Understanding the Mechanism of Cure in Testicular Cancer

by

Hayden Pearce

A thesis submitted to

The University of Birmingham

for the degree of

DOCTOR OF PHILOSOPHY

School of Cancer Sciences
College of Medical and Dental Sciences
The University of Birmingham
October 2013

ACKNOWLEDGEMENTS

Completing my PhD has been an immensely rewarding experience, mainly due to the people I have had the pleasure of working with.

First and foremost I would like to thank my supervisor, Prof. Paul Moss, for his inspiration and motivation throughout my PhD, and for allowing me the independence to make the project my own. Also, for his vital contribution in setting up the collaborations with the testicular cancer team at the QE hospital that has been vital to the success of this project. And for the incredible insight and enthusiasm in all aspects of this project.

The Moss group, past and present, which have been a great source of support, encouragement and friendship. I would like to give special thanks to Charlotte, Jo and Suzy for giving me excellent grounding in carrying out accurate and methodical experiments, and helping me maintain my sanity! Mark for being a great friend both at and away from the bench. I am also very grateful to Aaron and Kirsty for all their help, especially with the protein work. And to Ben for the wonderful cakes!

I'd like to thank urology oncologist Emilio Porfiri and urology surgeons Richard Viney and Prashant Patel at the QE hospital, for their generosity in giving up their time to advise me on the clinical aspects of testicular cancer, and for their help with sample collection. The pathologists Shalini Choudhri and Neeta Deshmukh for providing fresh tissue biopsies, and for our discussions relating to patient diagnosis. I would like to say a special thank you to Paul Hutton, who did a fantastic job of consenting patients for me over the last 3 years, and for providing me with patient information. I'd also like to mention the phlebotomists who kindly bled the patients for me.

And of course, I am extremely grateful to the guys who agreed to participate in this study, and the MRC for funding this Studentship.

Finally, I would like to thank my friends for keeping me going, and most of all, my family and partner Beth for their encouragement, patience and invaluable support throughout this PhD.

Thank you all

ABSTRACT

The expression of cancer testis antigens (CTAgs) is normally restricted to spermatogenic cells of the testis but is also present in many cancers including testicular germ cell tumours (TGCTs). CTAg-specific T cell responses have been identified in patients with other solid tumours, and here we identified CTAg-specific T cells in TGCT patients. MAGEA family-specific T cell responses were detected in 21/49 patients with a magnitude of up to 0.149% of total peripheral blood mononuclear cells. Responses to multiple MAGEA antigens were frequently detected in seminoma patients irrespective of tumour stage. Conversely, NSGCTT patients only developed responses towards MAGEA3, which were strongly associated with disease progression. Longitudinal analysis revealed that the magnitude of MAGE-specific immune responses diminished over time by up to 95%, which correlated with the removal of tumour antigens. MAGE-specific CD8 T cells demonstrated cytotoxic potential against endogenously presented antigen.

Tumour infiltrating T cells were antigen experienced, recently activated, oligoclonal populations; many of which expressed the inhibitory molecules, TIM-3 and PD-1. Proliferation and cytokine secretion was suppressed *in vivo* but was rescued with *in vitro* stimulation, indicative of an exhausted T cell phenotype.

Our findings have significant implications in the development of novel CTAg-specific immunotherapy in patients with cancer.

TABLE OF CONTENTS

ACKNOWLEDGEMENTS ..... **ii**

ABSTRACT ..... **iii**

TABLE OF CONTENTS ..... **iv**

TABLE OF FIGURES ..... **xi**

TABLE OF TABLES ..... **xv**

LIST OF ABBREVIATIONS ..... **xvii**

CHAPTER 1: INTRODUCTION **1**

The Immune System 1

Innate Immunity 1

Adaptive Immunity 2

B Cells 3

T Cells 4

TCR Gene Rearrangement within the Thymus 4

Central Tolerance 5

Peripheral Tolerance 6

Antigen Processing and Presentation 8

MHC Class I Antigen Presentation Pathway 8

MHC Class II Antigen Presentation Pathway 9

Cross Presentation 9

Antigen Presenting Cells and Costimulation 12

T cell Memory and Activation 13

Helper CD4 T cell Response 16

NK Cells 17

Activating and Inhibitory Receptors 18
NK Cell Subsets....18
Human Testis Structure and Function 19
Histology of the Human Testis....20
Spermatogenesis 22
Testicular Immune Privilege....23
Testicular Germ Cell Tumours 26
Risk Factors....28
Pathology 28
Presentation, Diagnosis and Staging 29
Treatment....30
Cancer Immunology....32
Immune Mediated Tumour Destruction....32
Intratumoural Immune Responses and Prognosis 33
Immunoediting Model....34
Mechanisms of Tumour Escape....35
Introduction to Cancer Testis Antigens....37
Importance of CTAgs in Cancer 37
Expression Patterns of CTAgs 38
Regulation of CTAgs....38
Spontaneous Immune Responses to CTAgs....39
Making the Most of a CTAg-specific Response 39
Expression of Cancer Testis Antigens in Testicular Germ Cell Tumours....40
Role of the Immune System in Testicular Germ Cell Tumour Destruction....41

HYPOTHESIS **42**

AIMS **42**

CHAPTER 2: MATERIALS AND METHODS **43**

Patients 43

Patient Characteristics 44

Cell Culture Media and Solutions 45

Peptides 47

Isolation of TIL from Tumour Tissue 47

Isolation of PBMC from Whole Blood 47

Isolation of Patient Serum from Clotted Blood 48

Cryopreservation of Purified TIL and PBMC 48

Thawing of Cryopreserved TIL and PBMC 49

Maintenance of Healthy Donor LCLs and HT-29 Cell Line 49

Flow Cytometry 49

Characterisation of Lymphocyte Subsets by Cell Surface Staining 50

PMA/Ionomycin Stimulation 50

Intracellular Cytokine Staining 52

Combined Intracellular Cytokine and CD107a Staining of Peptide-Stimulated PBMC 52

Celltrace™ Violet Labelling of TIL 53

CD3/CD28 Dynabeads® Proliferation Assay of TIL 53

Generation of T cell Lines 54

HLA-Peptide Dextramer Staining 56

Enrichment of Dextramer Positive CD8 T Cells 56

T Cell Cloning by Limiting Dilution 57
Stimulation Assay for IFNγ ELISA 58
IFNγ ELISA 59
NK Cell Purification 59
NK Cell Cytotoxicity Assay (CD107a Mobilisation Assay) 60
Simultaneous Extraction of RNA and Protein from Human Tumour Tissue 61
RNA isolation *61*
Protein Isolation *62*
Protein Concentration Determination by BCA Assay 63
Sample Preparation for SDS-Polyacrylamide Gel Electrophoresis (SDS-PAGE) 63
SDS-PAGE Gel Preparation and Running 63
Western Blot Analysis 65
Re-Probing of Western Blots 67
Reverse Transcription of RNA 67
Quantitative Real Time Polymerase Chain Reaction (qRT-PCR) 68
DNA Extraction from Whole Blood 69
HLA Typing by Endpoint PCR 70
Agarose Gel Electrophoresis for HLA Typing PCR 70
IFNγ ELISPOT 73
Determination of TCRVβ Repertoire by Flow Cytometry 74
Data Handling and Statistical Analysis 74
General Introduction 76
CHAPTER 3: PHENOTYPE AND FUNCTIONALITY OF LYMPHOCYTES INFILTRATING TGCTs 77
Introduction 77

Results 79

αβ and γδ T cells Infiltrate TGCTs 79

CD4 and CD8 TIL Have an Effector Memory Phenotype 82

The Effector Memory T cell Compartment is Inflated in TGCT Patients 86

T Cells Infiltrating TGCTs Express Markers of Activation 94

Increased CD69 Expression on Peripheral Blood CD8 T Cells Following Chemotherapy 96

T Cells Isolated from TGCT Tissue Have a High Proliferative Capacity *in vitro* .101

Oligoclonal Populations of T Cells Develop within TGCT Lesions 105

TGCTs Contain Inflammatory Cytokine Secreting T Cells 108

Tumour Infiltrating T Cells Have Cytotoxic Capacity 109

T Cells Infiltrating TGCTs Express Inhibitory Receptors 113

TIM-3 Is Induced on CD8 T Cells Shortly After Chemotherapy 116

PD-1 Expressing CD8 T Cells Decline Following Tumour Removal 116

PD-1 Ligands Are Expressed in TGCT Tissue 121

Tumour Infiltrating NK Cells Are Predominantly $CD56^{hi}CD16^{-}$ NK Cells 124

NKG2D is Downregulated on Tumour Infiltrating NK Cells 127

Tumour Infiltrating NK Cells are Functional 131

TGCTs Express NKG2D-Activating Ligands 136

Expression of NK Cell-Associated Markers on Tumour Infiltrating CD4 and CD8 T Cells 139

CD4+CD161+ T Cells are elevated in TGCT Tissue 139

CD8+CD56+ T Cells are rarely found in TGCT Tissue 140

NKG2D Is Downregulated on CD8 T Cells Infiltrating TGCTs 140

Discussion 146

Phenotype and frequency of peripheral and tumour infiltrating lymphocytes in TGCT patients 146

Functional analysis of peripheral and tumour infiltrating lymphocytes in TGCT patients 154

Regulation of T cell function in TGCTs 159

The role of NK cells in TGCTs 163

Conclusion 168

CHAPTER 4: CANCER TESTIS ANTIGEN RESPONSES IN TGCT PATIENTS 169

Introduction 169

Cancer Testis Antigens are Expressed in TGCTs 170

MAGE-specific CD8 T Cells are Detectable in TGCT Patients 174

MAGEA3-specific T Cells Secrete Inflammatory Cytokines 180

MAGEA3-specific T Cells Recognise Endogenously Processed Antigen 181

MAGEA3-Specific T Cells Have High Cytolytic Potential 181

Quantitation of CTAg Responses in TGCT Patients 190

MAGEA-specific T Cells are elevated in TGCT Patients 191

NY-ESO-1 and MAGEB1-Specific Cells are Undetectable in TGCT Patients 196

The Ability to Generate a MAGE-specific Response is Independent of Age 204

The Magnitude of a MAGEA4-Specific T cell Response is Age-Dependent 204

Patient Age of Disease Onset Differs Between Tumour Types 207

Metastatic Potential of the Tumour is Associated with Elevated Levels of MAGEA3-specific T Cells in NSGCTT Patients 207

Generation of a MAGE-Specific Response is not determined by Tumour Stage in Seminoma Patients 208

Multiple MAGE Responses are Generated in TGCT Patients 211

MAGE-specific T cell Frequency Diminishes Over Time 214

MAGE-specific Cells are Predominantly Cytotoxic CD8 T Cells 221

Discussion 225

Dextramer analysis reveals MAGE-specific CD8 T cells in TGCT patients 225

The development of multiple MAGEA family specific T cell responses is dependent on tumour type 228

NY-ESO-1 and MAGEB1 –specific T cell responses are not generated in TGCT patients 231

The effects of age on MAGE-specific T cell responses in TGCT patients 232

MAGE-specific T cell responses diminish over time 233

The functionality of MAGE-specific T cells from TGCT patients 236

Conclusion 240

CHAPTER 5: GENERAL DISCUSSION 241

REFERENCES 251

APPENDIX 275

TABLE OF FIGURES

Figure 1. The generation of central tolerance in the thymus. 7
Figure 2. Antigen presentation pathways in APCs. 11
Figure 3. T cell fate under different conditions of TCR engagement. 14
Figure 4. Morphology and immune privilege in the human testis. 21
Figure 5. Development of testicular germ cell tumours from spermatogenic precursors 27
Figure 6. The stage specific treatment regimen for TGCTs at the University Hospital Birmingham Testicular Cancer Centre. 31
Figure 7. Gating strategies for identification of CD4, CD8 and γδ T cells. 80
Figure 8. Proportion of CD4, CD8 and γδ TCR^+ T cells in PBMC and TIL. 81
Figure 9. Memory phenotype of CD4 T cells in matched PBMC and TIL. 83
Figure 10. Memory phenotype of CD8 T cells in matched PBMC and TIL. 84
Figure 11. Age of healthy donors and TGCT patients. 87
Figure 12. Memory phenotype of peripheral blood CD4 and CD8 T cells of healthy donors and TGCT patients. 89
Figure 13. Memory phenotype of peripheral blood CD4 and CD8 T cells of TGCT patients before and after chemotherapy. 92
Figure 14. CD69 expression on αβ and γδ T cell subsets from PBMC and TIL. 95
Figure 15. Expression of CD38 on T cells from TIL and autologous PBMC. 97
Figure 16. CD69 expression on peripheral blood T cells of healthy donors and TGCT patients at pre and post treatment. 99
Figure 17. T cells isolated from TGCT tissues have a high proliferative capacity. 104
Figure 18. Flow cytometric analysis of Vβ usage. 106
Figure 19. The clonality of tumour infiltrating T cells. 107
Figure 20. Secretion of inflammatory cytokines by tumour infiltrating T cells following stimulation. 110
Figure 21. Degranulation of tumour infiltrating T cells. 112
Figure 22. Expression of negative regulatory receptors on T cells from PBMC and TIL. 114
Figure 23. Expression of inhibitory receptors TIM-3 and PD-1 on peripheral blood CD4 and CD8 T cells of healthy donors and TGCT patients. 117

Figure 24. Expression of inhibitory receptors TIM-3 and PD-1 on peripheral blood CD4 and CD8 T cells following chemotherapy..... 119
Figure 25. Expression of PD-1 ligands in primary TGCT tissue..... 122
Figure 26. Expression of PD-L2 protein in primary TGCT tissue. 123
Figure 27. Gating strategy for identification of NK cell subsets..... 125
Figure 28. Comparison of NK cell subsets in PBMC and TIL..... 126
Figure 29. NKG2D expression on NK cell subsets from PBMC and TIL. 129
Figure 30. Changes in the proportion of NK cell subsets and NKG2D expression following chemotherapy. 130
Figure 31. Gating strategy and representative flow cytometric analysis for functional studies of tumour infiltrating NK cells. 133
Figure 32. Functional analysis of tumour infiltrating NK cells. 134
Figure 33. Degranulation of tumour infiltrating NK cell subsets against an NK-resistant tumour cell line..... 135
Figure 34. Expression of NKG2D activating ligands in primary TGCT tissue..... 137
Figure 35. Protein expression of NKG2D ligands, MICA and ULBP2, in primary TGCT tissue..... 138
Figure 36. Gating strategy for NK-associated markers on T cells. 141
Figure 37. Identification of tumour infiltrating T cell subsets expressing NK-associated markers. 142
Figure 38. Expression of NKG2D on CD8 T cells from PBMC and TIL..... 143
Figure 39. Expression of CTAg transcripts in primary TGCT tissue. 171
Figure 40. Expression of CTAg protein in primary TGCT tissue. 173
Figure 41. Schematic demonstrating the procedure for identification and purification of MAGE-specific T cells..... 175
Figure 42. Detection of MAGE-specific T cells by peptide-MHC dextramer. 177
Figure 43. The rate of detection of MAGE-specific T cells from PBMC of TGCT patients. 179
Figure 44. Inflammatory cytokine secretion of an EVDP–specific TCC generated from PBMC of a seminoma patient, following stimulation with LCL pulsed with EVDP peptide. 185

Figure 45. Inflammatory cytokine secretion of an EVDP –specific TCC stimulated with endogenously presented MAGEA3 antigen. 186
Figure 46. Cytotoxic potential of an EVDP-specific TCC. 187
Figure 47. Cytotoxic capacity of an EVDP-specific T cell clone in relation to cytokine secretion. 188
Figure 48. Titration of EVDP peptide concentration to establish avidity of EVDP-specific TCC. 189
Figure 49. CTAg-specific responses determined by ELISPOT from PBMC of Healthy donors. 193
Figure 50. CTAg-specific responses from PBMC of a seminoma patient, determined by ELISPOT. 194
Figure 51. Frequency of MAGEA1-specific T cells in healthy donors and TGCT patients. 197
Figure 52. Frequency of MAGEA3-specific T cells in healthy donors and TGCT patients. 198
Figure 53. Frequency of MAGEA4-specific T cells in healthy donors and TGCT patients. 199
Figure 54. Frequency of NY-ESO-1-specific T cells in healthy donors and TGCT patients. 200
Figure 55. Frequency of MAGEB1-specific T cells in healthy donors and TGCT patients. 201
Figure 56. Overall frequency of CTAg-specific T cells in healthy donors and TGCT patients. 202
Figure 57. The effect of age on the possibility of generating a T cell response to MAGE antigens. 205
Figure 58. Correlation between frequency of CTAg-specific IFNγ secreting cells and age of seminoma patients. 206
Figure 59. Age of TGCT patients used in ELISPOT assay, categorised by tumour type. .. 209
Figure 60. Effect of tumour stage on the frequency of CTAg-specific IFNγ secreting cells in TGCT patients. 210
Figure 61. TGCT patients with single and multiple MAGEA family responses. 212
Figure 62. Frequency of responses to multiple MAGE antigens according to tumour type. 213
Figure 63. Kinetics of MAGE-specific responses determined using ELISPOT assay. 216

Figure 64. Kinetics of MAGE-specific responses in TGCT patients with a positive response prior to chemotherapy. 217
Figure 65. The reduction of MAGE-specific T cells following chemotherapy..... 218
Figure 66. Dynamics of a single epitope MAGE-specific CD8 T cell response following chemotherapy. 219
Figure 67. Kinetics of MAGE-specific responses in TGCT patients without a response prior to chemotherapy. 220
Figure 68. The secretion of inflammatory cytokines, IFNγ and TNFα, from CD4 and CD8 T cells following MAGE peptide stimulation. 222
Figure 69. The magnitude of degranulation of CD8 T cells that secrete single or multiple cytokines. 223
Figure 70. Summary of MAGE-specific T cell immunity in TGCT patients 224

TABLE OF TABLES

Table 1. Summary of Blood and Tissue Samples Obtained From TGCT Patients 44
Table 2. Anti-human antibodies to cell surface markers used for cell phenotyping 51
Table 3. Detailed list of peptides used in T Cell Line assays..... 55
Table 4. Separating and Stacking gel recipes..... 64
Table 5. SDS page Running buffer and Transfer buffer recipes. 65
Table 6. Antibodies used for western blot analysis. 66
Table 7. Primers used in qRT-PCR assay to determine expression levels of genes in TGCT and healthy testis tissue..... 71
Table 8. Primers for HLA typing..... 72
Table 9. Antibodies used for Vβ clonality analysis. 75
Table 10. Memory phenotype of CD4 and CD8 T cells in matched PBMC and TIL..... 85
Table 11. Memory phenotype of peripheral blood CD4 and CD8 T cells of healthy donors and TGCT patients. 90
Table 12. Memory phenotype of peripheral blood CD4 T cells of TGCT patients before and after chemotherapy 93
Table 13. Memory phenotype of peripheral blood CD8 T cells of TGCT patients before and after chemotherapy 93
Table 14. P values for memory phenotyping of peripheral blood T cells of TGCT patients before and after chemotherapy. 93
Table 15. CD69 and CD38 expression on αβ and γδ T cell subsets from PBMC and TIL.... 98
Table 16. Activation status of T cells from peripheral blood of healthy donors compared to that of TGCT patients. 100
Table 17. T cell activation of peripheral blood T cells in TGCT patients pre and post chemotherapy. 100
Table 18. P values for T cell activation of peripheral blood T cells in TGCT patients before and at intervals following chemotherapy. 100
Table 19. Single and dual cytokine secretion of tumour infiltrating T cells..... 111
Table 20. Expression of negative regulatory receptors on T cells from PBMC and TIL..... 115
Table 21. Expression of inhibitory receptors TIM-3 and PD-1 on peripheral blood CD4 and CD8 T cells of healthy donors and TGCT patients. 118

Table 22. Expression of inhibitory receptors TIM-3 and PD-1 on peripheral blood CD4 and CD8 T cells following chemotherapy. 120
Table 23. p values for expression of inhibitory receptors TIM-3 and PD-1 on peripheral blood CD4 and CD8 T cells following chemotherapy. 120
Table 24. Identification of tumour infiltrating T cell subsets expressing NK-associated markers. 144
Table 25. Summary of differences observed between T cells isolated from 145
Table 26. Summary of differences observed between NK cells and NK-like 145
Table 27. Detailed list of peptides used in T Cell Line assays and Dextramer complex. ... 176
Table 28. Overall frequency of CTAg-specific T cells in healthy donors and TGCT patients. 203
Table 29. Patient Information of Recruited TGCT Patients. 275

LIST OF ABBREVIATIONS

AIRE	Autoimmune Regulator
ADCC	Antibody-dependent cellular cytotoxicity
AF700	Alexa-fluor 700
AmCyan	Anemonia majano cyan
APC	Antigen presenting cell
APC (flow)	Allophycocyanin
APC-Cy7	Allophycocyanin-cyanine 7
BSA	Bovine serum albumin
BTB	Blood-Testis-Barrier
CCR	CC chemokine receptor
CD	Cluster of differentiation
CTAg	Cancer-Testis Antigen
CTL	Cytotoxic T lymphocyte
CTLA-4	Cytotoxic T-lymphocyte antigen 4
CXCR	CXC chemokine receptor
DC	Dendritic cell
DMSO	Dimethyl Sulphoxide
DNA	Deoxyribonucleic acid
DP	Double positive
EDTA	Ethylenediaminetetracetic acid
ER	Endoplasmic reticulum
FACS	Fluorescence-activated cell sorting
FCS	Foetal calf serum
FITC	Fluorescein isothiocyanate
FSC	Forward scatter
GM-CSF	Granulocyte macrophage colony-stimulating factor
HLA	Human leukocyte antigen
HS	Human Serum
IFN	Interferon
IHC	Immunohistochemistry
IL	Interleukin
IQR	Inter-quartile range
LCL	Lymphoblastic cell line
MDSC	Myeloid derived suppressor cell
MFI	Median fluorescence intensity
MHC	Major histocompatibility complex
MICA	Major histocompatibility complex class I-related chain A
mGCT	Mixed germ cell tumour
mRNA	Messenger ribonucleic acid

NK	Natural killer cell
NKT	Natural killer T cell
NSGCTT	Non-seminomatous germ cell testicular tumour
PBMC	Peripheral blood mononuclear cell
PBS	Phosphate buffered saline
PD-1	Programmed death 1
PDGF	Platelet derived growth factor
PD-L1	Programmed death 1 ligand 1
PD-L2	Programmed death 1 ligand 2
PE	R-phycoerythrin
PE-Cy5	Phycoerythrin cyanine 5
PE-Cy7	Phycoerythrin cyanine 7
PerCPCy5.5	Peridinin chlorophyll protein complex-cyanine 5.5
PHA	Phytohaemagglutinin
PMA	Phorbol myristate acetate
pMHC	Peptide MHC complex
qRT-PCR	Quantitative Reverse transcription polymerase chain reaction
SDS	Sodium dodecyl sulphate
SEM	Standard error of the mean
SP	Single positive
SSC	Side scatter
TAA	Tumour associate antigen
TAP	Transporter associated with antigen processing
TCC	T cell clone
TCL	T cell line
T_{CM}	Central memory T cell
TCR	T cell receptor
T_{EM}	Effector memory T cell
TEMED	Tetramethylethylenediamine
TEMRA	Terminal differentiated effector memory CD45RA revertants
TGCT	Testicular Germ Cell Tumour
TGF	Transforming growth factor
Th1/2	T helper cell 1/2
TIL	Tumour infiltrating lymphocyte
TIM-3	T cell membrane protein 3
TLR	Toll-like receptor
TNF	Tumour necrosis factor
Treg	Regulatory T cell
TSA	Tumour specific antigen
ULBP	UL16-binding protein

CHAPTER 1: INTRODUCTION

The Immune System

The immune system of higher mammals has evolved into a complex system in order to effectively protect the body against a wide range of pathogenic microorganisms and abnormal self, such as cancerous cells (Delves and Roitt, 2000). The immune system comprises of many specialised cell types and soluble factors, which work in unison to protect the body against internal and external threats. The immune response is self-regulating to circumvent excessive inflammation that would otherwise lead to tissue damage. It also discriminates against self and non-self, thereby only targeting foreign bodies and not the body's own cells; unless these have been altered as in the case of cancer. The inability of the immune system to distinguish between self and non-self can lead to the development of autoimmune disease. The immune system consists of 'innate' and 'adaptive' immunity, which work together to ensure rapid and efficient removal of invading pathogens. This project focuses primarily on T cell immunology, and the introduction focuses predominantly on the mechanisms of adaptive immunity, with a brief overview of innate immunity.

Innate Immunity

The innate immune response represents the most ancient form of immunity, in evolutionary terms. It involves the recognition of conserved features of pathogens via pattern recognition receptors, such as the Toll- like receptors (TLRs), expressed on the cell surface (Hoffmann *et al*., 1999). Neutrophils and macrophages are the most important phagocytic cells that patrol the body and destroy pathogens (Underhill *et al*., 1999). Other

important cells such as mast cells, basophils and eosinophils release inflammatory mediators such as histamine and proteolytic enzymes. The inflammatory environment recruits other innate cells such as dendritic cells to the site of pathological insult.

The innate immune system provides rapid responses, but the huge diversity of pathogens means the innate response may be ineffective or overwhelmed by the invading organism. The innate response is vital for the activation of the adaptive immune response and minimises the damage by pathogens while the adaptive immune response is developing.

Adaptive Immunity

The adaptive immune response can take several days to develop and therefore this response alone is ineffective at protecting against pathogens. However, the adaptive immune response has several advantages over the innate response. Firstly, when an antigen is encountered more than once, each subsequent encounter is more rapid and more efficient. This vital feature of adaptive immunity is known as immunological memory. Secondly, the adaptive response is highly specific for a particular antigen and is long lived. The greater specificity and selectivity of an adaptive immune response is attributable to the vast repertoire of receptors that are somatically generated as the cell develops. This process allows each cell to have a unique specificity for recognition of pathogens or abnormal cells that have evaded the innate immune system (Arstila *et al*., 1999).

The adaptive immune system encompasses two major types of lymphocyte subsets that originate from a common lymphoid progenitor in the bone marrow. Each lymphocyte

expresses a unique receptor on the cell surface that is specific for a single antigen. When a naive lymphocyte recognises its cognate antigen for the first time, along with appropriate stimulatory signals, it proliferates creating a clonal population of effector cells specific for that particular antigen. Once the infection has been resolved, the majority of clonally expanded cells die; the antigens that originally provoked a response are no longer at levels required to sustain it (Callan *et al*., 2000). However, a population of memory lymphocytes remain. This enables a rapid response against the possible reoccurrence of the pathogen. The two major types of lymphocytes are B lymphocytes (B cells) and T lymphocytes (T cells).

B Cells

B cells use their surface bound immunoglobulin protein to recognise foreign antigens on extracellular pathogens. When a B cell encounters and binds its cognate antigen with high affinity, it proliferates and the daughter cells differentiate into antibody-secreting plasma cells or B memory cells. Activated B cells undergo isotype subclass switching and somatic hypermutation of complementarity determining regions (CDR) to generate high affinity antibodies (Brack *et al*., 1978). The high affinity soluble antibodies released by the plasma cells are of the same specificity to the parent B cell from which they were derived. Secreted antibodies either neutralise the function of the pathogen or induce opsonisation whereby the pathogen is ingested by phagocytes. Bound antibodies also act as a receptor for the first component of the complement system and initiate activation of the classical complement cascade leading to destruction of the target antigen. Memory B cells persist in bone marrow conferring long-term immunity to that particular antigen.

T Cells

There are two major subtypes of T cells. Firstly, CD8 cytotoxic T cells, which when stimulated, directly kill virally infected cells or abnormal cells such as tumour cells. Secondly, CD4 helper T cells, which, during the adaptive immune response, activate other cells. Precursors of T cells (thymocytes) migrate from the bone marrow to the thymus where they mature and undergo selection processes. This ensures they are able to bind self-major histocompatibility complex (MHC) molecules (positive selection), yet not react strongly to self- antigens (negative selection) (Klein *et al*., 2009).

TCR Gene Rearrangement within the Thymus

During T cell development, thymocytes migrate through defined microenvironments of the thymus and rearrange their T Cell Receptor (TCR) genes. Predominantly, T cells express TCRs comprising an α and a β chain, which form a heterodimer that recognises antigenic peptides bound to MHC molecules. The α chain is encoded by the variable (V) and joining (J) segments, whereas the β chain is encoded by the variable (V), the joining (J) and an additional segment, the diversity (D) segment (Davis, 1990). Initially, the β chain rearranges (Saint-Ruf *et al*., 1994), and is subsequently expressed alongside the α chain and CD3 complex (Mallick *et al*., 1993). TCRs are associated with the CD3 complex, which is expressed by all T cells and is required for TCR surface expression and subsequent signalling (Reinherz *et al*., 1982). The α chain gene is subsequently rearranged to form a functional $\alpha\beta$ TCR (Petrie *et al*., 1993). The vast diversity of the TCR is due to the availability of numerous gene segments which can be differentially combined, as well as additional junction diversity where single nucleotide changes are introduced during gene rearrangement (Krangel, 2009). Ultimately, this leads to a large number of CD4 and CD8

double-positive (DP) thymocytes with a diverse repertoire of unique αβ TCRs with random specificity.

Central Tolerance

During maturation, thymocytes express a unique TCR on their surface. Importantly, thymocytes are unable to recognise antigen on their own. Instead they recognise antigens bound to MHC molecules. The TCR affinity for self-peptide:MHC (pMHC) complexes determines a thymocytes fate from this point forward. DP thymocytes expressing TCRs that do not bind self-pMHC complexes die by delayed apoptosis by a process termed "death by neglect". Those with a low affinity for self-pMHC receive pro-survival signals and differentiate into CD4 or CD8 single-positive (SP) thymocytes in the thymic cortex by a process termed positive selection. However, those with a high-affinity TCR for self-pMHC complexes are removed by apoptosis, in a process called negative selection. Medullary thymic epithelial cells (mTECs) play a crucial role in thymic tolerance in that they express a large number of tissue-specific self-antigens (TSAs) (Derbinski *et al*., 2001) under the regulation of the autoimmune regulator (AIRE) (Anderson *et al*., 2002). They induce apoptosis of tissue specific antigen (TSA)-specific thymocytes in the thymic medulla. Combined, these processes render developing T cells non-reactive to self and prevent the generation of autoimmune disease. Cells that survive the selection process leave the thymus and enter the bloodstream or the lymphatic system. This process of central tolerance is outlined in Figure 1.

Peripheral Tolerance

While central tolerance is able to remove the majority of self-reactive T cells, some low avidity self-reactive T cells escape this process. Peripheral tolerance is developed when T cells have completed maturation within the thymus and have entered the periphery, and is vital for the prevention of autoimmune disease (Caspi, 2006). Peripheral tolerance is achieved by a variety of mechanisms including organisation of 'immune-privileged' sites such as that of the testis. The localised inhibitory mechanisms at play within the human testis are detailed later in this chapter. Tolerance within these sites is mediated by passive mechanisms, for example, restricted access to specific sites, e.g. blood-testis barrier. In addition, tolerance is actively mediated by the generation of an immune-suppressive environment through the production of regulatory cytokines such as TGF-β and IL-10. Moreover, expression of inhibitory ligands, such as Fas ligand and PD-L1, in tissue such as testis could induce cell cycle arrest or apoptosis in infiltrating T cells.

Antigen recognition by a T cell without subsequent costimulation generally results in T cell anergy, or hypo-responsiveness. This is particularly relevant to self-reactive T cells that escape central tolerance due to a low avidity interaction between TCR and pMHC (Redmond and Sherman, 2005). In addition, chronic exposure to antigen without costimulation can lead to activation-induced cell death (reviewed in (Walker and Abbas, 2002)). Moreover, if immature DCs process and present antigen without subsequent maturation, they do so in a tolerogenic manner (Dhodapkar *et al*., 2001). Probably the most pertinent mechanism by which peripheral tolerance is mediated is through the action of CD4+FoxP3+ regulatory T cells (Tregs). The absolute requirement for Tregs to protect the host from autoimmune disease suggests these cells play a crucial role in maintaining self-

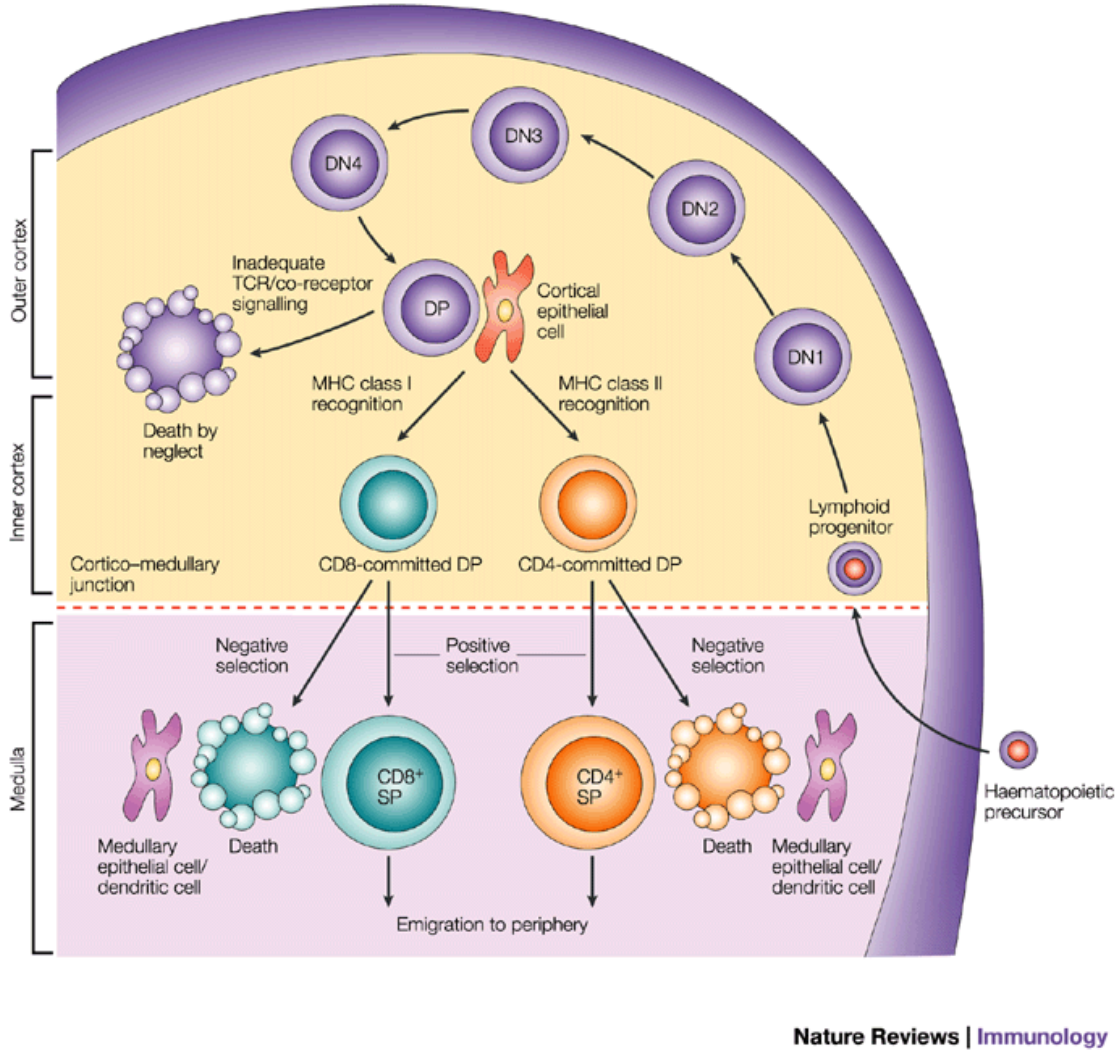

Figure 1. The generation of central tolerance in the thymus.
Common lymphoid progenitors arise in the bone marrow and migrate to the thymus. Early committed T cells lack expression of T-cell receptor (TCR), CD4 and CD8, and are termed double-negative (DN; no CD4 or CD8) thymocytes. As the thymocytes travel through the cortex they express the pre-TCR, which is composed of the non-rearranging pre-Tα chain and a rearranged TCRβ-chain. Thymocytes then become double positive (DP) replacement of the pre-TCRα-chain with a newly rearranged TCRα-chain occurs, yielding a complete $\alpha\beta$TCR. The thymocytes are then able to interact with cortical epithelial cells that express MHC class I and class II molecules associated with self-peptides. The fate of these DP thymocytes depends on signalling that is mediated by interaction of the TCR with these self-peptide–MHC ligands. The lack of pro-survival signalling results in apoptosis (death by neglect). In the medulla, too much signalling due to high avidity binding of self-antigens can induce pro-apoptotic signalling (negative selection). The appropriate, intermediate level of TCR signalling initiates effective maturation (positive selection). Thymocytes that express TCRs that bind self-peptide–MHC-class-I complexes become CD8 T cells, whereas those that express TCRs that bind self-peptide–MHC-class-II ligands become CD4 T cells. Mature cells leave the thymus and enter peripheral lymphoid tissues. SP, single positive. Adapted from (Germain, 2002) with consent (licence number: 3251880264723)

tolerance in the periphery (Sakaguchi *et al*., 2006). Importantly, many of these mechanisms outlined here are subverted in the course of tumour development, promoting tumour immune evasion and subsequently tumour growth.

Antigen Processing and Presentation

Antigens are derived from many sources including invading pathogens and self-proteins. T cells can only recognise antigens that are presented on the cell surface via MHC molecules. In humans, MHC molecules are also known as human leukocyte antigens (HLA), which are polygenic and very polymorphic. Consequently, there is huge variation in the exact peptides presented by the MHC (Horton *et al*., 2004). We all inherit multiple MHC class I genes (HLA-A, B and C) that present peptides to CD8 T cells, and MHC class II genes (HLA-DR, DP and DQ), which present antigenic peptides to CD4 T cells. The mechanism by which peptide processing occurs is different depending on whether peptides are presented on MHC class I or MHC class II. In general, antigens presented by MHC class I molecules are derived from endogenous proteins, whereas exogenous proteins taken up by endocytosis are presented by MHC class II. The concept of exogenous antigen presentation to CD8 T cells via the MHC class I pathway is known as 'cross-presentation' (Bevan, 1976). This latter concept is particularly important in the context of tumour immunology. The details of all three pathways are summarised below (Figure 2).

MHC Class I Antigen Presentation Pathway

MHC class I molecules are expressed on almost all nucleated cells and allow the cell to display peptides from endogenously synthesised proteins. These proteins are degraded by the proteasome into small peptides of around 9 amino acids in length and are then

transported into the endoplasmic reticulum by transporter associated with antigen processing (TAP) (Cresswell et al., 2005). Here, peptides are loaded into the MHC class I molecules and translocated to the cell surface with the help of chaperone proteins (Rock *et al*., 1994, Bouvier, 2003). In the context of tumour immunology, CD8 T cells are able to survey the host cell proteome for the presence of tumour-associated and tumour-specific proteins, then target these abnormal cells accordingly.

MHC Class II Antigen Presentation Pathway

The constitutive expression of MHC class II is restricted to professional antigen presenting cells (APCs), including B cells, macrophages and dendritic cells (DCs). However, MHC class II expression can be induced in other cell types, including fibroblasts and certain tumours (Steimle *et al*., 1994, Guermonprez *et al*., 2003). Peptides processed and subsequently presented by MHC class II are usually derived from exogenously acquired proteins following internalisation, i.e. those contained within endolysosomal compartments (Rudensky *et al*., 1991, Watts, 2004). Peptides with a size of around 15 amino acids are loaded onto nascent MHC class II molecules, and transported to the surface for recognition by CD4 T cells. Evidence suggests endogenously expressed proteins can also be presented by MHC class II molecules (Dengjel *et al*., 2005, Schmid *et al*., 2007).

Cross Presentation

Professional APCs are able to present exogenous antigens to CD8 T cells, in a process called 'cross-presentation' (Bevan, 2006). This phenomenon is extremely relevant in the context of tumour antigen presentation as it enables CD8 T cells to elicit a cytotoxic recall

response against tumour cells without requiring costimulation. Specifically, it allows a CD8 T cell response to be generated against an antigen that would otherwise be inaccessible to the MHC class I processing pathway. Proteins are potentially released from cells undergoing apoptosis or chemotherapy-induced-necrosis and endocytosed by neighbouring cells (usually DCs). This mechanism allows exogenous proteins to enter the MHC class II pathways. Importantly, mechanisms exist whereby extracellular proteins can enter the MHC class I pathway. Such mechanisms include DCs transporting endocytosed antigen from the endosome directly into the cytosol where it is degraded by the cytoplasmic proteasome. Peptides are then transported by TAP into the ER, and translocate to the cell membrane bound to MHC class I molecules, in a process similar to the classical MHC class I pathway (Ackerman and Cresswell, 2004, Nierkens *et al*., 2013). In addition, antigens can be degraded in the cytosol and imported into the recycling endosome by TAP molecules present in the endosomal membrane, where loading occurs on recycling MHC class I molecules (Albert *et al*., 1998). Another such mechanism is the degradation of antigens by endosomal proteases whereby these antigens are loaded onto MHC class I molecules in the endosomes, in a proteasome independent and TAP-independent manner (Gromme *et al*., 1999).

Alternative methods of cross presentation have been described which use mechanisms such as macroautophagy and trogocytosis, as well as the manipulation of gap junctions between DCs and tumour cells. Autophagy is an intracellular process, which degrades long-lived and misfolded proteins during cellular stress. Inhibition of autophagy results in the absence of cross presentation (Li *et al*., 2008). Trogocytosis is a process whereby MHC

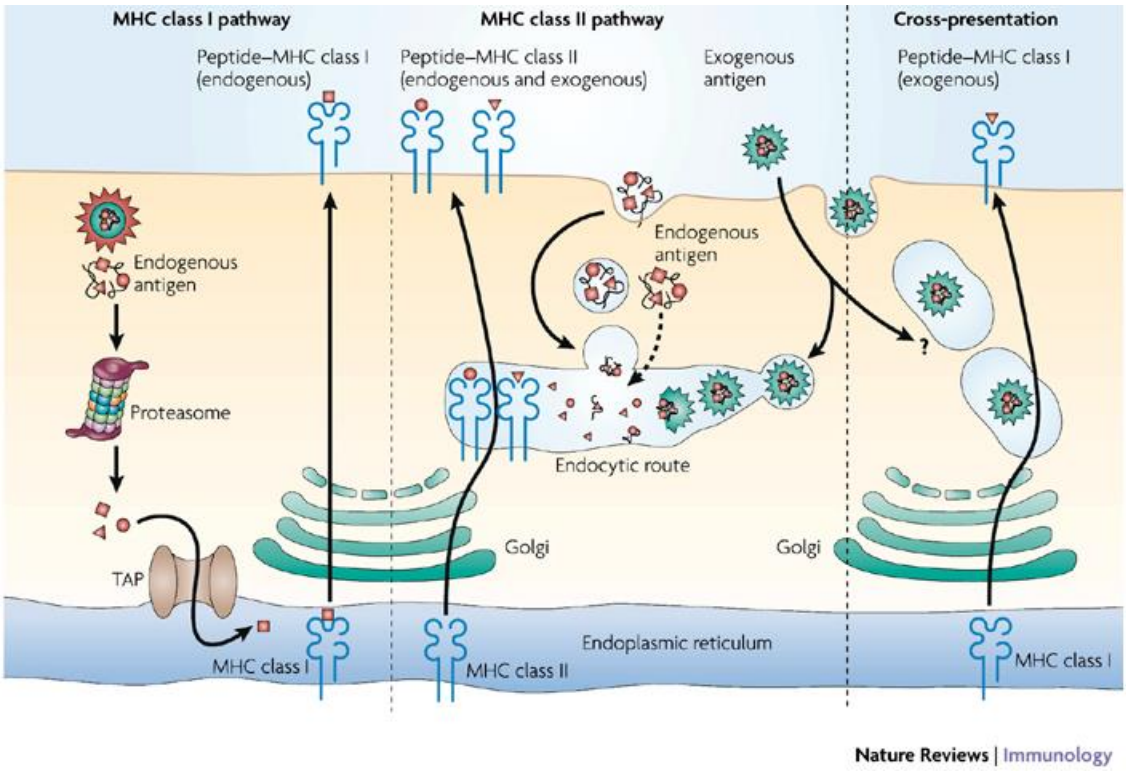

Figure 2. Antigen presentation pathways in APCs.
APCs have functional MHC class I and MHC class II presentation pathways. MHC class I molecules present peptides that are derived from proteins degraded mainly in the cytosol. MHC class II molecules acquire peptides that are generated by proteolytic degradation in endosomal compartments i.e. exogenous proteins. DCs have a unique ability to deliver exogenous antigens to the MHC class I pathway by 'cross-presentation'. TAP, transporter associated with antigen processing. Adapted from (Villadangos and Schnorrer, 2007) with consent (licence number: 3251880596676)

class I peptide complexes are transferred from the tumour to the DCs, allowing efficient presentation of tumour antigens to CD8 T cells and their subsequent activation (Wakim and Bevan, 2011, Wolfers *et al*., 2001). Tumour antigenic peptides could be transferred from the tumour cells to DCs via channels in gap junctions (Neijssen *et al*., 2005). Several publications demonstrate the transfer of peptides from apoptotic cells and tumour cells to DCs (Pang *et al*., 2009, Saccheri *et al*., 2010). Moreover, the transferred peptides were efficiently presented on MHC class I molecules and triggered activation of specific CD8 T cells.

Antigen Presenting Cells and Costimulation

Professional APCs are able to process antigen with great efficiency and induce complete activation of naive T cells that have not previously encountered cognate antigen. Immature DCs scout peripheral tissues and take up antigen at sites of infection or within a tumour mass. They migrate to secondary lymphoid organs where they mature and present captured epitopes to T cells.

APCs provide a second costimulatory signal at the point of TCR:pMHC interaction (Itano and Jenkins, 2003). This synergistic signalling by costimulatory molecules is necessary for optimal T cell proliferation and differentiation. Mature DCs are the most effective APC since costimulatory molecules are constitutively expressed following activation (Inaba *et al*., 1990), however, upon stimulation, B cells and macrophages can upregulate costimulatory molecules to act as professional APCs (Barker *et al*., 2002). The B7 superfamily of costimulatory molecules interact with CD28 on the surface of T cells. CD28 binding partners include CD80 (B7-1) and CD86 (B7-2), which are expressed on APCs. CD28 costimulation augments T-cell activation, and induces both T cell proliferation and IL-2 production. TCR engagement with pMHC in the absence of costimulation leads to a state of T cell anergy. Anergic T cells are characterised by their inability to secrete IL-2 and diminished proliferative capability, however their anergic state can be reversed due to their expression of CD25 (IL-2 receptor) (Schwartz, 2003).

After successful activation, proliferation and differentiation of naive T cells following TCR:pMHC interaction with costimulation, the requirement for costimulation is lost. Consequently, exposure to antigen alone is adequate for subsequent T cell activation.

Importantly, a high proportion of CD8 T cells express NKG2D on their surface, which can act to augment TCR-dependent activation when bound to its corresponding ligand (Roberts et al., 2001). In contrast, CTLA-4 is upregulated on the surface of activated CD4 T cells, which upon ligation of CD80 and CD86, can result in cell cycle arrest, and termination of the T cell response. Both CTLA-4 and CD28 have the same binding partners, but CTLA-4 transmits an inhibitory signal whereas CD28 transmits a stimulatory signal (London *et al*., 2000). These concepts have significant implications for the function of tumour-specific T cells, whereby costimulation would not be provided directly by the tumour cell initiating the response. T cell fate under different conditions of TCR engagement is illustrated in Figure 3.

T cell Memory and Activation

Activated T cells clonally expand and differentiate into effector T cells. During differentiation, T cells demonstrate extensive heterogeneity in the expression of molecules such as cytokines, chemokine receptors and costimulatory molecules. After the initial immune response, a small proportion of these cells persist as either effector memory (T_{EM}), or central memory (T_{CM}) T cells (Lanzavecchia and Sallusto, 2005, Tanchot et al., 1997). A highly differentiated memory subset of CD8 T cells (TEMRA) can also develop, however this population is less common in CD4 T cells. The fate of naive T cells is not decided prior to cell division as they have the capacity to produce effector and memory T cell progeny following activation (Stemberger *et al*., 2007). Memory cells persist at low frequencies for many years by an equilibrium of homeostatic proliferation and cell death (Gourley *et al*., 2004).

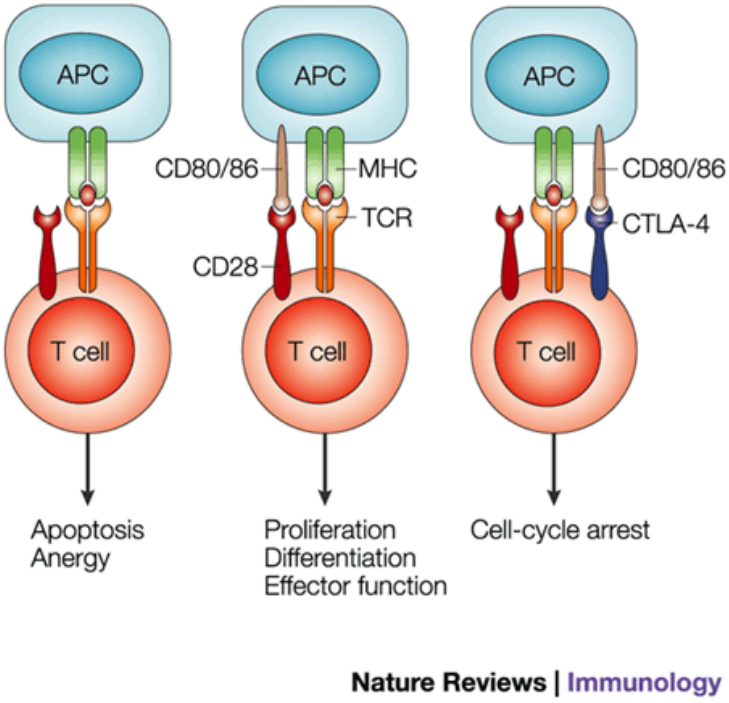

Figure 3. T cell fate under different conditions of TCR engagement.
Simultaneous recognition of a specific pMHC complex by the TCR, and of CD80 or CD86 by the costimulatory receptor CD28 results in T-cell activation, cytokine production, proliferation and differentiation. In the absence of CD28 costimulation, T cells become anergic or undergo apoptosis. After T-cell activation and upregulation of cytotoxic T-lymphocyte antigen 4 (CTLA-4), its ligation with the TCR results in cell-cycle arrest and termination of T-cell activation. Adapted from (Alegre *et al*., 2001) with consent (licence number: 3251880862396).

T cells can be separated into four major subsets based on the expression of chemokine receptor CCR7, and the CD45 high molecular weight isoform, CD45RA (Sallusto *et al*., 1999). These subsets are termed naive ($CCR7^+CD45RA^+$), T_{EM} ($CCR7^-$ $CD45RA^-$), T_{CM} ($CCR7^+CD45RA^-$), and the highly differentiated CD8 TEMRA ($CCR7^-CD45RA^+$). The expression of CCR7 is essential for the ability of naive and T_{CM} cells to circulate through lymph nodes and sample the environment for cognate antigen. The expression of CCR7 ligands, CCL19 and CCL21, in lymph nodes enables the migration of these cells into this

area (Rot and von Andrian, 2004). T_{CM} have the ability to differentiate into effector cells upon antigen stimulation, but lack immediate effector function. In contrast, T_{EM} downregulate CCR7 expression and upregulate the expression of tissue homing chemokine receptors e.g. CXCR3, enabling them to patrol peripheral tissues, including tumour sites. Upon antigen recognition, these cells are able to respond immediately with full effector function. TEMRA cells are produced primarily due to chronic viral-antigen stimulation, and re-express the CD45RA isoform. In this thesis, the detection of activated T cells *ex vivo* was required, and the markers used to distinguish activated cells from resting cells are outlined below.

T cell stimulation causes the upregulation of several cell surface molecules including CD69 and CD38. CD69 is a very early activation marker that is expressed on T cells within an hour of TCR:pMHC engagement. Moreover, it is the earliest known inducible cell surface glycoprotein acquired during T cell activation (Hara *et al*., 1986). CD38 is an ADP-ribosyl hydrolase expressed at variable levels on hematopoietic cells. It is highly expressed by subsets of thymocytes (Tenca *et al*., 2003) and antigen stimulated T cells (Sandoval-Montes and Santos-Argumedo, 2005, Shubinsky and Schlesinger, 1997).

T cells respond to antigen by secreting cytokines and/or directly lysing target cells. The appropriate mechanism(s) depends on the T cell subtype being stimulated and the environment in which activation occurs. Cytotoxic CD8 T cells directly kill infected, abnormal and cancerous cells which display antigenic peptides through MHC class I on their surface. Two populations of CD4 helper T cells exist, namely Th1 and Th2. Both of these populations recognise peptides in the context of MHC class II on APCs (Mosmann

and Coffman, 1989). Classification into these distinct subsets is based on the cytokines secreted by the cells. Antigen dose and cytokines present in the environment when the cells are activated dictates the pathway the cells will follow (Rogers and Croft, 1999). Once naive Th0 cells have been polarised into Th1 or Th2 cells, commitment is not reversible, even under opposing polarising conditions (Murphy *et al*., 1996).

Helper CD4 T cell Response

The role of CD4 T cells in the adaptive immune response is to orchestrate and promote the function of other effector cells. This is achieved by the secretion of soluble factors including cytokines and chemokines. In addition, activation-induced expression of Fas ligand by CD4 T cells can mediate apoptosis in tumour cells expressing Fas.

Th1 cells are polarised by IL-12 and type I interferons through induction of the transcription factors STAT4 and T-bet (Cho *et al*., 1996). They secrete IFNγ and TNFα, in order to instigate delayed-type hypersensitivity responses effective in the clearance of virally infected or cancerous cells. These inflammatory cytokines mediate the activation of phagocytes and the induction of opsonising and compliment activating antibodies. Furthermore, Th1 associated cytokines augment the cytotoxic T cell response by supporting CD8 T cell activation and up-regulating MHC class I expression on APCs.

Th2 cells are polarised by the induction of STAT-6 and GATA3 (Rengarajan *et al*., 2000). They secrete IL-4, IL-5, and IL-13 and are important for the control of extracellular pathogens and allergies by mediating humoral immune responses. Additional CD4 T cell subsets have also been described. For example, Th17 cells, which secrete IL-17 and are

associated with many autoimmune diseases (Harrington *et al*., 2005, Park *et al*., 2005), and FoxP3+ Tregs, which play a crucial role in the suppression of immune responses (Asano *et al*., 1996, Takahashi *et al*., 1998).

Cytotoxic CD8 T cell response

CD8 T cells induce apoptosis in target cells by the release of cytolytic granules, which contain perforin and granzyme (Lieberman, 2003). Perforin binds to the target cell membrane and polymerises to form a transmembrane pore which allows granzyme to enter (Keefe et al., 2005). Granzyme consists of proteases that trigger caspase dependent apoptosis (Russell and Ley, 2002). Interaction between Fas ligand, expressed by CD8 T cells, and Fas receptor, expressed by the target cell, is another mechanism by which CD8 T cells mediate their cytotoxic effects. Engagement of these two molecules induces apoptosis of the target cells (Rouvier *et al*., 1993). Furthermore, activation of CD8 T cells induces the production of the effector cytokines IFNγ and TNFα. Secreted IFNγ can synergise with TNFα to activate macrophages and recruit them to sites of inflammation. In addition, target cells up-regulate MHC class I molecules, increasing the likelihood of transformed cells being recognised by CD8 T cells (Zhou, 2009).

NK Cells

NK cells link the innate and adaptive arms of the immune system and have important anti-viral and anti-tumour functions. NK cells are large granular lymphocytes, derived from the common lymphoid progenitor, which circulate in lymphoid organs and peripheral tissues (Cooper and Caligiuri, 2004).

Activating and Inhibitory Receptors

NK cells can be activated by stimulation via their activating receptors or by the lack of signal through their inhibitory receptors (Hamerman *et al*., 2005). Primarily, inhibitory receptors are specific for highly polymorphic MHC molecules, which enable them to mediate 'missing self-recognition'- the ability to respond to self-cells that have lost expression of MHC class I molecules (Ljunggren and Karre, 1990). In addition, activating receptors expressed by NK cells, such as NKG2D, can bind ligand which is barely detectable in resting conditions but frequently expressed upon cellular stress. Such ligands include MICA and members of the ULBP family. Moreover, DNA lesions associated with tumour development activate the DNA damage response (DDR), resulting in the upregulation of NKG2D ligands and the subsequent killing of cancerous cells (Gasser *et al*., 2005). In summary, tumour cells can downregulate the necessary antigens identifying them as 'self' and also upregulate activating ligands, leading to NK cell mediated cytotoxicity.

NK Cell Subsets

NK cells are defined as a population of lymphocytes which express CD56, but are negative for CD3 and are subdivided into two subsets, namely $CD56^{low}CD16^{+}$ and $CD56^{hi}CD16^{-}$. NK cells found in peripheral blood are predominantly the $CD56^{low}CD16^{+}$ subset, accounting for approximately 90% of circulating NK cells. This subset has a greater cytolytic potential in the resting state, expressing high levels of cytotoxic granules, compared to the $CD56^{hi}CD16^{-}$ subset. $CD56^{hi}CD16^{-}$ NK cells are enriched in secondary lymphoid tissues and demonstrate superior production of inflammatory cytokines including IFNγ, TNFα, and GM-CSF (Cooper and Caligiuri, 2004).

NK cells direct their cytotoxic effects in two ways. Firstly, NK cells constitutively express cytotoxic granules and are capable of inducing apoptosis in target cells via a MHC-independent mechanism. Secondly, CD16 (FcγRIIIA immunoglobulin Fc receptor) expression allows NK cells to target cells to which a humoral response has been mobilized and to lyse cells through antibody-dependent cellular cytotoxicity (ADCC) (Tarkkanen *et al*., 1986). Moreover, the lysis of target cells directed by NK cell cytotoxicity could lead to cross-presentation of antigens released from target cell by a subset of DCs. This in turn could lead to activation of CD8 T cells and subsequent anti-tumour responses (Krebs *et al*., 2009). Importantly, both NK cell subsets may be recruited by chemokines to sites of inflammation following tumour formation.

Human Testis Structure and Function

The testis has two key functions: the generation of gametes (spermatozoa) and the production and controlled release of androgens, predominantly testosterone. The formation of the testis is controlled by the expression of the SRY gene, which directs the embryonic gonads into the testis development pathway by activating male-specific transcription factors. In humans, the primordial germ cells derived from pluripotent stem cells proliferate and migrate from the endoderm of the yolk sac into the undifferentiated gonad by the fourth week of gestation. Histological development of the testis is largely completed by the end of the third month of gestation (Shalet, 2009).

Histology of the Human Testis

The pubertal testis is a highly complex organ incorporating many specialised cell types including germ cells, Leydig cells and Sertoli cells. The testis is compartmentalised histologically and functionally, with androgen production and spermatogenesis being confined to separate regions. Spermatogenesis takes place in the seminiferous tubules and testosterone is synthesised by Leydig cells interspersed between the tubules. Germ cells are in intimate contact with Sertoli cells, which extend from the basal lamina toward the lumen of the tubules and constitute the main structural element of the seminiferous epithelium. They provide developmental signals and growth factors for germ cell differentiation. Surrounding the tubules are myoid peritubular cells that provide structural support and peristaltic properties to transport the immotile spermatozoa along the tubule. Tight junctions between neighbouring Sertoli cells generate the blood-testis barrier (BTB), dividing the seminiferous tubules into distinct compartments to protect the developing germ cells from the immune system. Immune cells such as macrophages, dendritic cells, mast cells, and T cells also reside in the interstitial space located between the tubules (Hedger, 1997, Rival et al., 2006). Macrophages are the largest population of immune cells located in the testis. These cells are derived from peripheral blood monocytes and migrate into the testis, where they mature (Frungieri *et al*., 2002). T cells constitute approximately 10 to 20% of the immune cells present in the human testis (Pollanen and Niemi, 1987). Natural killer cells and dendritic cells are also present within the interstitial space, but at relatively low numbers (Hedger, 2011). Testis morphology and cells likely to be involved in immune privilege is summarised in Figure 4.

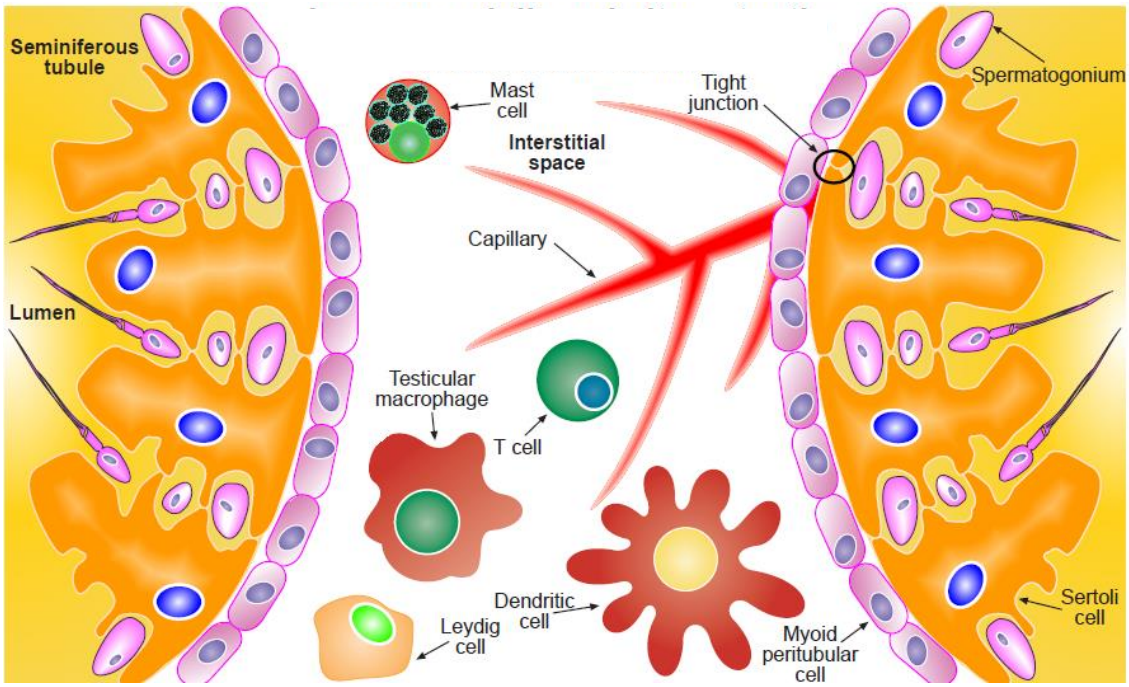

Figure 4. Morphology and immune privilege in the human testis.
Sertoli cells traverse the entire radius of the seminiferous tubules. Spermatogonia and more differentiated germ cells are in intimate contact with Sertoli cells at all stages of maturation. The myoid peritubular cells surround and protect the seminiferous tubules, and together with tight junctions between adjacent Sertoli cells form an impermeable physical barrier. This barrier forms the basis of the 'blood–testis barrier', although immune modulatory mechanisms play a fundamental part in protecting the germ cells from immune mediated damage. The interstitial space located between the tubules contains the Leydig cells and immune cells such as macrophages, dendritic cells and T cells. Since immune cells exist in such close proximity to highly antigenic germ cells, an immune response would be generated without appropriate tolerance mechanisms (Adapted from (Immunopaedia.org, 2010) with permission).

Spermatogenesis

Spermatogonial stem cells reside at the luminal side of the basal membrane, where they develop into highly specialised haploid spermatozoa by a tightly regulated process termed spermatogenesis. Spermatogenesis is a series of processes that produce an exceptionally large number of spermatozoa from a finite population of stem cells. This involves the mitotic proliferation of spermatogonial stem cells to form spermatogonia. DNA replication and differentiation of these cells generate primary spermatocytes. Two successive meiotic divisions follow to form haploid spermatids. Spermiogenesis completes the maturation process in the seminiferous tubules to produce highly differentiated spermatozoa. Sperm are then transported through the rete testis into the epididymis where they are concentrated and further matured ready for ejaculation.

Regulation of spermatogenesis is a complex interplay of endocrine and paracrine signals and involves the synthesis and release of gonadotropin releasing hormone (GnRH) from the anterior hypothalamus. In turn, GnRH stimulates the synthesis and secretion of follicle stimulating hormone (FSH) and luteinising hormone (LH) from the anterior pituitary gland. Both FSH and LH are released into circulation in bursts and act synergistically in spermatogenesis. Although the exact mechanisms are not fully understood, FSH binds to its receptor on Sertoli cells and activates several signalling pathways (Walker et al., 1995), (Sharma et al., 1994). The Sertoli cells stimulated by FSH produce a paracrine factor that prevents apoptosis of differentiated spermatogonia. The survival of these cells amplifies the basal level of germ cell production, which is maintained by testosterone secreted by Leydig cells following the binding of LH (Plant and Marshall, 2001).

Testicular Immune Privilege

During the process of spermatogenesis, a multitude of surface and intracellular proteins are expressed, which should be seen as foreign and eradicated accordingly. Surprisingly, these are tolerated by the testis and immunogenicity of these antigens is not diminished (Tung *et al*., 1981, Suescun *et al*., 1994).

Sertoli cells play a pivotal role in immunological privilege. Highly specialised tight junctions between adjacent Sertoli cells form a blood-testis barrier (BTB), which restricts and regulates the passage of large molecules through the intercellular spaces (Cheng and Mruk, 2002) (Figure 4). This process creates a unique microenvironment for the developing germ cells and ensures that the composition of the tubular fluid differs considerably from that of the interstitium (Tuck *et al*., 1970, Setchell, 1990). Importantly, mitotically active spermatogonia reside in the basal compartment that is not protected by the BTB, whilst the rest of the germ cells can be found in the immune privileged apical compartment (Rival et al., 2006). The majority of immunogenic germ cells are sequestered behind this barrier, physically protected from the immune system (Li *et al*., 2009). However, the spermatogonia lie within the non-immune privileged basal compartment suggesting that other mechanisms must be used to protect these cells from the host immune system (Yule *et al*., 1988, Saari *et al*., 1996). Moreover, the BTB is incomplete in the rete testis, a location where immense numbers of spermatozoa exist yet no immune response is provoked (Dym and Romrell, 1975, Koskimies *et al*., 1971). In addition, all cell types required to initiate an immune response are present in the interstitial space surrounding the tubules including APCs, T cells and NK cells (Hedger, 1997). Significantly, antibodies and lymphocytes specific for spermatogenic antigens can be found in the peripheral blood of fertile men

(Turek and Lipshultz, 1994). Finally, immunisation with testicular auto-antigens or passive transfer of testicular auto-antigen-specific T cells can disrupt immune privilege (Tung et al., 1987). It is therefore clear that the BTB alone cannot account for all the manifestations of testicular immune privilege.

Immune privilege is due to the failure of antigen recognition or the lack of a response following antigen exposure in the testis. MHC class I is expressed at low levels by seminiferous epithelium, which enables developing germ cells to avoid direct recognition by T cells. The immunoregulatory MHC antigen HLA-E is expressed by spermatogenic cells (Fiszer *et al*., 1997), which exerts an inhibitory effect on CD8 T cells and NK cells. Inactivation and deletion of antigen-specific T cells contributes to successful testicular immune privilege. In general terms, activated T cells can be regulated and subsequently deleted by the Fas-mediated signalling pathway (Ju *et al*., 1995). FasL is expressed by Sertoli cells and may be responsible for the death of activated CD8 T cells, thus suppressing adaptive immunity in a highly localised manner (Sanberg *et al*., 1996, Bellgrau *et al*., 1995). A protective effect of FasL has been demonstrated in studies involving melanoma cells (Hahne *et al*., 1996), and allogeneic colon carcinoma cells (Arai *et al*., 1997), however, other studies show increased FasL expression on certain tumour cell lines which in fact provoke an inflammatory response (Allison *et al*., 1997, Miwa *et al*., 1998). Testicular immune privilege is also mediated by the tryptophan-metabolising enzyme indoleamine 2,3 dioxygenase (IDO). IDO inhibits T cell mediated immunity and stimulates regulatory T cells (Fallarino *et al*., 2009).

Immune privilege is also mediated by antigen-specific control mechanisms within the testis. Injection of soluble antigens into the testis produces specific suppression of T cell responses against such antigens (Ditzian-Kadanoff, 1999, Verajankorva *et al*., 2002). In addition, activated and memory CD8 T cells directed against pancreatic islet allografts in the mouse testis are targeted for destruction when they enter the testis environment. Moreover, graft specific Treg cells are produced altering the balance between memory and regulatory T cells (Nasr et al., 2005). As summarised in (Meinhardt and Hedger, 2011), these studies indicate a switch from a response that is associated with cell-mediated immunity, to a response that is principally immunoregulatory and tolerogenic. A substantial proportion of interstitial macrophages demonstrate an immunoregulatory phenotype, characterised by an increase in suppressive functions and a reduction in pro-inflammatory cytokine secretion (Kern *et al*., 1995, Hedger, 2002).

As well as their role in the establishment of the BTB, Sertoli cells are central to testicular immune privilege in other ways. Immunoprotection of allografts and xenografts in the testis is provided by Sertoli cells (Mital *et al*., 2011). FasL, IDO and constitutively expressed TGFβ are all produced by Sertoli cells and have been implicated in graft survival (Bellgrau *et al*., 1995). In addition, Sertoli cells express inhibitors of complement (Lee *et al*., 2007), secrete inhibitors of granzyme B (Bladergroen *et al*., 2001, Sipione *et al*., 2006) and express PD-L1 (Cheng *et al*., 2009), all of which negatively regulate a cytotoxic T cell response. The production of macrophage-migration-inhibitory factor (MIF) by Leydig cells (Okuma *et al*., 2005), may also contribute to immune privilege by inhibiting the destructive potential of NK cells and cytotoxic CD8 T cells (Apte *et al*., 1998, Abe *et al*., 2001).

The roles of Sertoli cells, Leydig cells and testicular immune cells in creating immune privilege are still not fully understood. However, it is apparent that multiple factors are involved and what is most important is the balance between the suppression of an immune response to protect the spermatogenic cells from attack and the ability to initiate an immune response to protect against infection and cancer.

Testicular Germ Cell Tumours

Testicular cancer is a relatively rare cancer with an unusual age-distribution. It occurs predominantly in young and middle-aged men and is the most common cancer in men aged 15-44 years. Although the incidence of testicular cancer is low throughout the world, it is estimated to have nearly doubled in the last 40 years in the USA (McGlynn *et al*., 2003), Europe and the UK (Toledano *et al*., 2001, Swerdlow *et al*., 1998). It is evident that this increase has occurred mainly in younger men, predominantly the white Caucasian populations in industrialised countries such as Western and Northern Europe (Statistical Information Team, 2007). Notably, testicular cancer is rare in non-Caucasian populations especially in Eastern Asia and Western Africa (GLOBOCAN, 2002). Despite the significant rise in incidence, mortality from testicular cancer has fallen considerably. The decline in mortality has been noticeable since the 1970s, correlating with the introduction of better cancer management, in particular the therapeutic platinum-based chemotherapy regimens used for metastatic germ cell tumours. Unlike many other cancers, testicular cancer has a high cure rate, even in patients with metastatic disease.

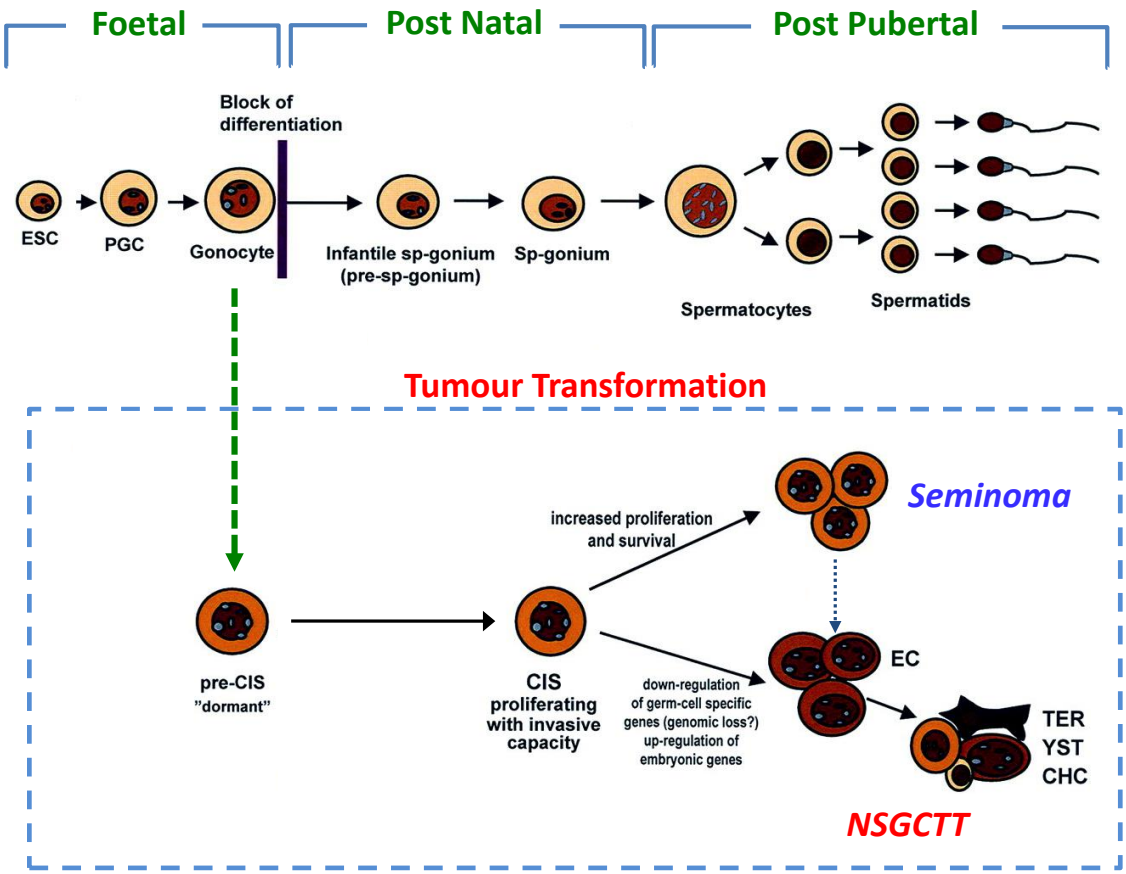

Figure 5. Development of testicular germ cell tumours from spermatogenic precursors
The process of spermatogenesis (top) and the hypothesised route to tumour transformation (bottom) are illustrated. The premalignant carcinoma in situ (CIS) is thought to develop from an undifferentiated gonocyte, but CIS does not develop into an invasive overt TGCT until after the onset of puberty. Then, CIS may transform into a seminoma or NSGCTT. Embryonal carcinoma (EC) is the most undifferentiated form of a NSGCTT. EC cells are pluripotent, and usually differentiate further into somatic tissues like teratomas (TER), and extra-embryonic tissues, like choriocarcinomas (CHC) and yolk sac tumour (YST). Sometimes, seminoma and various NSGCTT elements co-exist within the same tumour mass and are known collectively as mixed germ cell tumours (mGCT).

Risk Factors

The reasons behind the increased occurrence of testicular cancer are not fully understood but the rapid increase over a short period of time would suggest that critical changes in environmental factors are contributing to the development of these tumours. It has been postulated that increased maternal age and high oestrogen levels *in utero* may affect foetal germ cells and disrupt germinal epithelium (Richie, 2005, Group, 1994b, Group, 1994a, Coupland *et al*., 1999). A high prevalence of cryptorchidism, testicular maldescent, and infertility has been associated with an increased risk of developing testicular cancer. Other risk factors include inguinal hernias, hydrocele and a family history of testicular cancer, which suggests that defects in urological development and genetic predisposition may contribute to observed incidence (Tollerud *et al*., 1985, Rapley *et al*., 2000). A variety of genetic abnormalities have been described in testicular cancer, such as the isochromosome 12p (Oliver, 1997). Patients with Klinefelter's syndrome (47XXY) or XY dysgenesis have a higher risk of developing testicular cancer (Nichols *et al*., 1987, Levin, 2000). In addition, associations between a sedentary lifestyle or immunosuppression and testicular cancer have also been proposed, but there is no clear consensus from these studies (Leibovitch *et al*., 1996, Garner *et al*., 2003).

Pathology

Over 95% of testicular tumours originate from germ cells. Histologically, testicular germ cell tumours (TGCT) have two main subtypes - pure seminoma (45%) and non-seminomatous germ cell testicular tumours (NSGCTT) (55%). NSGCTTs may remain undifferentiated as embryonal carcinoma, or subsequently undergo extra-embryonic differentiation to form yolk sac tumours, choriocarcinomas, and mature teratomas. In

addition, NSGCTTs can include elements of seminoma to generate mixed germ cell tumours (mGCT). The tumour transformation process is summarised in Figure 5. NSGCTTs tend to occur on average ten years earlier than seminomas. It is recognised that seminomas have a indolent clinical course, whereas NSGCTTs behave more aggressively.

TGCT develop from a malignant transformation of a non-invasive lesion called carcinoma *in situ* (CIS), which is influenced by hormones at or after puberty (Rajpert-De Meyts *et al*., 1996, Rajpert-De Meyts and Skakkebaek, 1994). These lesions are found growing within seminiferous tubules and express transcription factors commonly expressed by embryonic stem cells, suggesting a pluripotent gonocyte origin. Despite a common origin, testicular cancers are histologically, pathologically and clinically distinct.

Presentation, Diagnosis and Staging

The classic presentation of a TGCT is a hard painless mass within the testis. Further diagnosis involves a testicular ultrasound and baseline measurements of tumour markers including Alpha-fetoprotein (AFP), human chorionic gonadotropin (HCG), and lactate dehydrogenase (LDH). AFP is an embryonic protein expressed by yolk sac elements of a tumour but not by pure seminoma, whereas HCG is secreted by both seminomas and non-seminomas. LDH is also a germ cell tumour product but is less tumour-specific and is generally used to monitor treatment (Andreyev *et al*., 1993, von Eyben *et al*., 2001).

Following positive diagnosis of a TGCT, a radical inguinal orchidectomy is performed. Between 5 and 10% of TGCTs are present at an extragonadal site, predominately at the retroperitoneum or mediastinum. Due to predictable patterns of lymphatic or

haematogenous spread, staging of the tumour is completed by an abdominal CT scan or chest x-ray. The tumour is assigned a stage on the basis of primary tumour size, the involvement of regional lymph nodes, the presence of distant metastases and the levels of various serum tumour markers (Fizazi *et al*., 2004).

Treatment

At University Hospital Birmingham, TGCT patients receive a stage specific treatment regime, as outlined in Figure 6. Stage 1 seminoma patients receive carboplatin monotherapy. A few patients, for whom chemotherapy is inappropriate or who decline it, may be offered radiotherapy. Stage 2A seminoma patients are treated with retroperitoneal radiotherapy or a combination of cisplatin and etoposide. Tumours categorised as Stage 2B or above are treated with four cycles of the same combination therapy. Stage 1 NSGCTT patients receive active surveillance or 2 cycles of the combination therapy bleomycin+etoposide+cisplatin (BEP). Patients receiving only surveillance have a recurrence rate of 15 – 20% but this is reduced to <2% with adjuvant chemotherapy. Stage I NSGCTT patients who exhibit lymphovascular invasion (LVI) receive two cycles of BEP. Higher stage NSGCTTs are separated into prognostic groups and treated accordingly. These patients are usually treated with 3-4 cycles of BEP chemotherapy followed by surgical resection of residual masses (Heidenreich *et al*., 2009).

The well-documented improvements in mortality from the mid-1970s appear to coincide with the introduction of cisplatin as a therapeutic agent for metastatic TGCTs. Chemotherapy regimens based on cisplatin were subsequently developed along with improvements in tumour imaging and developments in surgery for residual disease.

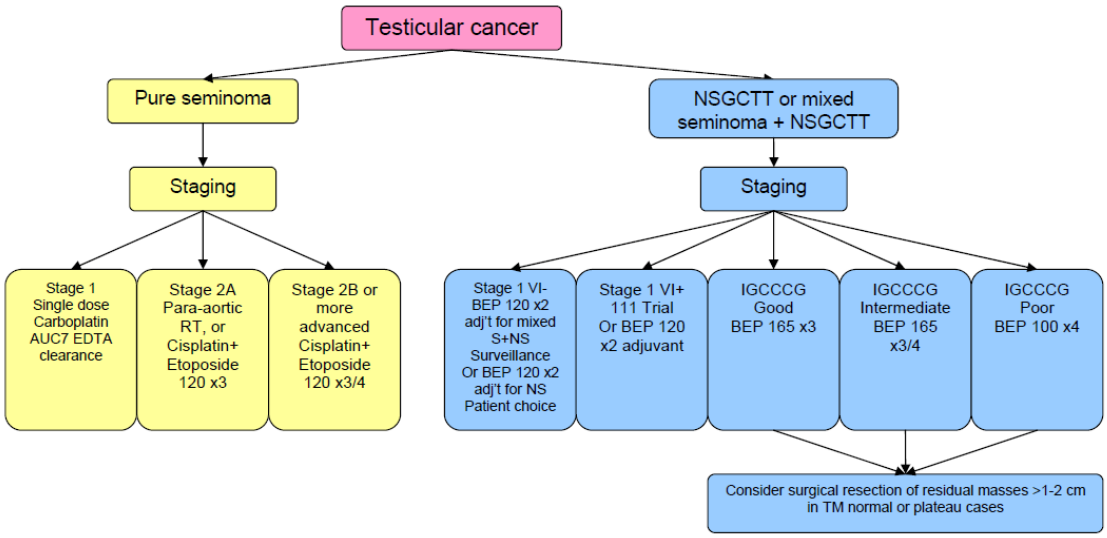

Figure 6. The stage specific treatment regimen for TGCTs at the University Hospital Birmingham Testicular Cancer Centre. Flow diagram illustrating the treatment plans according to tumour type and stage. Designed and approved by Paul Hutton, UHB, UK.

Cancer Immunology

The expression of immunogenic tumour antigens on the surface of tumour cells can mediate an adaptive immune response. Tumour growth suggests that either anti-tumour immunity is suppressed, or that it is insufficiently induced to destroy the cancer. This may be due to the inhibition of activation and differentiation, or induction of tumour-specific immune cell dysfunction, as well as the down-regulation of MHC on tumour cells.

Immune Mediated Tumour Destruction

The expression of tumour antigens on a transformed cell provokes an immune response, which generally involves the recognition and elimination of emerging tumour cells by lymphocytes (Dunn *et al*., 2002, Swann and Smyth, 2007). Many tumour antigens have been shown to induce cytotoxic T cell responses *in vitro* and *in vivo* and can be divided into several subgroups. Firstly are antigens that are products of mutated proto-oncogenes or tumour suppressor genes, such as the cell cycle regulator p53 (Goh *et al*., 2010) and caspase 8 (Mandruzzato *et al*., 1997). Secondly are atypical or over-expressed normal cellular proteins including HER-2 and AFP (Ioannides *et al*., 1993). Third are viral proteins, such as those derived from human papillomavirus, which can be processed and presented on the surface of a virus- induced cancerous cell (Ostrand-Rosenberg, 2004). Finally, cancer testis antigens (CTAgs), which are expressed exclusively in germ cells of the testis and various malignancies but are silent in normal somatic tissue (Caballero and Chen, 2009b). It is highly likely that the immunogenicity of these antigens is due to the lack of central tolerance during T cell development.

In addition, NK cells, which express NKG2D, can respond to transformed cells expressing NKG2D ligands, such as MICA/B and ULBPs (Guerra *et al*., 2008). Endogenous 'danger' signals are induced early during tumour development (Matzinger, 1994). These include DNA, heat shock proteins and IFNα, which promote the induction of adaptive anti-tumour immune responses (Gallucci and Matzinger, 2001). Furthermore, healthy, non-malignant cells surrounding the tumour are often damaged due to tumour growth and invasion, and as a result display substances such as hyaluronan fragments on their surface. This allows the recruitment of immune cells to the tumour site (Sims *et al*., 2010).

Intratumoural Immune Responses and Prognosis

Solid tumours often contain immune cell infiltrates consisting predominantly of tumour infiltrating lymphocytes (TILs). T cells are the main effector cell type of the adaptive immune response involved in the destruction of a tumour cell, in particular cytotoxic CD8 T cells. The infiltration of CD8 T cells, Th1 CD4 T cells and the presence of proinflammatory cytokines have been associated with improved prognosis (Prestwich *et al*., 2008, Ghiringhelli *et al*., 2009). The majority of tumour antigens described are restricted to presentation through MHC class I and are therefore recognised by CD8 T cells (Rosenberg, 2001). Interestingly, the distribution of CD8 T cells within particular tumour types is a determinant of prognosis in colorectal cancer, ovarian cancer, breast cancer and glioblastoma (Naito et al., 1998, Sato et al., 2005, Pages et al., 2005a, Yoshimoto et al., 1993, Palma et al., 1978). The presence of infiltrating NK cells is also associated with a favourable prognosis in several cancers (Ishigami *et al*., 2000, Takanami *et al*., 2001, Coca *et al*., 1997).

It is important to note that not all infiltrating lymphocytes have a beneficial effect on anti-tumour responses. TILs in this category would include the immunosuppressive cells types including Tregs and myeloid derived suppressor cells (MDSC) (Khaled *et al*., 2013). Tregs can be found in tumour draining lymph nodes (Munn and Mellor, 2006) as well as the tumour tissue itself (Woo *et al*., 2002), where they suppress the anti-tumour immune responses. Tregs can inhibit effective anti-tumour immunity by directly or indirectly inhibiting CD8 T cells, NK cells, NKT cells and B cells (Taams *et al*., 2001). Specifically, Tregs inhibit the proliferation of tumour-specific T cells restricting activation and subsequent effector functions of CD8 T cells (Shevach, 2002). An increased proportion of Tregs within tumours has been associated with poor prognosis in several tumours (Wolf *et al*., 2005, Petersen *et al*., 2006). The depletion of Tregs augments the effectiveness of T cell therapy (Antony and Restifo, 2005).

The important role played by the immune system in tumour development and patient prognosis is evident in immune comprised transplant patients, as these patients have an increased risk of developing certain tumours (Sheil *et al*., 1997, Birkeland *et al*., 1995).

Immunoediting Model

Despite the diverse range of immune mechanisms which target transformed cells, the high prevalence of cancer would indicate that the immune response is unable to sufficiently control its growth and spread (Dranoff, 2009). This has led to an updated hypothesis termed immunoediting, based on Burnet's immunosurveillance model, but incorporates a selection pressure in certain tumour cells, favouring escape from immune destruction (Dunn *et al*., 2002, Dunn *et al*., 2004a).

Cancer immunoediting is an extrinsic tumour suppressor mechanism that engages following cellular transformation and only when intrinsic tumour suppressor mechanisms are unsuccessful at controlling these transformed cells. The model is split into three sequential phases termed elimination, equilibrium and escape. The elimination phase focuses on the continual eradication of newly forming tumour cells that express 'danger' signals (Gallucci and Matzinger, 2001) by an anti-tumour immune response. If successful, this process leads to the complete destruction of early tumours before they are clinically apparent. Over time, a proportion of cancer cells may acquire mutations generating a cancer cell variant that is not destroyed in the elimination phase and consequently enter the equilibrium phase, in which its outgrowth is prevented by immunologic mechanisms. During the equilibrium phase, elimination of transformed cells continues and consequently results in the selection of mutated cells. If the immune system is too overwhelmed by tumour development, immunological control is lost and the balance is shifted towards tumour growth. These cells are now said to have entered the escape phase. In addition, spontaneous generation of poorly immunogenic cancer cells may enter directly into the escape phase. Tumour cells in this phase may accumulate together and cause clinically apparent disease (reviewed in (Schreiber *et al*., 2011))

Mechanisms of Tumour Escape

Cancer cells can evade the immune system using a combination of strategies. The well documented down regulation of MHC class I on tumour cells stops the cell from presenting tumour antigens and in turn reduces the ability of CD8 cytotoxic T cells recognise and lyse the cell (Bubenik, 2004). This may occur due to the downregulation or mutation of β2M, or by modifications to TAP, therefore disrupting the MHC class I

processing pathway (Benitez et al., 1998), (Bai et al., 2003). A reduction in the CD4 T cell response has also been described, which is due to the disruption in the formation and expression of MHC class II peptide complexes (Marsman *et al*., 2005). Tumour cells are able to inhibit the initiation or activation of a specific immune response. In particular, they fail to induce the maturation of DCs and in essence induce anergy in tumour specific T cells resulting in their failure to recognise the tumour as foreign (Kowalczyk, 2002). In addition, the expression of IDO by tumour cells leads to a depletion of tryptophan in the tumour microenvironment, thus inhibiting T cell proliferation (Avril *et al*., 2010). During tumour-induced angiogenesis, the disrupted interaction between lymphocytes and the tumour microvasculature has been shown to interrupt the infiltration of immune cells into the tumour (Ryschich *et al*., 2002).

The secretion of immune suppressive cytokines, such as TGFβ from tumour cells, can contribute to an immunosuppressive microenvironment and is usually associated with poor prognosis (Moses, 2010). TGFβ can modulate the activity and secretion of IFNγ by NK cells, which is required for successful clearance of tumour cells involving Th1 CD4 T cells. There are numerous additional roles for TGFβ in cancer immunosuppression that involve both innate and effector immune cells (Flavell *et al*., 2010). Importantly, TGFβ directly inhibits CTL function by suppressing the expression of several cytolytic genes, including the genes encoding IFNγ, granzyme B and FasL (Thomas and Massague, 2005). The sustained release of the anti-inflammatory cytokine IL-10 favours tumour escape from immune surveillance by stimulating cancer cell proliferation and inhibiting apoptosis (Alas *et al*., 2001, Kawamura *et al*., 2002). Ectopic expression of FasL in tumour cells is another means of immune escape since it encourages apoptosis of Fas-expressing activated

T cells that infiltrate the tumour tissue (Strand *et al*., 1996). Moreover, down regulation, genetic mutations or epigenetic gene silencing of Fas in tumour cells results in the inability of immune cells to induce apoptosis in these cells (Butler *et al*., 1998, Real *et al*., 2001). Furthermore, cytotoxic killing mechanisms can be inhibited, for example, the impaired binding of perforin to the tumour cell surface reduces the ability of granzyme B to penetrate the cell membrane (Lehmann *et al*., 2000).

Introduction to Cancer Testis Antigens

CTAg expression is limited to germ cells of the testis (Boon T, 1997) and many tumours. In particular, CTAgs are predominantly expressed by spermatogonia but are also expressed by cells in the later stages of spermatogenesis (Takahashi K, 1995, Jungbluth AA, 2002, Gjerstorff MF, 2006, Jungbluth AA, 2001, Jungbluth AA, 2000). In brief, CTAgs can be divided into two groups, those produced by genes on the X chromosome, named CT-X antigens, and those produced by genes on autosomes, termed non-CT-X antigens (Caballero and Chen, 2009a).

Importance of CTAgs in Cancer

More than 40 CTAg families have been described (Scanlan MJ, 2002, van der Bruggen P, 1991), but the biological function for many is unknown. The CTAg families with known functions are mainly the non-CT-X antigens which play important roles in spermatogenesis and cancer, including the MAGEA family. MAGEA1 is a transcriptional repressor and is thought to repress the expression of differentiation genes (Laduron *et al*., 2004). Within healthy testis it prevents differentiation of spermatogonia in order to maintain a population of cells for continuous spermatogenesis. Expression of MAGEA

family genes by tumour cells can cause resistance to TNF-mediated cytotoxicity (Park *et al*., 2002). In addition, MAGEA expression confers resistance to chemotherapy drugs including doxorubicin (Glynn *et al*., 2004). MAGEA2 suppresses the activation and function of p53, resulting in resistance to the chemotherapeutic drug etoposide (Monte *et al*., 2006). MAGEA3 is able to suppress p53-dependent apoptosis (Yang *et al*., 2007). Certain members of the GAGE family are able to suppress the apoptotic functions of Fas and IFNγ (Cilensek *et al*., 2002).

Expression Patterns of CTAgs

CTAg expression varies between different tumours. For example, melanoma appears to have the greatest frequency of expression, with lung and breast cancer also demonstrating high expression levels (reviewed in (Matthew *et al*., 2002) (Ugur *et al*., 1998)). In addition, NY-ESO-1 is very rarely found in the absence of MAGEA3 suggesting CTAgs are co-expressed and their regulation is part of a coordinated gene expression programme. Peripheral tolerance to CTAgs is not established as the germ cells of the testis are located within an immune privileged site (Bart *et al*., 2002) and do not express HLA molecules on their surface (Fiszer D, 1998). This makes CTAgs an ideal target for vaccination-based therapy which would stimulate the patient's immune system and induce an anti-tumour response.

Regulation of CTAgs

A universal mechanism for CTAg expression in germ cells and cancer is suggested by the lower levels of CpG methylated DNA within gene promoters of germ cells compared to somatic tissues (Reik *et al*., 2001) and the inclination towards genome-wide demethylation

in cancer (De Smet C, 1996). Hypomethylation of CpG islands is the most widely accepted mechanism for activation of CTAg expression in cancerous cells (reviewed in (Simpson *et al*., 2005)). Treatment with DNA methyl-transferase 1 inhibitor, 5-aza-2-deoxycytidine, leading to the progressive loss of DNA methylation, induces MAGE expression and apoptosis in cancer cells (Weiser *et al*., 2001). Histone deacetylase inhibitors, in combination with 5-aza-2-deoxycytidine, or independently, can also induce the expression of NY-ESO-1 and MAGE (Shigeki *et al*., 1996). Nevertheless, methylation states and histone deacetylation alone doesn't explain the non-coordinated pattern of CTAg expression in certain cancers (Jungbluth *et al*., 2000). It has been hypothesised that the expression of CTAgs in cancer cells results from the activation of a gametogenic differentiation program which aids the successful development of the tumour (Old, 2001).

Spontaneous Immune Responses to CTAgs

A range of immunogenic tumour antigens recognised by CD8 T cells (Boon and Old, 1997, Kawakami and Rosenberg, 1997, Robbins *et al*., 1997) or antibodies (Stockert *et al*., 1998, Scanlan *et al*., 1998) have been described. The MAGE family encode tumour–specific antigens, which have been shown to be presented by MHC class I molecules (Traversari *et al*., 1992, Van den Eynde and Boon, 1997, van der Bruggen *et al*., 1991). Furthermore, MAGEA1, MAGEA3 and NY-ESO-1 induce coordinated humoral and cell mediated immune responses (Caballero and Chen, 2009a, Marie et al., 1999, Scanlan et al., 1999).

Making the Most of a CTAg-specific Response

CTAgs are excellent targets for cancer vaccines as they are expressed in many tumour types but are absent in healthy tissue. A clinical trial which vaccinated with a known

MAGEA3 immunogenic peptide revealed tumour regression in 7 out of 25 patients even though a large CD8 T cell population was not present (Marie *et al*., 1999). Interestingly, CD8 T cells play a role in tumour regression in animal models (Coulie, 1997) and peptide based vaccination strategies have shown promise in some cancer patients (Khazaie *et al*., 2009). A vaccination approach using peptide and recombinant MAGEA3 and NY-ESO-1 has been developed for treatment of melanoma. These vaccines induce regression of individual melanoma nodules but infrequently lead to complete tumour regression (Jager *et al*., 2006, Marchand *et al*., 1999). A more recent study described synergistic effects and a beneficial clinical outcome when combining NY-ESO-1 with CTLA-4 blockade (Yuan *et al*., 2008), suggesting tumour-specific T cells are inhibited through regulatory receptors on their cell surface.

Expression of Cancer Testis Antigens in Testicular Germ Cell Tumours

The expression of MAGEB1, MAGEB2, MAGEA1, GAGE, NY-ESO-1 and/or CAGE has been described in seminoma. Interestingly, these CTAgs are not expressed in teratomatous elements and only 18% of NSGCTTs expressed one or more of these CTAgs (Yuasa *et al*., 2001). This suggests that TGCTs have different developmental pathways and may arise from different precursor cells. Previous research conducted by Hara *et al*., 1999 supports the conclusion that the expression of MAGE genes are more frequent in seminoma than in NSGCTT and suggested that seminomas share numerous traits with normal germ cells of the testis. Additional studies have confirmed protein expression of numerous MAGEA family members in seminoma (Cheville and Roche, 1999, Aubry *et al*., 2001, Nonomura *et al*., 1999). Studies using immunohistochemistry show NY-ESO-1 expression primarily in

carcinoma *in situ* and spermatocytic seminoma, but a lack of expression during tumour progression (Satie *et al*., 2002).

Role of the Immune System in Testicular Germ Cell Tumour Destruction

T cell tolerance to peptides derived from CTAg proteins is not generated in healthy individuals as these antigens do not cross the BTB and are not expressed in tissues at other sites. Therefore CTAg-specific T cell are present in the periphery which may have the ability to detect CTAg expression by tumours (Boon and van der Bruggen, 1996). To our knowledge, there are no reported studies describing in detail, the presence of CTAg-specific T cell responses in patients with testicular cancer.

As discussed previously, chemotherapy treatment results in high cure rates of TGCTs, however, some chemotherapeutic agents cause damage to the testis, most notably the BTB (Pereira and Garcia e Costa, 2007). Consequently, chemotherapy-associated damage may break down testicular immune privilege and expose remnants of CTAg expressing cells to the immune system. As a result, the immune system may encounter these antigens and subsequently prime anti-tumour immune cells which may then be involved in the elimination of residual disease post orchidectomy. In addition, the development of TGCTs may also break down testicular immune privilege (Fink *et al*., 2006), allowing the priming of cytotoxic CD8 T cells specific to antigens derived from germ cells and/or tumour cells. Taken together, it is conceivable that CTAg-specific T cells would be detectable in these patients, and may serve as a primary anti-tumour protective mechanism, or aid the destruction of residual tumour cells.

HYPOTHESIS

Chapter one of this thesis focuses on the hypothesis that T cells within testicular tumours contain clonally expanded, antigen-experienced populations. It also deals with the hypothesis that T cells and NK cells in TIL have been reversibly anergised or rendered dysfunctional within the tumour, but regain their function upon removal from this suppressive environment. The second chapter concerns the hypothesis that cell mediated immune responses are generated towards TGCTs. Specifically, CTAg expression in TGCTs provokes a T cell mediated immune response, which is detectable in peripheral blood of TGCT patients, but not in healthy controls.

AIMS

The aims of this work were:

- To investigate the memory phenotype, activation status and clonality of T cells infiltrating TGCTs, and possible regulatory mechanisms at play that may influence T cell function
- To investigate the functional capabilities of T cells that infiltrate testicular tumours following their removal from a potentially suppressive environment
- To determine whether other immune cells are present at the tumour site and how they may function
- To investigate the presence of CTAg-specific immunity in TGCT patients, and to study the kinetics of these responses following the removal of tumour burden
- To examine the functional capacity of CTAg-specific T cells isolated from peripheral blood of TGCT patients

CHAPTER 2: MATERIALS AND METHODS

Patients

Fresh human biopsies of TGCT tissue, adjacent normal testis tissue, and 50 ml heparinised blood and 6 ml clotted blood were obtained from patients undergoing radical orchidectomy at the New Queen Elizabeth Hospital, Birmingham, UK. Fresh tissue specimens were acquired immediately after surgical removal, and provided directly by the histopathology department.

Up to 30 ml heparinised blood and 6 ml clotted blood were also obtained from patients prior to adjuvant chemotherapy and at regular intervals following treatment. The follow-up samples coincide with mandatory clinic visits at the Cancer Centre, University Hospitals Birmingham, UK. Between 50-80 ml of blood was donated by healthy volunteers, which were used as controls.

Written informed patient consent and local ethical committee approval (South Birmingham research ethics committee LREC reference 09/H1207/161, study reference RRK3953) were obtained prior to sample collection. Patients were 18 years or above, and competent to give full informed consent. Patients were excluded from the study if they were known to be infected with HIV, HBV or HCV.

Patient Characteristics

Blood samples used in this study were collected from 74 TGCT patients prior to chemotherapy. Tumour tissue was collected from 10 patients, and healthy testicular tissue from 7 patients. Matched blood and tissue samples were obtained from 8 patients. Tumour type and tumour stage of samples obtained are summarised in Table 1. Blood samples from 14 healthy controls were age- and gender-matched to TGCT patients. Each patient is assigned a patient ID, consisting of a unique number and the patients initials. Further information about all patients recruited into this study including the patients' age, tumour type, staging and chemotherapy regime, can be found in the appendix Table 29.

Table 1. Summary of Blood and Tissue Samples Obtained From TGCT Patients

Tumour Type (Stage)	n	Blood		Tissue	
		PBMC	Serum	Tumour	Normal
NSGCTT	**14**	**12**	**11**	**3**	**1**
Localised	5	4	4	1	1
Metastatic	9	8	7	2*	-
Embryonal Carcinoma	**2**	**1**	**1**	**0**	**1**
mGCT	**11**	**9**	**10**	**3**	**0**
Localised	10	8	9	3	-
Metastatic	1	1	1	-	-
Seminoma	**48**	**46**	**43**	**6**	**3**
Stage I	39	37	35	6	3
Stage II-IV	9	8	8	-	-
Total	**75**	**68**	**65**	**12**	**5**

* patients with metastatic disease where primary tumour tissue was collected

Cell Culture Media and Solutions

Wash media

RPMI 1640 (Gibco BRL)

100 U/ml Penicillin (Gibco BRL)

100 μg/ml Streptomycin (Gibco BRL)

GM media

RPMI 1640 (Gibco BRL)

100 U/ml Penicillin (Gibco BRL)

100 μg/ml Streptomycin (Gibco BRL)

2mM Glutamine (Gibco BRL)

10% Foetal Calf Serum (SBS Biologicals)

TCL media

RPMI 1640 (Gibco BRL)

100 U/ml Penicillin (Gibco BRL)

100 μg/ml Streptomycin (Gibco BRL)

2 mM Glutamine (Gibco BRL)

10% Human Serum (HD Supplies)

Freezing media

Foetal Calf Serum (SBS Biologicals)

10% DMSO (Sigma)

MACS buffer (sterile filtered)

1 x PBS (University of Birmingham)

0.5% Bovine serum albumin (Sigma)

2 mM EDTA (Sigma)

TCC media

RPMI 1640 (Gibco BRL)

100 U/ml Penicillin (Gibco BRL)

100 μg/ml Streptomycin (Gibco BRL)

2 mM Glutamine (Gibco BRL)

5% Human Serum (HD Supplies)

5% Foetal Calf Serum (SBS Biologicals)

ELISA coating buffer

1 x PBS (University of Birmingham)

0.1M Na2HPO4 (Sigma)

adjust to pH 9 with 0.1 M NaH2PO4

TBE Buffer

89 nM Tris HCL

89 nM Boric Acid

3 mM EDTA

ELISA blocking buffer

1 x PBS (University of Birmingham)

1% Bovine serum albumin (Sigma)

0.05% Tween 20 (Sigma)

ELISA Wash buffer (PBS-T)

1x PBS

0.05% Tween 20

ELISA stop buffer

1M HCL

Sample Buffer (Laemmli)

0.0625M Tris-HCl pH 6.8

2%SDS,

10% glycerol,

5% 2- mercaptoethanol

1M DTT.

DMEM-C

100 U/ml Penicillin (Gibco BRL)

100 μg/ml Streptomycin (Gibco BRL)

2 mM Glutamine (Gibco BRL)

10% FCS

10 x HLA-typing PCR buffer

670 mM Tris base (pH 8.8)

166mM ammonium sulphate

1% Tween-20

HLA-typing TDMH mix

2.6 x PCR buffer

460 mM dNTPs

6.25 mM $MgCl_2$

10x gel electrophoresis loading buffer

16g sucrose,

0.25% (w/v) Bromophenol Blue

40ml dH_2O

Peptides

Single peptides were synthetic 9mer peptides generated using 9-fluorenylmethoxy-carbonyl chemistry. They were dissolved in DMSO to a final concentration of 5 mg/ml. The MAGEB1 peptide library consisted of a series of 15mer peptides, overlapping by 11 amino acids, covering the entire MAGEB1 protein sequence. The lyophilised peptides were resuspended in DMSO to a final concentration of 5 mg/ml. The MAGEA1, A3, A4 and NY-ESO-1 overlapping peptide mixes, and the CEFT peptide pool, where purchased from JPT, Germany. Each vial contained 25 μg of each overlapping peptide and was dissolved in a minimal volume of DMSO.

Isolation of TIL from Tumour Tissue

Between 4 and 10 mm^3 of tumour tissue was washed twice in RPMI media then cut with fine scissors into 1 mm^3 pieces followed by non-enzymatic disaggregation. Briefly, tissue pieces were forced through a 70 μm filter to remove tissue aggregates. The resulting single cell suspension was layered over Lymphoprep™ density gradient solution (NycoMed) and centrifuged at 800 x g for 30 minutes (brake off). The buffy layer at the density gradient interface was carefully removed and washed in RPMI media and centrifuged at 600 x g for 10 minutes. The final cell suspension contained predominantly lymphocytes, as determined by light microscopy. On average, approximately 5 x 10^3 lymphocytes were harvested from each 1 mm^3 of tumour tissue.

Isolation of PBMC from Whole Blood

PBMCs were isolated from 10 to 40 ml of heparinised venous blood under sterile conditions. Heparinised blood was mixed at a ratio of 1:1 with RPMI media and layered

over Lymphoprep™ density gradient solution (NycoMed) at a ratio of 2:1, and centrifuged at 800 x g for 30 minutes at room temperature (brake off). The PBMCs at the density gradient interface were carefully removed with a transfer pipette, transferred into fresh RPMI media, and centrifuged at 600 x g for 10 minutes. This wash step removes any residual serum proteins that were in the buffy layer. Cells were washed again in RPMI media and centrifuged at 600 x g for 10 minutes. The final wash was performed in TCL media and centrifuged at 300 x g for 10 minutes. This relatively slow spin removes contaminating platelets that may interfere with downstream assays. The number of lymphocytes was determined using a haemocytometer. Cells were used immediately for assays or cryopreserved, as described below.

Isolation of Patient Serum from Clotted Blood

Whole blood collected in vacutainers containing clotting factor were centrifuged at 800 x g for 5 minutes. The supernatant containing serum proteins devoid of blood cells and clotting factors were transferred to a 2ml cryovial. Serum was frozen at -80°C for later use.

Cryopreservation of Purified TIL and PBMC

Cell suspensions were pelleted by centrifugation at 300 x g for 10 minutes, and resuspended in ice cold Freezing media. Cells were frozen at -80°C in a Mr Frosty (Nalgene) containing isopropanol to allow cooling at a constant rate of 1°C per minute. Cells were then transferred to liquid nitrogen (-180°C) after 24 hours, for long term storage.

Thawing of Cryopreserved TIL and PBMC

Cryopreserved cells were removed from liquid nitrogen and placed in a water bath at 37°C. When completely thawed, cells were immediately transferred to pre-warmed TCL media and washed by centrifuging at 280 x g for 10 minutes before resuspension in an appropriate volume for downstream assays.

Maintenance of Healthy Donor LCLs and HT-29 Cell Line

All cells were grown in a humidified incubator at 37°C, 5% CO_2. LCLs were generated from healthy donor PBMCs. They were grown in GM media, which was replenished twice weekly. HT-29 colorectal adenocarcinoma cell lines were grown in tissue culture flasks and maintained in DMEM-C media. Cell lines were passaged when 80% confluent by removing media, washing cells with sterile PBS, and trypsinising with Trypsin- EDTA to detach adherent cells from the flask. Trypsin was neutralised with the addition of fresh DMEM-C media, centrifuged at 500 x g for 5 minutes, resuspended in an appropriate volume of DMEM-C media and transferred to a new flask.

Flow Cytometry

Flow cytometric analysis was carried out using a BD LSRII machine with BD FACS DIVA acquisition software (Version 6.1.3; BD Biosciences). Further offline analysis was performed with either FACS DIVA or FlowJo analysis software (TreeStar). The use of multi-colour flow cytometry requires compensation techniques to account for spectral overlap of fluorochromes. This was achieved by running anti mouse IgG-CompBeads (BD) stained separately with each fluorochrome conjugated antibody. The auto-compensation

function was used to effectively compensate spectral overlap. Cells were gated using FSC-H vs. FSC-A to identify single cells; single lymphocytes were then identified by their FSC-A and SSC-A properties. Dead cells were gated out using Propidium Iodide (PI). Live T cells were identified as PI^- $CD3^+$ cells. T-helper cells and T-cytotoxic cells were determined by surface expression of CD4 or CD8, respectively. Cells bearing both CD4 and CD8 were excluded. NK cells were determined by gating on $CD3^-$ $CD56^+$ cells and divided into 2 subsets by differential expression of CD56 and CD16.

Characterisation of Lymphocyte Subsets by Cell Surface Staining

PBMCs or TIL were resuspended in 100 µl MACS buffer at a final concentration of 0.5-1x10^7 cells/ml. Cells were surface stained for 20 minutes at 4°C, as previously described, with various combinations of antibodies as detailed in Table 2. Cells were washed once in MACS buffer and resuspended in an appropriate volume for cytometric analysis. At least 50,000 lymphocytes were recorded based on size and granularity using a FSC vs. SSC scatter plot.

PMA/Ionomycin Stimulation

PBMC or TIL were resuspended at a concentration of 1x10^6 /ml in TCL media. To a 96w round bottom plate, 100 µl of each cell suspension with or without 0.02 µg/ml PMA, 2 µg/ml Ionomycin was added. The cells were incubated at 37°C, 5% CO_2. After 1 hour, 100 µl of TCL media containing 10 µg/ml Brefeldin-A, and 1.25 µg/ml Monensin was added to each well. Cells were incubated for a further 5 hours at 37°C, 5% CO_2. Cells were subsequently washed ready for intracellular cytokine staining.

Table 2. Anti-human antibodies to cell surface markers used for cell phenotyping

Target Antigen	Conjugate	Stock	Dilution	Clone	Source
CD3ε	APC-Cy7	50μg/ml	1:20	HIT3a	Biolegend
CD4	PerCP-Cy5.5	200μg/ml	1:50	FU50	Biolegend
CD8α	AmCyan	0.1mg/ml	1:20	SK1	BD
CD56	PE-Cy7	50μg/ml	1:30	1:HOD56	Biolegend
CD16	PE	0.1mg/ml	1:30	B73.1	eBioscience
CD45RA	eFluor-450	0.1mg/ml	1:20	HI100	eBioscience
CCR7	PE	25μg/ml	1:20	3D12	eBioscience
TIM-3	PE	25μg/ml	1:20	F38 2E2	eBioscience
PD-1	PerCP-efluor710	25μg/ml	1:20	MIH4	eBioscience
CD107a	FITC	0.1mg/ml	1:50	H4A3	BD
CD161	eFluor-488	50μg/ml	1:20	HP-3G10	eBioscience
NKG2D	APC	0.1mg/ml	1:20	D11	eBioscience
γδTCR	FITC	0.8mg/ml	1:20	B1.1	eBioscience
CD4	FITC	-	1:20	VIT4	Miltenyi
CD69	Alexa-fluor-647	0.4mg/ml	1:20	FN20	Biolegend
CD38	PE-Cy7	0.3mg/ml	1:20	HIT-2	eBioscience

Intracellular Cytokine Staining

Cells were then washed in MACS buffer and stained with appropriate surface antibodies at 4°C for 20 minutes. Cells were then washed in PBS and fixed with 2% paraformaldehyde at room temperature for 10 minutes. Cells were washed with MACS buffer, resuspended in the residual volume and permeabilised with 0.5% saponin at room temperature for 10 minutes. In the presence of 0.5% saponin, intracellular cytokine staining was subsequently conducted with IFNγ-AF700 and TNFα-PE-Cy7 for 30 minutes at room temperature. Cells were washed 2x in MACS buffer and resuspended in an appropriate volume for flow cytometric analysis.

Combined Intracellular Cytokine and CD107a Staining of Peptide-Stimulated PBMC

Multiparameter flow cytometry was used to simultaneously examine CD4 and CD8 T cells for intracellular expression of IFNγ and TNFα, and degranulation (CD107a surface expression) following stimulation with peptide. Cells were stimulated with either 10 μg/ml single peptide or 40 ng/ml overlapping peptides. PBMCs were resuspended at a concentration of $1x10^6$ /ml in TCL media. To a 96w round bottom plate, 100 μl of each cell suspension containing peptide(s) and 20 ng/ml CD107a-FITC (stimulated) or 20 ng/ml CD107a-FITC antibody only (unstimulated), was added. The cells were incubated at 37°C, 5% CO_2. After 1 hour, 100 μl of TCL media containing 10 μg/ml Brefeldin-A, and 1.25 μg/ml Monensin was added to each well. Cells were incubated for a further 5 hours at 37°C, 5% CO_2. Cells were then washed in MACS buffer and stained with CD3-APC-Cy7, CD4-PerCP-Cy5.5 and CD8-AmCyan at 4°C for 20 minutes. Cells were then washed in PBS and intracellular cytokine stained, as previously described.

Celltrace™ Violet Labelling of TIL

TIL and PBMCs were resuspended at a concentration of $1x10^6$ cells/ml in PBS. A 5 mM Celltrace™ Violet dye stock solution was prepared following the manufacturers guidelines. Briefly, 20 µl of DMSO was added to one vial of Celltrace™ Violet reagent and mixed well by vortexing. The reconstituted Celltrace™ Violet was added to the cell suspension at a final concentration of 5 µM and incubated for 20 minutes at 37°C, 5% CO_2, with occasional agitation. Five times the original staining volume of TCL media was added to the cells and incubated for 10 minutes at 37°C to sequester any unbound dye remaining in solution. Cells were pelleted by centrifugation at 600 x g for 10 minutes then resuspended in pre-warmed TCL media at a concentration of $1x10^6$ cells/ml. Cells were incubated for a further 15 minutes to allow acetate hydrolysis of Celltrace™ Violet molecules.

CD3/CD28 Dynabeads® Proliferation Assay of TIL

Following Celltrace™ Violet labelling of TIL, cells were incubated at a 1:1 ratio with Dynabeads® Human T-Activator CD3/CD28 beads (Invitrogen), in the absence of protein transport inhibitors, for 4-5 days at 37°C, 5% CO_2. Beads were subsequently removed from the cell suspension by transferring cells to a 15ml Falcon tube and placing them in the EasySep® magnet for 5 minutes. Cells were decanted, washed in MACS buffer and centrifuged at 600 x g for 10 minutes. Cell pellets were resuspended in residual volume and stained with CD3-APC-Cy7, CD4-PerCP-Cy5.5 and CD8-AmCyan at 4°C for 20 minutes. Cells were washed twice in MACS buffer and resuspended in an appropriate volume for flow cytometric analysis.

Generation of T cell Lines

A panel of 8 peptides (Generon) from 5 CTAg gene families was chosen on the basis of having been previously identified as CD8 T cell epitopes that cover the most common HLA types, and HLA-peptide dextramers were available. The peptides, gene derivation, and MHC Class I restriction are detailed in Table 3. Freshly isolated PBMC were resuspended in 500 μl of Wash media. If using cryopreserved PBMC, cells were thawed as previously described, resuspended at $1x10^6$ /ml in TCL media and rested overnight in a 48 well tissue culture plate ($1x10^6$ cells/well). The following morning, cells were washed in Wash media to remove serum proteins and resuspended in 500 μl Wash media. Peptides were added either individually or in pools at a final concentration of 10 μg/ml. Cells were incubated at 37°C, 5% CO_2 for 1 hour, with occasional agitation. Following peptide loading, cells were washed in TCL media and resuspended in 500 μl TCL media containing 25 ng/ml IL-7 (Peprotech) and 2 ng/ml IL-15 (Peprotech). Each 500 μl cell suspension was transferred to one well of a 48 well cell culture plate and incubated at 37°C, 5% CO_2. A further 500 μl of TCL media supplemented with 50 U/ml IL-2 (Peprotech) was added on day 3. Cell cultures were fed twice weekly with TCL media containing 50 U/ml IL-2, following the removal of half the spent media. A proportion of cells were subsequently harvested 10-12 days later for dextramer analysis. If peptide stimulated cells contained a dextramer positive population, these cells were set up for limiting dilution T cell cloning.

Table 3. Detailed list of peptides used in T Cell Line assays.

Gene product	HLA restriction	HLA frequency(#) (%)	Peptide (aa Sequence)	Position
NY-ESO-1	A2	42.6	MLMAQEALAFL	1-11
MAGEA1	A2	42.6	KVLEYVIKV	278-286
	B7	21.4	RVRFFFPSL	289-298
MAGEA2	A2	42.6	YLQLVFGIEV	157-166
MAGEA3	A1	29.1	EVDPIGHLY	168-176
	A2	42.6	KVAELVHFL	112-120
MAGEA4	A2	42.6	GVYDGREHTV	230-239

(#) HLA prevalence in England was determined using **www.allelefrequencies.net**, as described in (Gonzalez-Galarza et al., 2011)

HLA-Peptide Dextramer Staining

Following peptide stimulation of T cell cultures, cells were washed in MACS buffer and stained with pMHC complexes (Dextramers; Immudex) at room temperature for 20 minutes. Cells were washed in MACS buffer before antibody staining of surface markers. A negative HLA-matched dextramer was used that contained an irrelevant peptide. Cells that stained positive with this dextramer were classified as background and were subtracted from the CTAg-specific T cell frequency. This enabled us to determine a more accurate final frequency of a particular CTAg-specific T cell population. A result was only considered positive if a dextramer positive population was greater than 0.1% of the total frequency of CD8 T cells.

Enrichment of Dextramer Positive CD8 T Cells

Dextramer positive CD8 T cells were obtained by positive selection using MACS technology (Miltenyi Biotec) under sterile conditions. Antigen specific T cells were enriched using a manual magnetic cell sorting method using anti-PE magnetic beads and QuadroMACS (midi) separator. Anti-PE magnetic beads bind to PE-conjugated dextramers and enable high purity enrichment through MS columns. Cells were washed in MACS buffer and stained with dextramers as previously described. Cells are resuspended in 90 μl of MACS buffer and 10 μl of anti-PE beads was added. Cells were incubated for 30 minutes at 4°C with occasional agitation. Following incubation, cells were washed to remove unbound beads and passed through 2 pre-equilibrated MS columns (double sort). Dextramer positive cells bind to the column and are eluted with MACS buffer. Enriched dextramers positive cells were pelleted by centrifugation at 300 x g for 10 minutes. Cells were resuspended in either MACS buffer for flow cytometric analysis to determine purity

of sort, or TCL media for limiting dilution cloning. The post purification flow cytometric analysis was used to determine dilutions required for cloning by limiting dilutions. Negative fractions were also collected and used as autologous feeder cells, as required.

T Cell Cloning by Limiting Dilution

CTAg-specific T cells were cloned using this method to enable further characterisation of their function. Feeder cells are required to provide stimulatory signals and growth factors that support the clonal expansion of isolated T cells. If autologous PBMCs (or negative fraction of MACS sort) were unavailable or insufficient, allogeneic PBMCs from 3 apheresis "cones" (National Blood Service) were used as feeder cells. To generate feeder cells, PBMCs were stimulated overnight at 37°C, 5% CO_2 in TCC media containing 5 μg/ml PHA. The following morning, cells were washed thoroughly in TCC media before irradiation (40Gy). HLA-matched LCLs were also used and loaded with 10 μg/ml relevant peptide prior to irradiation. The irradiated feeder cells were washed 3 times in TCC media and resuspended at $1x10^6$/ml PBMC and $1x10^5$/ml LCL. The mixture was supplemented with 20 U/ml IL- 2; 10 ng/ml IL-7; 8 ng/ml of both IL-15 and IL-21. To this cloning mix, T cells to be cloned were added to give concentrations of 0.3 cells, 1 cell and 3 cells per 100 μl/well. The resulting mixes were added to 96 well round bottom tissue culture plates and incubated at 37°C, 5% CO_2. On day 3, 100 μl of TCC media supplemented with 25 U/ml IL-2 was added to each well. Between days 14 and 28, the plates were monitored for clonal expansion. If enlargement of cell pellet was observed, the entire contents of that well were resuspended in 500 μl TCC media containing fresh feeder cells and cytokines. The cell suspension was subsequently transferred to a well of a 48 well tissue culture plate. Cells were replenished with fresh TCC media containing 50 U/ml IL-2 twice weekly. If required,

cells were given irradiated feeder cells at the same cell concentrations as the original cloning procedure. Clones were screened by dextramer staining prior to further characterisation. If cells were dextramer positive, functional analysis was determined at least 7 days after the most recent addition of feeder cells.

Stimulation Assay for IFNγ ELISA

This assay was used to test the specificity and avidity of T cells through their ability to secrete IFNγ when co-cultured with antigen specific targets. Antigen specificity was confirmed with a range of targets consisting of peptide loaded LCLs and HT-29 colorectal adenocarcinoma cell line (endogenously presented MAGEA3 through HLA-A1). In addition, LCLs loaded with irrelevant peptide, HLA-mismatched LCLs loaded with test peptide, LCLs alone and T cells alone, were also used as controls. LCLs and T cells were washed twice in TCL media to remove any residual IFNγ present in tissue culture supernatant. LCLs were resuspended in TCL media at a concentration of $3x10^5$ cells/ml; T cells were resuspended at $3x10^4$ cells/ml in TCL media supplemented with 50 U/ml IL-2. T cells were seeded in triplicate in 96 well round bottom plates at a density of $3x10^3$ per well. Targets were peptide loaded as required. For a peptide titration assay to determine the avidity of a T cell response, LCLs were loaded with 10 fold dilutions ranging from 10^{-5} to 10^{-12} M peptide. Target cells were added to T cells at an Effector:Target (E:T) ratio of 1 to 10. To determine the ability of T cells to respond to endogenously presented antigen, HT-29 cells were added instead of peptide loaded LCLs at various E:T ratios. The plates were centrifuged at 300 x g for 5 minutes to enhance cell-to-cell contact, and then incubated at 37°C, 5% CO_2 overnight. The following morning, plates were centrifuged at 600 x g for 5

minutes and 150 μl of supernatant was harvested. The cell culture supernatants were either assayed immediately or frozen at -80°C prior to IFNγ ELISA.

IFNγ ELISA

A Maxisorp™ plate (Nunc) was coated with 0.75 μg/ml anti-human IFNγ antibody (Pharmingen) in 50 μl/well Coating Buffer. The plate was sealed and incubated overnight at 4°C. The plates were washed 5 times with 200 μl PBS-T buffer, blotted, and then 200 μl of ELISA Blocking Solution was added to each well. The plates were incubated for 2 hours at room temperature. The plates were then washed 3 times in PBS-T and 50 μl test supernatants, as well as standards (2000 pg/ml to 15 pg/ml IFNγ in doubling dilutions) were added. The plate was washed 5 times as before then 50 μl/well of 0.75 μg/ml biotinylated anti-human IFNγ antibody (Pharmingen) was added. The plate was incubated for 1 hour at room temperature. The plate was washed 5 times then 50 μl/well of 1:1000 streptavidin-HRP (MabTech) was added, and incubated for 45 minutes at room temperature. The plate was washed extensively before 100 μl/well of TMB substrate (Tebu Bio) was added. The plate was left in the dark at room temperature for up to 20 minutes. The reaction was stopped by the addition of 100 μl 1M HCl and the plate was read at an absorbance wavelength at 450nm. IFNγ levels of supernatants were calculated by reference to the standard curve.

NK Cell Purification

To examine the function of infiltrating NK cells, they were first purified using MACS technology, in sterile conditions. When TIL numbers were available, the cells were washed in MACS buffer and stained with anti-CD56-PE. Cells were washed in MACS buffer,

stained with anti-PE microbeads and positively selected using MS columns, as previously described. Following enrichment, cells were resuspended at $1x10^5$/ml in TCL media containing 50 U/ml IL-2 and rested in a well of a 96 well tissue culture plate for up to 48 hours at 37°C, 5% CO_2. Following incubation, NK cells were used in the NK cell cytotoxicity assay, as described below.

NK Cell Cytotoxicity Assay (CD107a Mobilisation Assay)

To determine NK cell cytolytic potential, rested NK cells were plated into a 96 well round-bottom tissue culture plate, at a final concentration of $1x10^5$cells/ml of TCL media containing 20 U/ml IL-2. K562 or Daudi cells were subsequently added to each well at a concentration of $1x10^5$cells /ml in TCL media containing 20ng/ml CD107a-FITC, to give a E:T ratio of 1:1. When cells were required at varying E:T ratios (range 10:1 to 1:10), NK cells were diluted accordingly. Cell-to-cell contact was improved by centrifuging the plate at 200 x g for 4 minutes. Cells were incubated at 37°C, 5% CO_2. After 1 hour, Brefeldin-A and Monensin were added at a final concentration of 10 μg/ml and 1.25 μg/ml, respectively. Following a further 5 hour incubation, cells were washed and surface stained with CD3-APC-Cy7, CD56-PE-Cy7 and CD16-PE. Where appropriate, cells were fixed and permeabilised, and stained for intracellular cytokines as previously described. Cells were subsequently analysed for CD107a levels and cytokine secretion by flow cytometry. NK cells cultured with TCL media alone (containing CD107a-FITC and protein transport inhibitors) were considered background and the value subtracted from each test sample.

Simultaneous Extraction of RNA and Protein from Human Tumour Tissue

RNA isolation

RNA and protein were isolated for semi-quantitative reverse transcription-polymerase chain reaction (RT-PCR) and Western blot analysis, respectively. RNA and Protein were simultaneously extracted using a phenol-chloroform method. Following precipitation, total RNA was purified further using an RNeasy Lipid Tissue Mini Kit (Qiagen). Between 30 and 50 mg of snap-frozen tissue was placed in a tube containing 1 ml of QIAzol Lysis Reagent. The tip of a homogeniser probe was submerged into the tube and homogenised on ice for 1 minute on setting 5. Next, the homogenate was left to stand for 3 minutes at room temperature to allow foaming to subside. To ensure complete dissociation of nucleoprotein complexes, the suspension was incubated for a further 5 minutes at room temperature. To the homogenate, 200 μl of chloroform was added and shaken vigorously for 20 seconds. To allow phase separation to occur, the sample was incubated for 10 minutes at room temperature before centrifuging at 12,000 x g for 15 minutes at 4°C.

Following centrifugation, the sample separates into 3 distinct phases: an upper aqueous phase containing RNA; an interphase; and a lower organic phase containing protein. The upper aqueous phase was transferred to an RNase-free tube and 1 volume of 70% ethanol was added, mixed thoroughly by vortexing, transferred to an RNeasy Mini spin column and centrifuged at 10,000 x g for 20 seconds. The organic phase containing protein was transferred to an eppendorf and placed on ice while the RNA purification procedure was completed. The RNA, now bound to the membrane of the RNeasy column was washed with Buffer RW1, followed by 2 washes with Buffer RPE. The RNA was then eluted from the membrane with 50 μl of RNase-free water, and frozen at -80°C or used immediately for

generation of cDNA. RNA concentration was measured with a Nano-Drop 3300 (Thermo Scientific). Pure RNA samples would have an A260/A280 ratio of 2.0, and samples were rejected if a value of 1.7 or below were obtained, indicating unacceptable levels of contamination. For all reactions, 1 μg of RNA was prepared for reverse transcription by dilution with sterile DEPC-treated water.

Protein Isolation

Protein, contained within the organic fraction, was precipitated using alcohol precipitation. Firstly, DNA contamination was removed by the addition of 0.3ml of 100% ethanol per 1 ml QIAzol Lysis Reagent used. The tube was inverted 10 times, until a homogenous solution was achieved, before being incubated at room temperature for 5 minutes. The solution was subsequently centrifuged at 2000 x g to pellet the DNA. The supernatant was further precipitated to isolate protein immediately, or stored at -80°C for later purification. Briefly, 1.5 ml of acetone was added per 1 ml QIAzol Lysis Reagent used for the initial homogenation. The sample was incubated for 10 minutes on ice before being centrifuged at 12,000 x g for 10 minutes at room temperature. Following centrifugation, the supernatant was discarded and the pellet, containing the protein, was washed 3 times in 95% ethanol containing 0.3 M guanidine hydrochloride. During each wash, the solution was incubated for 20 minutes at room temperature before being centrifuged at 8000 x g for 5 minutes at 4°C. After the third wash, the pellet was resuspended in 100% ethanol, incubated for 20 minutes at room temperature, and centrifuged at 10,000 x g at 4°C. The supernatant was removed and the protein pellet was air dried for 10 minutes before being resuspended in PBS containing 1% SDS. To aid pellet dissolution, the sample was

incubated at 50°C for 10 minutes. Following complete resuspension, protein concentration was determined using the BCA assay or stored at -80°C for downstream applications.

Protein Concentration Determination by BCA Assay

Protein levels in healthy testis and TGCT lysates were quantified using BCA assay as described in the manufacturers protocol (Pierce). Bovine serum albumin (BSA) standards were prepared from a 2 mg/ml stock solution and ranged from 0 to 2000 μg/ml. Twenty five μl of each sample/standard and 200 μl of Working Reagent (50:1, Reagent A:B) was added to a 96 microplate well and mixed well on a plate shaker for 30 seconds. The plate was sealed and incubated for 30 minutes at 37°C. The plate was subsequently cooled to RT then absorbance was measured at 550nm. A standard curve was generated using the known standards and the equation of the line (linear) was used to determine the relative concentrations of each samples.

Sample Preparation for SDS-Polyacrylamide Gel Electrophoresis (SDS-PAGE)

Protein samples were denatured in Sample Buffer and boiled at 100°C for 5 minutes. Tubes were placed on ice for 3 minutes before being centrifuged at 10,000 x g for 5 minutes to remove insoluble material. Following centrifugation, tubes were left on ice until ready to load on gel.

SDS-PAGE Gel Preparation and Running

Protein samples were separated on homemade SDS-polyacrylamide gels assembled using Atto apparatus according to manufacturer's instructions. Separating gels were made containing 100mM Tris-HCl, 0.1% SDS, and 0.01% TEMED which were diluted with H_2O

to give a 15% acrylamide gel, as outlined in Table 4. Immediately before casting, a final concentration of 0.02% APS was added to initiate acrylamide polymerisation. The gel was poured and allowed to set at room temperature for 10 minutes. Isopropanol was layered on top of the separating gel to warrant level setting and to prevent the gel from drying out. The isopropanol was removed, stacking gel was poured above the separating gel and comb inserted. The gel was set following 15 minute incubation at room temperature. SDS-PAGE running buffer was prepared as detailed in Table 5, and added to the upper and lower gel-tank reservoirs.

The denatured samples (up to 50 μg) were then loaded into each lane. A pre-stained, broad range molecular marker (NEB) was run simultaneously to allow determination of protein separation and molecular weight estimation. The gel was run at 100V through the Stacking gel then increased to 200V through the separating gel. The gel was run for 2 hours or until the dye front (bromophenol blue) had migrated to the bottom of the gel.

Table 4. Separating and Stacking gel recipes.

Separating gel components (15%)	**Volume**	**Stacking gel components**	**Volume**
30 % Acrylamide	3.75 ml	30 % Acrylamide	1.0 ml
H20	1.34 ml	H20	4.5 ml
1M Tris Buffer pH 8.8	1.88 ml	1M Tris Buffer pH 6.8	1.9 ml
SDS 10% (w/v)	100 μl	SDS 10 % (w/v)	100 μl
APS 10% (w/v)	100 μl	APS 10 % (w/v)	100 μl
TEMED	5μl	TEMED	7.5 μl
Total Volume	7.2 ml	Total Volume	7.61 ml

Table 5. SDS page Running buffer and Transfer buffer recipes.

Running buffer (1x)		Transfer Buffer (1x)	
Tris Base	1.5 g	Tris Base	3.0 g
Glycine	7 g	Glycine	14.4 g
SDS	0.5 g	SDS	0.1 g
		Methanol	200 ml
Water	Up to 500ml	Water	800 ml
Total Volume	500 ml	Total Volume	1000 ml

Western Blot Analysis

Following electrophoresis, Western blotting was conducted by wet transfer electroblotting. SDS-PAGE resolved proteins were transferred to 0.45 μm nitrocellulose membrane. Briefly, gels, membrane, sponges and 3mm blotting filter paper were equilibrating in Transfer buffer. A single gel was laid onto a pre-cut nitrocellulose membrane, sandwiched between 4 pieces of 3 mm blotting paper and two blotting sponge pads, and placed in a transfer cassette (Bio-Rad). The assembled cassettes were inserted into a transfer tank filled with Transfer buffer. Proteins were transferred to the membrane overnight at 4°C at a constant 30V. Following transfer, the blots were stained with Ponceau S to allow visual inspection of protein transfer. Ponceau S was easily removed from the membrane by 3 washes in PBS-T, with constant agitation.

Table 6. Antibodies used for western blot analysis.

Target Antigen	Host	Isotype	Stock	Dilution	Clone	Source	Secondary Antibody	Stock	Dilution	Source
GAPDH	Rabbit	IgG	200μg/ml	1:3000	Polyclonal	SCBT	Anti-rabbit HRP	1mg/ml	1:1000	Invitrogen
MAGEA1	Mouse	IgG1	200μg/ml	1:200	MA454	Thermo	Anti-mouse HRP	1mg/ml	1:5000	Promega
MAGEA3	Mouse	IgG1	200μg/ml	1:2000	1H1	Abcam	Anti-mouse HRP	1mg/ml	1:5000	Promega
MAGEA4	Rabbit	IgG	1mg/ml	1:1000	Polyclonal	Sigma	Anti-rabbit HRP	1mg/ml	1:1000	Invitrogen
PD-L2	Goat	IgG	500μg/ml	1:200	Polyclonal	R&D	Anti-goat HRP	1mg/ml	1:1000	Invitrogen
MICA/B	Goat	IgG	200μg/ml	1:1000	Polyclonal	SCBT	Anti-goat HRP	1mg/ml	1:1000	Invitrogen
ULBP2	Mouse	IgG2a	1mg/ml	1:200	MM0593-7F33	Abcam	Anti-mouse HRP	1mg/ml	1:5000	Promega

Prior to detection, membranes were incubated with blocking solution (PBS containing 3% BSA and 0.05% Tween-20) for 1 hour to prevent primary antibodies binding non-specifically. The membranes were washed in PBS-T for 5 minutes at room temperature before being probed overnight at 4°C with primary antibody (prepared in blocking solution). Post incubation, blots were subjected to 3 x 10 minute washes in PBS-T. Secondary horseradish peroxidase (HRP) conjugated antibodies were prepared in blocking solution and incubated with the membranes for 1-2 hours at room temperature. The blot was subsequently washed as described before. Primary and secondary antibody combinations are detailed in Table 6. Residual wash buffer was removed from the blot and a chemiluminescence substrate (ECL-Plus) was applied directly to the membrane for 2 minutes. Proteins were visualised on the ChemiDoc system (Bio-Rad) using GeneTools software. Equal loading of samples was confirmed by blotting for GAPDH. Densitometry was performed using GeneTools software.

Re-Probing of Western Blots

To probe for different proteins using the same blot, the membranes were stripped using Restore™ Western Blot Stripping Buffer (Pierce) for 15 minutes at room temperature, with constant agitation. The membranes were washed 3 times in PBS-T before incubation in blocking solution. The membranes were then ready for re-probing.

Reverse Transcription of RNA

QuantiTect reverse transcription kit (Qiagen) was used to reverse transcribe RNA to cDNA. Template RNA and kit components were thawed on ice, mixed by flicking the tubes and centrifuged briefly to collect residual liquid from the sides of the tubes. The

genomic DNA elimination reaction was prepared by mixing 2 µl gDNA Wipeout Buffer, 1 µg template RNA, and topped up with RNase-free water to a total volume of 14 µl. The solution was incubated at 42°C for 5 minutes, and then placed immediately on ice. In a separate tube, the reverse-transcription master mix was prepared by combining 1 µl Quantiscript Reverse Transcriptase, 4 µl Quantiscript RT Buffer, and 1 µl RT Primer Mix. The mixture was vortexed briefly and stored on ice. The entire genomic DNA elimination reaction (14 µl) was added to the reverse-transcription master mix, and mixed by gentle pipetting. The reaction mixture was subsequently incubated at 42°C for 15 minutes for reverse transcription to occur, followed by 95°C for 3 minutes to inactivate the reverse transcriptase enzyme. The newly generated cDNA was used immediately for qRT-PCR reaction or stored at -20°C for later use.

Quantitative Real Time Polymerase Chain Reaction (qRT-PCR)

All qRT-PCR reactions were performed on an Applied Biosystems 7500 real-time PCR system using Sybr Green technology and QuantiTect Primer Assays (Qiagen). QuantiTect primers contain a mixture of forward and reverse primers at equal proportions, and are outlined in Table 7. The QuantiTect primers were reconstituted in 1.1 ml TE buffer, pH 8.0, and mixed by vortexing the tube 5 times, to give a 10x primer mix. For a single reaction of a gene of interest, 12.5 µl of 2x QuantiTect SYBR Green PCR Master Mix, 2.5 µl of appropriate QuantiTect Primers, and RNase-free water up to 20 µl, were combined in a microcentrifuge tube. The reaction mixture was gently vortexed and dispensed into PCR plates. To each well 100ng of appropriate template cDNA (5 µl of 20 ng/µl) was added, mixed by pipetting, and the plate was sealed and centrifuged at 300 x g for 3 minutes. The

plate was placed in the qRT-PCR machine and run with the following conditions: An initial PCR activation step for 15 minutes at 95°C, followed by 40 cycles of 30 seconds at 94°C (denaturation), 30 seconds at 55°C (annealing), and 30 seconds at 72°C (extension). A melt curve analysis step was added at the end of the PCR run to verify the specificity of PCR products. A housekeeping gene (GAPDH) was always run alongside the genes of interest. Each sample was run in triplicate. The $2^{-\Delta\Delta Ct}$ method was used to compare expression levels between tumour tissue and healthy testis tissue, and normalised to GAPDH. Fluorescence below the threshold after 40 cycles was classified as a negative result.

DNA Extraction from Whole Blood

DNA extraction from whole blood was carried out using the Qiagen DNeasy Blood and Tissue Kit. Briefly, 20 µl proteinase K was pipetted into a 1.5 ml microcentrifuge tube. Between 50 and 100 µl anticoagulant-treated blood was added to the tube and adjusted to 220 µl with PBS. The suspension was mixed before adding 200 µl Buffer AL and vortexing. The suspension was incubated at 56°C for 10 minutes, and 200 µl absolute ethanol was added, mixed by vortexing briefly and pipetted into a DNeasy Mini spin column placed in a 2 ml collection tube. The tube was centrifuged at 6000 x g for 1 minute, and the flow-through and collection tube was discarded. The spin column was placed in a new 2 ml collection tube and 500 µl Buffer AW1 was added, centrifuged for 1 minute at 6000 x *g*, and flow-through and collection tube were discarded. The spin column was placed in a new 2 ml collection tube and 500 µl Buffer AW2 was added, centrifuged for 3 minutes at 20000 x g, and flow-through and collection tube were discarded. The spin column was transferred to a new 1.5 ml microcentrifuge tube, and DNA was eluted by adding 50 µl

Buffer AE to the centre of the spin column membrane. The spin column was incubated for 1 minute at RT, and then centrifuged for 1 minute at 6000 x g. The eluted DNA was used immediately for HLA-typing PCR or frozen at -20°C for long-term storage.

HLA Typing by Endpoint PCR

To verify HLA-type of patients with a positive dextramer response, patient and control DNA samples were used to identify those expressing HLA A1, A2 and B7, as previously described (Bunce *et al*., 1995). A PCR master mix containing 70.87 µl TDMH, 35 µl nuclease-free water, 2 µM of each adenomatous polyposis coli control primers and 3.75 units of Taq polymerase (Bioline) was prepared in a small eppendorf. For a no DNA control tube, 8.5 µl of master mix was removed. One hundred ng of DNA/ reaction (1.5 µg) was then added to the master mix, and was aliquoted into 0.2 ml domed PCR tubes that contained various primer combinations for each HLA type to be tested, as per Table 8. PCR was carried out using the following conditions: 60 seconds (96°C), 5 cycles of 25 seconds (95°C), 45 seconds (70°C), 45 seconds (72°C) followed by 21 cycles of 25 seconds (95°C), 50 seconds (65°C), 45 seconds (72°C) followed by 4 cycles of 25 seconds (96°C), 60 seconds (55°C) and 120 seconds (72°C), then 72°C for 10 minutes. At the end of the run, samples were held at 4°C before being run on an agarose gel.

Agarose Gel Electrophoresis for HLA Typing PCR

Agarose gels were made by adding 1% (w/v) agarose powder to 1xTBE buffer and heating in a microwave to dissolve the agarose. Agarose was cooled to 55°C before the addition of a final concentration of ~0.5 µg/ml ethidium bromide solution. The gel was then poured with an appropriate toothed comb. A 10x loading buffer was added to all samples before

loading into appropriate lanes in the gel. Agarose gels were immersed in 1xTBE buffer before samples were loaded and gels ran at 120V for approximately 55 minutes. The size of DNA fragments were assessed by comparing their migration to a 100 base pair DNA marker ladder (Invitrogen). Gels were examined and recorded using an ultraviolet transilluminator.

Table 7. Primers used in qRT-PCR assay to determine expression levels of genes in TGCT and healthy testis tissue.

Gene	Qiagen Primer Reference	Amplicon Size
MAGEA1	QT01669430	109bp
MAGEA3	QT00064799	106bp
MAGEA4	QT00008862	118bp
NY-ESO-1	QT00088956	140bp
MAGEB1	QT00012362	126bp
PD-L1	QT00082775	72bp
PD-L2	QT00089761	127bp
ULBP1	QT00084532	108bp
ULBP2	QT01026291	80bp
ULBP3	QT00049728	121bp
MICA	QT00245112	120bp
GAPDH	QT00079247	95bp

Table 8. Primers for HLA typing.

HLA	Sense primer sequence	Anti-sense primer sequence	Final concentration (μM)
A1	5-CGACGCCGCGAGCCAGAA	5-AGCCCGTCCACGCACCG	3.3
A2	5-GTGGATAGAGCAGGAGGGT	5-CCAAGAGCGCAGGTCCTCT	3.3
B7.1	5-GGAGTATTGGGACCGGAAC	5-TACCAGCGCGCTCCAGCT	3.3
B7.2	5-GAGCCTGCGGACCCTGCT	5-TACCAGCGCGCTCCAGCT	3.3
Positive Control	5- ATGATGTTGACCTTTCCAGGG	5- TTCTGTAACTTTTCATCAGTTGC	2
No DNA Control	5- ATGATGTTGACCTTTCCAGGG	5- TTCTGTAACTTTTCATCAGTTGC	2

IFNγ ELISPOT

PBMC used for the ELISPOT assay were removed from liquid nitrogen and thawed as previously described. Cells were resuspended and washed in TCC media and centrifuged at a reduced speed of 100 x g for 15 minutes to avoid cell clumping. Cell were resuspended in TCC media at a final concentration of 10^6 cells/ml, and rested overnight at 37°C, 5% CO_2. Ninety six well Millipore Immobilon-P PVDF plates were activated for 30 seconds with 70% Ethanol. Plates were then washed 3 times with sterile PBS and subsequently coated with 15 μg/ml of anti-IFNγ mAb (clone:D1K, Mabtech) diluted in PBS overnight at 4°C. The following morning the plate was washed 5 times with PBS, then once with RPMI 1640 and subsequently blocked for 1 hour with TCC media. During this blocking stage, rested cells were washed and counted. Trypan blue was used to disregard dead cells. Between 250,000 and 300,000 PBMCs were added to duplicate wells in 100 μl of TCC media, to which overlapping peptides were added at a final concentration of 1 μg/ml of each peptide. The plate was incubated for 16-18 hours at 37°C, 5% CO_2. Following incubation, cells were removed and the plates were washed 6 times with PBS-T. Fifty μl of 1 μg/ml biotinylated anti-IFNγ-mAb (clone: 7-B6-1, Mabtech) diluted in PBS was added to the wells and incubated for 3 hours at RT. The plates were washed 6 times with PBS-T. Fifty μl of streptavidin conjugated alkaline phosphatase was added to the wells for 1 hour at RT, and the plates were washed 6 times with PBS-T, and 4 times with PBS. The chromogenic substrate BCIP/NBT-plus was added to the wells and allowed to develop in the dark until dark spots emerged. The reaction was by washing the plate extensively with tap water and allowing it to dry in the dark overnight. The number of spots were read using an AID automated ELISPOT reader. Each spot is representative of one reactive IFNγ secreting T cell. Data was transformed to give the number of IFNγ secreting cells per 10^6 PBMC.

Determination of TCRVβ Repertoire by Flow Cytometry

All TCRVβ-specific antibody reagents were part of the TCRVβ repertoire kit from Beckman Coulter. Detection of individual TCRVβ families was carried out on TIL and autologous PBMC. Briefly, up to 1×10^5 cells were surface stained simultaneously with CD3-PE-Cy5 and a set of three antibodies (A-H), directed against TCRVβ families as listed in Table 9. Antibodies directed against TCR families were labelled with either FITC or PE, or dual labelled with PE and FITC. Flow cytometric analysis was performed on LSRII, as previously described. Cells were gated on the CD3+ population, and individual TCRVβ families were evaluated based on exclusive staining for either FITC or PE or dual staining of both. Thus, 24 individual TCRVβ families were analysed, covering over 80% of the TCRVβ repertoire, using only eight individual tubes.

Data Handling and Statistical Analysis

Statistical analysis was performed using GraphPad Prism version 5 (GraphPad Software). To determine differences between two groups, a non-parametric Mann-Whitney test was performed. A non-parametric Kruskal–Wallis test was used when comparing more than 2 groups, with a Dunn's multiple comparison post hoc test. A Wilcoxon matched-pairs signed-rank test was used to compare non-parametric matched data. A linear regression was performed to assess the relationship between two variables. Spearman's non-parametric test was used to determine correlations. Normal distribution was assessed using the D'Agostino & Pearson test, where appropriate. The null hypothesis was rejected at a p value of <0.05. Confidence intervals of 95 -99.9 % were used. * indicates of $p < 0.05$, ** indicates $p < 0.01$, *** indicates $p<0.001$.

Table 9. Antibodies used for Vβ clonality analysis.

Tube	Vβ Family	Fluorochrome	Clone	Isotype (species)
A	*Vβ 5.3*	PE	3D11	IgG1 (mouse)
	Vβ 7.1	PE + FITC	ZOE	IgG2a (mouse)
	Vβ 3	FITC	CH92	IgM (mouse)
B	*Vβ 9*	PE	FIN9	IgG2a (mouse)
	Vβ 17	PE + FITC	E17.5F3	IgG1 (mouse)
	Vβ 16	FITC	TAMAYA1.2	IgG1 (mouse)
C	*Vβ 18*	PE	BA62.6	IgG1 (mouse)
	Vβ 5.1	PE + FITC	IMMU157	IgG2a (mouse)
	Vβ 20	FITC	ELL1.4	IgG (mouse)
D	*Vβ 13.1*	PE	IMMU222	IgG2b (mouse)
	Vβ 13.6	PE + FITC	JU74.3	IgG1 (mouse)
	Vβ 8	FITC	56C5.2	IgG2a (mouse)
E	*Vβ 5.2*	PE	36213	IgG1 (mouse)
	Vβ 2	PE + FITC	MPB2D5	IgG1 (mouse)
	Vβ 12	FITC	VER2.32	IgG2a (mouse)
F	*Vβ 23*	PE	AF23	IgG1 (mouse)
	Vβ 1	PE + FITC	BL37.2	IgG1 (rat)
	Vβ 21.3	FITC	IG125	IgG2a (mouse)
G	*Vβ 11*	PE	C21	IgG2a (mouse)
	Vβ 22	PE + FITC	IMMU546	IgG1 (mouse)
	Vβ 14	FITC	CAS1.1.3	IgG1 (mouse)
H	*Vβ 13.2*	PE	H132	IgG1 (mouse)
	Vβ 4	PE + FITC	WJF24	IgM (rat)
	Vβ 7.2	FITC	ZIZOU4	IgG2a (mouse)

General Introduction

Tumour-infiltrating lymphocytes (TIL), particularly T cells, are found within the lesions of many types of human tumours including TGCTs. The contribution of the immune infiltrate in recognition and elimination of tumour cells is unclear for the majority of cancers. Numerous studies in a variety of cancer types have shown that tumour residing T cells express markers of activation and display a phenotype typical of effector memory differentiation (Pages et al., 2005b, Yoshino et al., 1992). In addition, previous literature has described the ability of CD8 T cells to recognise tumour cells via the expression of tumour-specific antigens. Nevertheless, tumour progression is common especially in the case of TGCTs, suggesting immune escape mechanisms play an important role in tumour growth and survival.

A detailed phenotypic and functional analysis of cells infiltrating TGCT lesions, and the knowledge of negative regulatory mechanisms at play within the tumour can help increase our understanding of tumour mediated immune evasion. This opens up the possibility of creating alternative immunotherapies, not only relevant for use in TGCTs, but also as a universal treatment for other cancers exhibiting a large lymphocytic infiltrate. Knowledge gathered from the identification and in-depth analysis of CTAg-specific T cells from TGCT patients would be relevant for other tumour types where CTAg expression is demonstrated. In addition, understanding the dynamics of a CTAg response would enable us to generate more effective T cell-mediated therapy regimens in the future.

CHAPTER 3: PHENOTYPE AND FUNCTIONALITY OF LYMPHOCYTES INFILTRATING TGCTs

Introduction

Since lymphocytes are abundant in TGCTs, particularly seminoma, the emphasis of previous studies has primarily concerned T cells and their potential anti-tumour function. In addition, earlier reports have predominantly used immunohistochemistry to examine the phenotype of infiltrating cells. Although this methodology allows the identification, localisation, and potential interaction of TIL with tumour cells *in situ*, phenotypic analysis is restricted and functionality is difficult to determine.

Here, this chapter aims to further characterise the phenotype of T cells that are recruited into the TGCT, not only in seminoma, but within all TGCTs containing seminomatous elements. In particular, the memory phenotype of infiltrating T cells will be examined and compared to that of autologous peripheral blood derived T cells. Furthermore, the activation status of these T cell subsets will be investigated, along with the expression of inhibitory receptors known to negatively regulate an immune response. This will aid in our understanding of whether tumour infiltrating T cells retain effective anti-tumour functionality. This may be important in the context of developing T cell immunotherapies whereby blocking of such receptors may favour a successful cytotoxic immune response and thereby improve anti-tumour immunity.

The functionality of these cells with regard to cytokine secretion, proliferative ability and cytotoxic potential will be examined to determine the activity of these cells once removed from the tumour environment. The clonality of tumour infiltrating T cells will also be compared to that of autologous peripheral blood T cells (PBMC) to help determine whether antigen-specific expansion of T cells occurs within the tumour. Investigating the functional characteristics of these cells will increase our understanding of anti-tumour immunity in the context of TGCTs.

Although the presence of T cells within TGCT lesions has been well documented, little is known about NK cells which infiltrate these tumours. Since all TGCTs are derived from undifferentiated primordial germ cells, it has been suggested that MHC expression on these cells may be low or absent. Consequently, T cell mediated immunity, in particular cytotoxic CD8 T cell responses, may be ineffective at targeting and subsequent killing of tumour cells. NK cells can target transformed cells without the need of prior sensitisation. The frequency, phenotype and function of NK cells within these tumours will therefore be examined.

In this study, immune cells are analysed *ex vivo*, directly following mechanical tumour dissociation, an approach which allows a more informative examination of multiple phenotypic and functional attributes of TIL.

Results

αβ and γδ T cells Infiltrate TGCTs

Following the isolation of lymphocytes from TGCT tissues by gentle mechanical dissociation, cells were stained with appropriate antibodies against cell surface antigens and analysed by flow cytometry. Cells were first gated to remove doublet cells, before gating on live lymphocytes. T cells were identified by their expression of CD3 and were subsequently defined by differential expression of CD4, CD8 and γδ TCR. All three T cell subtypes were detected in TIL (Figure 7).

The median CD4:CD8 ratio in TIL (n=7) is 1.12:1 (interquartile range [IQR]: 0.65-1.15) demonstrating CD4 and CD8 cells are present at approximately equal proportions. In PBMC, there is approximately twice as many CD4 T cells than CD8 T cells (median ratio: 1.99 IQR: 1.26-3.04) demonstrating that TILs are significantly enriched for CD8 T cells (p=0.0156) (Figure 8a).

γδ T cells were also present in TIL, but at relatively low frequency compared to αβ T cells (median: 3.07% of CD3+ T cells) (Figure 8b). There was no significant difference between the proportion of γδ T cells in TIL (3.07 IQR: 1.61-9.57) compared to PBMC (3.42 IQR: 1.54-6.90) (p=0.5703).

Overall, our results indicate that αβ T cells are the dominant T cell population infiltrating TGCT masses, with the tumour environment being enriched for CD8 T cells.

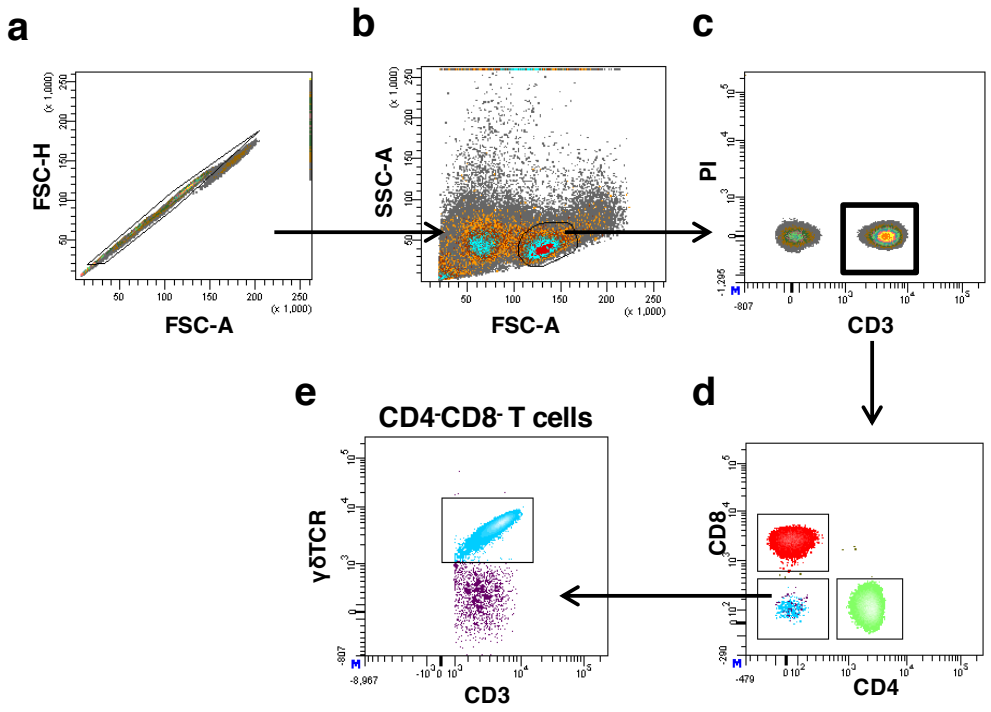

Figure 7. Gating strategies for identification of CD4, CD8 and γδ T cells.
Cells were first gated to remove doublet cells (a), before gating on lymphocytes based on FSC-A and SSC-A properties (b). Live T cells were classified as being propidium iodide (PI) negative and CD3 positive cells (c). CD4 (green) and CD8 (red) T cells were gated from the $CD3^{+}PI^{-}$ population (d). γδ T cells (blue) were identified as γδ TCR positive cells from the $CD3^{+}$ $CD4^{-}$ $CD8^{-}$ subset (e). Plots shown are representative of TIL isolated from TGCT tissue of a single individual.

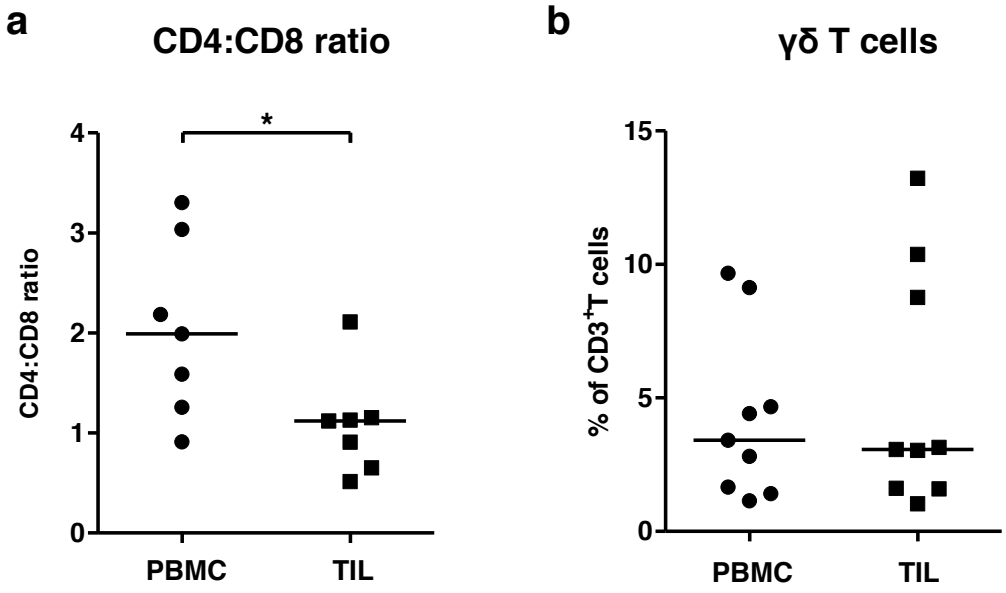

Figure 8. Proportion of CD4, CD8 and γδ TCR$^+$ T cells in PBMC and TIL.
The proportion of CD4 and CD8 T cells in matched PBMC and TIL was calculated, and expressed as a CD4:CD8 ratio (a). The proportion of γδ T cells was determined and expressed as a percentage of total CD3$^+$ T cells (b). Each symbol represents an individual patient. Horizontal lines indicate the median. Data analysed by Wilcoxon matched-pairs signed-rank test, * denotes $p<0.05$.

CD4 and CD8 TIL Have an Effector Memory Phenotype

The memory phenotype of CD4 and CD8 T cells from PBMC and TIL was determined by flow cytometry following antibody staining for CD45RA and the chemokine receptor CCR7. The expression of these markers classified cells into the following memory phenotypes: TEMRA ($CD45RA^{+}CCR7^{-}$), naive ($CD45RA^{+}CCR7^{+}$), effector memory (T_{EM}, $CD45RA^{-}CCR7^{-}$) and central memory (T_{CM}, $CD45RA^{-}CCR7^{+}$) T cells. Table 10 shows the distribution of CD4 (Figure 9) and CD8 (Figure 10) T cells in these memory subsets within both PBMC and TIL. The proportion of naive T cells was markedly lower in TIL compared with autologous PBMC (CD4 median 1.35% vs. 46.44%; CD8 median 2.22% vs. 30.49%). These changes were reciprocated by a significant enrichment of T_{EM} in TIL compared to PBMC (CD4 median 78.22% vs. 20.54%; CD8 median 85.76% vs. 38.30%). In addition, the proportion of TEMRA cells in the CD4 compartment was significantly reduced. The same serves true for CD8 TEMRA although the decrease does not reach statistical significance. There was no significant difference in the proportion of CD4 and CD8 T_{CM} cells isolated from tumour compared to PBMC. In conclusion, T cells with an T_{EM} phenotype are the predominant tumour infiltrating cells.

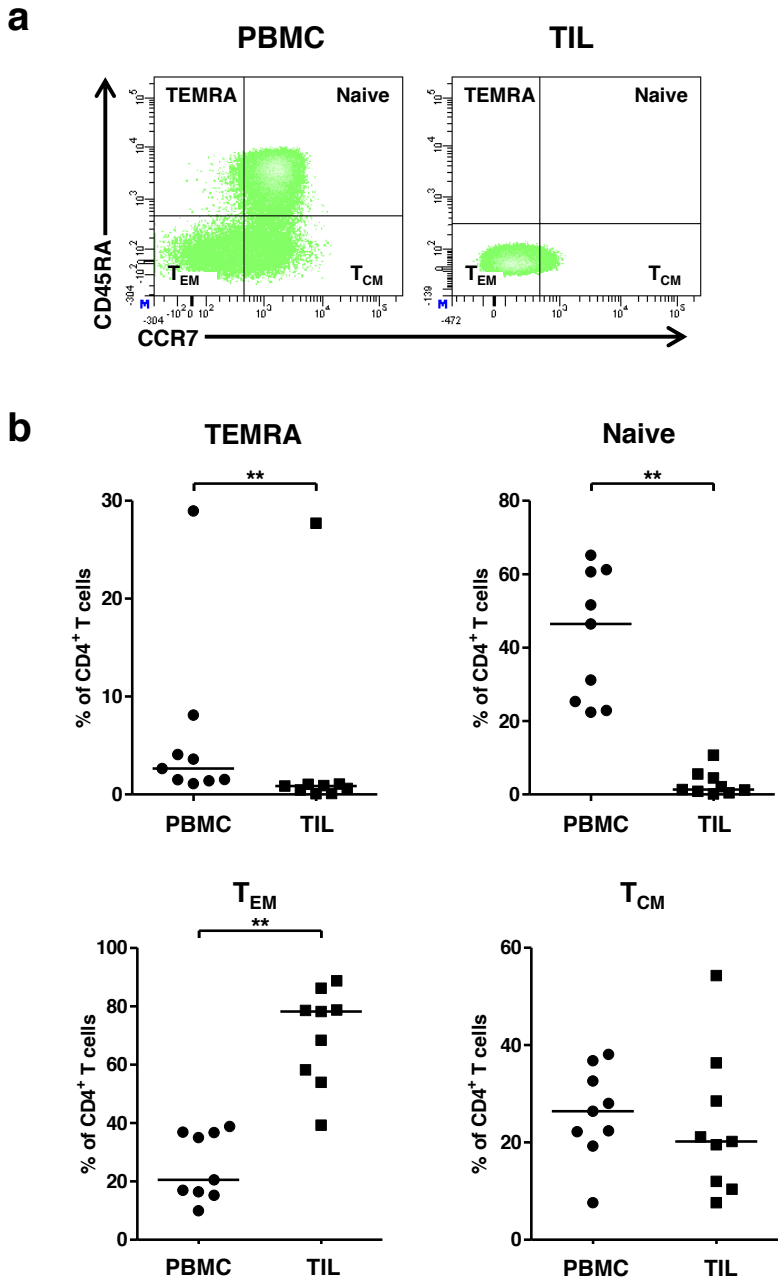

Figure 9. Memory phenotype of CD4 T cells in matched PBMC and TIL.
Expression of CCR7 and CD45RA on CD4 T cells was determined to show TEMRA ($CD45RA^+CCR7^-$), naive ($CD45RA^+CCR7^+$), effector memory (T_{EM}, $CD45RA^-CCR7^-$), and central memory (T_{CM}, $CD45RA^-CCR7^+$) T cells (a). Proportions of CD4 T cells in each memory subset are shown (b). Each symbol represents an individual patient. Horizontal lines indicate the median. Data analysed by Wilcoxon matched-pairs signed-rank test,
** denotes $p<0.01$.

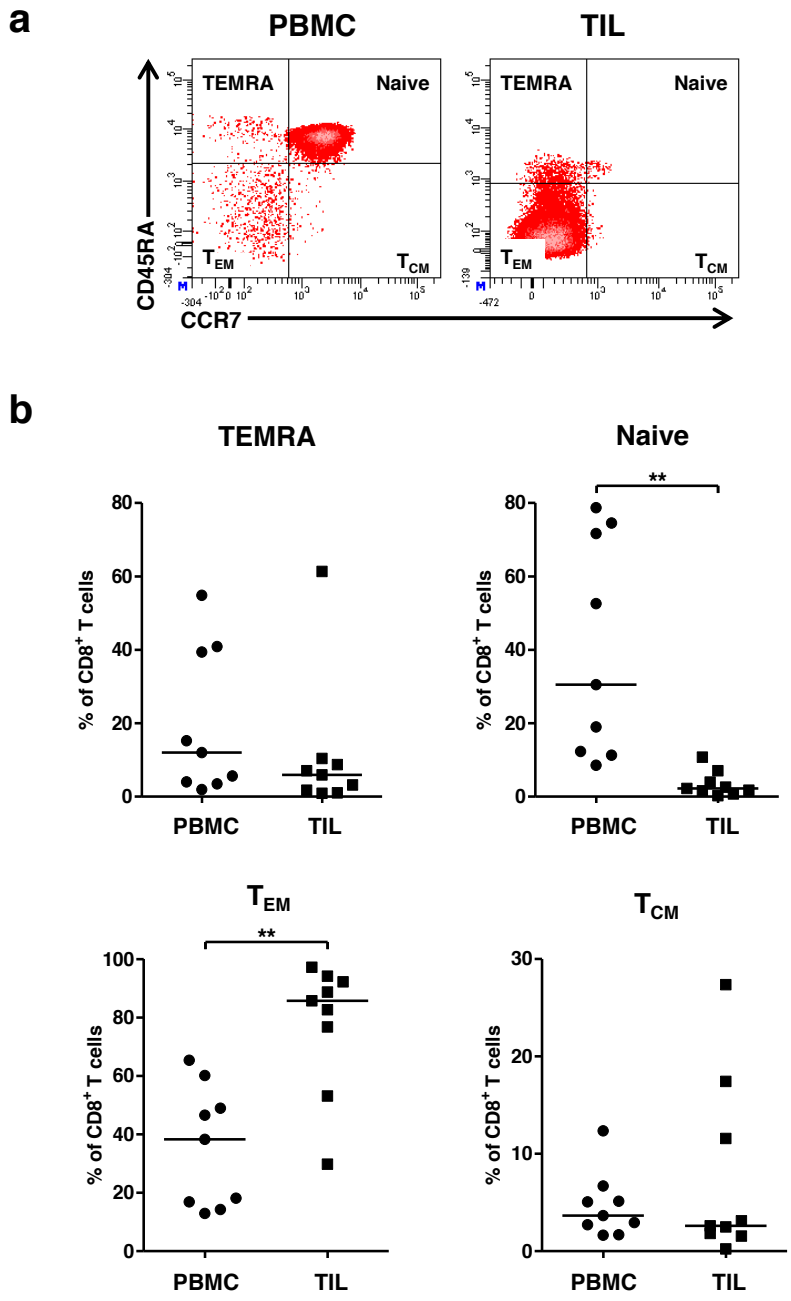

Figure 10. Memory phenotype of CD8 T cells in matched PBMC and TIL.
Expression of CCR7 and CD45RA on CD8 T cells was determined to show TEMRA ($CD45RA^+CCR7^-$), naive ($CD45RA^+CCR7^+$), effector memory (T_{EM}, $CD45RA^-CCR7^-$), and central memory (T_{CM}, $CD45RA^-CCR7^+$) T cells (a). Proportions of CD8 T cells in each memory subset are shown (b). Each symbol represents an individual patient. Horizontal lines indicate the median. Data analysed by Wilcoxon matched-pairs signed-rank test,
** denotes $p<0.01$.

Table 10. Memory phenotype of CD4 and CD8 T cells in matched PBMC and TIL.

	CD4 (n=9)							CD8 (n=9)						
	PBMC			TIL			p	PBMC			TIL			p
	Median	25th	75th	Median	25th	75th		Median	25th	75th	Median	25th	75th	
TEMRA	2.66	1.45	6.10	0.86	0.29	28.71	**0.0039**	12.01	3.74	40.15	5.94	1.40	9.58	0.1641
Naive	46.44	24.12	60.69	1.35	0.66	10.71	**0.0039**	30.49	11.81	73.09	2.22	1.16	5.52	**0.0039**
T_{EM}	20.54	15.85	36.79	78.22	56.10	82.43	**0.0039**	38.30	15.56	54.52	85.76	64.69	93.18	**0.0039**
T_{CM}	26.43	20.74	34.71	20.22	11.21	32.43	0.2500	3.65	2.21	5.91	2.61	1.69	14.51	0.6523

Data expressed as median with 25th and 75th quartile. Significant differences are highlighted in bold type.

The Effector Memory T cell Compartment is Inflated in TGCT Patients

We could reasonably hypothesise that T cells infiltrating the tumour may re-enter circulation and would therefore result in a systemic increase in tumour specific cells in peripheral blood. Since effector memory T cells are elevated in TIL, we investigated whether memory subsets were increased in the circulation of patients with testicular cancer, compared to healthy controls. TGCT patients and healthy donors were gender-matched and age-matched, to enable effective comparison (Figure 11). We observed different proportions of peripheral blood memory subsets in TGCT patients, compared to healthy donors (Figure 12 and Table 11). Peripheral blood effector memory CD4 and CD8 T cells were significantly elevated in TGCT patients. This effect was reciprocated by a statistically significant reduction in the proportion of naive T cells. We speculate that tumour development leads to the generation and expansion of tumour specific T cells that may enter circulation and subsequently inflate the peripheral blood memory T cell pool.

Furthermore, we characterised the memory phenotype of peripheral T cells from a small cohort of seminoma patients before (n=10), two weeks (n=10) and three months (n=6) post chemotherapy. No significant difference was observed in the proportions of CD4 and CD8 T cells within each memory subset shortly after chemotherapy (two weeks). However, three months post chemotherapy revealed decreased proportions of T_{EM} cells and increased proportions of naive T cells for both the CD4 and CD8 T cell compartments within the circulation (Table 12, Table 13 and Figure 13). P values and significance between each time point for CD4 and CD8 T cells are outlined in Table 14. Together, our data suggest the removal of tumour burden and/or the onset of chemotherapy could lead to a reduction in anti-tumour specific immunity.

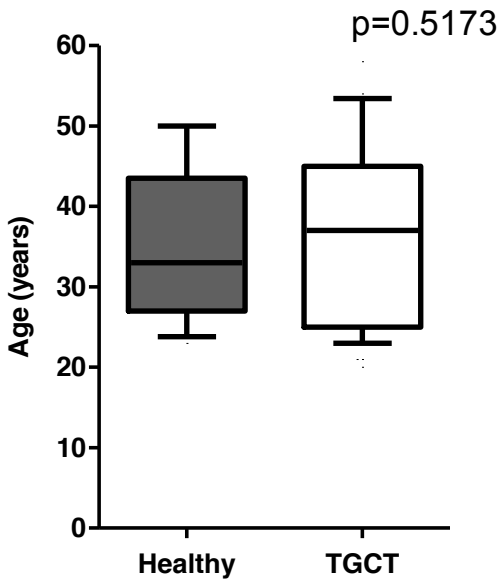

Figure 11. Age of healthy donors and TGCT patients.
The age of healthy donors and TGCT patients is shown. There is no significant difference in the age of healthy donors and TGCT patients used in this study. Box represents 25th and 75th percentile, line represents median, and whiskers represent 10-90 percentile. Data analysed by Mann-Whitney test.

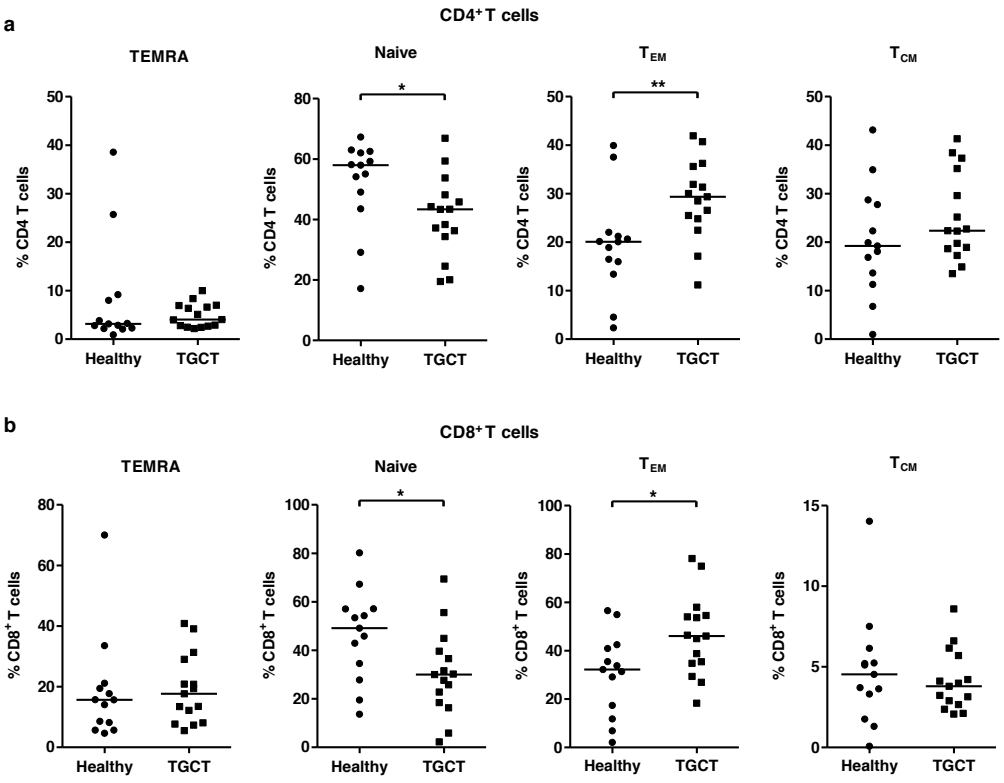
a
CD4+ T cells
TEMRA
Naive
TEM
TCM
% CD4 T cells
Healthy
TGCT
*
**
b
CD8+ T cells
% CD8+ T cells

Figure 12. Memory phenotype of peripheral blood CD4 and CD8 T cells of healthy donors and TGCT patients.

Expression of CCR7 and CD45RA on CD4 (a) and CD8 (b) T cells was determined to define TEMRA, Naive, T_{EM} and T_{CM} subsets. Proportions of cells in each memory subset of healthy donors and TGCT patients were compared. Each symbol represents an individual patient. Horizontal line indicates the median. Data analysed by Mann Whitney test,
* denotes $p<0.05$, ** denotes $p<0.01$.

Table 11. Memory phenotype of peripheral blood CD4 and CD8 T cells of healthy donors and TGCT patients.

	CD4							CD8						
	Healthy (n=13)			TGCT (n=15)			p	Healthy (n=13)			TGCT (n=15)			p
	Median	25th	75th	Median	25th	75th		Median	25th	75th	Median	25th	75th	
TEMRA	**3.16**	2.24	8.60	**4.06**	2.70	6.93	0.5804	**15.70**	6.96	20.29	**17.69**	8.08	29.06	0.6450
Naive	**57.96**	46.29	62.30	**43.36**	34.34	48.36	***0.0270***	**49.16**	31.18	57.10	**29.99**	18.47	39.64	***0.0341***
T_{EM}	**20.08**	14.70	21.64	**29.35**	24.81	35.61	***0.0099***	**32.26**	14.59	41.71	**46.05**	34.81	54.59	***0.0382***
T_{CM}	**19.21**	12.48	28.23	**22.37**	18.64	35.18	0.2136	**4.54**	2.54	5.69	**3.80**	2.66	5.70	0.7125

Data expressed as median (bold) with 25th and 75th quartile. Significant differences are highlighted in bold italic type.

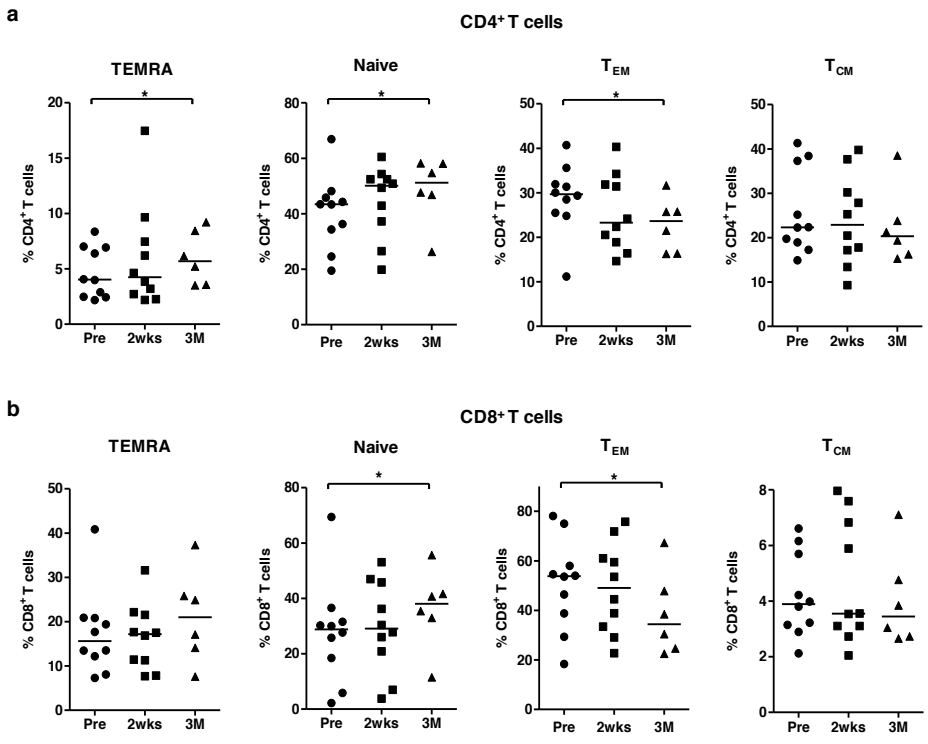
a
CD4+ T cells
TEMRA
Naive
TEM
TCM
% CD4+ T cells
Pre
2wks
3M
b
CD8+ T cells
% CD8+ T cells

Figure 13. Memory phenotype of peripheral blood CD4 and CD8 T cells of TGCT patients before and after chemotherapy.
Expression of CCR7 and CD45RA on CD4 (a) and CD8 (b) T cells was determined to define TEMRA, Naive, T_{EM} and T_{CM} subsets. Proportions of cells in each memory subset at pre, 2wks and 3M post chemotherapy is shown. Each symbol represents an individual patient. Horizontal line indicates the median. Data analysed by Wilcoxon matched-pairs signed-rank test, * denotes $p<0.05$.

Table 12. Memory phenotype of peripheral blood CD4 T cells of TGCT patients before and after chemotherapy

	Pre (n=10)			2wks (n=10)			3M (n=6)		
	Median	**25th**	**75th**	**Median**	**25th**	**75th**	**Median**	**25th**	**75th**
TEMRA	**4.03**	2.46	6.95	**4.24**	2.69	8.01	**5.69**	3.57	8.64
Naive	**43.40**	31.90	46.39	**50.12**	34.58	52.93	**51.22**	41.70	58.12
T_{EM}	**29.69**	25.32	32.83	**23.27**	18.28	32.44	**23.64**	16.35	27.27
T_{CM}	**22.33**	18.50	37.60	**22.89**	16.24	32.07	**20.34**	16.22	27.49

Data expressed as median (bold) with 25th and 75th quartile.

Table 13. Memory phenotype of peripheral blood CD8 T cells of TGCT patients before and after chemotherapy

	Pre (n=10)			2wks (n=10)			3M (n=6)		
	Median	**25th**	**75th**	**Median**	**25th**	**75th**	**Median**	**25th**	**75th**
TEMRA	**15.61**	11.16	20.86	**17.18**	10.43	21.70	**21.00**	12.48	28.70
Naive	**28.83**	15.32	32.82	**29.09**	17.39	46.07	**38.07**	27.62	45.16
T_{EM}	**53.83**	36.42	62.23	**49.03**	32.34	63.69	**34.42**	24.10	52.67
T_{CM}	**3.89**	3.08	5.81	**3.55**	3.01	7.02	**3.44**	2.71	5.35

Data expressed as median (bold) with 25th and 75th quartile.

Table 14. P values for memory phenotyping of peripheral blood T cells of TGCT patients before and after chemotherapy.

	CD4				CD8			
	TEMRA	**Naive**	**T_{EM}**	**T_{CM}**	**TEMRA**	**Naive**	**T_{EM}**	**T_{CM}**
Pre vs. 2wks	0.1309	0.2324	0.2754	0.1602	0.6250	0.5566	0.7695	0.3223
Pre vs. 3M	***0.0313***	***0.0313***	***0.0313***	0.0938	0.5625	***0.0313***	***0.0313***	0.3125
2wks vs. 3M	1.000	0.3215	0.2188	0.3125	0.3125	0.5625	0.1563	0.5625

Significant differences are highlighted in bold italic type.

T Cells Infiltrating TGCTs Express Markers of Activation

T cells isolated from TGCT tissue are predominantly T_{EM}. This suggests tumour infiltrating T cells are antigen-experienced i.e. they have previously been activated by, and are responding to, cognate antigen presented through MHC complexes. Although these cells are antigen experienced, this alone does not indicate whether the recognition of antigen has occurred recently. By assessing the expression of activation markers on T cells from TIL, and comparing this to PBMC, we are able to determine whether these cells have been activated within the tumour.

Expression of CD69 was examined on CD4 and CD8 T cells from PBMC and TIL by flow cytometry. CD69 is the earliest inducible cell surface glycoprotein acquired during T cell activation (Testi et al., 1994). Expression of CD69 was significantly increased on both CD4 ($p=0.0025$) and CD8 T cells ($p=0.0025$) in TIL compared to PBMC (Figure 14 and Table 15). The median expression of CD69 on TIL was 46.70% and 44.56% of total CD4 and CD8 T cell subsets, respectively. In contrast, less than 1% of CD4 and CD8 T cells from PBMC expressed CD69. Expression levels of CD69 on $\gamma\delta$ T cells were similar to that of $\alpha\beta$ T cells, with a median of 51.77% for TIL vs. 0.79% for PBMC. This data suggests that approximately half the T cell population infiltrating TGCT has very recently been activated, indicative of stimulation within the tumour.

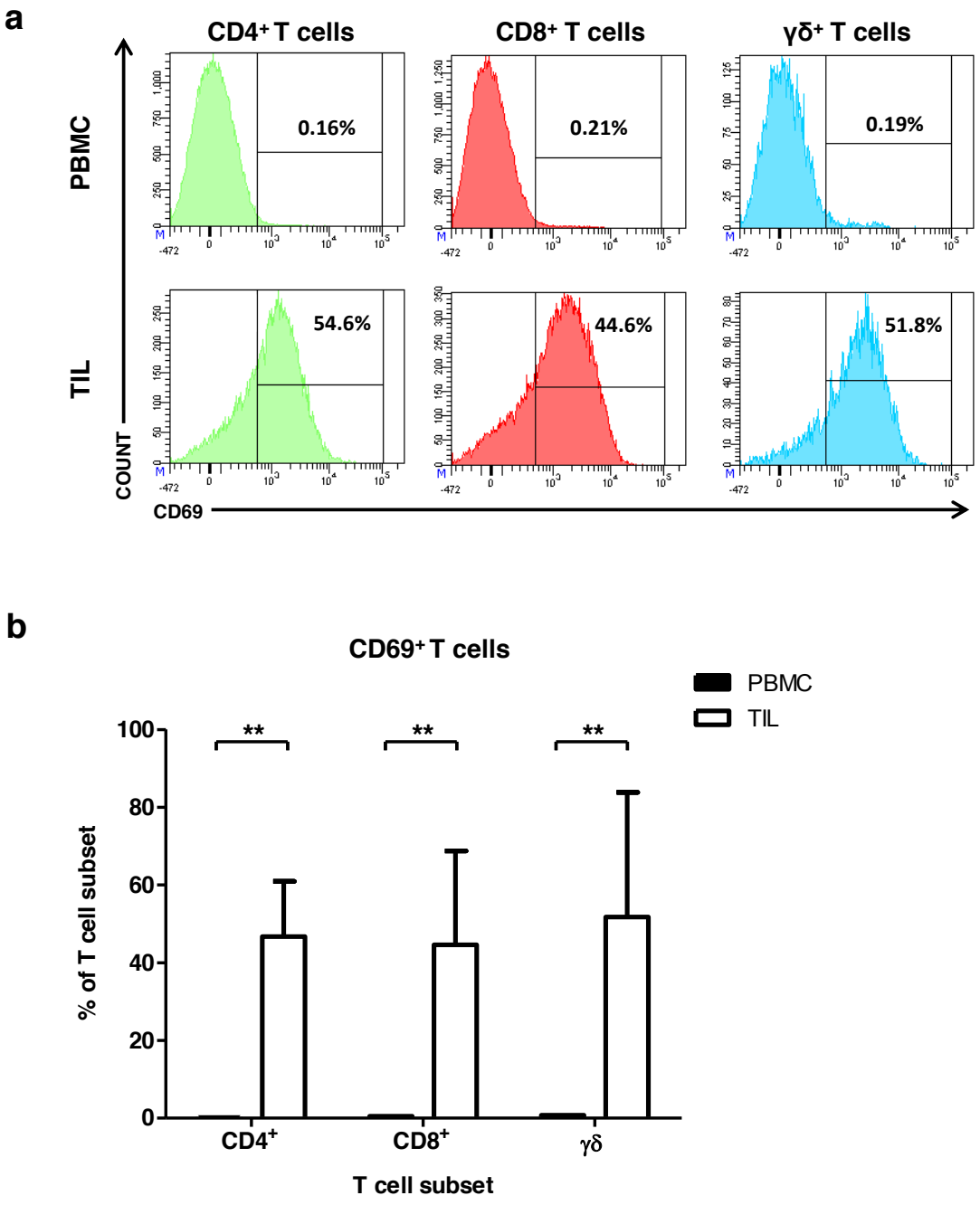

Figure 14. CD69 expression on αβ and γδ T cell subsets from PBMC and TIL.
Expression of CD69 was determined on CD4, CD8, and γδ T cells by flow cytometry and representative histograms are shown (a). Bar chart shows significant increase in CD69 expression on all T cell subsets (b) in TIL (open bar) compared to PBMC (filled bar). Bars represent median. Error bars represent upper range. Data analysed by Mann-Whitney test, * *denotes $p<0.01$.

To corroborate the observation that T cells are activated, CD38 expression was also analysed on matched PBMC and TIL. CD38 expression on resting T cells is low but is highly expressed on activated T cells. The cell surface density of CD38 (median fluorescence intensity [MFI]) on CD4 and CD8 T cells was far greater on TIL (CD4: 1310, CD8: 1036) than on PBMC (CD4: 454, CD8: 406), in all patients analysed (Figure 15 and Table 15). A 4-fold increase in CD38 density was found on CD8 T cells in TIL compared to PBMC. Similarly, a 5-fold increase was observed for CD4 T cells in TIL. Differences in CD38 MFI of T cells from PBMC and TIL did however not reach statistical significance, likely due to small sample size (n= 3). It is clear from Figure 15a that the increase in MFI in TIL was primarily due to a large population of T cells expressing very high levels of CD38. This cell population was present in both the CD4 and CD8 compartments, but was completely absent on T cells from peripheral blood.

Increased CD69 Expression on Peripheral Blood CD8 T Cells Following Chemotherapy

A high proportion of tumour infiltrating T cells are activated, which led us to examine the expression of CD69 on peripheral blood T cells from TGCT patients (pre-treatment) compared to healthy controls. No difference in CD69 expression was apparent on either the CD4, CD8 or γδ T cell subsets from TGCT patients compared to healthy donors (Figure 16a and Table 18). However, the proportion of CD8 and γδ T cells expressing CD69 was increased shortly after (two weeks) chemotherapy (Figure 16b, Table 17 and Table 18), compared to levels prior to treatment. Although statistically significant, the overall increase in CD69 expressing cells is minimal, and therefore its biological significance unknown.

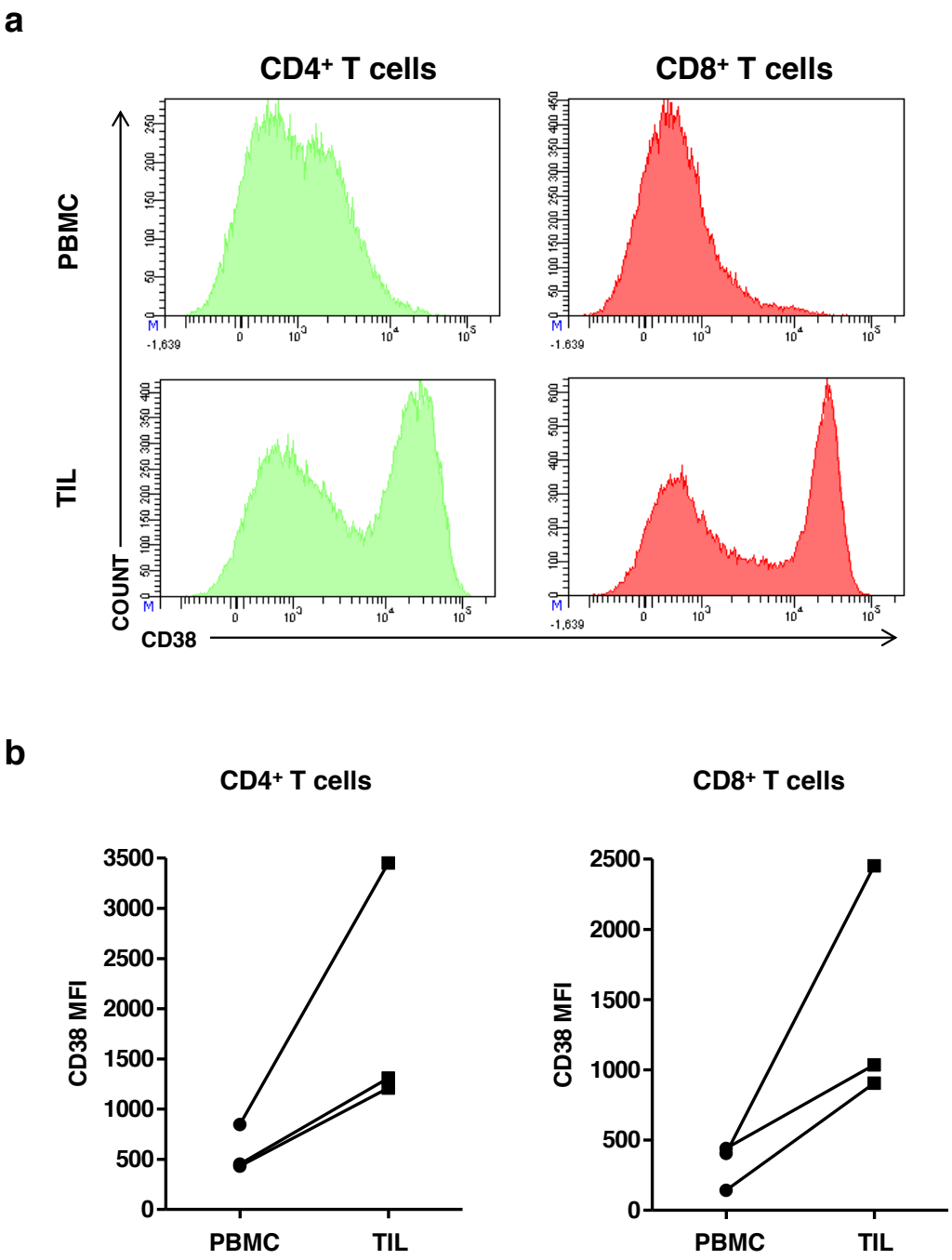

Figure 15. Expression of CD38 on T cells from TIL and autologous PBMC.
Representative histograms show the expression of CD38 on CD4 and CD8 T cells in PBMC and TIL (a). CD38 MFI was calculated and is shown for CD4 and CD8 T cells in PBMC and TIL (b). Lines join PBMC and TIL from the same patient. Data analysed by Wilcoxon matched-pairs signed-rank test.

Table 15. CD69 and CD38 expression on αβ and γδ T cell subsets from PBMC and TIL.

	CD4							CD8						
	PBMC			TIL			p	PBMC			TIL			p
	Median	25th	75th	Median	25th	75th		Median	25th	75th	Median	25th	75th	
CD69 (n=6)	**0.17**	0.04	0.44	**46.70**	17.85	57.76	***0.0025***	**0.52**	0.12	1.00	**44.59**	17.16	62.38	***0.0025***
CD38 (n=3)	**454**	431	847	**1310**	1211	3451	0.2500	**406**	142	440	**1036**	905	2452	0.2500

	γδ						
	PBMC			TIL			p
	Median	25th	75th	Median	25th	75th	
CD69 (n=6)	**0.79**	0.19	1.56	**51.77**	26.08	71.23	***0.0025***

Data expressed as median (bold) with 25th and 75th quartile. Significant differences are highlighted in bold italic type.

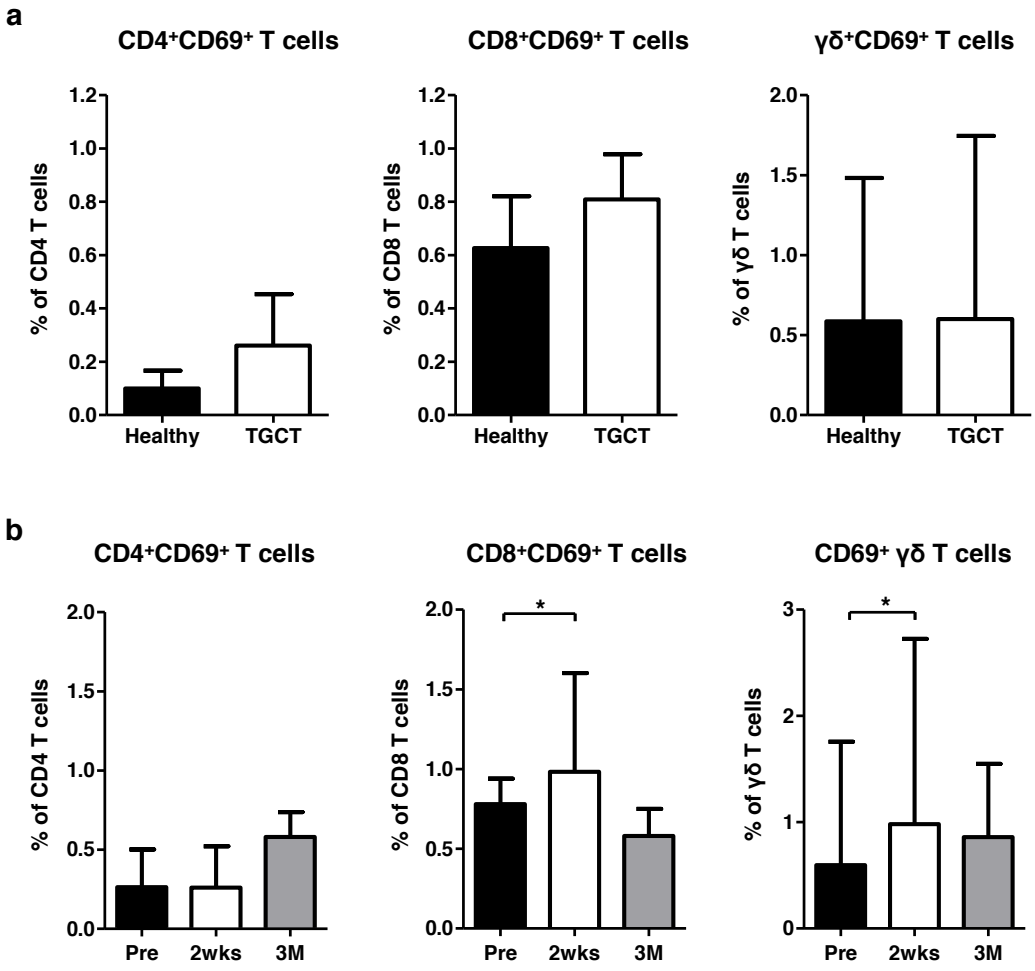

Figure 16. CD69 expression on peripheral blood T cells of healthy donors and TGCT patients at pre and post treatment.

Expression of CD69 was determined by flow cytometry. Bar charts compare the proportion of CD69 expressing CD4, CD8 and γδ T cells in healthy donors and TGCT patients (a) Bars represent median. Error bars indicate upper quartile. Data analysed by Mann-Whitney test. CD69 expression on CD4, CD8 and γδ T cells from TGCT patients at pre, 2wks and 3M post chemotherapy. Bars represent median. Error bars indicate upper quartile. Data analysed by Wilcoxon matched-pairs signed-rank test, *denotes $p<0.05$.

Table 16. Activation status of T cells from peripheral blood of healthy donors compared to that of TGCT patients.

	Healthy (n=13)				TGCT (n=15)				p
	Median	**25th**	**75th**	**n**	**Median**	**25th**	**75th**	**n**	
$CD4^+CD69^+$	**0.10**	0.08	0.17	13	**0.26**	0.09	0.45	15	0.0538
$CD8^+CD69^+$	**0.63**	0.44	0.82	13	**0.81**	0.42	0.98	15	0.4070
$CD69^+\gamma\delta$	**0.59**	0.28	1.48	13	**0.60**	0.36	1.75	15	0.4336

Data expressed as median (bold) with 25th and 75th quartile. Significant differences are highlighted in bold type.

Table 17. T cell activation of peripheral blood T cells in TGCT patients pre and post chemotherapy.

	Pre (n=10)			2wks (n=10)			3M (n=6)		
	Median	**25th**	**75th**	**Median**	**25th**	**75th**	**Median**	**25th**	**75th**
$CD4^+CD69^+$	**0.26**	0.12	0.50	**0.26**	0.15	0.32	**0.58**	0.40	0.74
$CD8^+CD69^+$	**0.78**	0.39	0.94	**0.98**	0.60	1.60	**0.58**	0.47	0.75
$CD69^+\gamma\delta$	**0.60**	0.59	1.76	**0.98**	0.55	2.73	**0.86**	0.61	1.55

Data expressed as median (bold) with 25th and 75th quartile.

Table 18. P values for T cell activation of peripheral blood T cells in TGCT patients before and at intervals following chemotherapy.

	$CD4^+CD69^+$	$CD8^+CD69^+$	$CD69^+\gamma\delta$
Pre vs. 2wks	0.3570	***0.0137***	***0.0273***
Pre vs. 3M	0.4375	0.3125	0.4375
2wks vs. 3M	0.6875	0.1875	1.000

Significant differences are highlighted in bold italic type.

T Cells Isolated from TGCT Tissue Have a High Proliferative Capacity *in vitro*

We have shown that T cells within TGCT lesions are predominantly recently activated T_{EM} cells. Following activation, T cells enter the cell cycle and clonally expand in order to generate an effective immune response. Next, we determined the extent of T cell proliferation with and without *in vitro* stimulation. Cells were either unstimulated (IL-2 only) or stimulated *in vitro,* for 5 days. TCR-mediated stimulation was achieved by stimulating with CD3/CD28 Dynabeads with IL-2. Prior to cell culture, cells were stained with a Celltrace™ proliferation dye, which is distributed equally between the daughter cells during each successive cell division thus cellular fluorescence intensity is halved. As a result, the proportion of cells that have undergone a particular number of cell divisions can be determined by flow cytometry.

If T cells received the appropriate stimulus to proliferate within the tumour microenvironment, we would expect them to continue dividing *in vitro* without additional TCR stimulation. However, we showed that only a minority of CD4 (3.83% IQR 0.67-15.31) and CD8 (1.91% IQR 0.31-20.40) T cells were found to proliferate when cultured without *in vitro* stimulation (Figure 17a). This suggests that although T cells have been activated by cognate antigen very recently, the majority of T cells within the tumour are not proliferating. Next, we investigated the extent of proliferation following *in vitro* TCR-dependant stimulation, to determine whether proliferation could be restored. Stimulation of these cells *in vitro* would determine whether they are proliferatively dysfunctional due to chronic stimulation (cell intrinsic) and whether being previously present in the tumour microenvironment influences their proliferative potential.

Following stimulation, the majority of CD4 (84.73% IQR 77.83-87.83) and CD8 (83.59% IQR 75.99-92.91) T cells underwent at least one division (Figure 17b). In addition, we found there was no significant difference in the proliferative potential of CD4 T cells vs. CD8 T cells regardless of whether they were stimulated (p=1.000) or not (p=1.000). This suggests proliferation is suppressed in both T cell subtypes within the tumour microenvironment. However, the inability to proliferate is reversed by signalling through the TCR with appropriate costimulation.

The extent of proliferation of CD4 and CD8 T cells was determined following TCR-dependant stimulation. A small proportion of unstimulated cells showed proliferation, with the majority of these cells undergoing a single cycle of cell division (CD4: 2.48% out of 3.83%, CD8 1.74% out of 1.91%). This suggests cells directly isolated from the tumour have a very low proliferative potential. In contrast, the majority of *in vitro* stimulated CD4 and CD8 T cells isolated from TGCTs underwent multiple rounds of cell division (Figure 17). Combined, this suggests that T cells isolated from TGCTs are not incapable of proliferation, but are inhibited in doing so directly by the tumour and/or the milieu.

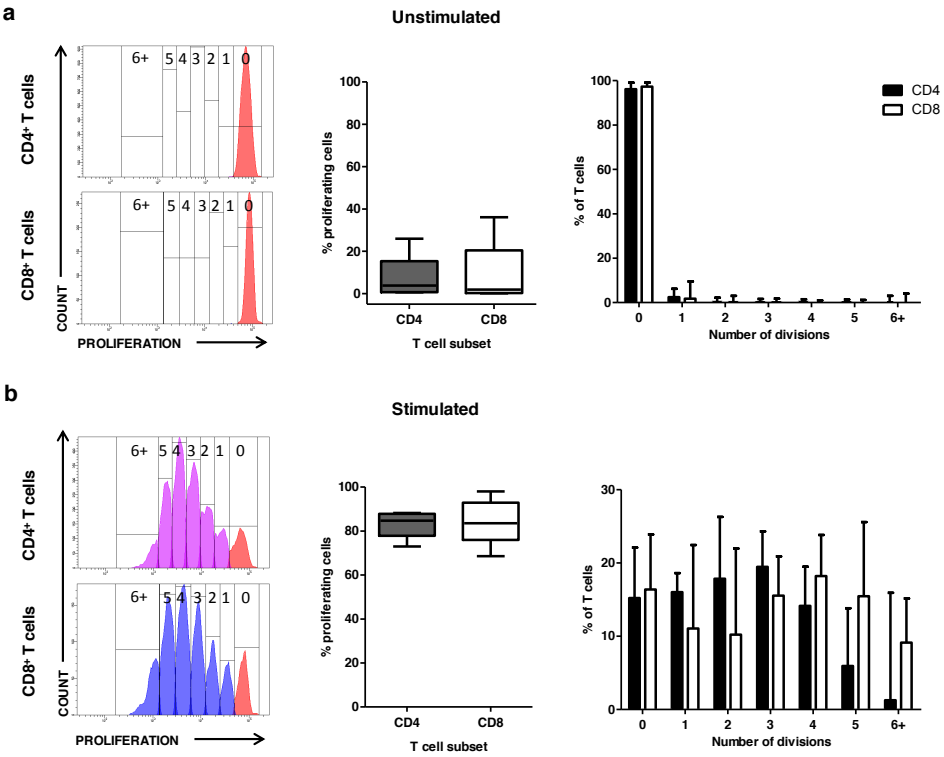
a
Unstimulated
CD4+ T cells
CD8+ T cells
6+ 5 4 3 2 1 0
COUNT
PROLIFERATION
% proliferating cells
CD4
CD8
T cell subset
% of T cells
Number of divisions
b
Stimulated

Figure 17. T cells isolated from TGCT tissues have a high proliferative capacity.
Representative histograms (left) show the numbers of cell divisions of unstimulated (a) and stimulated (CD3/CD28 Dynabeads + IL-2) CD4 and CD8 T cells (b). Each peak (CD4, purple; CD8, blue) represents a cell division. Red peaks represent non-dividing cells. Percentages of total proliferating CD4 and CD8 T cells when unstimulated and stimulated are shown (middle). Box represents 25^{th} and 75^{th} percentile, line represents median, and whiskers represent 10-90 percentile. Percentages of T cells that have undergone 0 to 6^{+} divisions when unstimulated or stimulated were determined (right). Black bars represent CD4 T cells; white bars represent CD8 T cells. Bars represent median. Error bars indicate upper quartile. Data analysed by Wilcoxon matched-pairs signed-rank test.

Oligoclonal Populations of T Cells Develop within TGCT Lesions

We hypothesise that T cells infiltrating TGCT are tumour specific. Consequently, we would expect oligoclonal populations of tumour specific cells to accumulate within the tumour mass. If this were true the TCR Vβ usage in TIL would be different to that of PBMC. We compared the CD3+ TCR Vβ repertoire of PBMC with that of TIL by flow cytometry using a commercially available antibody kit. Figure 18 demonstrates the gating strategy used to quantify the proportion of cells expressing a particular Vβ chain.

We examined the clonality of T cells isolated from matched peripheral blood and TIL in NSGCTT (n=1), mGCT (n=1) and seminoma (n=3) patients. Figure 19a illustrates the proportion of each Vβ family represented in PBMC and TIL expressed as a percentage of total T cells in a NSGCTT, mGCT and Seminoma patient. Clear differences were observed in the Vβ repertoire in all tumour types examined, and the data is summarised in the form of a discontinuous heat map (Figure 19b). Our results show that a median of 11 Vβ families (range: 6-12) are enriched in TIL when compared to matched peripheral blood, and that this can be an increase in excess of 200%. As expected, large increases in particular Vβ families in TIL were reciprocated with large reductions in other Vβ families. The greatest difference was observed in a NSGCTT patient who had an increase of 265% in Vβ13.1 T cells, which made up 11.6% of the total T cell infiltrate. Similar increases in this particular Vβ family were observed in 4 out of 5 patients. Vβ families 17 and 13.6 were increased in all patients examined, while Vβ18 was always at lower levels in TIL compared to PBMC. The results indicate that oligoclonal populations of T cells within TGCT do exist, suggestive of clonal expansion of tumour-specific T cells to multiple epitopes.

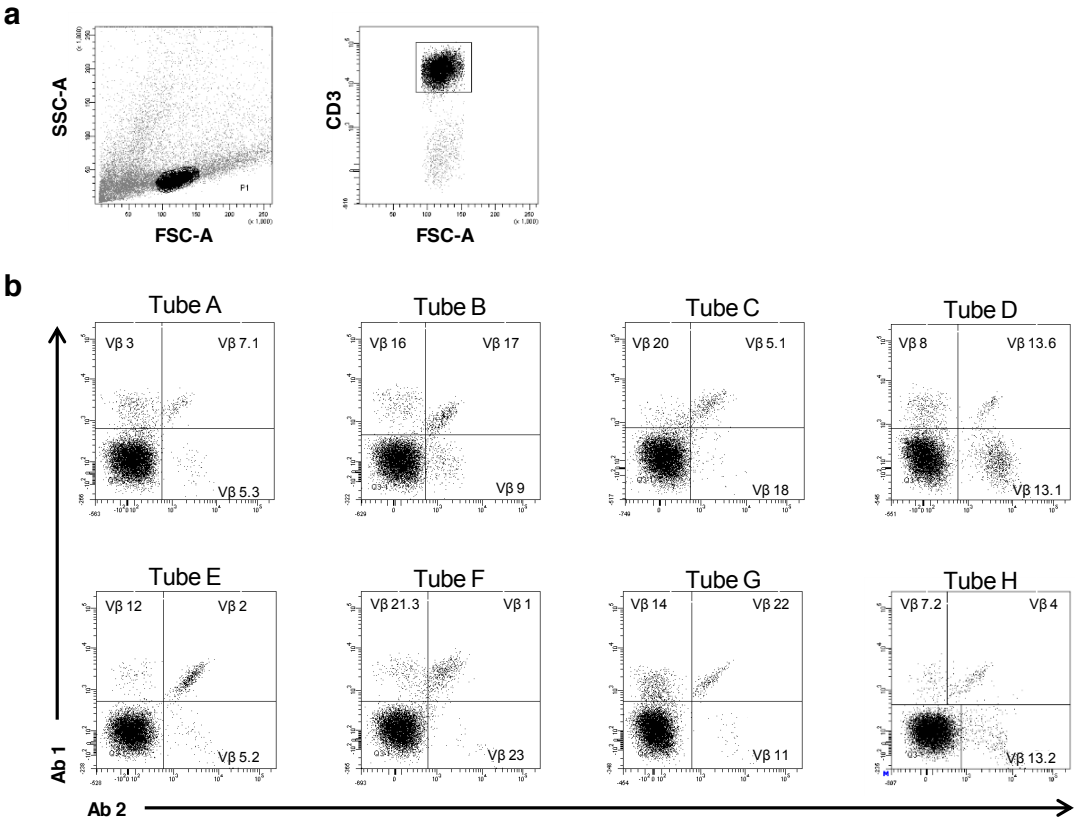

Figure 18. Flow cytometric analysis of Vβ usage.
Total CD3⁺ T cells were analysed (a). Cells were stained with a cocktail of Vβ monoclonal antibodies, all conjugated to different fluorochromes. The dot plots depict the quantitative analysis of the TCR Vβ repertoire of T cells from PBMC in a representative TGCT patient (b). Quadrants show the indicated Vβ families.

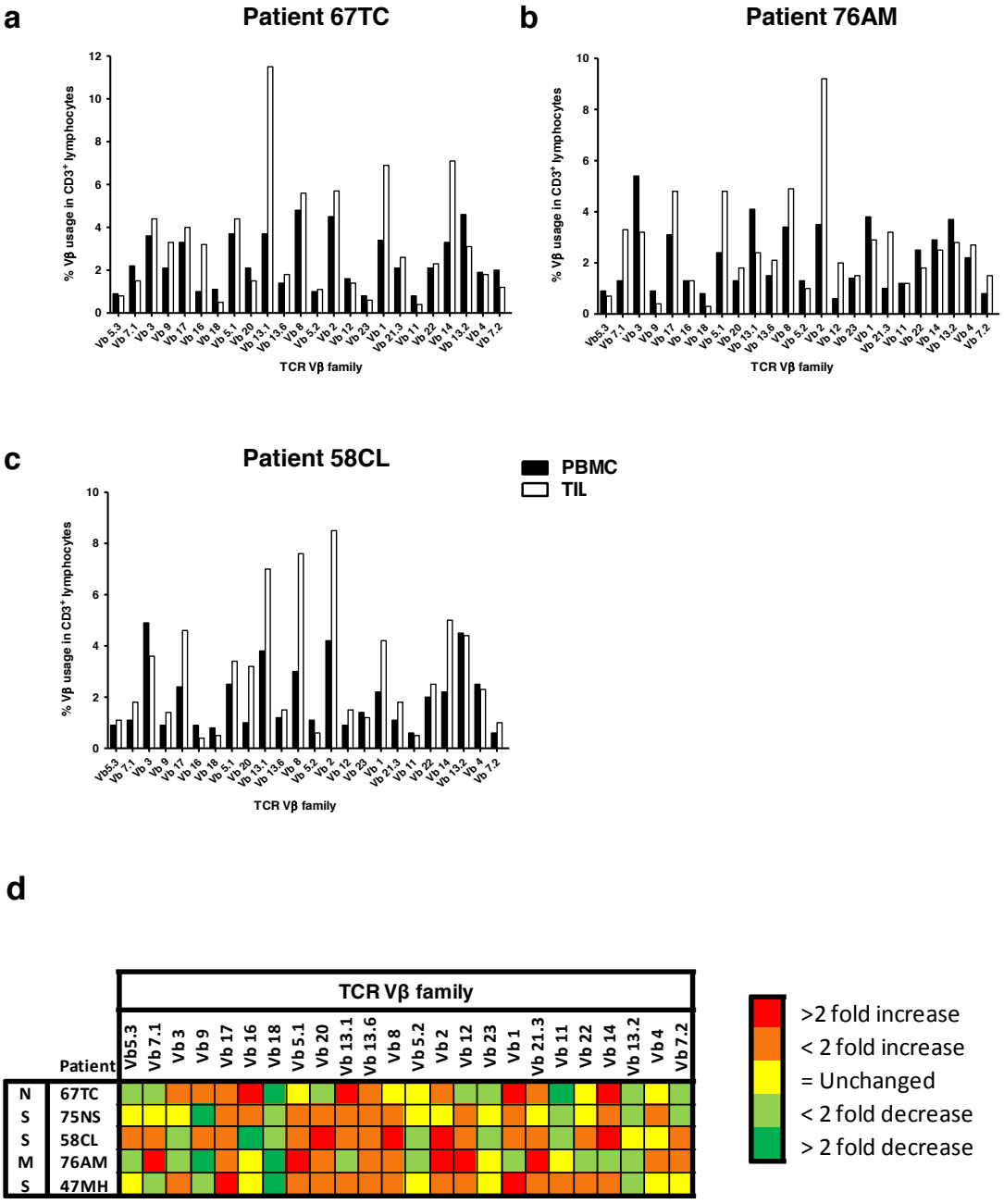

Figure 19. The clonality of tumour infiltrating T cells.

The proportion of each Vβ family is represented as a percentage of total T cells. The representative bar charts compare the frequency of each Vβ family in PBMC (filled bar) and TIL (open bar), for a NSGCTT (a), mGCT (b), and Seminoma (c) patient. Each graph represents a single patient. The discontinuous heat map demonstrates the degree of change in TIL of each Vβ family, compared to PBMC (d). N, NSGCTT; S, Seminoma; M, mGCT.

TGCTs Contain Inflammatory Cytokine Secreting T Cells

We have determined that CD4 and CD8 T cells infiltrating TGCTs are activated; antigen experienced and presumably clonally expanded cells. Next, we determined whether T cells isolated directly from the tumour were producing IFNγ and TNFα by intracellular cytokine staining. Flow cytometric analysis revealed that inflammatory cytokines are not produced by T cells without *in vitro* stimulation (Figure 20a), suggesting cells are not producing inflammatory cytokine within the tumour mass.

Stimulation with PMA/Ionomycin followed by intracellular staining for the cytokines IFNγ and TNFα was performed on CD4 and CD8 T cells from TIL, to verify that these cells are able to produce cytokine. Both CD4 and CD8 TIL release IFNγ and TNFα following *in vitro* stimulation (Figure 20b), suggesting these cells are able to produce cytokine but their ability to do this *in vivo* is repressed. We used the same stimulation protocol to define and quantify inflammatory T cell effector subsets. Cytotoxic CD8 T cells and CD4 Th1 cells can be classified by the production of IFNγ and TNFα. The cytokine profile of CD4 T cells (Figure 20c) and CD8 T cells (Figure 20d) from TIL was compared to that of autologous PBMC. We examined the proportion of dual cytokine secreting T cells ($IFN\gamma^{+}TNF\alpha^{+}$) as well as single cytokine secretors ($IFN\gamma^{+}TNF\alpha^{-}$ or $IFN\gamma^{-}TNF\alpha^{+}$), and non-secretors ($IFN\gamma^{-}TNF\alpha^{-}$). There was no significant difference in the cytokine profile of T cells isolated from the tumour compared to those from peripheral blood (Table 19). Our results suggest the effector function of CD4 and CD8 TIL may be compromised within the tumour but, similarly to that observed with proliferative capacity of TIL, it can be rescued with additional stimulation *in vitro*.

Tumour Infiltrating T Cells Have Cytotoxic Capacity

Our results indicate that T cells isolated from TGCT tissue are able to produce inflammatory cytokines upon stimulation. Next, we examined the cytotoxicity of T cells by measuring CD107a surface expression. CD107a is transiently mobilised to the surface of T cells as a prerequisite of degranulation in response to stimulus (Betts *et al*., 2003). CD107a was examined on the surface of CD4 and CD8 TIL and compared with that of autologous PBMC, following stimulation with PMA/Ionomycin (n=4) (Figure 21).

There was a significant increase in the proportion of both CD107a expressing CD4 and CD8 T cells in TIL (CD4, 24.83 IQR: 22.80-51.67; CD8, 48.70 IQR: 40.67-71.99) compared to PBMC (CD4, 2.59 IQR: 1.30-2.97; CD8, 10.20 IQR: 8.78-15.89) ($p=0.0286$) with CD4 T cells isolated from PBMC having the least potential to degranulate. Stimulated CD8 T cells from TIL had a greater proportion of $CD107a^+$ cells than CD4 T cells (Figure 21c) ($p=0.0579$); an observation which could be explained by the natural cytotoxicity of CD8 T cells. These results suggest cytotoxic activity of CD8 T cells isolated from TIL remains, and that CD4 T cells may acquire this activity within the tumour as illustrated by an increased ability to degranulate when compared to healthy PBMC controls.

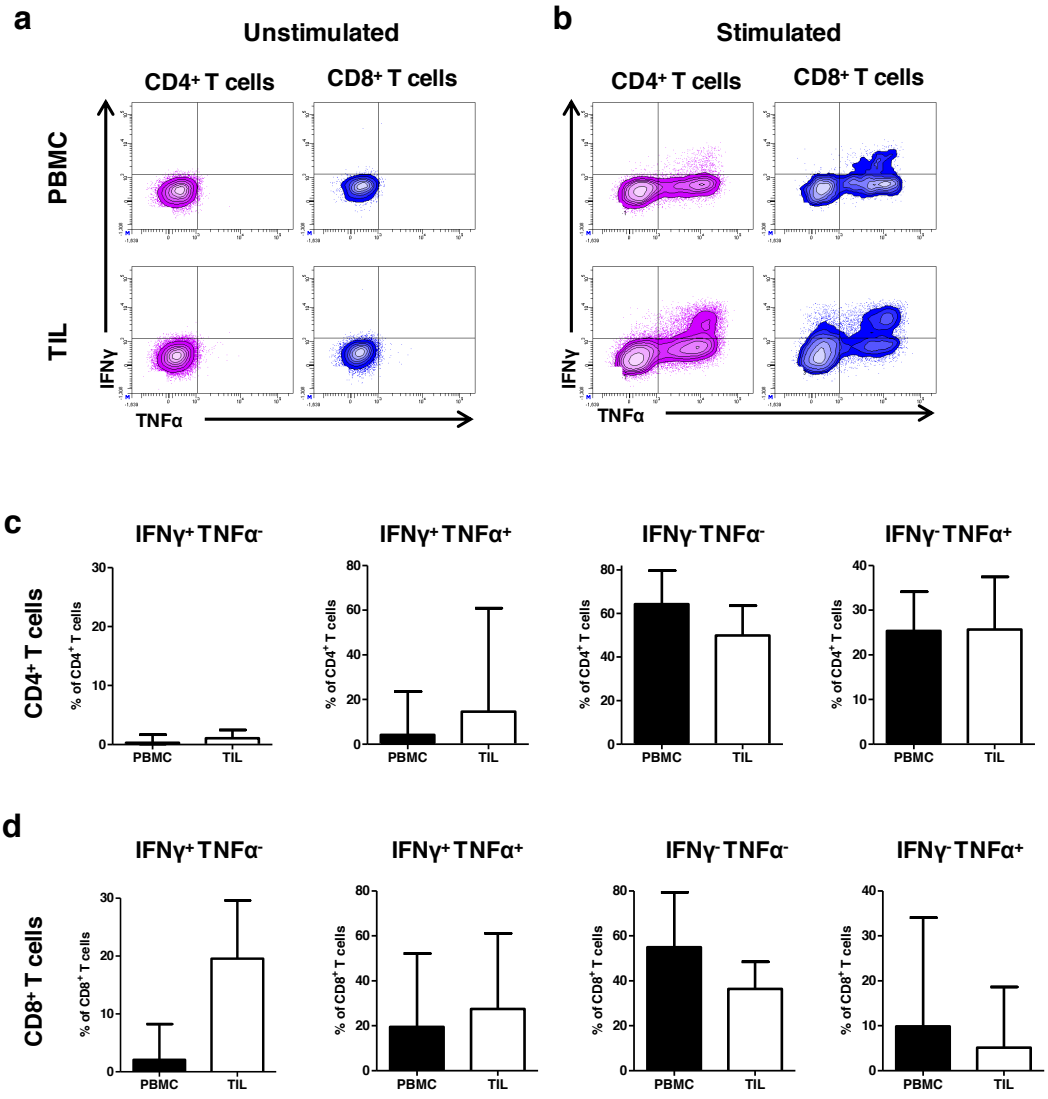

Figure 20. Secretion of inflammatory cytokines by tumour infiltrating T cells following stimulation.

IFNγ and TNFα release is shown for unstimulated (a) and PMA/Ionomycin stimulated (b) CD4 and CD8 T cells from TIL and autologous PBMC. Bar graphs compare the percentage of total CD4 (c) and CD8 T cells (d) from PBMC and TIL that are IFNγ^{+}TNFα^{-}, IFNγ^{+}TNFα^{+}, IFNγ^{-}TNFα^{-} and IFNγ^{-}TNFα^{+} following PMA/Ionomycin stimulation. Bars show median. Error bars indicate upper quartile range. All data analysed by Wilcoxon matched-pairs signed-rank test.

Table 19. Single and dual cytokine secretion of tumour infiltrating T cells.

	CD4 (n=4)							CD8 (n=4)						
	PBMC			TIL			p	PBMC			TIL			p
	Median	25th	75th	Median	25th	75th		Median	25th	75th	Median	25th	75th	
IFNγ⁺TNFα⁻	**0.28**	0.08	1.68	**1.07**	0.85	2.46	0.1250	**2.08**	1.04	8.25	**19.54**	13.42	29.61	0.1250
IFNγ⁺TNFα⁺	**4.13**	1.12	23.59	**14.55**	11.31	60.88	0.1250	**19.51**	5.40	52.17	**27.53**	23.82	61.15	0.2500
IFNγ⁻TNFα⁻	**64.72**	46.99	79.67	**49.95**	20.99	63.53	0.1250	**55.00**	27.30	79.38	**36.42**	13.19	48.44	0.1250
IFNγ⁻TNFα⁺	**25.39**	18.65	34.14	**25.69**	11.30	37.43	0.8750	**9.84**	5.97	34.06	**5.16**	3.09	18.63	0.1250

Data expressed as median (bold) with 25th and 75th quartile.

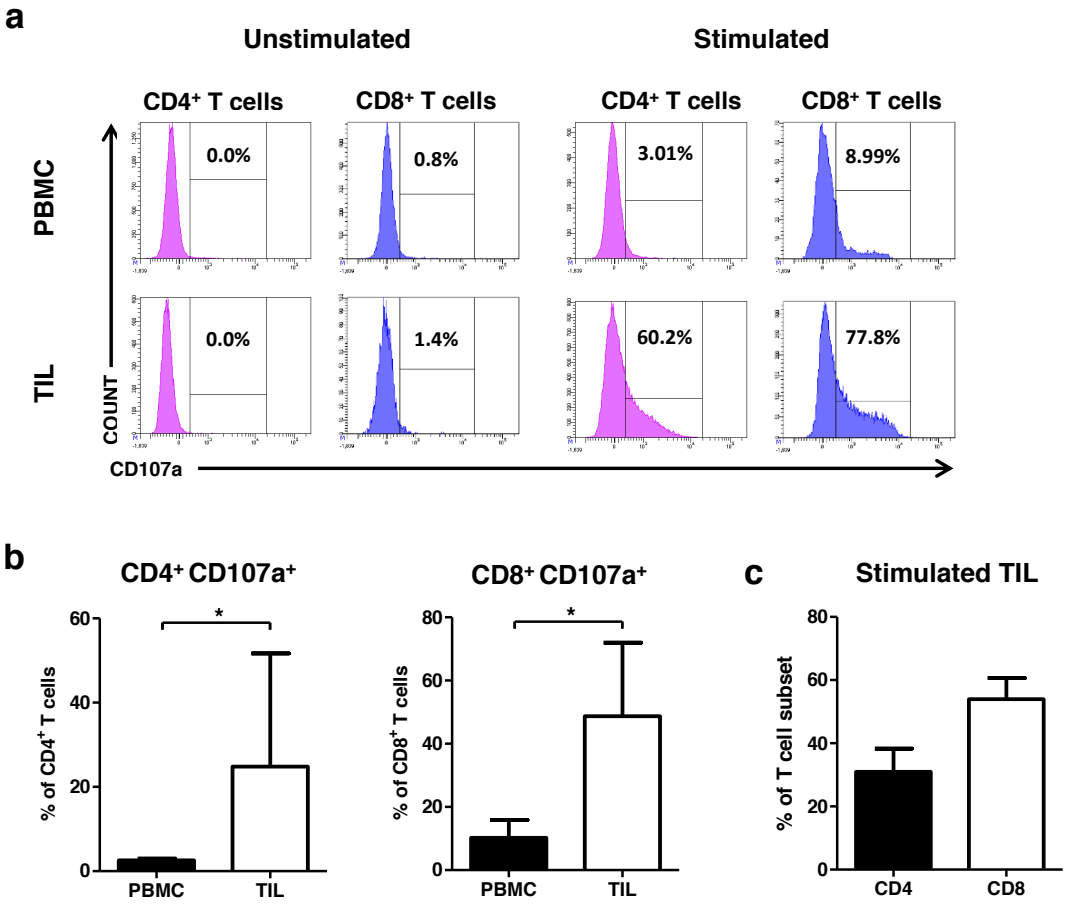

Figure 21. Degranulation of tumour infiltrating T cells.
CD107a expression was used as a marker of degranulation. Representative histograms show the expression levels of CD107a on CD4 and CD8 T cells from PBMC and TIL, with or without PMA/Ionomycin stimulation (a). Bar graphs compare median expression of CD107a on CD4 T cells and CD8 T cells (b) in PBMC and TIL. The proportion of $CD107a^+$ TIL was compared between CD4 and CD8 T cells (c). Error bars indicate upper quartile. Data analysed by Wilcoxon matched-pairs signed-rank test.* denotes $p<0.05$.

T Cells Infiltrating TGCTs Express Inhibitory Receptors

Negative regulatory receptors on the surface of T cells are upregulated following activation. If these receptors bind their respective ligands, T cell function becomes impaired (Barber *et al*., 2006, Freeman *et al*., 2000). Exhausted or dysfunctional T cells are regulated by multiple inhibitory receptors during an active immune response, which include the negative costimulatory receptors TIM-3 and PD-1. We examined the expression of these inhibitory receptors on CD4 and CD8 TIL and compared it to autologous PBMC (n=7) (Figure 22 and Table 20).

Both CD4 and CD8 TIL have increased expression of TIM-3 (Figure 22b) and PD-1 (Figure 22c), compared to autologous PBMC. In addition, the proportion of CD4 and CD8 T cells that were double positive for TIM-3 and PD-1 was significantly greater in TIL than PBMC (Figure 22d). In fact, double positive cells were practically absent in the peripheral blood of all patients examined. Moreover, the expression of both inhibitory receptors was more prominent on CD8 T cells (median: 18.01%) than CD4 T cells (median: 5.60%) in TIL.

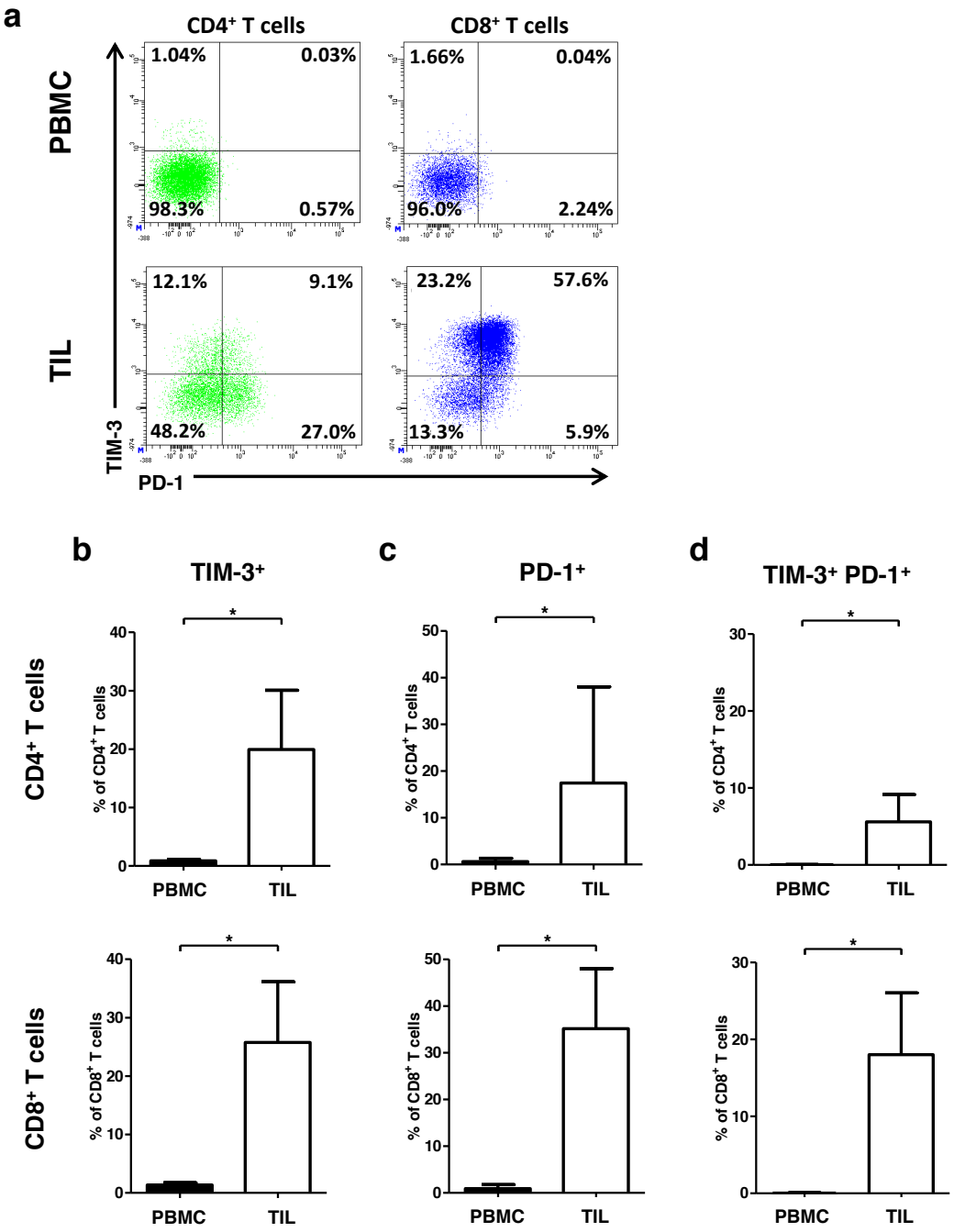

Figure 22. Expression of negative regulatory receptors on T cells from PBMC and TIL. TIM-3 and PD-1 expression was determined on CD4 and CD8 T cells from PBMC (filled bar) and TIL (open bar) by flow cytometry (a). Proportions of CD4 and CD8 T cells that are TIM-3$^+$, PD-1$^+$ or TIM-3$^+$PD-1$^+$ are shown (b). Bars represent median. Error bars represent upper quartile range. Data analysed by Wilcoxon matched-pairs signed-rank test, *denotes $p<0.05$.

Table 20. Expression of negative regulatory receptors on T cells from PBMC and TIL.

	CD4 (n=7)							CD8 (n=7)						
	PBMC			TIL			p	PBMC			TIL			p
	Median	25th	75th	Median	25th	75th		Median	25th	75th	Median	25th	75th	
TIM3⁺	**0.87**	0.38	1.11	**19.95**	9.54	30.08	***0.0156***	**1.37**	0.65	1.75	**25.74**	14.00	36.14	***0.0156***
PD-1⁺	**0.61**	0.23	1.31	**17.42**	7.22	38.02	***0.0156***	**0.91**	0.30	1.77	**35.14**	2.62	48.00	***0.0156***
TIM3⁺PD-1⁺	**0.04**	0.03	0.05	**5.60**	4.39	9.14	***0.0156***	**0.04**	0.01	0.08	**18.01**	2.29	26.05	***0.0156***

Data expressed as median (bold) with 25th and 75th quartile. Significant differences are highlighted in bold italic type.

TIM-3 Is Induced on CD8 T Cells Shortly After Chemotherapy

There was no significant difference in the expression of TIM-3 or PD-1 on CD4 and CD8 T cells between PBMC of seminoma patients and healthy controls (Figure 23 and Table 21). T cells expressing both inhibitory receptors were virtually undetectable in PBMC from TGCT patients and healthy controls, however, shortly after chemotherapy (2wks) TIM-3 was significantly upregulated on a proportion of CD8 T cells by up to 58% (Figure 24a, Table 22 and Table 23). Three months after chemotherapy, elevated levels of TIM-3 were not maintained and dropped to levels similar to those prior to chemotherapy. TIM-3 can be induced on T cells following activation (Canaday *et al*., 2013). Here we show a simultaneous increase in CD69 and TIM-3 expressing cells shortly after chemotherapy suggesting activation of cells may be induced by chemotherapy treatment.

PD-1 Expressing CD8 T Cells Decline Following Tumour Removal

A step wise decrease in PD-1 expression by CD8 T cells was observed over time post chemotherapy (Figure 24b), although statistical significance was not reached (Pre vs. 3M, p=0.0625). This is likely to be associated with the availability of tumour antigens following orchidectomy, and the decline in T_{EM} cells that may express this ligand. In contrast, no differences were observed in the CD4 T cell compartment for either inhibitory receptor.

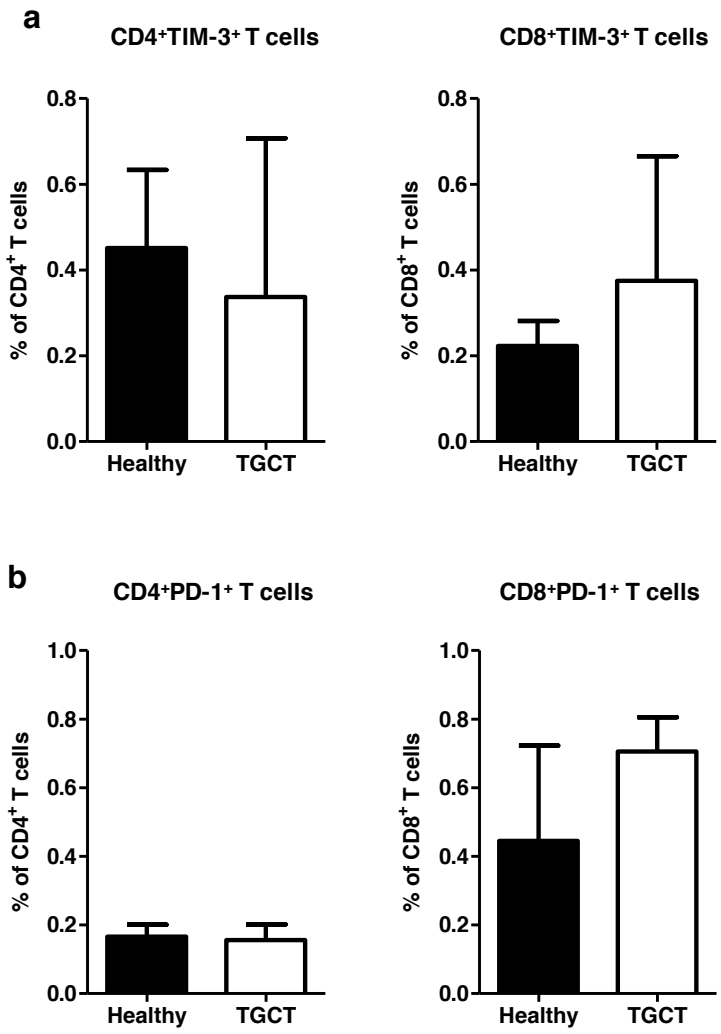

Figure 23. Expression of inhibitory receptors TIM-3 and PD-1 on peripheral blood CD4 and CD8 T cells of healthy donors and TGCT patients.

TIM-3 and PD-1 expression was determined on peripheral blood CD4 and CD8 T cells of healthy donors and TGCT patients. Proportions of CD4 and CD8 T cells that are TIM-3$^+$ (a) and PD-1$^+$ (b) are shown. Bars represent median. Error bars indicate upper quartile. Data analysed by Mann-Whitney test.

Table 21. Expression of inhibitory receptors TIM-3 and PD-1 on peripheral blood CD4 and CD8 T cells of healthy donors and TGCT patients.

	CD4							CD8						
	Healthy (n=13)			TGCT (n=15)			p	Healthy (n=13)			TGCT (n=15)			p
	Median	25th	75th	Median	25th	75th		Median	25th	75th	Median	25th	75th	
TIM3⁺	**0.45**	0.24	0.63	**0.34**	0.15	0.70	0.7125	**0.22**	0.15	0.28	**0.38**	0.17	0.67	0.0812
PD-1⁺	**0.17**	0.10	0.20	**0.17**	0.11	0.20	0.8178	**0.45**	0.36	0.72	**0.71**	0.38	0.80	0.3109

Data expressed as median (bold) with 25th and 75th quartile.

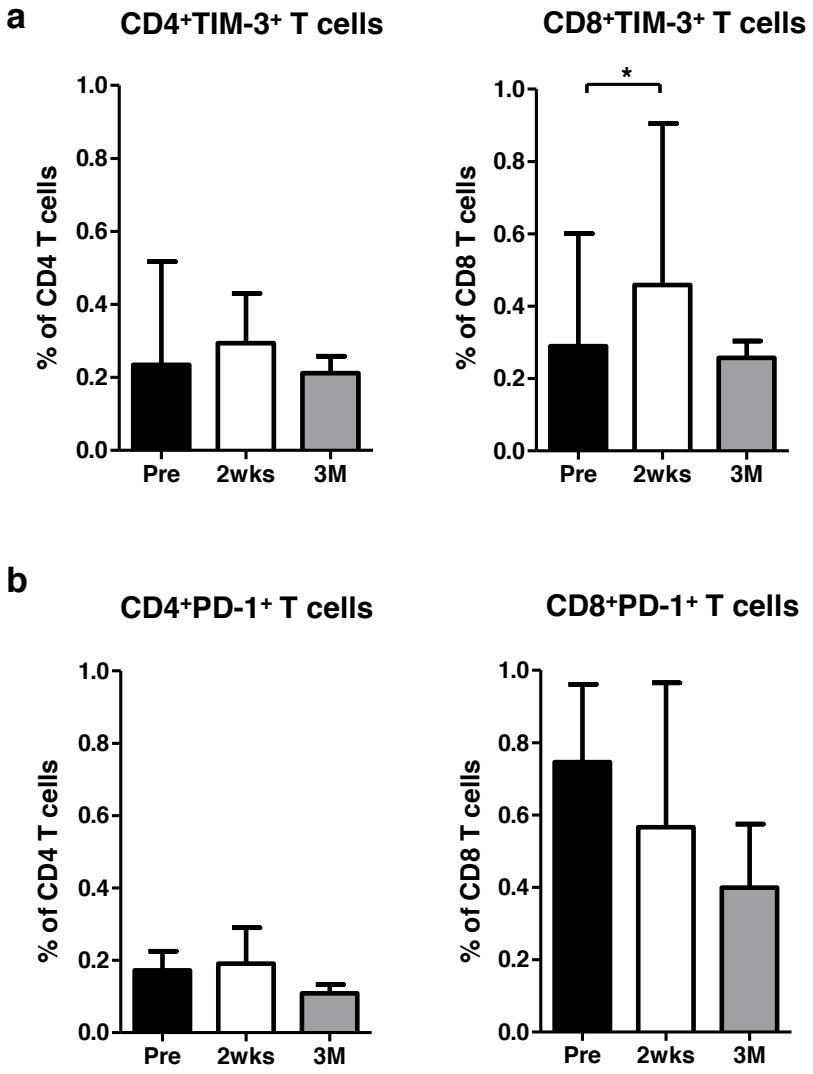

Figure 24. Expression of inhibitory receptors TIM-3 and PD-1 on peripheral blood CD4 and CD8 T cells following chemotherapy.

TIM-3 and PD-1 expression was determined on peripheral blood CD4 and CD8 T cells at pre, 2wks and 3M post chemotherapy by flow cytometry. Proportions of CD4 and CD8 T cells that are TIM-3$^+$ (a) and PD-1$^+$ (b) are shown. Bars represent median. Error bars indicate upper quartile. Data analysed by Wilcoxon matched-pairs signed-rank test, *denotes $p<0.05$.

Table 22. Expression of inhibitory receptors TIM-3 and PD-1 on peripheral blood CD4 and CD8 T cells following chemotherapy.

	Pre (n=10)			2wks (n=10)			3M (n=6)		
	Median	**25th**	**75th**	**Median**	**25th**	**75th**	**Median**	**25th**	**75th**
$CD4^+TIM\text{-}3^+$	**0.23**	0.12	0.52	**0.29**	0.17	0.43	**0.21**	0.15	0.26
$CD8^+TIM\text{-}3^+$	**0.29**	0.16	0.60	**0.46**	0.24	0.90	**0.26**	0.15	0.30
$CD4^+PD\text{-}1^+$	**0.17**	0.11	0.23	**0.19**	0.17	0.29	**0.11**	0.06	0.13
$CD8^+PD\text{-}1^+$	**0.75**	0.38	0.96	**0.57**	0.26	0.97	**0.40**	0.30	0.58

Data expressed as median (bold) with 25th and 75th quartile.

Table 23. p values for expression of inhibitory receptors TIM-3 and PD-1 on peripheral blood CD4 and CD8 T cells following chemotherapy.

	$CD4^+TIM\text{-}3^+$	$CD8^+TIM\text{-}3^+$	$CD4^+PD\text{-}1^+$	$CD8^+PD\text{-}1^+$
Pre vs. 2wks	0.4316	***0.0195***	0.3750	0.5566
Pre vs. 3M	0.4375	0.4325	0.0625	0.0625
2wks vs. 3M	1.000	0.8438	0.0625	0.4375

Significant differences are highlighted in bold italic type.

PD-1 Ligands Are Expressed in TGCT Tissue

A high proportion of tumour infiltrating CD4 and CD8 T cells express PD-1. Ligation of PD-1 by its ligands, PD-L1 or PD-L2, attenuates T cell function and induces cell cycle arrest (Bennett *et al*., 2003, Chemnitz *et al*., 2004, Latchman *et al*., 2001, Sharpe *et al*., 2007). Since we detect the expression of PD-1 on tumour infiltrating T cells, we investigated the expression of these corresponding ligands in a variety of primary TGCT tissues.

The level of PD-1 ligand transcripts was determined in fresh TGCT specimens and healthy testis following orchidectomy, using qRT-PCR analysis. Expression levels in tumour tissue were compared to healthy testis tissue and were normalised to GAPDH, using the $2^{-\Delta\Delta Ct}$ method. PD-L1 transcripts were found in all TGCTs examined, and were found at levels up to 2.5-fold higher than those in healthy testis (Figure 25a). In addition, all TGCT samples examined in this study exhibited increased PD-L2 expression when compared to normal testis (Figure 25b). The highest expression of both PD-1 ligands was generally found in seminoma tissues.

Next, we determined the expression and abundance of the PD-1 ligand, PD-L2, in TGCTs by Western blot and densitometry, respectively (Figure 26). Western blot analysis revealed protein expression in normal healthy testis and TGCT tissue. In all cases, protein expression was greater in TGCT tissue than in healthy testis. Transcript levels correlate well with protein abundance in seminoma and mGCT, but correlation was less clear in NSGCTT samples. Here, we demonstrate for the first time that TGCTs express PD-1 ligands, which may have a detrimental effect on anti-tumour T cell responses, thus contributing to tumour evasion mechanisms.

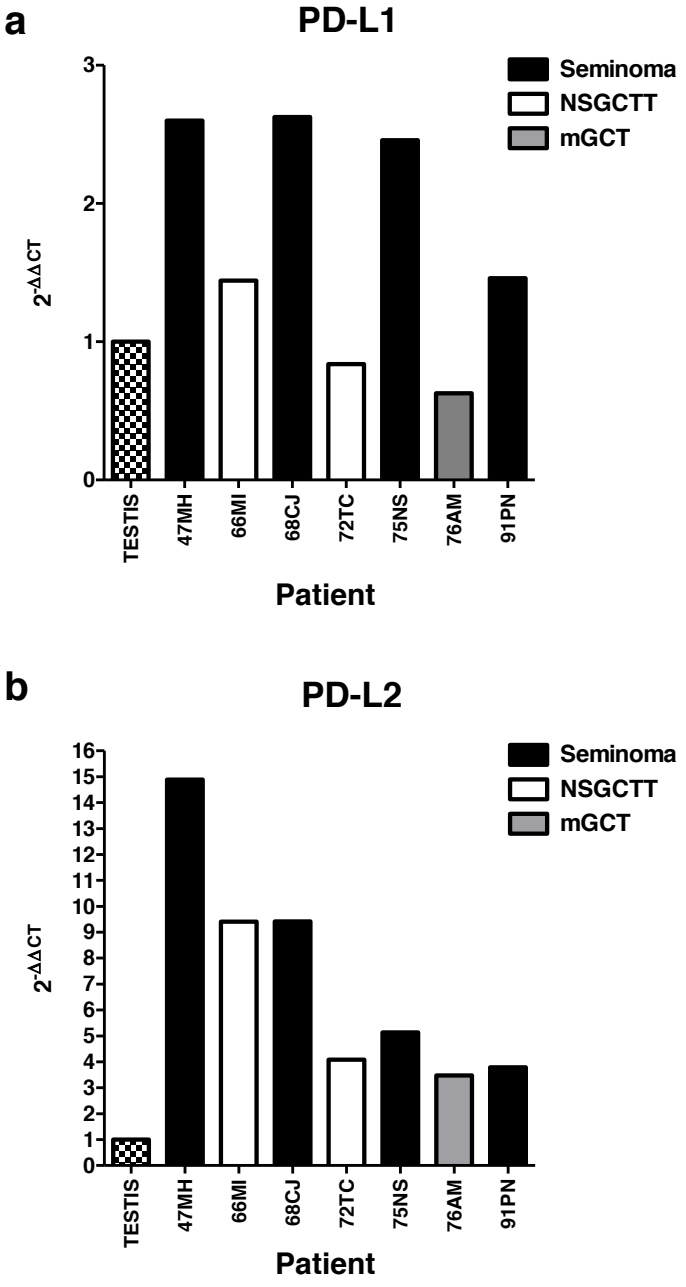

Figure 25. Expression of PD-1 ligands in primary TGCT tissue.
The mRNA levels of PD-L1 (a), and PD-L2 (b) were determined by qRT-PCR. Each bars represent relative expression levels of individual patients. "TESTIS" represents the mean expression level in normal testis tissue of 3 patients. Expression is relative to testis and normalised to GAPDH. Each bar represents an individual patient.

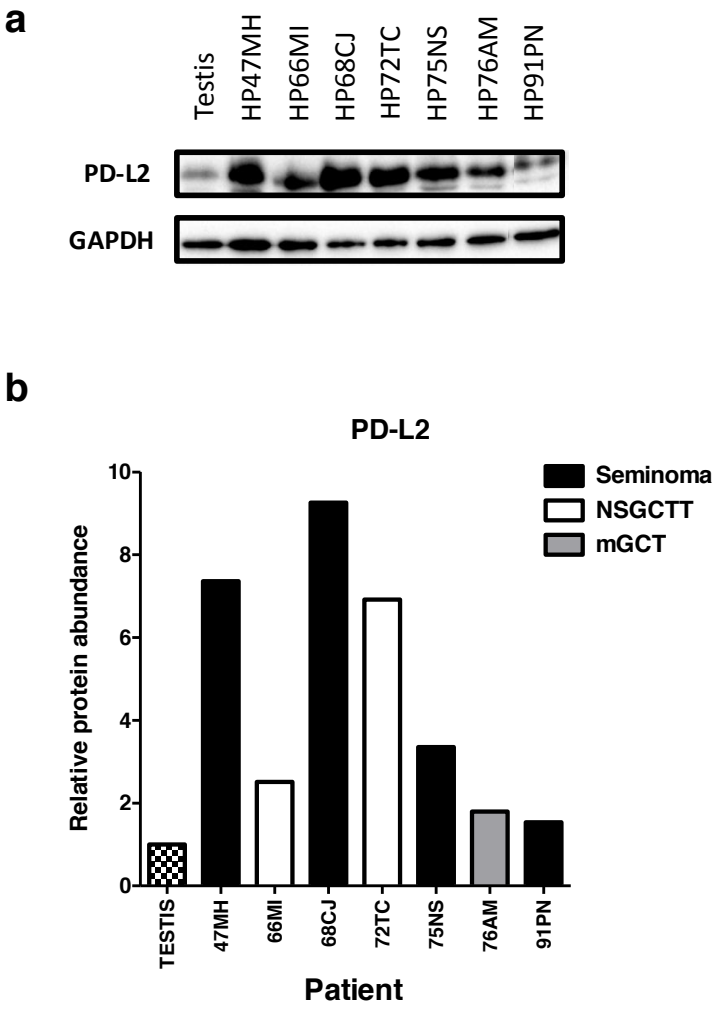

Figure 26. Expression of PD-L2 protein in primary TGCT tissue.
Western blot analysis was used for the detection of PD-L2 protein expression in TGCT tissue (a). GAPDH was used as a loading control and to determine relative protein abundance between patients. Relative abundance of PD-L2 was calculated by densitometry, relative to testis, and normalised to GAPDH (b). Each bar represents an individual patient.

Tumour Infiltrating NK Cells Are Predominantly $CD56^{hi}CD16^{-}$ NK Cells

We have demonstrated that T cells infiltrating TGCTs are antigen experienced, activated and are potentially capable of cytotoxic function under the appropriate stimulation. Since MHC expression on TGCTs may be low or absent (Hadrup *et al*., 2006), NK cells may play an important role in the recognition and subsequent cytolysis of tumour cells.

Expression of CD56 and CD16 define two subsets of NK cells found in peripheral blood: $CD56^{low}CD16^{+}$ and $CD56^{hi}CD16^{-}$. We have used flow cytometry to identify both NK cell subsets in PBMC and TIL (Figure 27). In the cohort of patients used in this study, we identify approximately 6.7 (IQR: 3.43-7.76) T cells for every NK cell in PBMC, compared to 60.1 (IQR: 23.01-109.4) T cells for every NK cell in TIL (Figure 28a). This difference in T cell to NK cell ratio in PBMC and TIL is highly significant (p=0.0078). Moreover, the $CD56^{low}CD16^{+}$ subset dominate in PBMC (95.43%, IQR: 88.93-97.26%), yet only a minority of this subtype are observed in TIL (36.78% IQR: 27.92-47.35%) (p=0.0078), therefore the NK cells infiltrating TGCTs are predominantly $CD56^{hi}CD16^{-}$ (Figure 28b). Even though NK cells comprise only a small proportion of infiltrating lymphocytes, their ability to recognise and respond effectively to tumour cells makes them an important cell type within TGCTs.

Next, we determined whether the increased proportions of $CD56^{hi}CD16^{-}$ NK cells in TIL was also evident in the periphery. We determined the proportion of each NK cell subset in peripheral blood of TGCT patients and healthy controls. There was no difference in the proportion of peripheral blood NK cell subsets between TGCT patients and healthy controls (Figure 28c).

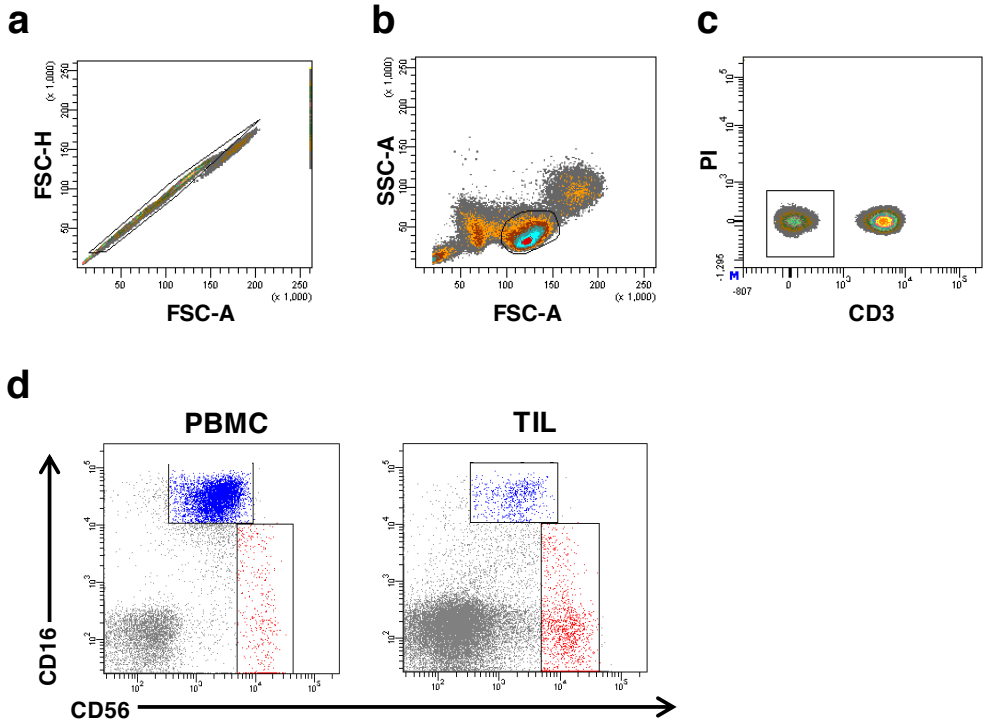

Figure 27. Gating strategy for identification of NK cell subsets.
Doublets were excluded (a) and FSC-A and SSC-A properties were used to set the lymphocyte gate (b) Only live cells (PI negative) which lacked expression of CD3 were analysed (c). Expression of CD56 and CD16 define two subsets of NK cells in PBMC and TIL (d); $CD56^{low}CD16^{+}$ (blue), $CD56^{hi}CD16^{-}$ (red).

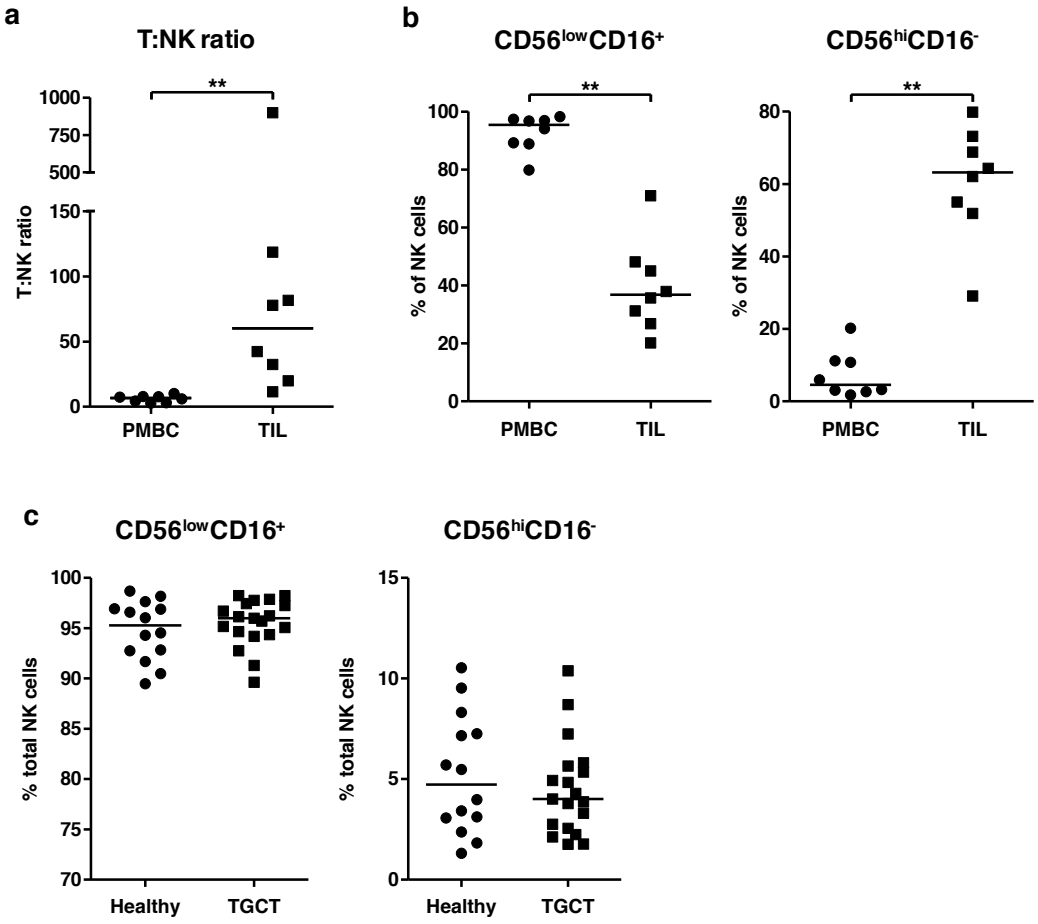

Figure 28. Comparison of NK cell subsets in PBMC and TIL.
Comparison of the proportions of NK and $CD3^+$T cells in PBMC and TIL expressed as the T cell:NK cell ratio (a). The proportion of $CD56^{low}CD16^+$ and $CD56^{hi}CD16^-$ NK cells in PBMC and TIL were compared and represented as a percentage of total NK cells (b). The proportion of $CD56^{low}CD16^+$ and $CD56^{hi}CD16^-$ NK cells in healthy donors and TGCT patients represented as a percentage of total NK cells (c). Each symbol represents an individual patient. Horizontal lines represent median. Horizontal line represents the median. Data analysed by Wilcoxon matched-pairs signed-rank test (a,b) or Mann-Whitney test (c). ** denotes $p<0.01$.

NKG2D is Downregulated on Tumour Infiltrating NK Cells

NKG2D is an activating cell surface receptor which can mediate NK cell cytotoxicity against tumour cells which express its corresponding ligand(s). Tumour induced down-regulation of NKG2D on NK cells has been shown to aid tumour immune evasion (Wiemann *et al*., 2005). Accordingly, we determined the density of NKG2D expression on the surface of NK cells, and compared this to peripheral blood NK cells. MFI was used to determine the density of NKG2D molecules on the surface of cells.

NKG2D cell surface density was markedly reduced on the $CD56^{low}CD16^{+}$ NK subset in TIL (MFI 832 IQR: 595-1239), compared to PBMC (MFI 2004 IQR: 1251-2196) ($p=0.0313$). The downregulation of NKG2D was even more pronounced in the $CD56^{hi}CD16^{-}$ subset of TIL (MFI 779 IQR: 547-1077), compared to PBMC (MFI 2867 IQR: 2123-3247) ($p=0.0022$). There was no difference in NKG2D expression between either NK subset in TIL (Figure 29a,b), suggesting downregulation of NKG2D in both NK subsets to similarly low levels.

We show a greater level of expression of NKG2D on $CD56^{hi}CD16^{-}$ NK cells in PBMC from both TGCT patients and healthy donors ($p=0.0313$) (Figure 29c). This suggests NKG2D expression is universally higher on peripheral blood derived $CD56^{hi}CD16^{-}$ NK cells, and is therefore not likely to be a direct consequence of testicular tumour development.

We analysed the proportions of both NK cell subsets in peripheral blood of TGCT patients before chemotherapy, 2wks and 3 months post treatment. There was no statistical difference in the proportion of either NK cell subset between these time points (Figure 30a), suggesting neither the loss of tumour antigens nor chemotherapy alter NK cell subset ratios.

Furthermore, we determined NKG2D expression on NK cells at the same intervals pre and post chemotherapy. Interestingly, we detected a stepwise increase in NKG2D expression on $CD56^{hi}CD16^{-}$ NK cells, which was statistically significant between pre and 3 months post chemotherapy ($p=0.0313$) (Figure 30b). This may indicate that NK cells within the tumour, which have significantly reduced NKG2D expression, may re-enter circulation during tumour development subsequently lowering NKG2D MFI. Following tumour removal, these cells are not subjected to NKG2D downregulation, leading to a gradual increase of NKG2D density on NK cells over time.

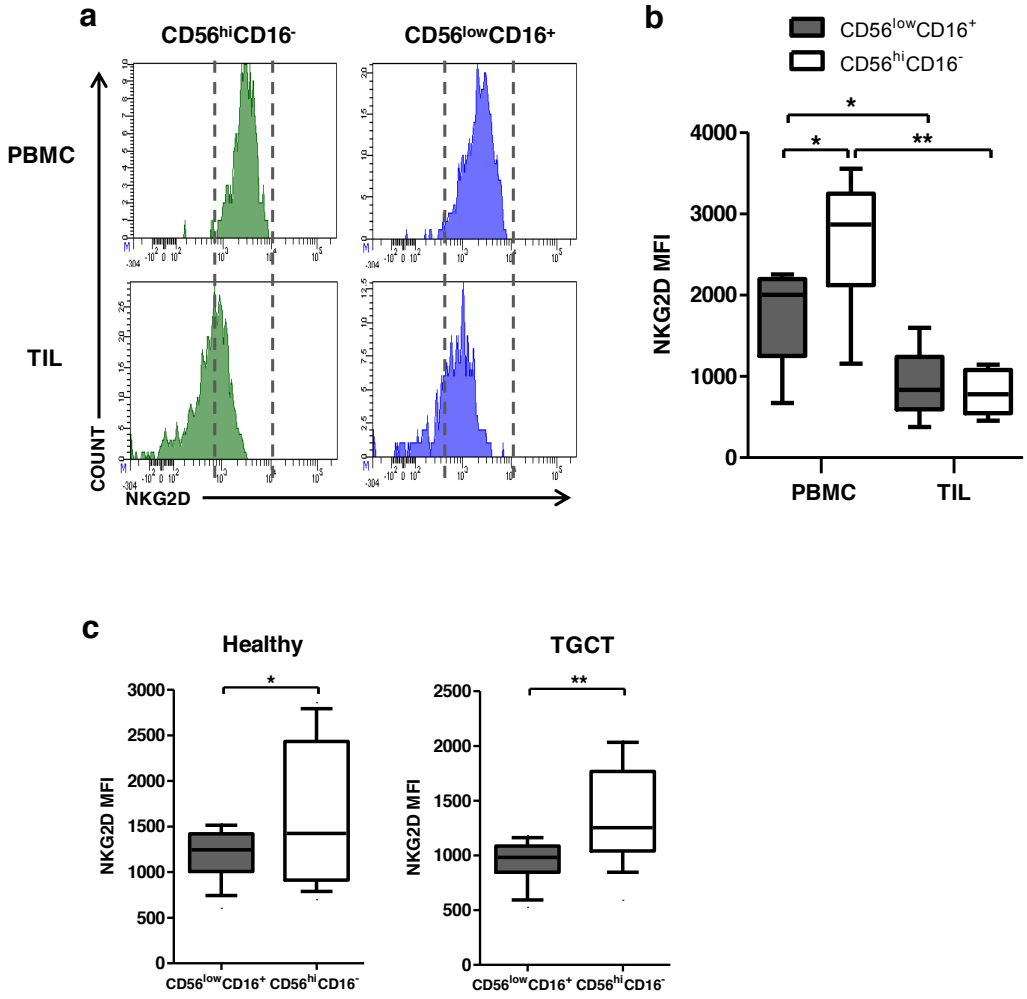

Figure 29. NKG2D expression on NK cell subsets from PBMC and TIL.
Differential expression of NKG2D is shown for both NK subsets (a). Comparison of NKG2D MFI on $CD56^{low}CD16^{+}$ and $CD56^{hi}CD16^{-}$ cells within PBMC and TIL is shown (b). Comparison between NKG2D MFI on $CD56^{low}CD16^{+}$ and $CD56^{hi}CD16^{-}$ NK cells in healthy donors and TGCT patients (c). Box represents 25th and 75th percentile, line represents median, and whiskers represent 10-90 percentile. Data analysed by Wilcoxon matched-pairs signed-rank test (b) or Mann-Whitney test (c). *denotes $p<0.05$, ** denotes $p<0.01$.

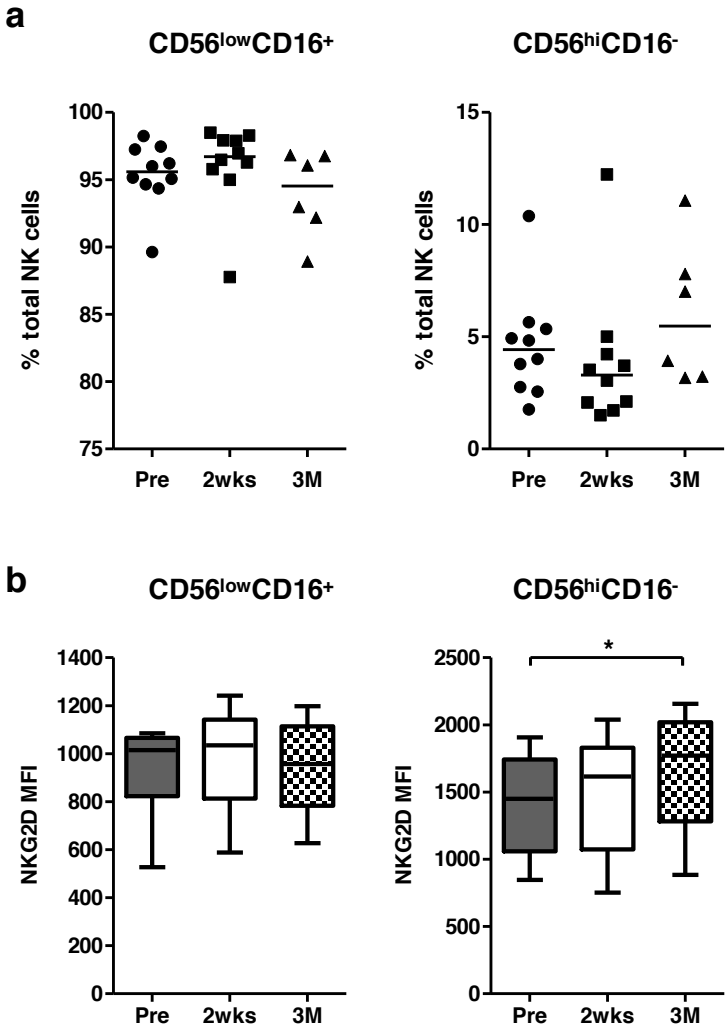

Figure 30. Changes in the proportion of NK cell subsets and NKG2D expression following chemotherapy.

The proportion of $CD56^{low}CD16^{+}$ and $CD56^{hi}CD16^{-}$ NK cells at pre, 2wks and 3M post chemotherapy (a). Each symbol represents an individual patient. Horizontal lines represent median. Comparison of NKG2D MFI on $CD56^{low}CD16^{+}$ and $CD56^{hi}CD16^{-}$ NK cells at pre, 2wks and 3M post chemotherapy is shown (b). Box represents 25^{th} and 75^{th} percentile, line represents median, and whiskers represent 10-90 percentile. Data analysed by Wilcoxon matched-pairs signed-rank test, *denotes $p<0.05$.

Tumour Infiltrating NK Cells are Functional

Next, we examined the functionality of NK cells isolated from TGCTs using an *in vitro* co-culture method with an MHC-deficient tumour cell line (K562), and measured cytokine production and cytotoxic capacity (degranulation). Degranulation was determined by the mobilisation of CD107a to the surface of NK cells, as assessed by flow cytometry. Noticeably, CD56 expression on the $CD16^{+}$ subset of NK cells was increased following tumour cell co-culture presumably due to *in vitro* culture conditions.

IFNγ and TNFα production was detected only in the $CD56^{hi}CD16^{-}$ subset of NK cells (Figure 31a). Both NK subsets degranulated in response to K562 co-culture (Figure 31b). T cells were used as a negative control and as expected, did not secrete cytokine (data not shown) or degranulate in response to K562 co-culture (Figure 31c). Unexpectedly, the proportion of NK cells which mobilise CD107a upon stimulation was significantly higher in the $CD56^{hi}CD16^{-}$ (61.60% IQR: 48.38-64.44%) subset than in the $CD56^{low}CD16^{+}$ (20.78% IQR: 17.03-25.62) subset ($p=0.0079$) (Figure 32a). Generally, peripheral blood derived $CD56^{low}CD16^{+}$ NK cells are naturally cytotoxic, whereas the $CD56^{hi}CD16^{-}$ subset has low natural cytotoxicity, the opposite to what we observe in NK cells isolated from TGCTs.

In a smaller cohort of patients (n=3), we determined whether the difference in cytotoxic potential of both NK cell subsets was consistent at different Effector:Target ratios (Figure 32b). At all NK:K562 ratios examined the $CD56^{hi}CD16^{-}$ subset had increased expression of CD107a in comparison to its $CD16^{+}$ counterpart. Degranulation was greatest at an E:T ratio of 1:5 for both NK subsets. Two-way ANOVA statistical analysis revealed that NK cell phenotype accounts for 48.66% of total variance ($p<0.0001$) and E:T ratio accounts for

26.81% of total variance (p=0.0032). A Bonferroni post hoc analysis indicated that differences were significantly different for ratios of 1:1, 1:5, and 1:10. Although statistical significance was not reached for ratios of 5:1 and 10:1, there was a clear trend towards greater cytotoxicity in the $CD56^{hi}CD16^{-}$ subset. This data suggests that NK cells within TGCT lesions have the potential to lyse tumour cells under the appropriate stimulus, and the $CD56^{hi}CD16^{-}$ subset shows the greatest cytotoxic potential.

The co-culture method used involved resting NK cells in media supplemented with IL-2. High dose IL-2 induces lymphokine-activated killer (LAK) activity in NK cells enabling them to effectively kill Daudi cells, which are otherwise resistant to NK cell lytic activity. The generation of LAK cells has been demonstrated *in vitro*, but their development *in vivo* is highly speculative. To confirm cytotoxicity was specifically induced by the NK cell subsets described and not due to the development of LAK cells, we co-cultured rested NK cells with the Daudi cell line at a ratio of 1:1, and assessed the extent of degranulation.

All tumour infiltrating NK cells had greatly diminished cytotoxic responses towards the Daudi cell line compared to the K562 cell line (Figure 33). CD107a upregulation was virtually absent on the $CD56^{low}CD16^{+}$ subset following stimulation with Daudi cells (mean 1.63%; SEM 1.21). Surface expression was marginally higher on the $CD56^{hi}CD16^{-}$ subset following Daudi cell co-culture (mean 6.68%; SEM 2.25). Nevertheless, the difference in expression of CD107a between the Daudi and K562 cell lines was highly significant for the $CD56^{low}CD16^{+}$ (p=0.0052) and the $CD56^{hi}CD16^{-}$ (p=0.001) subset. In conclusion, NK cells do not degranulate in response to Daudi cell stimulation, suggesting tumour infiltrating NK cells do not acquire LAK activity following short term culture or within the tumour.

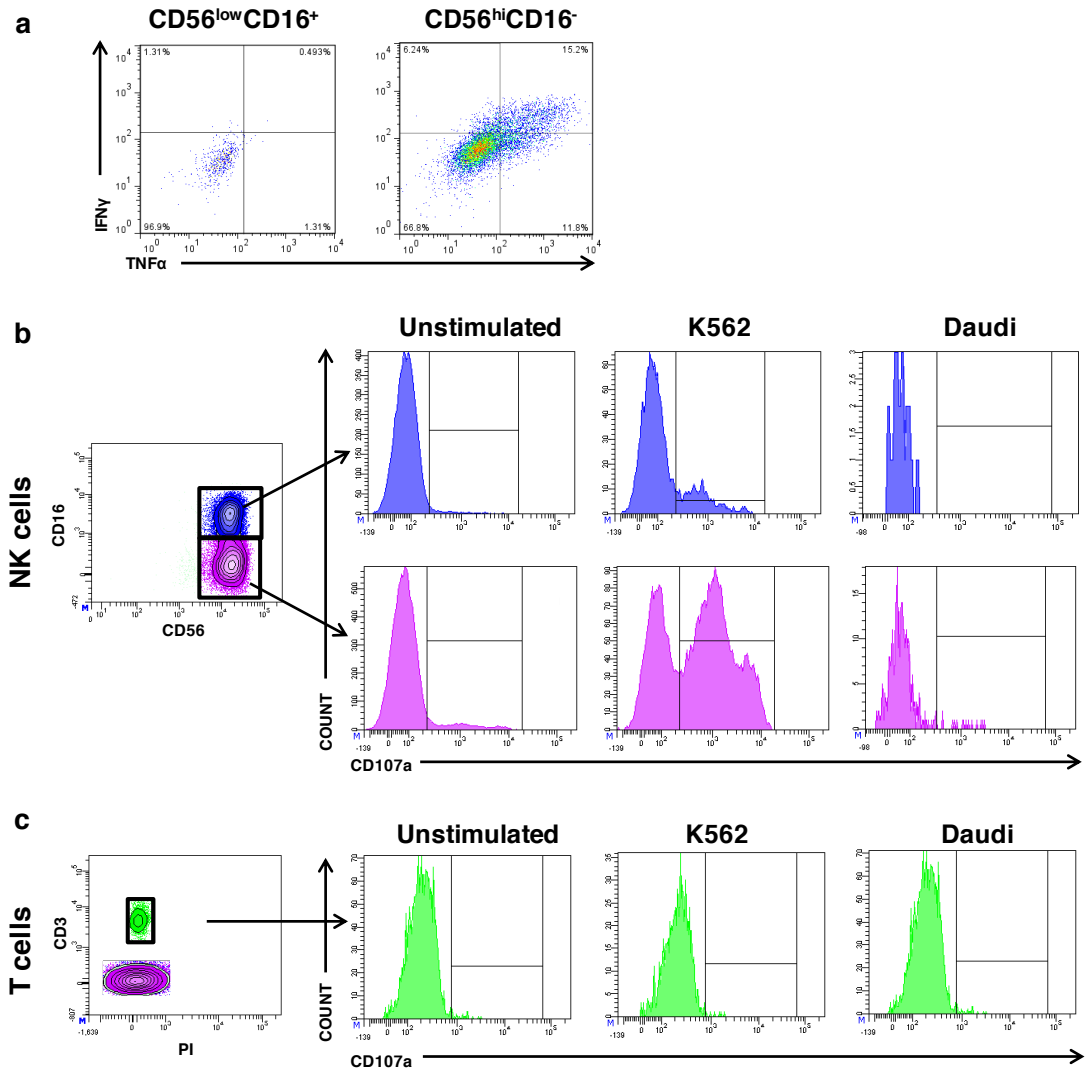

Figure 31. Gating strategy and representative flow cytometric analysis for functional studies of tumour infiltrating NK cells.

Production of IFNγ and TNFα by tumour infiltrating NK cell subsets following K562 co-culture is shown (a). $CD56^{hi}CD16^{-}$ (purple) and $CD56^{low}CD16^{+}$ (blue) NK cells were gated and analysed for their expression of CD107a without stimulation (unstimulated), and following co-culture with either K562 or Daudi cell lines (b). Representative histograms are shown. T cells (green) were also analysed for CD107a expression without stimulation, and following co-culture with K562 and Daudi cell lines (c).

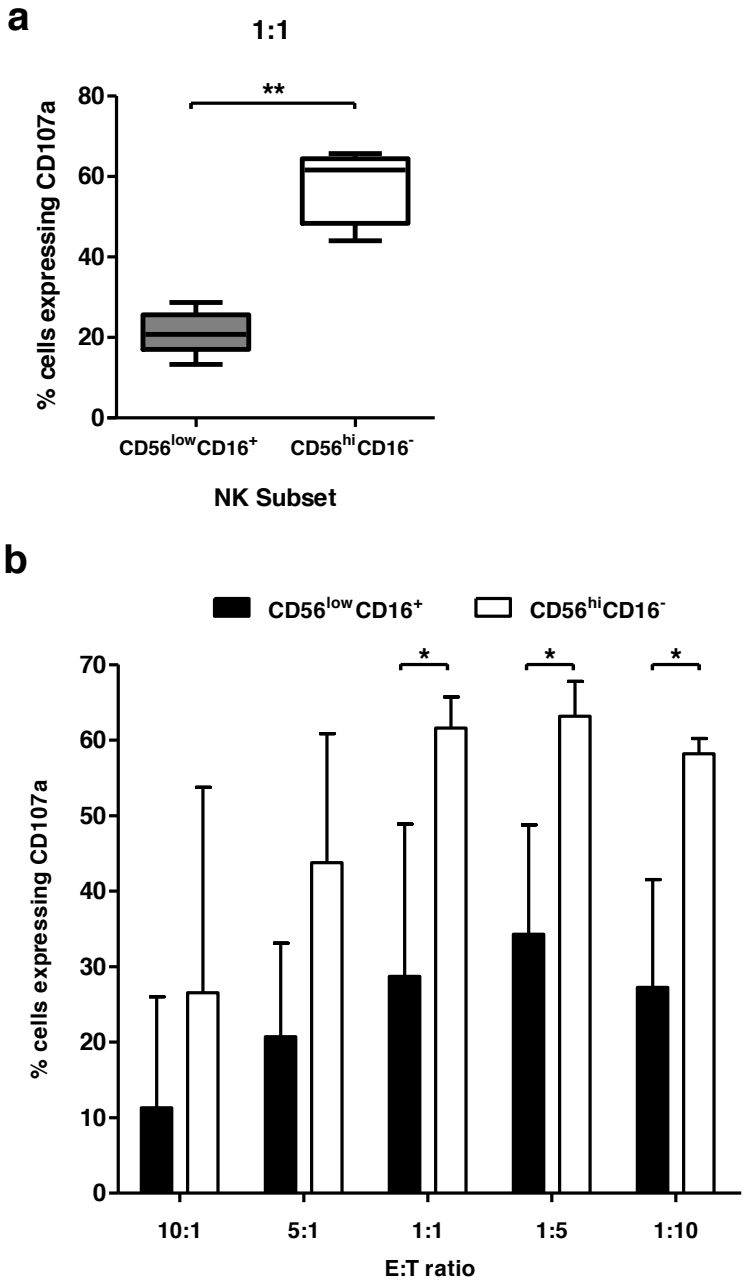

Figure 32. Functional analysis of tumour infiltrating NK cells.
NK cells were co-cultured with K562 tumour cell line at a ratio of 1:1. The expression of CD107a on each NK subset was determined and expressed as a proportion of total NK cells within that subset (a). Box represents 25th and 75th percentile, line represents median, and whiskers represent 10-90 percentile. Data analysed by Mann-Whitney, **denotes $p<0.01$. The expression of CD107a on CD16^{+} (open bars) and CD16^{-} (filled bars) NK subsets at E:T ratios of 10:1, 5:1, 1:1, 1:5 and 1:10 is shown (b). Bars represent median, error bars indicate upper quartile. Data analysed by a two-way ANOVA with Bonferroni post-test, *denotes $p<0.05$.

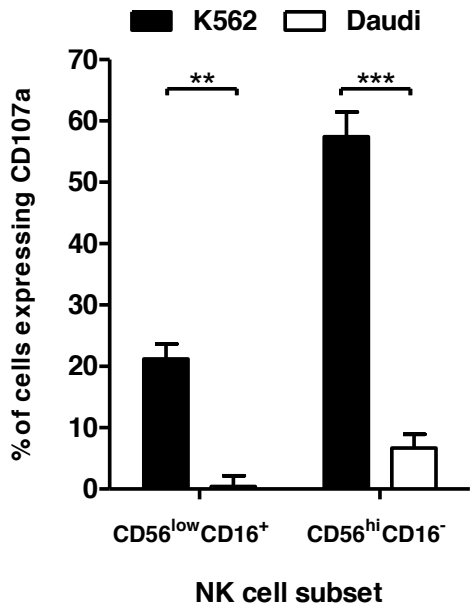

Figure 33. Degranulation of tumour infiltrating NK cell subsets against an NK-resistant tumour cell line.

The ability of both NK cell subsets to degranulate in response to an NK sensitive tumour cell line was determined. NK cells were co-cultured with K562 (filled bar) and Daudi (open bar) tumour cell line at a ratio of 1:1. The expression of CD107a on each NK subset was determined and expressed as a proportion of total NK cells within that subset. Bars represent mean, error bars indicate SEM. Data analysed by paired t test, having passed D'Agostino & Pearson omnibus normality test. **denotes $p<0.01$ *** denotes $p<0.001$.

TGCTs Express NKG2D-Activating Ligands

NK cells express many different cell surface receptors that deliver either activating or inhibitory signals. It is the relative balance of these signals that regulates NK cell activity. If activating stimulation exceeds that of inhibitory, NK cells respond by producing inflammatory cytokines and releasing cytolytic granzymes. Engagement of NKG2D by tumour-expressing ligands can trigger NK cell cytolytic activity. A number of NKG2D ligands (MICA, ULBP1, 2, and 3) were determined in TGCT tissue by qRT-PCR (Figure 34). Transcript levels of all ligands were compared directly to healthy testis. MICA transcripts were found in all TGCTs examined, but were present at less than half the level found in healthy testis. Expression of ULBP1 and 3 was virtually absent in TGCT tissue, regardless of tumour type, whereas ULBP2 transcripts were detectable in TGCTs at levels lower than healthy testis. Protein expression of MICA and ULBP2 was confirmed in all TGCT samples using Western blot analysis (Figure 35a). Densitometry revealed MICA protein was present in TGCT tissue at levels comparable to healthy testis (Figure 35b). ULBP2 protein expression was greater in TGCT tissue than in healthy testis, in a proportion of tumour samples. Expression levels of ULBP2 were independent of tumour type (Figure 35c). This data reveals the expression of NKG2D ligands in TGCT tissue which may contribute to NK cell activation and subsequent tumour cell lysis.

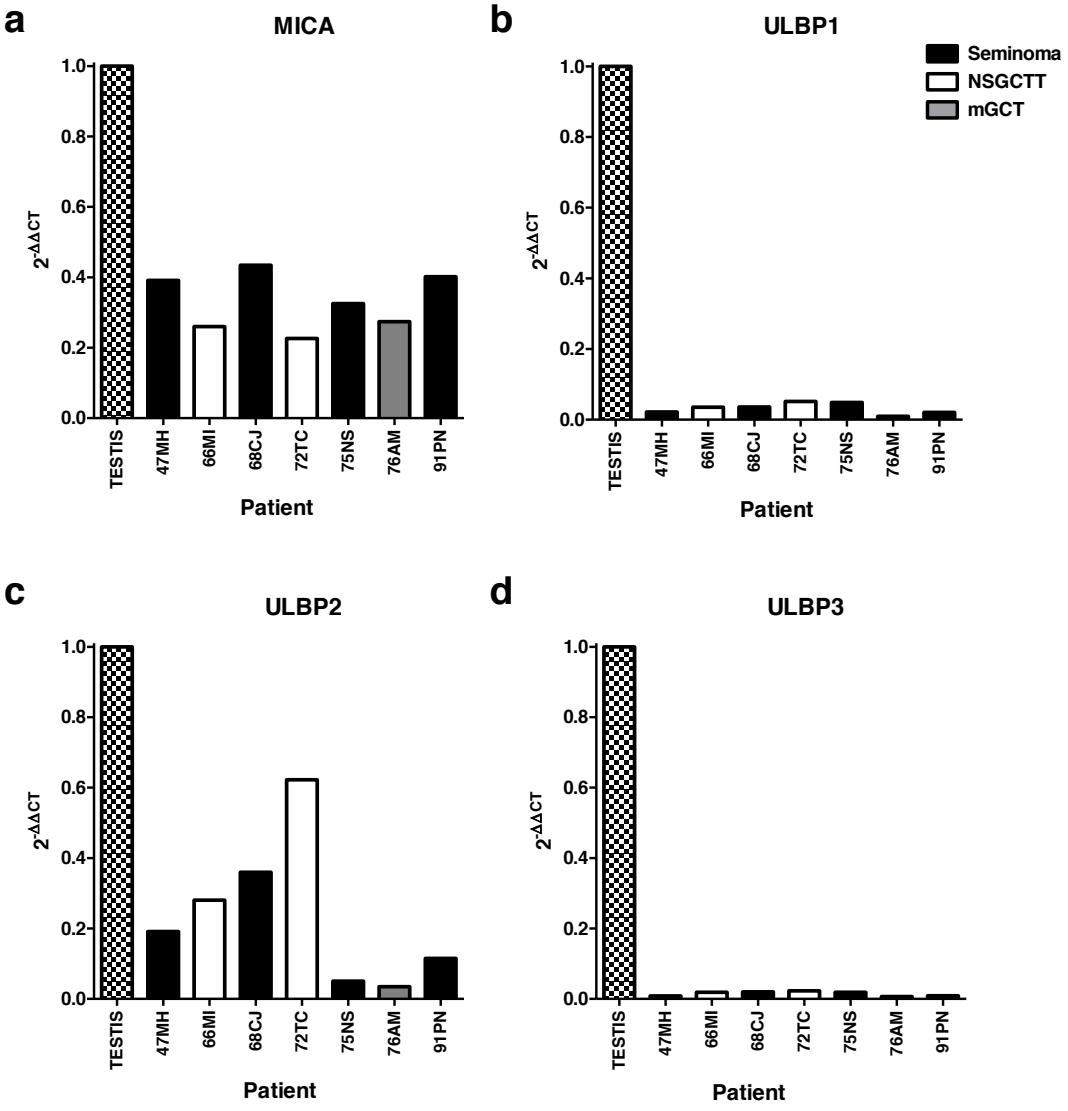

Figure 34. Expression of NKG2D activating ligands in primary TGCT tissue.
The mRNA levels of MICA (a), ULBP1 (b), ULBP2 (c) and ULBP3 (d) is shown. Black bars represent relative expression levels of individual patients and grey bars represent the mean expression level in normal testis tissue of 3 patients. Expression is relative to testis and normalised to GAPDH.

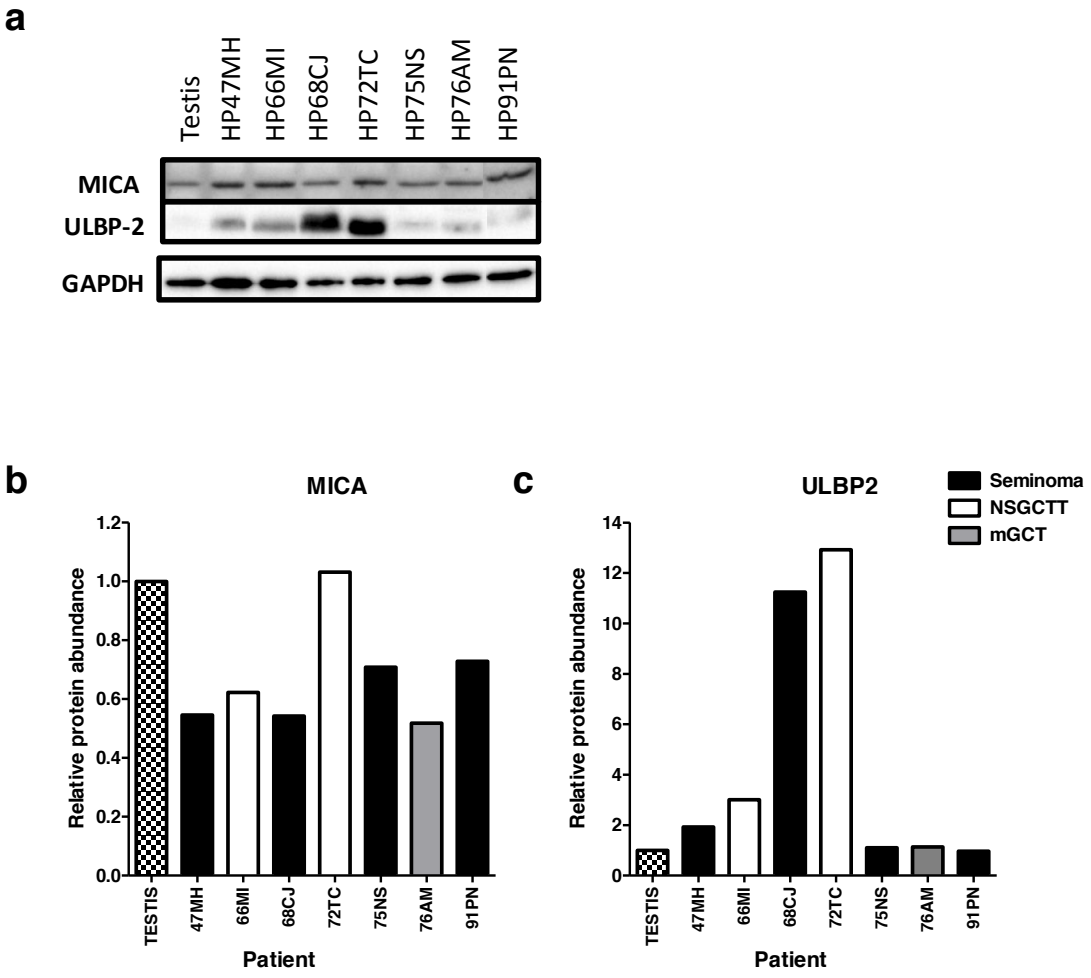

Figure 35. Protein expression of NKG2D ligands, MICA and ULBP2, in primary TGCT tissue.

Western blot analysis of MICA and ULBP-2 to determine protein expression in TGCT tissue (a). GAPDH was used as a loading control and to determine relative protein abundance between patients. Relative protein abundance was calculated by densitometry, relative to testis, and normalised to GAPDH. Each filled bar represents an individual patient.

Expression of NK Cell-Associated Markers on Tumour Infiltrating CD4 and CD8 T Cells

T cells are the predominant lymphocyte subset infiltrating TGCT lesions. However, cytotoxic NK cells are also present but at lower frequencies. It has been shown previously that the expression of NK-associated markers may regulate T cell effector function in cancer patients (Speiser *et al*., 1999), thus we investigated the expression of the NK cell markers, CD161 and CD56, on tumour infiltrating T cells. The proportion of T cells which express NK cell-associated markers in TIL was compared to those in autologous PBMC, using flow cytometry. Figure 36 represents the gating strategy used for the numeration of each T cell subset. Table 24 summarises the expression levels of each NK marker on T cell subsets, with corresponding statistical significance.

CD4+CD161+ T Cells are elevated in TGCT Tissue

CD161 expressing CD4 and CD8 T cells are a minor population of cells found in peripheral blood, which are described as containing all IL-17 producing cells. In the context of CD8 T cells, CD161 expression is correlated with diminished proliferative and cytotoxic capacity (Takahashi *et al*., 2006). We show the proportion of CD161+CD8 T cells was significantly lower in TIL (1.29 IQR: 0.44-3.46) compared to autologous PBMC (5.51 IQR: 2.49-12.89) ($p=0.0059$). Conversely, the proportion of CD161+CD4 T cells was significantly higher in TIL compared to matched PBMC ($p=0.0039$) (Figure 37a). Interestingly, the proportion of CD161+CD4 T cells in peripheral blood decreases over time to a significantly lower proportion at 3 months post chemotherapy (8.71 IQR: 6.38-10.09), compared to pre-treatment (12.11 IQR: 10.24-14.02) ($p=0.0313$) (Figure 37b).

CD8+CD56+ T Cells are rarely found in TGCT Tissue

$CD56^+$ T cells have been described as a subset which demonstrates enhanced MHC-unrestricted cytotoxicity (Kelly-Rogers *et al*., 2006). Consequently we examined the presence of these cells within TGCT tissue. We determined the frequency of $CD56^+$CD8 T cells in TIL and peripheral blood, and found this subset was at significantly lower levels in TIL compared to autologous PBMC ($p=0.0059$) (Figure 37c). It has been suggested that CD8 T cell effector function correlates with CD56 surface expression, whereby greater CD56 expression relates to increased cytokine production and cytotoxic capacity (Ohkawa *et al*., 2001).

NKG2D Is Downregulated on CD8 T Cells Infiltrating TGCTs

We have previously shown a reduction of NKG2D surface expression on tumour infiltrating NK cells, hence we determined the proportion of CD8 NKG2D+ T cells in TIL and peripheral blood (Figure 38a). We found a significant reduction in the proportion of CD8 T cells expressing NKG2D in TIL, compared to PBMC (Figure 38b). This suggests NKG2D is globally down-regulated by the tumour microenvironment, and is not specific to NK cells alone.

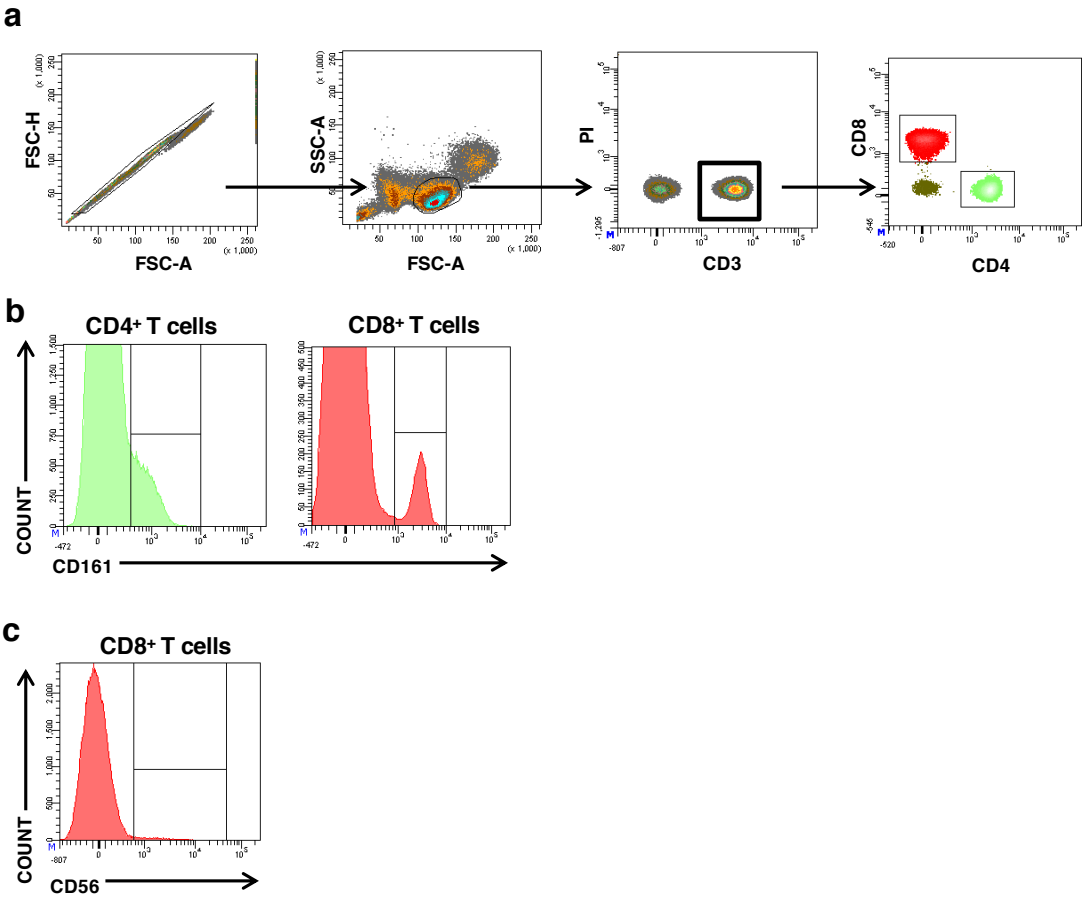

Figure 36. Gating strategy for NK-associated markers on T cells.
Cells were first gated to remove doublet cells before gating on lymphocytes based on FSC-A and SSC-A properties. Dead cells were subsequently removed by gating on propidium iodide (PI) negative cells along with CD3. CD4 (green) and CD8 (red) T cells were subsequently gated from the $CD3^{+}PI^{-}$ population (a). Representative histograms show expression of CD161 (b) on CD4 and CD8 T cells, and CD56 (c) expression on CD8 T cells.

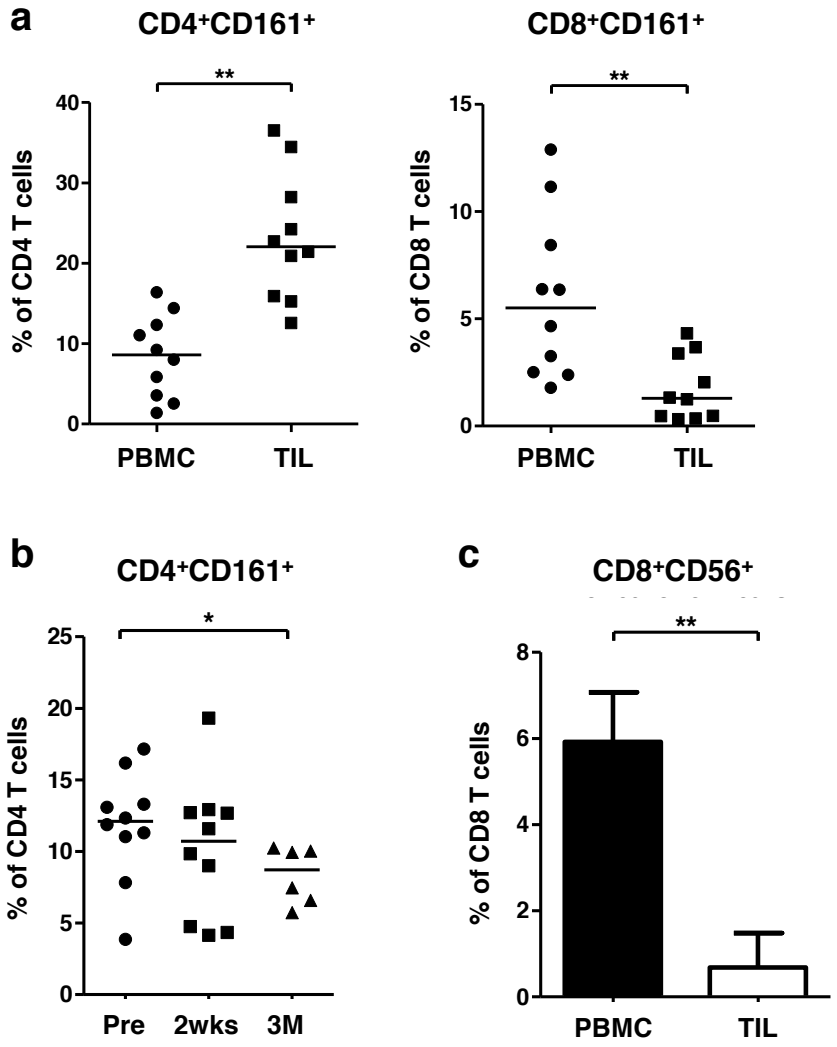

Figure 37. Identification of tumour infiltrating T cell subsets expressing NK-associated markers.

CD161 expression was determined on CD4 and CD8 T cells from PBMC and TIL (a). Comparison of CD161 expression on CD4 T cells at pre, 2wks and 3M post chemotherapy is shown (b). Each symbol represents an individual patient. Horizontal line represents the median. Data analysed by Wilcoxon matched-pairs signed-rank test. * denotes $p<0.05$, ** denotes $p<0.01$. Expression of CD56 on CD8 T cells was determined and represented as a proportion of total CD8 T cells (c). Bars represent median. Error bars represent the upper quartile. Data analysed by Wilcoxon matched-pairs signed-rank test. ** denotes $p<0.01$.

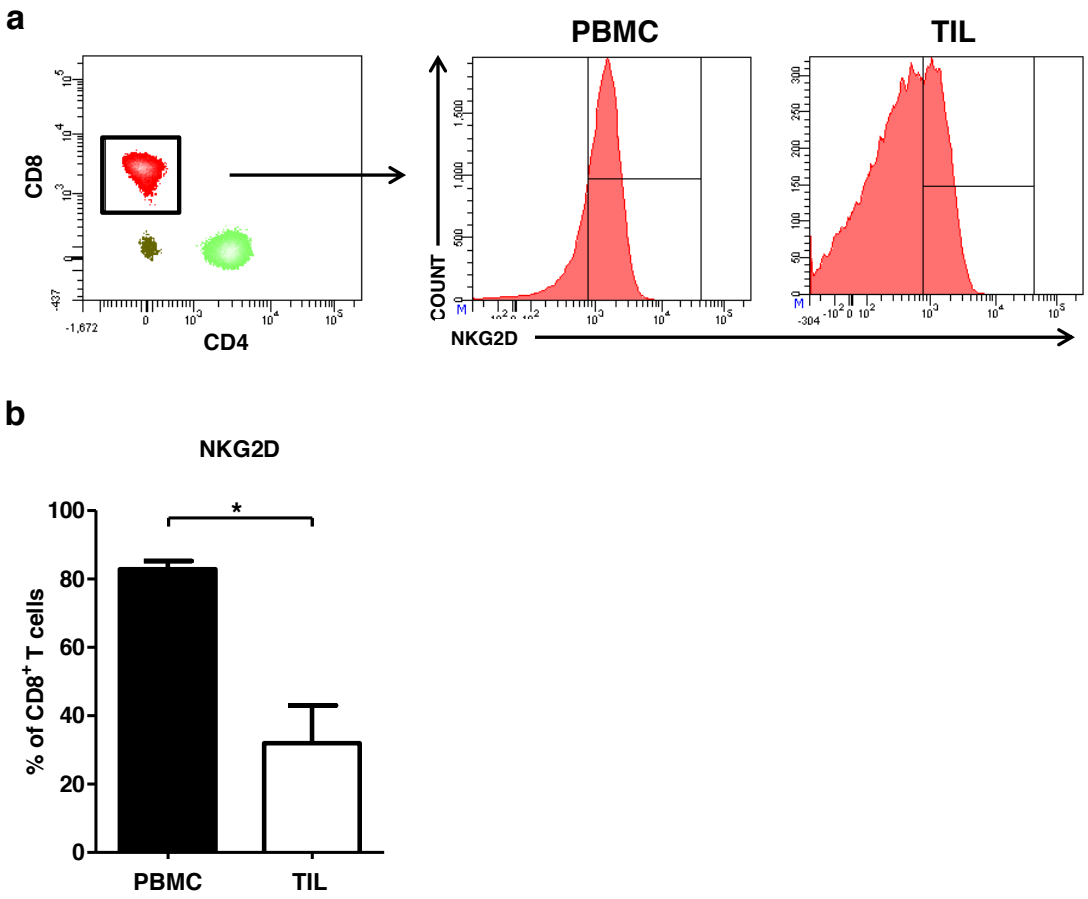

Figure 38. Expression of NKG2D on CD8 T cells from PBMC and TIL.
Representative histogram showing NKG2D expression on CD8 T cells in PBMC and TIL (a). Expression of NKG2D on CD8 T cells is significantly reduced in TIL compared to PBMC (b). Bars represent median. Error bars indicate upper quartile. Data analysed by Wilcoxon matched-pairs signed-rank test, *denotes $p<0.05$.

Table 24. Identification of tumour infiltrating T cell subsets expressing NK-associated markers.

	PBMC			TIL			p
	Median	**25th**	**75th**	**Median**	**25th**	**75th**	
$CD4^+CD161^+$ (n=10)	**8.61**	3.32	12.86	**22.07**	15.74	29.79	***0.0039***
$CD8^+CD161^+$ (n=10)	**5.51**	2.49	12.89	**1.29**	0.44	3.46	***0.0059***
$CD8^+CD56^+$ (n=9)	**5.92**	1.13	7.07	**0.68**	0.49	1.48	***0.0059***
$CD8^+NKG2D^+$ (n=6)	**82.83**	80.67	85.23	**31.96**	19.51	42.96	***0.0313***

Data expressed as median (bold) with 25th and 75th quartile. Significant differences are highlighted in bold italic type.

Table 25. Summary of differences observed between T cells isolated from peripheral blood and TIL

Description/Characteristic	Difference in TIL compared to PBMC[($)]
CD4:CD8 ratio	↓
T cell memory phenotype	
Naive	↓
T_{EM}	↑
Activation markers	
CD69 expression	↑
CD38 density	↑
TCR diversity	↓
Degranulation potential of T cells *in vitro*	↑
Negative regulatory molecule expression	
TIM-3	↑
PD-1	↑

[($)] Arrows represent properties that are increased or decreased in TIL compared to PBMC.

Table 26. Summary of differences observed between NK cells and NK-like cells isolated from peripheral blood and TIL

Description/Characteristic	Difference in TIL compared to PBMC[($)]
T:NK cell ratio	↑
Proportion of NK cell subset	
$CD56^{hi}CD16^{-}$	↑
$CD56^{low}CD16^{+}$	↓
NKG2D expression	
NK cells	↓
CD8 T cells	↓
Proportion of CD161 expressing cells	
CD4 T cells	↑
CD8 T cells	↓
Proportion of $CD8^{+}CD56^{+}$ T cells	↓

[($)] Arrows represent properties that are increased or decreased in TIL compared to PBMC.

Discussion

This chapter described the phenotype and function of lymphocytes that infiltrate TGCTs. The differences in phenotype and cell proportions of T cells (Table 25) and NK cells (Table 26) observed between PBMC and TIL are summarised. In addition, changes in circulating lymphocytes were monitored following tumour removal and the onset of chemotherapy.

Phenotype and frequency of peripheral and tumour infiltrating lymphocytes in TGCT patients

Although large frequencies of lymphocytic infiltrates are found in many TGCTs, spontaneous regression is extremely rare (Balzer and Ulbright, 2006, Sarid *et al*., 2002), suggesting tumour immune escape mechanisms are at play. The phenotype and function of immune infiltrates have been examined in multiple tumour types. However, the significance of this infiltrate has been subject to conflicting reports. Tumour-infiltrating T cells have demonstrated effective anti-tumour activity in some malignancies (Clark *et al*., 1989, Clemente *et al*., 1996, Pages *et al*., 2010) but support tumour growth and development in others (Curiel *et al*., 2004). In the majority of cases, the presence and proportion of cytotoxic vs. regulatory cell subsets has been correlated with disease progression and prognosis (Chin *et al*., 1992, Shah *et al*., 2011, Wakabayashi *et al*., 2003).

Studies using IHC techniques have identified T cells, B cells and macrophages surrounding TGCT tissue (Torres *et al*., 1997, Grobholz *et al*., 2000). One such study showed increased numbers of T cells and macrophages per unit area in seminoma compared to NSGCTTs. Interestingly, in this study the frequency of B cells was the same. Another study using IHC revealed equal proportions of CD4 T cells, CD8 T cells, and B

cells within seminoma lesions (Bols *et al*., 2000). Conversely, CD4:CD8 T cell ratios greater than one were reported in some seminoma lesions, suggesting CD4 T cells were the dominant T cell subset (Grobholz *et al*., 2000). In the present study, we show a predominance of αβ T cells within TGCTs. In agreement with (Bols *et al*., 2000), we found near equal proportions of CD4 and CD8 T cells within these tumour lesions. This suggests both T cell subsets are migrating into TGCT lesions with similar efficiency.

Naive T cells circulate the peripheral blood and lymphatics, and enter secondary lymphoid organs where they are antigen-primed and clonally expand before entering inflamed tissue (Mackay, 1993). We hypothesise that priming of tumour-specific T cells in TGCT patients occurs in tumour draining lymph nodes where T cells subsequently expand and infiltrate the tumour at similar frequencies. Alternatively, T cells may enter the tumour at the CD4:CD8 T cell ratio found in peripheral blood (approximately 2:1), but once inside the tumour mass CD8 T cells preferentially activate in response to cognate antigen and proliferate *in situ*, thereby lowering CD4:CD8 towards a 1:1 ratio. If TGCT cells express MHC class I, or expression is induced on tumour cells by the inflammatory environment, it would allow presentation of antigen directly to CD8 T cells at the tumour site. Conversely, most tumours lack MHC class II expression and therefore CD4 T cells cannot be activated through these TCR dependant mechanisms within the tumour without the presence of APCs. In turn, this may allow greater CD8 T cell activation and subsequent inflation of the CD8 T cell pool in TGCT tissue. It would be interesting to consider the possibility that CD8 T cells are able to directly target tumour cells that express MHC class I, and that CD4 T cells are present to help the cytotoxic response, and aid the development of long-lived memory cells (Bevan, 2004).

If tumour infiltrating T cells have limited specificity i.e. are tumour antigen restricted, it is likely that the TCRVβ repertoire observed would be less diverse than that of peripheral blood, and the subsequent enrichment of specific Vβ chains may be observed. Examination of the TCRVβ repertoire of T cells by flow cytometry, revealed an enrichment of certain TCRVβ in all TGCTs examined, irrespective of tumour type, confirming a restriction of the repertoire. Importantly, this was not confined to a single TCRVβ family suggesting there is no single dominant epitope responsible for the lymphocytic infiltrate, but instead suggests the generation of oligoclonal T cell populations which are specific to multiple tumour antigens. In support of this, a previous study demonstrated that most seminomatous tumours comprise numerous clonally expanded T cells (Hadrup *et al*., 2006). An additional study revealed a polyclonal population of T cells (Grobholz *et al*., 2000), again indicative of multiple T cell populations specific to numerous tumour targets. We did observe, however, an increase in Vβ13.1 in all patients examined suggesting tumours may share the expression of certain antigens that provoke a response through this family. Further analysis including deep sequencing of the CDR3 region of these Vβ13.1 T cells is required to determine whether the specificity of these cells in the same between patients.

Overall, our data suggests clonally expanded T cells are present within tumour lesions as a result of either a) recognition of cognate antigen presented directly by the tumour or by APCs co-inhabiting tumour lesions, or b) preferential migration of these cells into the tumour following expansion in secondary lymphoid organs. A recent publication describes the selective recruitment of naive T cells into the tumour mass, where subsequent activation and effector differentiation of CD8 T cells occurs (Thompson *et al*., 2010). In this paper, they demonstrated antigen presentation directly by the tumour or

through cross-presentation by APCs to initiate CD8 T cell activation. This would support the notion of clonal expansion within the tumour. The methods used in our study did not allow location of T cell expansion to be determined, nor did it allow the discrimination of CD4 and CD8 T cells. Our experimental setup compared the TCRVβ repertoire of TIL with autologous PBMC, and as a result may underestimate the degree of oligoclonality as tumour-specific T cells may enter circulation, thereby increasing the same TCRVβ subset in peripheral blood. We speculate that an abundance of tumour-specific T cells with multiple antigen specificities reside within TGCT lesions. The location of activation and clonal expansion of these T cells remains unclear.

Antigen experienced T cells downregulate CD45RA expression, and upregulate CD45RO expression, and subsequently differentiate into central or effector memory T cells. Differentiation between central and effector memory populations and naive and effector populations is achieved by the addition of the chemokine receptor CCR7, or the costimulatory molecule, CD28. Loss of CCR7 expression allows the migration of T cells from secondary lymphoid tissue to inflamed peripheral tissues i.e. to the tumour site. To determine whether TIL was categorically antigen-experienced we examined the expression of CCR7 and CD45RA on tumour infiltrating T cells. The majority of T cells found within TGCT lesions had lost expression of both CCR7 and CD45RA. This was observed in both the CD4 and CD8 T cell compartments, whereby up to 90% of cells were negative for both molecules, indicative of T_{EM} cells. This suggests the majority of T cells within TGCT lesions have experienced cognate antigen. In comparison, PBMC from TGCT patients had a much lower proportion of T_{EM} cells than that observed in TIL; the majority of peripheral blood T cells were naive. In agreement with our findings, a previous study demonstrated the

expression of CD45RO on the majority of tumour infiltrating T cells in TGCT patients (Grobholz *et al*., 2000). Another study looked at the expression of both CD45RO and CD28 to define memory phenotypes, and observed an expression profile indicative of T_{EM} cells (Hadrup *et al*., 2006). The increased effector memory T cell pool we and others have observed in TIL of TGCT patients is not a unique feature to this tumour type, and has been used as a prognostic factor in a wide range of tumours (Rauser *et al*., 2010, Koulis *et al*., 1997, Attig *et al*., 2009). In this context, elevated proportions of antigen experienced T cells generally indicate improved prognosis.

Furthermore, we observed a striking increase in the proportion of peripheral blood T_{EM} cells in TGCT patients compared to gender and age matched healthy individuals. This increase in T_{EM} cells was directly reciprocated with a statistically significant decrease in the proportion of naive T cells. We speculate that the rise in T_{EM} cells in peripheral blood during active disease can occur by one of two mechanisms. Firstly, tumour infiltrating T cells, presumably tumour-specific, re-enter the systemic circulation from the tumour by an unknown mechanism. Secondly, and more likely, APCs such as DCs residing in tumour lesions sample the environment and become activated following tumour antigen uptake. Following maturation, DCs migrate into tumour draining lymph nodes, where they present processed tumour antigens to T cells. Recently activated tumour-specific T cells could potentially enter peripheral blood before migrating into tumour tissue, thereby elevating the frequency of T_{EM} cells in PBMC.

To substantiate our claim of tumour-specific T cells entering systemic circulation, we monitored the proportion of memory subsets over time following tumour removal.

Longitudinal analysis demonstrated a reduction in the peripheral blood T_{EM} cell pool following the removal of tumour burden, in agreement with the kinetics of a cell-mediated immune response. Based on the short life-span of T_{EM} cells in the absence of cognate antigen, we hypothesise that removal of the tumour restricts the supply of antigen, resulting in the death of the majority of antigen-specific cells. We assume long-lived tumour-specific T cells are generated following the primary immune response, which reside within the effector and central memory pools, to enable a rapid secondary response following subsequent antigen encounter. Unfortunately, blood samples prior to disease onset where unobtainable in this study so we were unable to determine the extent of change in the memory T cell pool during tumour development.

Blood samples for longitudinal analysis were taken at time points that coincided with the onset of adjuvant chemotherapy. All patients within this cohort received the same adjuvant chemotherapy regimen (single dose carboplatin) and samples were acquired at the same time points pre- and post- chemotherapy. The mode of action of platinum-based chemotherapeutics is mediated by its interaction with DNA to form intrastrand DNA adducts (Siddik, 2003). It is not cell specific and can potentially mediate cytotoxic effects towards immune cells, which ultimately triggers apoptosis in cycling cells. Tumour-specific T cells, predominantly T_{EM} cells, are likely to be proliferating in response to tumour antigens, and as a result they could be more sensitive to the cytotoxic effects of carboplatin than naive T cells. This would also lead to diminishing levels of T_{EM} cells following chemotherapy, increasing the proportion of the naive cell pool, as we have observed in this study.

Both chemotherapy and immune response kinetics may contribute to a reduction of T_{EM} cells in peripheral blood over time. We cannot categorically determine the extent of which these two mechanisms are involved as we are unable to distinguish between the effects of chemotherapy and the reduction of tumour antigen load. Future work would ideally include *in vitro* studies to determine whether particular T cell subsets are more prone to the effects of chemotherapy drugs, and correlate this with full blood counts to determine the extent of T cell depletion *in vivo.* In addition, longitudinal analysis of T cell memory phenotype in patients with testicular cancer who did not receive chemotherapy (surveillance) would allow us to accurately determine the effect of reduced tumour antigen load alone.

The T_{EM} phenotype infiltrating TGCTs demonstrates they have previously encountered cognate antigen but gives no indication as to when this recognition event occurred. Moreover, the memory phenotype does not indicate the extent of tumour-specific versus "irrelevant" bystander T-cell recruitment into the tumour. To date, the activation status of TIL from TGCTs is unknown therefore we investigated this on freshly isolated tumour residing T cells. We examined the surface expression of CD69 and CD38, and found a substantial proportion of both CD4 and CD8 T cells expressing these molecules. CD69 is induced within an hour of activation and its expression is only transient (Demaria *et al*., 1994). The rapid upregulation and transient nature of CD69 expression following activation suggests T cells are activated within the tumour, independent of locality of initial antigen encounter. T cell activation was confirmed using CD38, a marker which is upregulated on the surface of activated leukocytes (Malavasi *et al*., 2006).

CD69 is known to trigger proinflammatory responses by inducing T cell proliferation (Cebrian *et al*., 1988) and cytokine secretion (Santis *et al*., 1992) in CD8 T cells; directly contributing to the inflammatory response. However, the functional consequences of CD69 expression on CD4 T cells is less clear. Recently, populations of CD69+ CD4 T cells with specific regulatory functions have been described. (Han *et al*., 2009) described a tumour-induced CD69+CD4+CD25− T cell subset, which increased during tumour progression, and was capable of suppressing CD4 T cell proliferation by expression of surface-bound TGF-β. Another paper described the ability of CD69+ T cells to induce the expression of IDO in tumour residing macrophages (Zhao *et al*., 2012). IDO inhibits the proliferation (Uyttenhove *et al*., 2003, Frumento *et al*., 2002) and cytotoxic capability (Gajewski *et al*., 2006) of antigen-specific T cells, and enhances the suppressive activity of Tregs (Zou, 2006). We speculate that activated CD4 T cells present within TGCT lesions, may contain populations of potentially regulatory cell subsets, contributing to tumour immune escape mechanisms, however, further investigation is needed to confirm this.

Following removal of the tumour mass by radical orchidectomy, chemotherapy is given to reduce the high rates of relapse (20%) observed in testicular cancers, even in the absence of secondary metastasis. Interestingly, in this study we observe a significant increase in CD69 expression on CD8 T cells shortly after chemotherapy in a number of TGCT patients. This suggests that a high frequency of residual tumour cells may be circulating in these patients, and that chemotherapy induces lysis of these residual tumour cells allowing the release of numerous tumour antigens. Released antigens could be captured, processed and cross-presented to CD8 T cells by DCs, leading CD8 T cell activation and hence upregulation of CD69. As the primary tumour has already been removed through surgery,

these activated T cells may then accumulate in the peripheral blood. It would be interesting to determine the specificity of these cells, as this may aid the development of immunotherapeutics to treat residual disease in instances where adjuvant chemotherapy is not appropriate, and minimise side effects of standard chemotherapy regimens. However, we should also consider the direct effects of chemotherapeutic drugs on T cell activation. The effect of platinum-based chemotherapy on the activation of T cells is unknown, however, one publication demonstrated that other types of chemotherapy drugs can induce atypical CD69 surface expression on peripheral blood T cells in the absence of costimulation (Morgan and Holguin, 2002).

Functional analysis of peripheral and tumour infiltrating lymphocytes in TGCT patients

Activation following stimulation through the TCR and costimulatory molecules, ultimately leads to clonal expansion, a requirement for effective immune responses. We found that T cells isolated directly from TGCTs did not proliferate in the presence of IL-2 alone. However, stimulation of T cells through the TCR with appropriate costimulation resulted in multiple cell divisions over a 5 day period. Combined, these results suggest T cells are not clonally expanding within the tumour but regain proliferative capability when stimulated outside the tumour environment. We speculate that various regulatory mechanisms are at play, which suppress the proliferation of T cells, and induce a state of reversible anergy mediated directly by the tumour or its milieu. This temporary state has been described previously where T cell exhaustion was efficiently reversed with addition of exogenous IL-2 (Beverly *et al*., 1992). Reduced proliferative potential of T cells within the tumour could be mediated by the lack of costimulation. MHC class I expressing tumours

are able to present antigens, but the lack of costimulatory molecules on tumour cells promotes anergy and tolerance, thus exerting detrimental effects.

With these in mind, we hypothesise that T cells proliferate within secondary lymphoid organs and subsequently migrate to the tumour, as opposed to proliferating *in situ*. Alternatively, chronic antigenic stimulation within the tumour may have generated a cell phenotype typically associated with exhaustion, whereby T cells are rendered proliferatively incompetent. Ki-67 is a nuclear protein associated with proliferation and is used as a marker to differentiate between clonally expanding cells and the resting population. During progression through the cell cycle, Ki-67 can be detected within the nucleus by intracellular staining techniques. In future studies, we would use this marker to assess the proliferation of T cells *ex vivo.*

The absence of costimulation and/or high co-inhibition is sufficient to induce cell cycle arrest and inhibit cytokine production in antigen-specific T cells. In the inflammatory environment of the tumour we may expect high levels of proliferation. However, we have illustrated a potentially detrimental effect of the tumour microenvironment on T cell proliferation within the tumour mass. We therefore also investigated the ability of these cells to secrete inflammatory cytokines and undergo degranulation following *in vitro* stimulation. We show that *ex vivo* production of IFNγ and TNFα is practically absent in T cells directly isolated from TGCTs. Activated cytotoxic CD8 T cells and CD4 Th1 cells should secrete these cytokines as part of the inflammatory response towards the tumour. This was not observed, further substantiating our claim that T cell effector function is actively inhibited by the tumour microenvironment, inducing T cell dysfunction.

Following stimulation by a TCR independent mechanism using PMA/Ionomycin, a high proportion of CD4 and CD8 T cells secrete both these cytokines, suggestive of defects in proximal signal transduction, in addition to inhibitory signalling. We postulate that cytokine production in response to TCR stimulation may be defective in tumour residing T cells. This stimulation method is universally used to determine the effector subtype of T cells. The secretion of IFNγ and TNFα by CD4 T cells suggests a proportion of tumour infiltrating CD4 T cells are Th1 cells. Th1 effector cells stimulate an inflammatory response by recruiting APCs into the tumour mass, which would further increase tumour antigen presentation to infiltrating T cells. In addition, Th1 cells can aid a cytotoxic T cell response by stimulating dendritic cells to produce more costimulatory molecules. Furthermore, IFNγ secretion increases the efficiency of antigen processing and presentation to cytotoxic CD8 T cells, and induces MHC class I expression on tumour cells. These qualities make Th1 cells an important cell type in the generation of an inflammatory response against the tumour.

We show populations of CD4 Th1 cells and CD8 T cells within TGCTs, which could be explained by the increased migration of these particular cell subtypes to tumour tissue. CXCR3 is expressed primarily on activated cytotoxic CD8 T cells and CD4 Th1 cells, but not on Th2 cells (Qin *et al*., 1998, Loetscher *et al*., 1996). Importantly, it is also expressed on T cells infiltrating TGCTs (Schweyer *et al*., 2002). Its chemokine ligand, IP-10, is consistently expressed on seminoma-associated endothelial cells (Schweyer *et al*., 2002), enhancing the recruitment of lymph node-activated CD8 T cells and CD4 Th1 cells. It was also shown that IFNγ is produced directly by the tumour. We speculate that IFNγ produced by both the tumour and the functional T cell repertoire, could augment the

expression of IP-10, further contributing to the recruitment and polarization of effector T cells. This could also help explain the vast numbers of lymphocytes observed in seminoma compared to NSGCTTs.

It is important to note that other CD4 T cell subsets could be present within TIL. This includes the Th2 subset which secretes IL-4, IL-5 and IL-13. These cytokines mediate a regulatory and anti-inflammatory effect on other immune cells, which may actively contribute to tumour immune evasion. In addition, Tregs, which are important in regulating an immune response, may be present in TGCTs. In the context of tumour immunology, secretion of TGFβ and IL-10 by Tregs has been implicated in the inhibition of anti-tumour immune responses, thereby preventing tumour clearance. Increased frequencies of Tregs is associated with poor prognosis in many tumour types including breast and colorectal cancers (Dranoff, 2005). Future studies would establish the presence of Tregs in TGCTs, and would involve *in vitro* assays to determine their ability to inhibit antigen-specific T cell effector function, and to decipher the exact inhibitory mechanisms involved.

Interestingly, we also observed an increase in the proportion of CD4+CD161+ T cells within TIL, compared to PBMC. All IL-17 secreting T cells are contained within this cell population (Cosmi *et al*., 2008), suggesting an elevated presence of Th17 cells within these tumours. Th17 cells also produce IFNγ (Annunziato *et al*., 2007) and recruit granulocytes into inflamed tissues. We therefore speculate that Th17 cells contribute to the generation of an inflammatory environment within TGCT lesions. We also observe a decrease in the proportion of CD161+CD4 T cells in circulation following tumour removal, suggesting

these cells are increased in numbers during tumour development and fall to baseline levels upon tumour removal. Combined, it suggests these cells may play a potentially important role in tumour immunity and further studies are warranted to elucidate their function.

Next, we investigated the cytotoxic potential of T cells isolated from the tumour, and compared it to T cells from autologous PBMC. We found that tumour residing CD8 T cells had a greater capacity to degranulate in response to *in vitro* stimulus compared to their peripheral blood counterparts. In agreement with our results, a previous publication showed that CD8 T cells expressed markers of cytotoxic potential, and were in direct contact with apoptotic TGCT cells (Yakirevich *et al*., 2002). Combined, this suggests tumour cell death in tumour lesions may be mediated by cytotoxic granule release by CD8 T cells. Another study examined the cytotoxicity of tumour infiltrating CD8 T cells by examining *ex vivo* CD107a surface expression and *in situ* granzyme B expression (Hadrup *et al*., 2006). They reported increased frequencies of $CD107a^{+}$ cells in TIL, as well as increased intracellular cytotoxic granzyme in tumour immune cells. We found cytolytic activity in PBMC was restricted to CD8 T cells; however we observed a surprisingly high percentage of CD4 T cells isolated from TGCT tissue that degranulated upon stimulation.

Comparable results were reported in CD4 T cells isolated from renal cell carcinomas (Attig *et al*., 2009). Many articles describe the ability of CD4 T cells to direct cytotoxicity towards viral and bacterial antigens (Appay, 2004, van de Berg *et al*., 2008, Brown, 2010). A recent publication showed that antigen-specific CD4 T cells can exert significant MHC class II-restricted cytotoxicity (Hildemann *et al*., 2013). This paper shows that mobilization of CD107a to the cell surface, and the ability to secrete cytotoxic granules was comparable in

magnitude to CD8 T cells. Others have shown CD4 T cell populations with increased levels of intracellular perforin (Appay *et al*., 2002) and cytotoxic granzymes (Zaunders *et al*., 2004). Although the majority of studies have focused predominantly on virus-specific cytotoxic CD4 T cells, it would be interesting to investigate whether CD4 T cells isolated from TGCT tissue could potentially contribute to the direct killing of tumour cells, should the tumour environment allow. The physiological relevance of this to TGCTs is not fully clear due to the low or absent MHC class II expression on TGCTs. Future studies would extend this work to analyse cytotoxic granule release and autologous tumour lysis by both CD4 and CD8 T cells isolated from TIL. In addition, the generation of tumour-specific cytotoxic CD4 T cell clones from tumour residing T cells may be an attractive approach in targeting tumour cells where MHC class II is induced or constitutively expressed.

Regulation of T cell function in TGCTs

Anti-tumour T cells may become compromised following entry into the tumour milieu. T cells require both TCR signalling and costimulation to mount an effective immune response. However, if antigen-specific T cells were activated in lymphoid organs prior to tumour infiltration, there would be no requirement for costimulation within the tumour microenvironment for subsequent activation. Therefore, negative regulatory mechanisms, other than the availability of costimulatory molecules, may be regulating effector T cell function. Here we postulate various modes of regulation, which could suppress or restrict an efficient anti-tumour response.

Previous studies have revealed the lack of Fas-L expression on TGCTs, which would potentially suppress a cytotoxic immune response on cells expressing its receptor, Fas

(Bols *et al*., 2000). Consequently, immune suppressive mechanisms in addition to Fas-L may be present. Here we examined the expression of the inhibitory receptors TIM-3 and PD-1 on tumour infiltrating T cells. To our knowledge, we are the first to describe the expression of these molecules on T cells infiltrating TGCTs. We show a significant proportion of T cells expressed one or both of these receptors. This was particularly apparent for cytotoxic CD8 T cells, where expression of both receptors was observed on a high proportion of cells.

TIM-3 expression on IFNγ-secreting CD4 Th1 cells has also been shown to regulate Th1 immunity and tolerance *in vivo* (Hastings *et al*., 2009, Monney *et al*., 2002). Interaction of TIM-3 with its putative ligand galectin-9 (Gal-9) triggers apoptosis of TIM-3+ T cells. Recent studies have shown that TIM-3 is upregulated on exhausted CD8 T cells (Jones *et al*., 2008). TIM-3+ T cells are dysfunctional as they cannot produce cytokine or proliferate in response to stimuli. It is important to note that not all dysfunctional T cells express TIM-3, nor are all dysfunctional T cells rescued by blockade of the TIM-3-galectin 9 interaction. Further studies have demonstrated that exhausted T cells are characterised by sustained expression of the PD-1 (Barber *et al*., 2006). In agreement with our observations, PD-1 expression on tumour infiltrating T cells has been well documented in other solid tumours (Blank *et al*., 2006, Ahmadzadeh *et al*., 2009). Interference with PD-1 signalling restores functional T cell responses and improves clinical outcome in multiple tumour types (Zhang *et al*., 2009, Yamamoto *et al*., 2008), but this alone is not guaranteed to reverse T cell exhaustion (Blackburn *et al*., 2008). During a normal T cell response, recently activated T cells also upregulate surface PD-1 expression, therefore PD-1 may solely reflect an activated cell phenotype (Fourcade *et al*., 2009). Overall, the our data and previous

literature suggests both TIM-3 and PD-1 can function as negative regulators of T cell responses, and we speculate that signalling through both receptors may synergistically mediate T cell dysfunction in TGCTs.

Co-expression of TIM-3 and PD-1 is strongly correlated with immune dysfunction in patients with cancer (Fourcade *et al*., 2010, Sakuishi *et al*., 2010). This has important consequences in our study, whereby TIL that co-express TIM-3 and PD-1 were often observed among CD8 TIL. In addition, CD8 T cells expressing TIM-3 and PD-1 have been shown to produce IL-10, further limiting the magnitude of CD4 (Said *et al*., 2010) and CD8 (Jin *et al*., 2010) T cell responses. Simultaneous targeting of the both pathways may prove most effective in reversing T cell exhaustion. We speculate that T cells may acquire multiple inhibitory surface molecules during tumour progression, which effectively prevents efficient T cell activation.

We have also demonstrated for the first time the expression of PD-1 ligands, PD-L1 and PD-L2, in a variety of TGCT tissues. Interaction with these ligands can lead to cell cycle arrest and apoptosis of T cells expressing PD-1. Unfortunately, our methodology did not allow us to distinguish the cell type(s) that express these ligands, and we envisage determining this *in situ* by IHC. Expression of PD-L1 has been demonstrated on mouse Sertoli cells of the testis as part of normal testicular immune privilege (Dal Secco *et al*., 2008). If this is the case in human testis, we could be underestimating the level of PD-L1 expression in tumour tissue as we normalised PD-L1 levels to healthy testis. Expression of PD-L1 by Sertoli cells could in fact inadvertently contribute to T cell dysfunction and ultimately aid tumour immune evasion. In all cases, PD-L1 expression was greater in

seminoma tissue than any other testicular tumour type. This could be due to higher expression levels of PD-L1 on seminoma cells than non-seminoma cells. Many tumours express PD-L1 on their surface including renal cell carcinoma (Thompson *et al*., 2006), oesophageal cancers (Ohigashi *et al*., 2005) and breast cancer (Ghebeh *et al*., 2006), where it is associated with suppression of T cell function and poor prognosis. Alternatively, elevated numbers of APCs within the microenvironment of seminoma lesions and increased frequencies of activated T cells, both of which express this ligand, would also explain the higher expression level of PD-L1 we observed in seminoma. The contribution of each PD-L1-expressing subset to induce T cell dysfunction is unclear but here we outline a number of ways in which the tumour microenvironment may be regulating T cells.

We also demonstrated elevated expression of PD-L2 in all TGCTs examined. Generally, tumour cells express very low levels of PD-L2 or show focal expression (reviewed in (Rozali *et al*., 2012)). Interestingly, PD-L2 is expressed by tumour-associated fibroblasts (Nazareth *et al*., 2007), APCs (Latchman *et al*., 2001) and activated T cells (Messal *et al*., 2011). Together, this suggests immune cells and stromal cells of the tumour may express PD-L2, rather than the tumour cells themselves. We speculate that PD-1 ligands are expressed by multiple cell types that are present within the testicular tumour mass. We would hypothesise that the immune infiltrate may contribute to its own demise whereby tumour antigen-induced activation of the immune system leads to expression of inhibitory molecules on APCs and their receptors on activated T cells. This process could be exaggerated in tumour masses, leading to T cell anergy and an exhausted T cell phenotype.

In addition to PD-1 ligands, APCs and T cells are known to express Gal-9, the ligand for TIM-3 (Zhu *et al*., 2005). Gal-9-induced TIM-3 signalling mediates T cell dysfunction in the cancer setting (Li *et al*., 2012). We show TIM-3 expression is restricted to activated cytotoxic CD8 T cells and CD4 Th1 cells, leading to inhibition of T cell subsets specifically involved in anti-tumour immunity. Expression analysis of Gal-9 by qRT-PCR would not discriminate between internal and surface expression of Gal-9. Only surface expression of Gal-9 is able to interact with TIM-3 and subsequently induce T cell dysfunction. In the future, Gal-9 expression would be determined by digestion of TGCT tissue and subsequent surface staining with an anti-Gal-9 antibody.

The methodology used in this study does not allow a clear distinction of inhibitory ligand expression between tumour cell, immune cell and tumour stroma. Induction of T cell dysfunction through inhibitory receptors seems to be an important tumour immune escape mechanism in TGCT patients. Therefore, the expression of other inhibitory receptors, including Lag-3 and BTLA, would be investigated, and the correlation between cellular function and inhibitory receptor expression would be determined. Signalling through multiple inhibitory receptors may have an additive or synergistic effect on T cell dysfunction, and determining the contribution of each would enable the development of more effective cancer immunotherapies.

The role of NK cells in TGCTs

It has been shown that the generation of tumour-specific CD8 T cells is enhanced by activated NK cells, which promote the maturation of DCs and provide them with antigenic

material following tumour cell lysis (Kalinski *et al*., 2005). In addition, NK cells can directly kill target cells that lack MHC class I expression without prior sensitisation, as well as those displaying stress-induced molecules, including MICA/B and ULBPs. MHC class I expression on TGCTs is either low, focal or absent (Nouri *et al*., 1993, Bols *et al*., 2000, Hadrup *et al*., 2006). Together, this would suggest that TGCT-residing NK cells may play a fundamental role in the initial recognition and subsequent lysis of tumour cells. We and others (Grobholz *et al*., 2000, Hadrup *et al*., 2006), have shown few NK cells in TGCTs compared to T cell frequency, yet the phenotype and function of these NK cells has not been previously investigated.

We show the predominant NK cell subset within TGCTs is the $CD56^{hi}CD16^{-}$ population. We and others have shown that this subset represents only a minority subset in peripheral blood, ranging from approximately 5-10% of total NK cells (Sinkovics and Horvath, 2005), in contrast to sites of peripheral inflammation where $CD56^{hi}CD16^{-}$ NK cells represent 40–60% of total NK cells (Dalbeth *et al*., 2004). We speculate that the preferential accumulation of $CD56^{hi}CD16^{-}$ NK cells in TGCTs is in part due to increased CXCR3 surface expression (Campbell *et al*., 2001) and its corresponding chemokine, IP-10, being secreted by seminoma stroma. However, the migratory potential alone may not explain the increase of $CD56^{hi}CD16^{-}$ cells into TGCT tissues in all instances. Increased proliferation of these NK cells within the tumour would elevate the levels of $CD56^{hi}CD16^{-}$ cells. The interaction of the $CD56^{hi}CD16^{-}$ NK population with DCs induces proliferation in this subtype but not in the $CD56^{low}CD16^{+}$ population (Moretta *et al*., 2004). Therefore, local interaction with tumour residing DCs may result in elevated frequencies of $CD56^{hi}CD16^{-}$ NK cells.

Within peripheral blood, the $CD56^{hi}CD16^{-}$ subset of NK cells are predominantly cytokine secreting cells, with lower cytotoxic potential than their $CD56^{low}CD16^{+}$ counterparts (Cooper *et al*., 2001). Surprisingly, we observed enhanced cytokine secretion and cytotoxic capacity of tumour infiltrating $CD56^{hi}CD16^{-}$ NK cells following stimulation. It has been suggested that $CD56^{hi}$ NK cells are an activated form of $CD56^{low}$ cells (Cooper *et al*., 2001), which may indicate an activated phenotype of NK cells in TGCTs, a prerequisite for cytotoxic activity. This may also explain the increased CD56 expression on $CD16^{+}$ cells following *in vitro* stimulation in this study. Alternatively, IL-2 supplementation during *in vitro* stimulation, or its secretion by activated T cells within the tumour microenvironment, could lead to increased cytotoxicity of $CD56^{hi}CD16^{-}$ NK cells (Robertson *et al*., 1992). Overall, we consider NK cells to play an important role in anti-tumour immunity, yet the high frequency of infiltrating T cells, as well as tumour induced suppression mechanisms, may hinder their ability to effectively interact and lyse tumour cells.

In the present study, we demonstrate effective tumour killing by tumour residing NK cells *in vitro*, however, lysis in this system (using K562 cells) was mediated by the lack of MHC class I on the tumour cell line, and not through activation of NKG2D. NK cells expressing NKG2D specifically lyse tumours expressing NKG2D ligands including MICA/B and ULBPs (Arina *et al*., 2007), and blockade of NKG2D results in an impaired ability to kill transformed targets (Strid *et al*., 2008). We demonstrate expression of NKG2D activating ligands, MICA and ULBP2, on a number of tumour samples, but not ULBP1 or 3. Tumour cells may evade NKG2D-mediated immune surveillance by specifically shedding MICA and ULBP2 via metalloproteinases (Bauer et al., 1999, Waldhauer and Steinle, 2006), reducing the ability of NK cells to recognise the tumour. Soluble MICA and ULBP2 have

been show to promote the internalization and subsequent degradation of NKG2D in NK cells (Groh *et al*., 2002), rendering them less efficient at tumour cell lysis. This may help explain our observation of decreased NKG2D expression on both NK cell subsets that infiltrate TGCTs, and may render these cells unable to receive activating signals through NKG2D. These observations suggest a prominent role for MICA and ULBP2 in TGCT immune surveillance. By promoting the reduction of NKG2D ligands on the cell surface, tumour cells may efficiently escape innate immune recognition (Diefenbach and Raulet, 2002). Future studies would aim to determine the effect of NKG2D downregulation on the functionality of NK cells, through the use of tumour cells lines which provoke NK cell-mediated cytotoxicity through activating NKG2D.

Furthermore, we found that NKG2D expression on tumour-infiltrating CD8 T cells was extensively downregulated. NKG2D costimulates and augments TCR-mediated activation of CD8 T cells (Bauer et al., 1999, Roberts et al., 2001), but chronic stimulation with NKG2D ligands can lead to its internalisation (Cerboni *et al*., 2009), leading to functional impairment (Groh *et al*., 2002). In summary, NKG2D is downregulated on both NK cells and CD8 T cells, which is presumably mediated by the tumour. The negative regulation of NKG2D may be an important mechanism of tumour-induced immune suppression of both the innate and adaptive immune response in TGCT patients. Furthermore, TGFβ secreted by tumour stroma or Tregs may also downregulate NKG2D expression. Several publications have described TGFβ-induced downregulation of NKG2D on tumour residing NK cells and CD8 T cells, rendering them less efficient at tumour cell killing (Crane *et al*., 2010, Friese *et al*., 2004). Our results also show a reduction in NKG2D density on $CD56^{hi}CD16^{-}$ NK cells in peripheral blood. The expression of NKG2D over time was

significantly increased following tumour removal; suggesting NK cells with decreased NKG2D expression may be entering systemic circulation.

To determine the extent of NKG2D ligand shedding from the tumour surface and the potential role of TGFβ in mediating immune evasion in TGCT patients, levels of these molecules in patient sera during tumour development would need to be determined. We would expect higher levels of these molecules in TGCT patients with active disease than in post-operative patients or healthy donors. We show for the first time that NKG2D expression is downregulated on both the innate and adaptive immune cells that infiltrate TGCTs.

Finally, we demonstrated the presence of activated γδ T cells in TGCTs. In contrast to (Zhao et al., 1995), who observed a high percentage of γδ T cells in TIL, we observed proportions similar to those found in peripheral blood, and (Bols et al., 2000) demonstrated only focal staining of γδ T cells by IHC. Importantly, MICA and ULBP-expressing tumours are recognised and killed by γδ T cells (Bauer et al., 1999, Maeurer et al., 1996), mediated not only through their TCR but also by activation of the NKG2D signalling pathway (Rincon-Orozco *et al*., 2005). This suggests γδ T cells may be able to directly target TGCTs, although we assume that surface expression of NKG2D is also reduced on γδ T cells, and dysfunction extends to this cell type.

Conclusion

In conclusion, TGCTs are infiltrated by a variety of immune cells with putative anti-tumour activity. Of particular importance are the CD4 and CD8 T cell subsets, which predominate in TIL. Cell surface expression analysis suggests these T cells are antigen experienced, recently activated, oligoclonal populations; many of which have cytotoxic capacity. Our findings suggest T cells from TGCTs have high proliferative potential upon TCR stimulation *in vitro*, yet clonal expansion within the tumour masses may be restricted. The upregulation of inhibitory receptors on T cells and the down regulation of NKG2D on T cells and NK cells suggest multiple immune suppressive mechanisms exist within the tumour microenvironment; some of which span both the innate and adaptive arms of the immune system. The role of this immune infiltrate in controlling tumour growth, and the antigen specificity of T cells infiltrating these tumours is presently unknown.

CHAPTER 4: CANCER TESTIS ANTIGEN RESPONSES IN TGCT PATIENTS

Introduction

Tumour-specific antigens (TSAs) are expressed in a high proportion of tumours of various histopathological types, but are absent in healthy somatic tissue, with the exception of the CTAg family proteins (e.g. Melanoma-associated antigen - MAGE), which are expressed in testicular germ cells. These antigens are not presented to the developing immune system in the thymus hence central tolerance is not generated against them. In addition, the blood-testis barrier (BTB) prevents the presentation of CTAgs in the periphery. The tumour restricted expression of TSAs makes them excellent targets for anti-tumour immune responses mediated by cytotoxic CD8 T cells. MAGE antigens have been studied in great detail, and many T cell epitopes have been described (Traversari *et al*., 1992, Ottaviani *et al*., 2005, Zhang *et al*., 2002, Luiten and van der Bruggen, 2000). Elevated levels of MAGE-specific T cells in peripheral blood have been described in patients with various cancers (Zerbini *et al*., 2004, Goodyear *et al*., 2005) but are absent or at very low frequency in healthy donors. The importance of MAGE-specific T cells in anti-tumour immunity have been demonstrated by their ability to induce tumour regression in vaccine trials (Godelaine *et al*., 2003, Coulie *et al*., 2002, Karanikas *et al*., 2003).

In this chapter we examined the frequency and kinetics of MAGE-specific T cell responses in TGCT patients and in cancer-free healthy individuals. The functional characteristics of MAGE-specific T cells were also investigated.

Cancer Testis Antigens are Expressed in TGCTs

There is conflicting evidence regarding the expression profile of CTAgs in TGCTs, including MAGE family antigens (Grobholz *et al*., 2000, Chen *et al*., 2013, Hara *et al*., 1999). Therefore, we examined the transcript levels of various MAGE antigens and, where appropriate, the protein abundance in TGCT tissue and healthy testis.

Firstly, CTAg expression was determined in each tissue by qRT-PCR represented relative to healthy testis, and normalised to GAPDH. Gene transcripts for all CTAgs examined were abundant in healthy testis. MAGEA1 transcripts were detected in 50% of seminoma patients (2 out of 4), but were present at levels lower than that of healthy testis. MAGEA1 expression was not observed in NSGCTT (0 out of 2) or mGCT tissue (0 out of 1) (Figure 39a). MAGEA3 was expressed in 25% of seminoma tissues, with levels 1.58-fold greater than healthy testis, but was practically absent in all other tissue specimens (Figure 39b). Similarly, MAGEA4 was expressed in 25% of seminoma samples, but was undetectable in other TGCT specimens (Figure 39c). NY-ESO-1 was expressed at low levels in one seminoma specimen (Figure 39d). MAGEB1 expression was detected in healthy testis, but not in any TGCT tissues (Figure 39e).

Noticeably, patients with low, but detectable expression of MAGEA1 also had high expression of either MAGEA3 (patient 68CL) or MAGEA4 (patient 75NS). This suggests multiple MAGE antigens are expressed in a proportion of seminoma tumours.

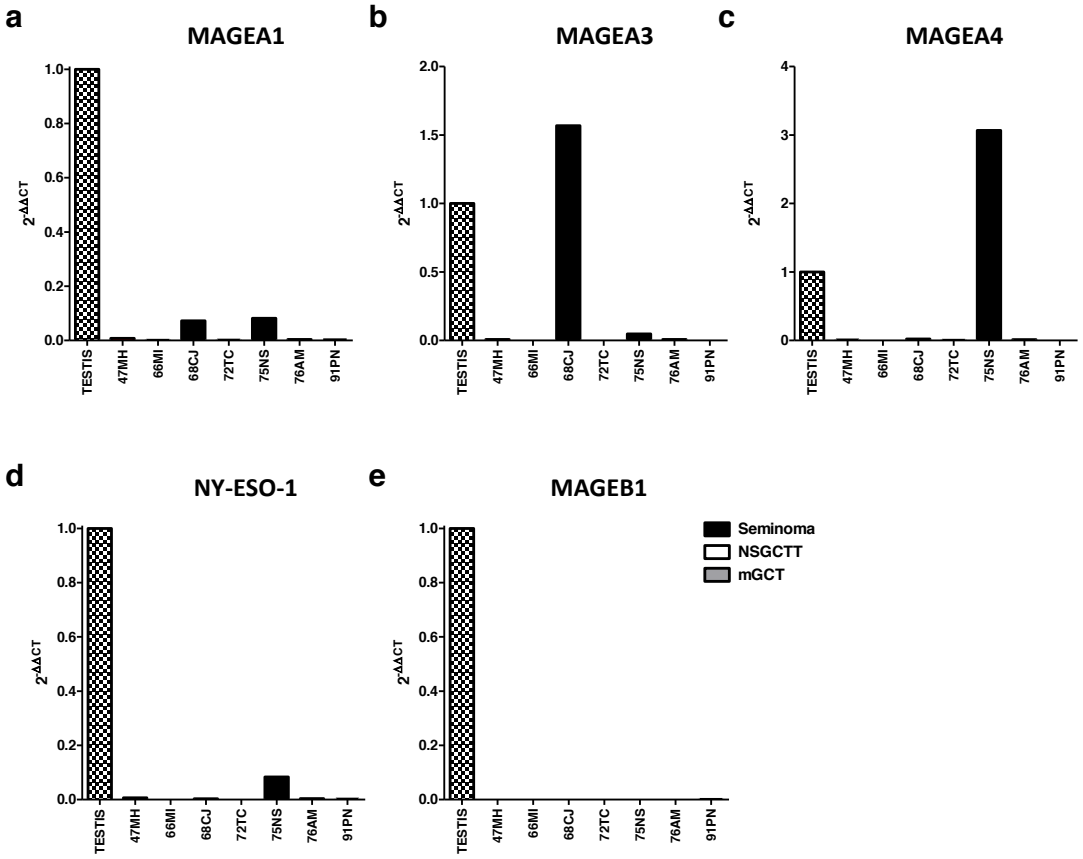

Figure 39. Expression of CTAg transcripts in primary TGCT tissue.
The mRNA levels of MAGEA1 (a), MAGEA3 (b), MAGEA4 (c), NY-ESO-1 (d), and MAGEB1 (e) is shown. Each bars represent relative expression levels of individual patients. "TESTIS" represents the mean expression level in normal testis tissue of 3 patients. Expression is relative to testis and normalised to GAPDH.

To verify whether transcript levels correlate with protein expression, we performed western blot analysis with specific MAGEA antibodies on healthy testis and TGCT samples (Figure 40a). Protein abundance was determined by densitometry. MAGEA1, A3 and A4 protein expression levels correlated well with transcript levels (Figure 40b,c,d).

We show differential expression of MAGEA antigens in TGCTs at both the mRNA and protein level. Expression of these antigens was only detectable in seminoma specimens. We also show a proportion of TGCTs that expressed more than one MAGEA family antigen. NY-ESO-1 and MAGEB1 are not expressed in TGCTs.

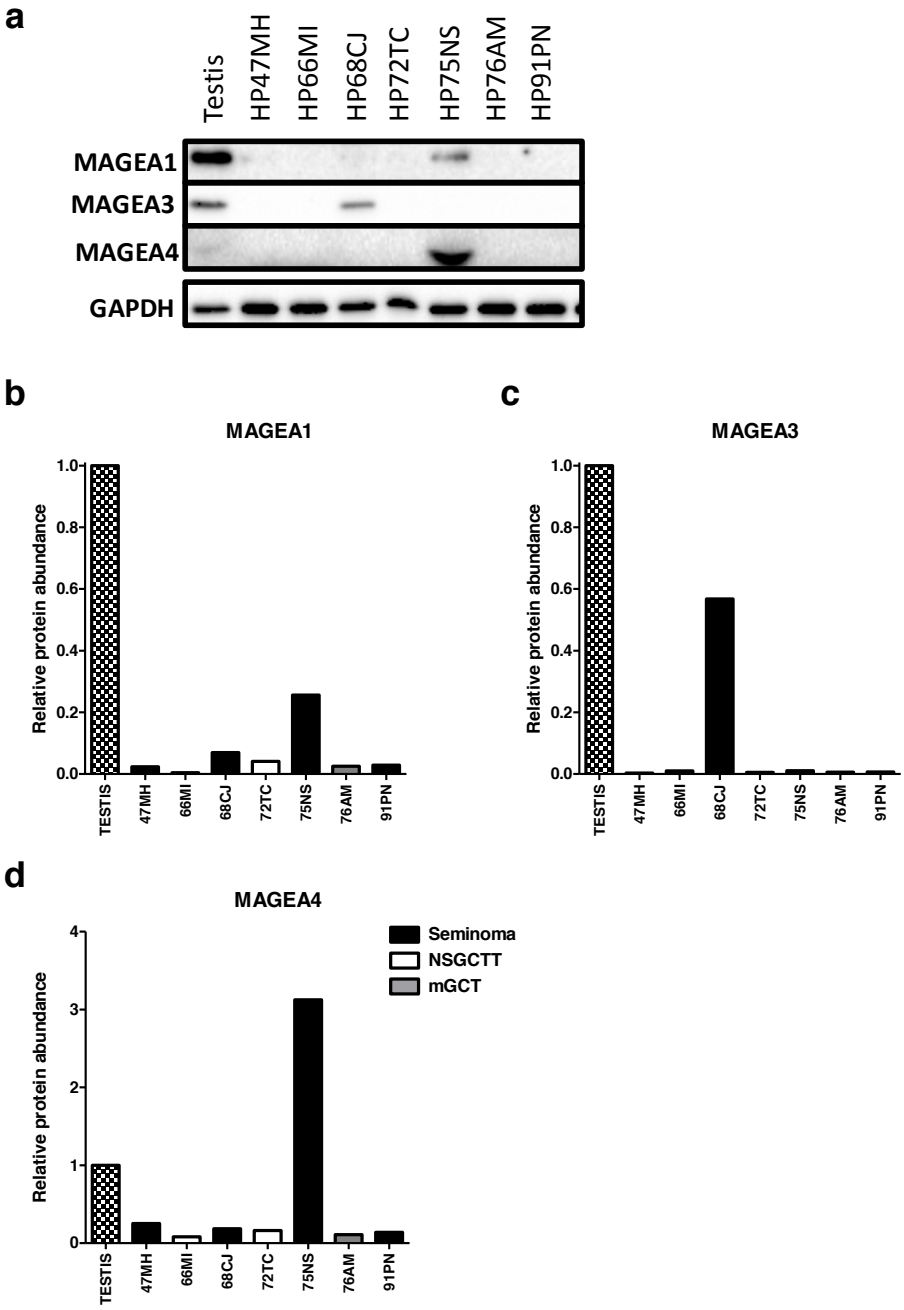

Figure 40. Expression of CTAg protein in primary TGCT tissue.
Western blot analysis of MAGEA1, MAGEA3 and MAGEA4 to determine protein expression in TGCT tissue (a). GAPDH was used as a loading control and to determine relative protein abundance between patients. Relative protein abundance was calculated by densitometry, for MAGEA1 (b), MAGEA3 (c) and MAGEA4 (d), relative to testis, normalised to GAPDH.

MAGE-specific CD8 T Cells are Detectable in TGCT Patients

A proportion of TGCTs express MAGEA family antigens and the vast majority of these tumours have an immune infiltrate. We therefore investigated whether cell mediated immune responses are generated against these antigens. If spontaneous MAGE-specific T cell responses are generated towards the tumour, we would expect to detect these cells in peripheral blood of TGCT patients.

We examined the frequency of MAGEA1, MAGEA3 and MAGEA4-specific T cells from PBMC of TGCT patients (n=22) by MHC-dextramer analysis, following ten day T cell line peptide culture (TCL). Peptide lines were set up with freshly isolated PBMCs, without prior enrichment of CD8 T cells. Figure 41 illustrates the experimental procedure used for dextramer staining, including an example of positive dextramer staining and subsequent purification. Table 27 details the peptides used in the TCL stimulation assay and those present in the MHC-peptide-dextramer complexes. Flow cytometry analysis was used to visualise dextramer positive (MAGE-specific) T cells.

Representative density plots show the presence of MAGE-specific CD8 T cells in peripheral blood of TGCT patients, following TCL culture (Figure 42). The specificity of dextramer staining was illustrated by the absence of staining of CD8-negative T cells (presumably CD4 T cells and NK cells) and low background staining with the negative dextramer (irrelevant peptide). A positive response was defined as a frequency of MAGE-specific cells greater than an arbitrary value of 0.05% of the total CD8 T cell pool. The percentage of cells binding to the negative control dextramer was deducted.

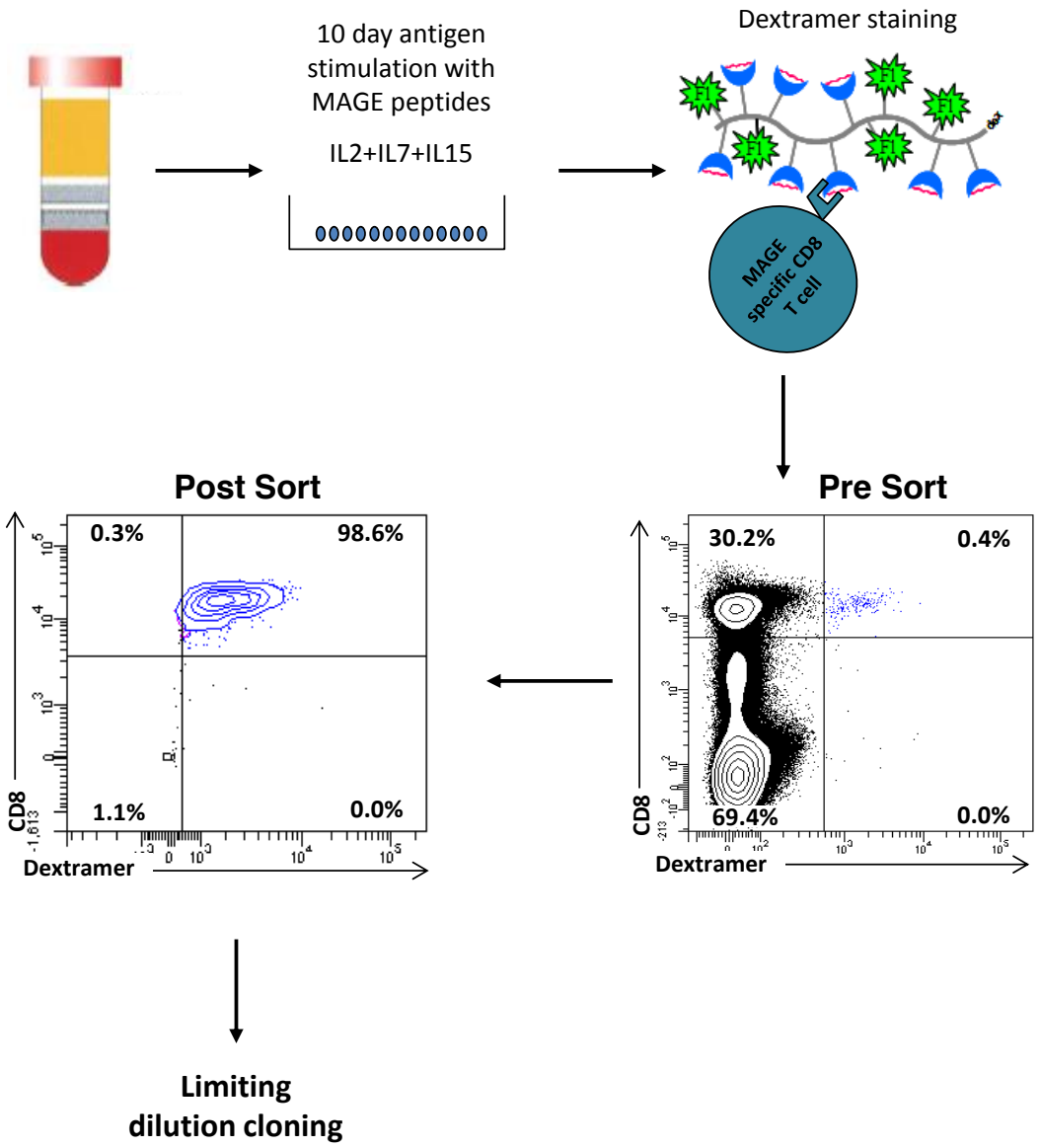

Figure 41. Schematic demonstrating the procedure for identification and purification of MAGE-specific T cells.

PBMCs were stimulated with immunogenic peptides corresponding to various MAGE antigens, in the presence of IL2, IL7 and IL15, for 10 days. MAGE-specific cells were detected using MHC-dextramer staining and analysed by flow cytometry. The 'Pre Sort' density plot (right) is representative of a patient with a positive response directly following TCL culture. 'Post sort' density plot (left) is the same sample following magnetic selection of dextramer positive cells. Where appropriate, cells were set up for limiting dilution cloning for functional analysis.

Table 27. Detailed list of peptides used in T Cell Line assays and Dextramer complex.

Gene product	HLA restriction	HLA frequency (%)	Peptide* (aa Sequence)	Position
NY-ESO-1	A2	42.6	**MLMA**QEALAFL	1-11
MAGEA1	A2	42.6	**KVLE**YVIKV	278-286
	B7	21.4	**RVRF**FFPSL	289-298
MAGEA2	A2	42.6	**YLQL**VFGIEV	157-166
MAGEA3	A1	29.1	**EVDPI**GHLY	168-176
	A2	42.6	**KVAE**LVHFL	112-120
MAGEA4	A2	42.6	**GVYD**GREHTV	230-239

* each letter represents an amino acid. Letters in bold are shorthand as referred to in the text

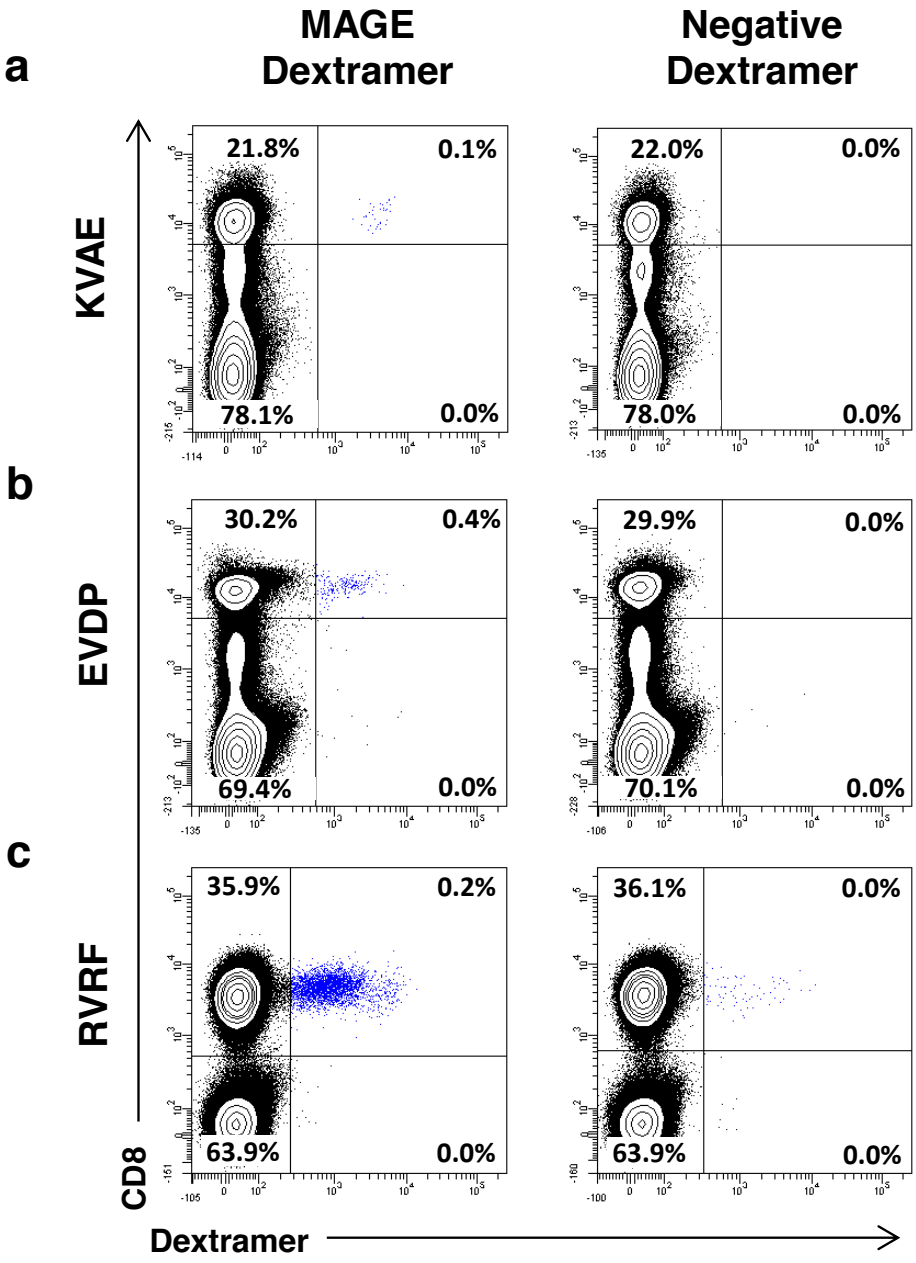

Figure 42. Detection of MAGE-specific T cells by peptide-MHC dextramer.
Flow cytometry contour plots illustrate the detection of MAGE- specific CD8 T cells in TGCT patients prior to chemotherapy, using MHC-peptide Dextramers. Representative plots show KVAE (a), EVDP (b) and RVRF (c) –specific T cells detected in TGCT patients, following 10 day peptide TCL expansion. The left column demonstrates cells stained positive for MAGE- specific dextramer and the right column with the non-specific dextramer (negative control). Dextramer positive cells are highlighted in blue.

The magnitude of a MAGE-specific response was calculated, and expressed as a proportion of total CD8 T cells (Figure 43a). MAGEA1 (RVRF) -specific T cells were detected in 9% of TGCT patients at frequencies of 0.06% to 0.58% of total CD8 T cells. Approximately a third (31%) of TGCT patients assessed had a MAGEA3 (combined EVDP and KVAE) response. Patients with an EVDP response had EVDP-specific cells at frequencies of 0.13% to 1.14% of total CD8 T cells. The frequency of KVAE-specific T cells in patients with a KVAE response was lower than that of EVDP, ranging from only 0.06% to 0.33% of total CD8 T cells. Interestingly, one seminoma patient had both a MAGEA1 (RVRF) and a MAGEA3 (EVDP) response. Another patient had responses to two MAGEA3 peptides (EVDP and KVAE) presented through different HLA molecules. In this patient cohort, no NY-ESO-1 (MLMA), MAGE-A2 (YLQL) or MAGEA4 (GVYD) –specific T cell responses were detected. Overall, MAGE-specific responses were detected in 36% (8 out of 22) of patients, one of whom developed responses to multiple MAGEA antigens. The HLA-type of patients with a positive response was subsequently determined to verify the validity of the response. In all cases, the observed responses to a particular HLA-restricted peptide were consistent with the HLA-type of the patient.

Next, we categorised responding TGCT patients according to tumour type - seminoma and NSGCTT (Figure 43b). All MAGEA1 (RVRF) responses were from seminoma patients, whereas MAGEA3 responses (combined KVAE and EVDP) were detected in both seminoma and NSGCTT patients. Our results reveal that MAGE-specific T cells are present in the peripheral blood of TGCT patients, presumably generated towards MAGEA family-expressing tumours.

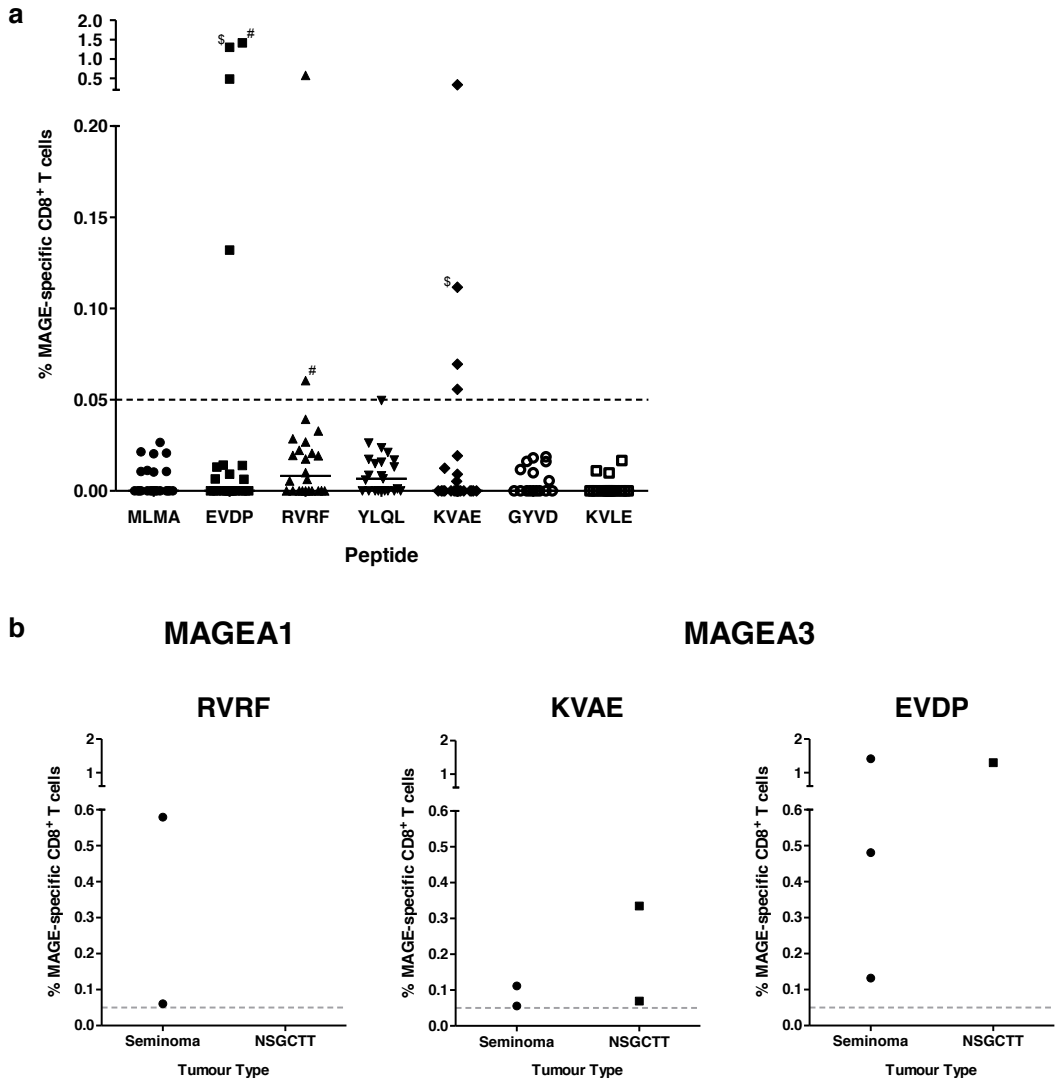

Figure 43. The rate of detection of MAGE-specific T cells from PBMC of TGCT patients. In TGCT patients in whom a MAGE-specific T cell response was detected the frequency of MAGE specific T cells is shown as a percentage of total CD8 T cells, following 10 day peptide TCL culture (a). The dotted line represents the threshold for a positive response. The threshold was set at an arbitrary value of 0.05% of total CD8 T cells, and is indicated by a dotted line. The frequency of cells stained positive with the non-specific dextramer was deducted for the MAGE-specific dextramer frequency. Positive responses were detected against EVDP, RVRF and KVAE peptides, and were categorised by tumour type (b). # represents points from the same patient with a MAGEA1 and MAGEA3 response.
$ represents points from the same patient with a MAGEA3 response to 2 peptides presented through different HLA serotypes.

MAGEA3-specific T Cells Secrete Inflammatory Cytokines

Next we addressed the function of MAGE-specific T cells through the use an EVDP-specific T cell clone generated from a seminoma patient prior to adjuvant chemotherapy. The generation of a MAGEA3 T cell clone (TCC) involved pulsing PBMC with EVDP peptide followed by short term *in vitro* culture, followed by enrichment using the EVDP-dextramer and MACS technology. Subsequent cloning of single cells was achieved by a limiting dilution cloning method. The procedure and representative enrichment from a short term culture is shown in Figure 41. Developing clones were visualised and tested for dextramer specificity between 14 days and 28 days following setup.

The enrichment of dextramer positive cells by MACS gave a purity of between 75% and 98% in the patients tested. Unfortunately, cloning efficiency was surprisingly low, and only a single T cell clone was generated. To our knowledge, this is the first MAGEA3-specific T cell clone generated from a patient with testicular cancer.

Next we determined the functional capabilities of these cells following peptide stimulation *in vitro.* The MAGEA3-specific clone was assessed for its ability to release IFNγ and TNFα, following co-culture with HLA-A1-positive EVDP-pulsed target cells (LCL). We determined the production of inflammatory cytokines by intracellular cytokine staining. The TCC produced both IFNγ and TNFα following co-culture with EDVP peptide pulsed LCLs at low E:T ratios (Figure 44). Interestingly, a higher proportion of cells released TNFα compared to IFNγ following stimulation at 1:10 (45.97 vs. 7.17) and 1:1 (15.48 vs. 2.06) E:T ratios. No cytokine release was observed following co-culture with LCL pulsed

with irrelevant peptide (KVAE), or with IL-2 alone. Representative dot plots show that the majority of MAGE-specific cells were producing TNFα only. All IFNγ secreting cells simultaneously produced TNFα and no IFNγ single-secreting cells were observed following stimulation with peptide-pulsed LCL (Figure 44a).

MAGEA3-specific T Cells Recognise Endogenously Processed Antigen

Next, we determined whether the MAGEA3-specific T cell clone was able to recognise endogenously processed and presented MAGEA3 antigen. This was achieved by co-culturing the TCC with an HLA-A1+ MAGEA3+ tumour cell line, HT-29, and examining the production of IFNγ and TNFα. This revealed a high proportion of cells which secrete TNFα but very few which secrete IFNγ (Figure 45), similar to that observed following co-culture with peptide pulsed LCL. HT-29 cells pulsed with peptide showed similar results to those not pulsed with peptide, suggesting HT-29 cells are effectively presenting MAGEA3. Incubation of HT-29 cells with an irrelevant CD8 T cell clone (virus-specific) does not induce cytokine production in these cells (Figure 45b). This confirms that the MAGEA3-specific TCC is recognising and responding to endogenously processed MAGEA3, and the HT-29 cell line is not inducing cytokine production independent of TCR engagement.

MAGEA3-Specific T Cells Have High Cytolytic Potential

The cytotoxic potential of cells cannot be solely predicted based on the cytokines they secrete. We used the mobilisation of CD107a on the cell surface as an indicator of degranulation, a prerequisite for cytotoxic granzyme release. The TCC was stimulated with LCL pulsed with either EVDP or an irrelevant peptide (KVAE), or with a HT-29 cell

line (Figure 46). We found that CD107a surface expression was induced on EVDP-specific CD8 T cells following co-culture with EVDP-pulsed LCL (Figure 46a,b) and HT-29 cell line (Figure 46c). We also show that increasing the proportion of target cells from 1:1 to 1:10 induces degranulation in a greater proportion of T cells, presumably due to an increase in the number of MHC molecules presenting EVDP peptide.

In addition, we examined the proportion of CD107a expressing cells according to their cytokine profile (Figure 47). We show that the majority of cells simultaneously secreting TNFα and IFNγ, or TNFα alone were strongly associated with CD107a expression. This suggests cytokine secretion is a good indicator of cytotoxic potential. Interestingly, HT-29 cells induced degranulation of a high proportion of T cells without inducing cytokine production (1:10 ratio, 42.60%). This was also observed following stimulation with EVDP-pulsed LCLs, but to a lesser extent (1:10 ratio, 8.56%). This suggests that a proportion of MAGE-specific T cells can mediate cytolytic activity without secreting inflammatory cytokines. In summary, we have observed that all EVDP-specific cytokine secreting cells are cytotoxic; however, we have identified a population of cytotoxic cells that fail to secrete inflammatory cytokines.

Finally, a peptide titration assay was used to determine the avidity of the EVDP-specific T cell clone. Cells were stimulated with 10-fold dilutions of peptide ranging from 10^{-5} to 10^{-11} M, and IFNγ levels in cell culture supernatant were determined by ELISA. A reduction in IFNγ secretion was demonstrated with diminishing concentrations of peptide (Figure 48a). This clone had fairly low avidity for peptide with 50% maximal IFNγ release at a peptide

concentration between 10^{-6} and 10^{-7} (Figure 48b). This is comparable however with MAGE-specific T cell clones generated from PBMC of multiple myeloma patients (Goodyear *et al*., 2005), but is considerably lower than viral specific clones generated in our laboratory (data not shown).

Overall, our results suggest that MAGEA3-specific T cells isolated from peripheral blood of TGCT patients have high cytotoxic potential, although the avidity of the TCR:pMHC interaction may be low. Moreover, this HLA-A1-restricted MAGEA3-specific T cell clone, but not an HLA-A1-restricted irrelevant (virus-specific) T cell clone, has the capacity to degranulate in response to tumour cells that have the capacity to present MAGEA3 through HLA-A1.

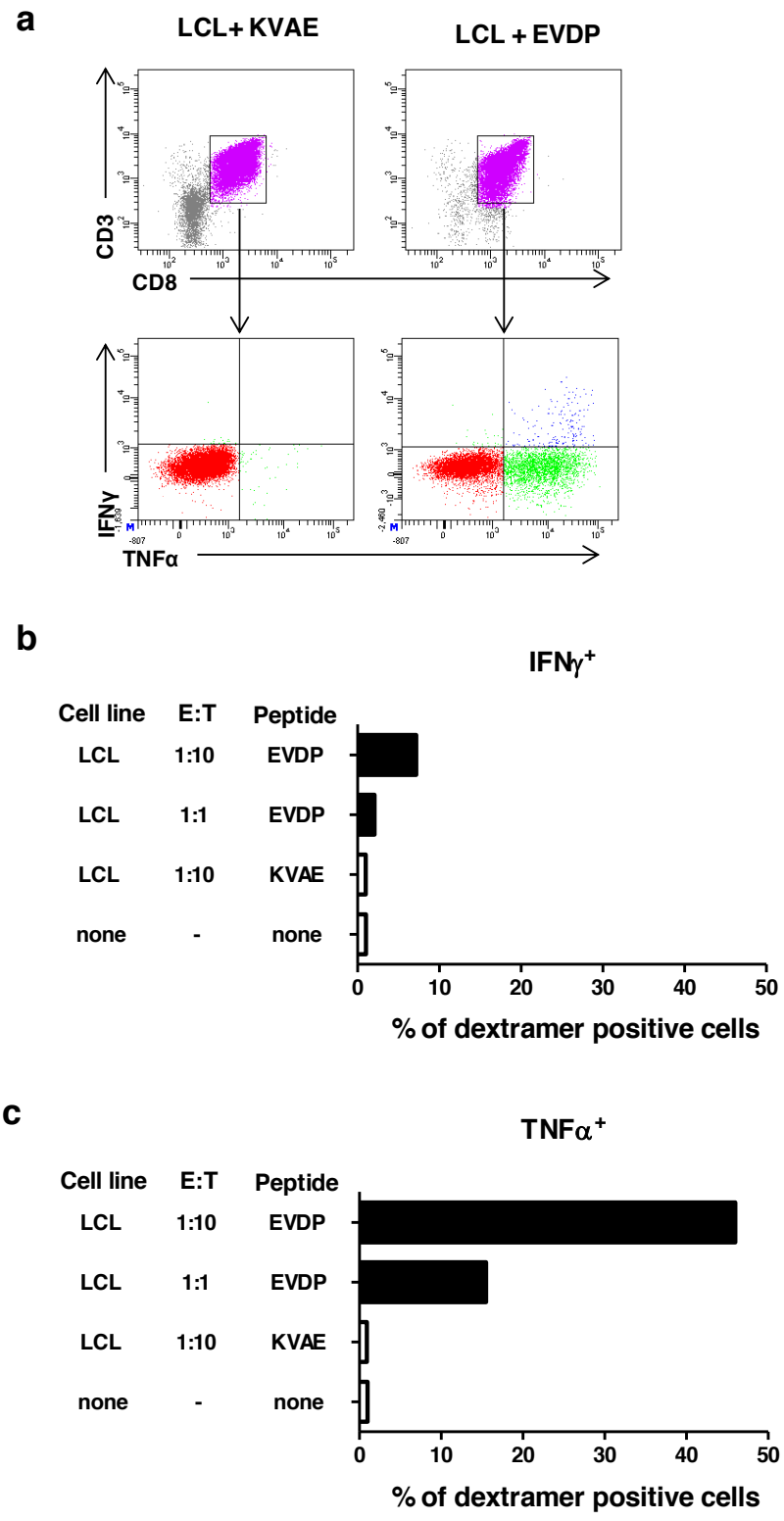
a
LCL+ KVAE
LCL + EVDP
CD3
CD8
IFNγ
TNFα
b
IFNγ+
Cell line
E:T
Peptide
LCL
1:10
EVDP
LCL
1:1
EVDP
LCL
1:10
KVAE
none
-
none
0
10
20
30
40
50
% of dextramer positive cells
c
TNFα+
Cell line
E:T
Peptide
LCL
1:10
EVDP
LCL
1:1
EVDP
LCL
1:10
KVAE
none
-
none
0
10
20
30
40
50
% of dextramer positive cells

Figure 44. Inflammatory cytokine secretion of an EVDP–specific TCC generated from PBMC of a seminoma patient, following stimulation with LCL pulsed with EVDP peptide.

Cell were stimulated with LCL pulsed with irrelevant peptide (LCL+KVAE) and with test peptide (LCL+EVDP). Flow cytometry dot plots illustrate the secretion of IFNγ and TNFα with irrelevant and test peptide (a). EVDP-specific T cells were stimulated with peptide loaded LCL at E:T ratios of 1:10 and 1:1 with test peptide EVDP (filled bars). Control experiments (open bars) were cells treated with irrelevant peptide KVAE at a 1:10 ratio, and T cells alone. The secretion of IFNγ (b) and TNFα (c) was quantified and represented as a percentage of total dextramer positive cells.

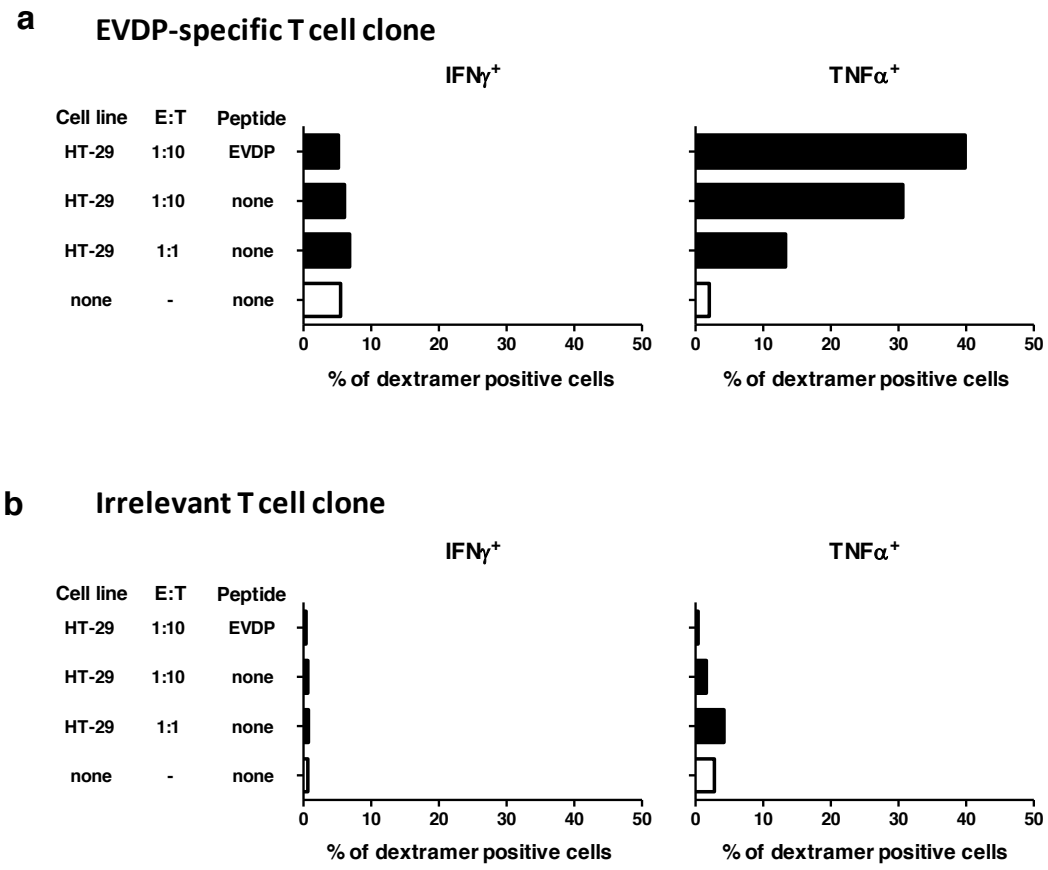

Figure 45. Inflammatory cytokine secretion of an EVDP –specific TCC stimulated with endogenously presented MAGEA3 antigen.

EVDP-specific T cells (a) and an irrelevant T cell clone (b) were stimulated with HT-29 tumour cell line at E:T ratios of 1:10 and 1:1. Negative control (open bar) was T cells alone. Positive control was HT-29 cells pulsed with EVDP peptide. The secretion of IFNγ and TNFα was quantified and represented as a percentage of total dextramer positive cells.

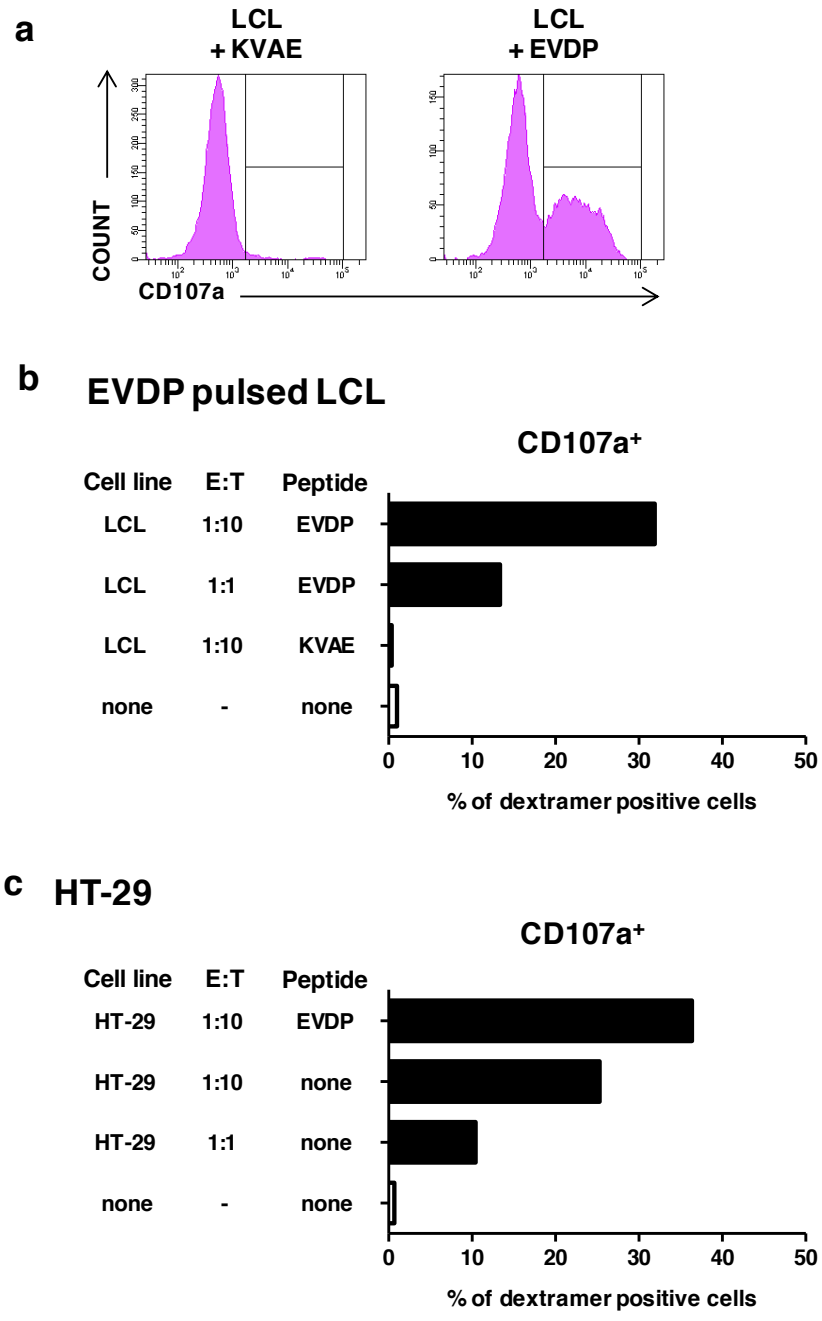

Figure 46. Cytotoxic potential of an EVDP-specific TCC.
CD107a was used as a marker of degranulation. Histograms illustrating the proportion of cells expressing CD107a following stimulation with test peptide is shown (a). The induction of surface CD107a expression of an EVDP –specific T cell clone stimulated with EVDP pulsed LCL (b) and HT-29 cell line (c), at E:T ratios of 1:10 and 1:1, is shown. CD107a expression was expressed as the percentage of total EDVP-specific cells. Negative control (open bar) was LCL pulsed with KVAE peptide and T cells alone in (b), and T cells alone in (c). Positive control in (c) was HT-29 cell line pulsed with EVDP peptide.

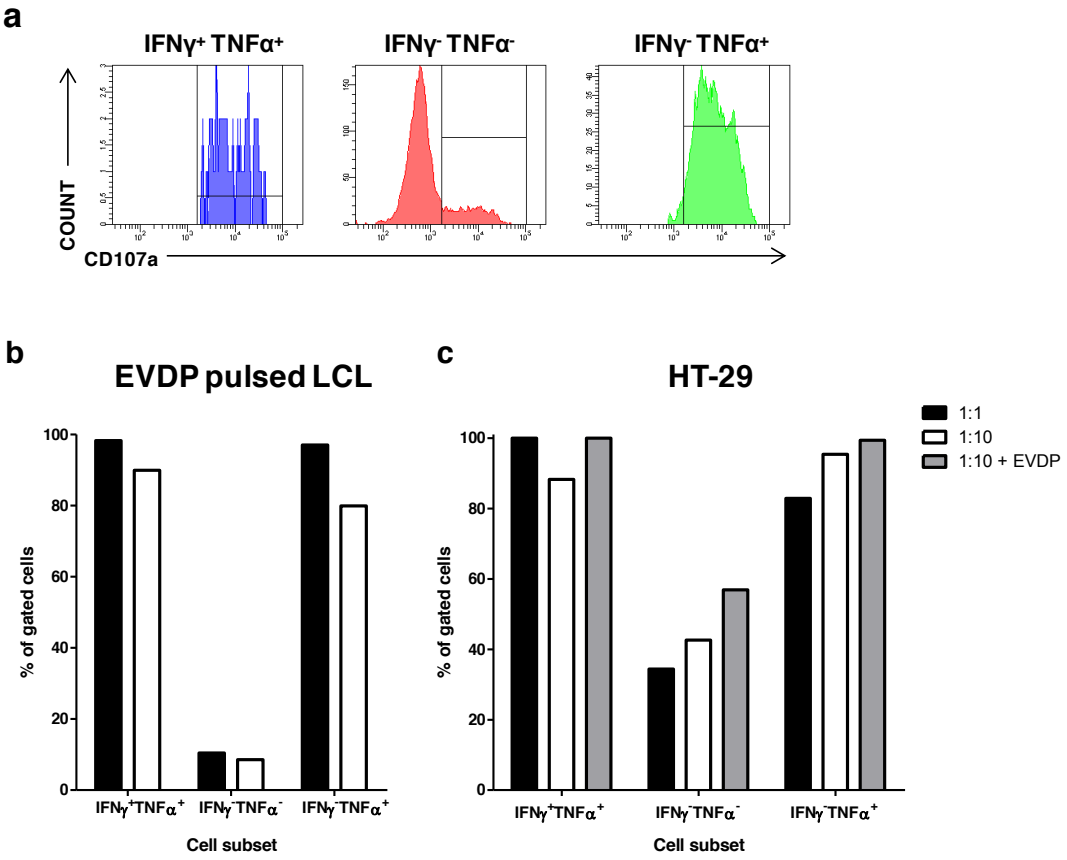

Figure 47. Cytotoxic capacity of an EVDP-specific T cell clone in relation to cytokine secretion.

The proportion of cells that are CD107a positive following stimulation was determined for each cytokine group. Histograms illustrating the proportion of cells expressing CD107a following stimulation with test peptide, within the IFNγ^{+}TNFα^{+} (blue), IFNγ^{-}TNFα^{-} (red), and IFNγ^{-}TNFα^{+} (green) quadrants is shown (a). The proportion of CD107a positive cells following stimulation with EVDP peptide pulsed LCL (b) and HT-29 (c) was represented as a percentage of cells within that cytokine group.

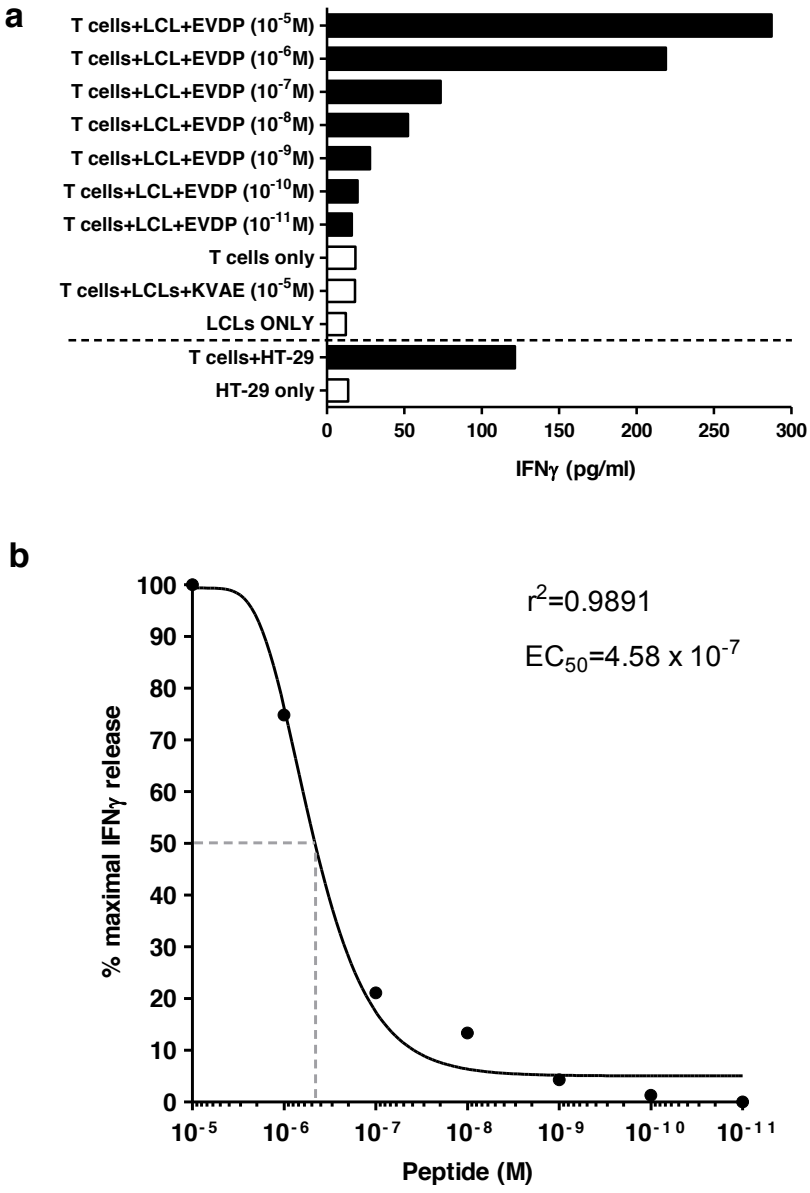

Figure 48. Titration of EVDP peptide concentration to establish avidity of EVDP-specific TCC.

EVDP-specific T cells were co-cultured with EVDP loaded LCLs or MAGEA3 expressing HT-29 cell line, and response was measured using IFNγ production (a). For peptide titration, LCLs were pulsed with 10-fold diminishing concentrations of peptide from 10^{-5}M to 10^{-11}M. Spontaneous IFNγ production (open bars) was tested by co-culture of clones with LCL pulsed with irrelevant peptide (KVAE), T cells alone, LCL alone, or HT-29 alone. A standard curve of the logarithmic relationship between concentration and absorbance was used to calculate the IFNγ concentration in cell culture supernatants. The maximum and minimum IFNγ release was calculated and used to determine the half maximal IFNγ release (EC_{50}) of the clone (b). The dotted line represents the EC_{50} for the clone, which was between 10^{-6}M to 10^{-7}M.

Quantitation of CTAg Responses in TGCT Patients

We have identified, isolated and analysed MAGE-specific CD8 T cells in peripheral blood of TGCT patients. Using dextramers we have shown the expression of MAGE antigens within testicular tumours. Dextramer analysis has its limitations as it requires prior knowledge of immunogenic epitopes and the HLA type of patients. In addition, dextramer analysis may underestimate the number of patients with a MAGE-specific response as only one or two epitopes are being examined. Dextramer analysis is further complicated by the need to expand antigen-specific cells *in vitro* to enable efficient detection. It is important to note that this experimental system only detects CD8 T cells and therefore does not provide information regarding MAGE-specific CD4 T cells, which are fundamental for an effective cell-mediated immune response.

We therefore quantitated CTAg responses in a large cohort of patients (n=45) using a combination of MAGE overlapping peptides, which span the entire length of the protein, and a highly sensitive IFNγ ELISPOT assay. The robustness of this assay is proven and permits its use in a clinical trial setting, such as those conducted in our institute. This assay allows the simultaneous detection of CD4 and CD8 T cell responses, which are HLA unrestrictive and fully quantitative. In addition, presentation of peptides is done so by autologous PBMCs, removing the use of artificial target cells, which may provoke non-specific IFNγ production.

MAGEA-specific T Cells are elevated in TGCT Patients

We determined the frequency of CTAg-specific cells in healthy donors. Cells were stimulated with overlapping peptides (or appropriate controls) in the ELISPOT assay for 16-18 hours. A single IFNγ secreting cell is represented as a single spot. In the peripheral blood of healthy donors absent or very low frequencies of CTAg-specific cells were present (Figure 49). The highest frequency of IFNγ secreting CTAg specific T cells were against the NY-ESO-1 antigen, with 41 cells per million PBMC detected (0.0041%). For MAGEA antigens the frequency of cells ranged from 0 to 40 cells. MAGEB1 specific cells were practically absent in healthy donors with a maximum of 9 cells per million PBMC. We set a positive response threshold at double the highest CTAg-specific cell frequency found in healthy donors (82 cells per million PBMC).

Next, we investigated the frequency of CTAg-specific cells in NSGCTT (n= 10), mGCT (n= 6), and seminoma (n= 29) patients. Clinically, mGCTs are classified as part of the NSGCTT subtype. This classification is used because the management of mGCT is the same as NSGCTT. However, in this study we have placed mGCT into its own category since these tumours contain elements of both seminoma and non-seminoma. Figure 50 is a representative ELISPOT readout, demonstrating the presence of MAGEA1, A3, and A4-specific T cells in the peripheral blood of a seminoma patient. Spots in the unstimulated well represent cells releasing IFNγ non-specifically, which were detectable at low levels in this patient. Patients with high background were excluded from analysis. NY-ESO-1 and MAGEB1-specific cells were undetectable in this patient. CEFT (positive control) induced a high frequency of spots demonstrating cells are responsive to antigenic peptide stimulation.

a

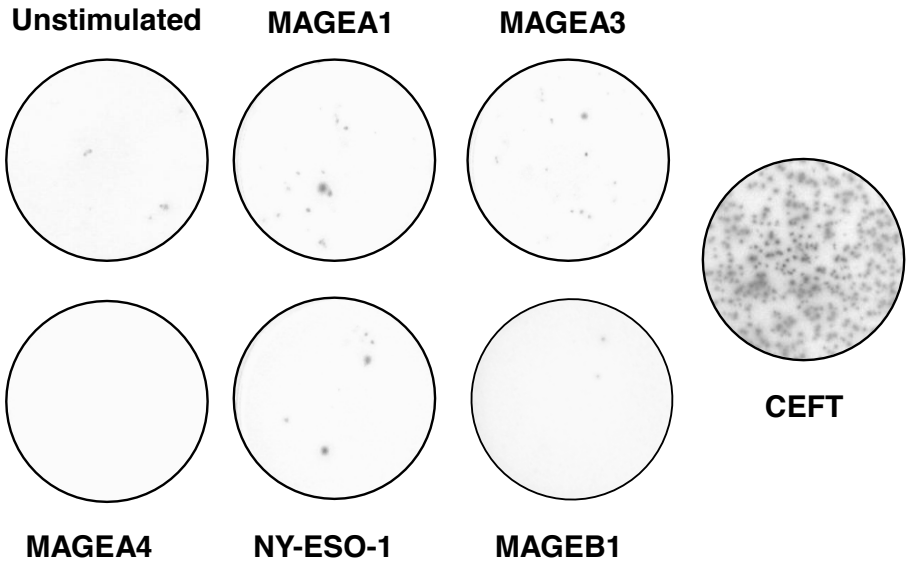
Unstimulated
MAGEA1
MAGEA3
CEFT
MAGEA4
NY-ESO-1
MAGEB1

b

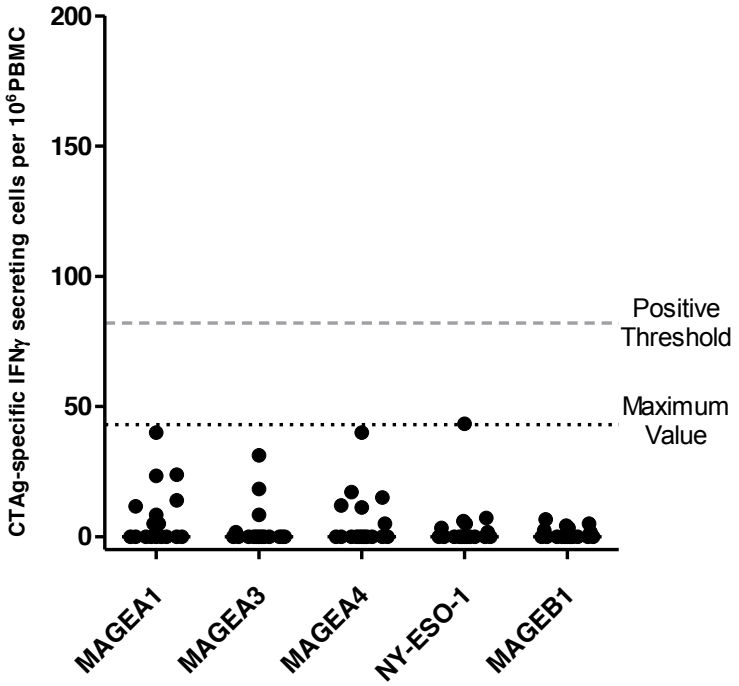
CTAg-specific IFNγ secreting cells per 10^6 PBMC
200
150
100
50
0
Positive Threshold
Maximum Value
MAGEA1
MAGEA3
MAGEA4
NY-ESO-1
MAGEB1

Figure 49. CTAg-specific responses determined by ELISPOT from PBMC of Healthy donors.

Representative ELISPOT spots from a healthy donor demonstrating an absence of specific cells to all CTAgs examined (a). Between 250,000 and 350,000 PBMC were stimulated with overlapping peptides spanning the full length of a CTAg protein. Each spot represents a single antigen-specific IFNγ secreting cell. The negative control was cells stimulated with vehicle only (DMSO, unstimulated). Spots in these wells were cells releasing IFNγ non-specifically, and were subsequently deducted from CTAg peptide stimulated values. Positive control was stimulation with CEFT peptide library, containing known antigenic peptides for CMV, EBV, Flu and Tetanus. Computational analysis was used to count the spots in each well. Values were converted to represent the frequency of IFNγ secreting cells per 10^6 PBMC for each CTAg (n=17) (b). Black dotted line represents the maximum number of CTA-specific cells found in healthy donors. Grey dashed line represents the threshold for a positive CTAg response.

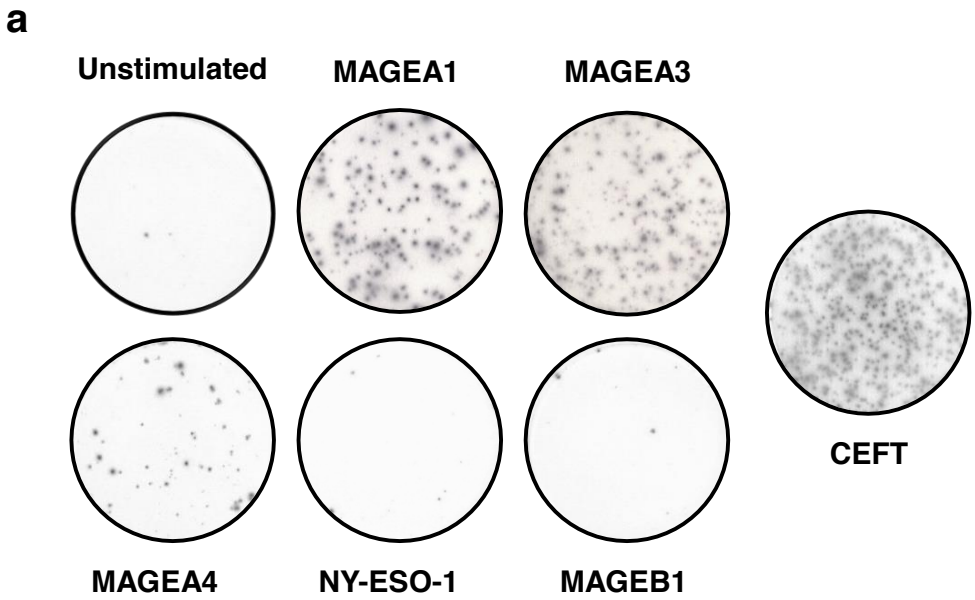

Figure 50. CTAg-specific responses from PBMC of a seminoma patient, determined by ELISPOT.

Representative ELISPOT spots from a TGCT patient with a MAGEA1, MAGEA3 and MAGEA4 response. Between 250,000 and 350,000 PBMC were stimulated with overlapping peptides spanning the full length of a CTAg protein. Each spot represents a single antigen-specific IFNγ secreting cell. The negative control was cells stimulated with vehicle only (DMSO, unstimulated). Spots in these wells were cells releasing IFNγ non-specifically, and were subsequently deducted from CTAg peptide stimulated values. Positive control was stimulation with CEFT peptide library, containing known antigenic peptides for CMV, EBV, Flu and Tetanus. Computational analysis was used to count the spots in each well. Values were converted to frequency of IFNγ secreting cells per 10^6 PBMC. Patients with a high frequency of spots in the unstimulated wells were excluded from further analysis.

The frequency of cells specific to MAGEA1 (Figure 51), MAGEA3 (Figure 52), MAGEA4 (Figure 53), NY-ESO-1 (Figure 54), and MAGEB1 (Figure 55) in healthy donors and patients with various TGCTs, are shown. Table 28 summarises the frequency of each CTAg response according to tumour type.

A direct comparison of the frequency of cells in healthy donors and TGCT patients was depicted according to the CTAg they were stimulated with (Figure 56). We observed positive MAGEA1 responses in 17% of mGCT patients and 31% of seminoma patients. MAGEA1-specific responses were absent in all NSGCTT patients analysed (Figure 56a). Furthermore, the magnitude of positive MAGEA1 responses was far greater in seminoma patients (up to 0.149% of PBMC) compared to mGCT patients (0.0248% of PBMC). The median frequency of MAGEA1-specific cells was statistically higher in seminoma patients than in healthy donors ($p=0.0009$) and NSGCTT patients ($p=0.0307$). No significant differences were observed between other tumour types. MAGEA3 responses were detected in patients across all testicular tumour types (Figure 56b), and we show that 31% of seminoma, 50% of mGCT and 30% of NSGCTT patients developed a spontaneous immune response to this antigen. The magnitude of responses was similar across all TGCT types, with up to 0.07% of total PBMC being specific to MAGEA3. The median frequency of MAGEA3-specific cells was significantly greater in both seminoma ($p= 0.0072$) and NSGCTT ($p=0.0292$) patients, compared to that of healthy donors. MAGEA4 responses were detected in 33% of mGCT and 28% of seminoma patients, with median frequencies significantly greater in the seminoma than in healthy donors ($p=0.0226$). Conversely, no positive responses were identified in NSGCTT patients.

NY-ESO-1 and MAGEB1-Specific Cells are Undetectable in TGCT Patients

We show expression of MAGEA family proteins in TGCTs and spontaneous cell mediated immune responses towards these antigens. We showed that NY-ESO-1 and MAGEB1 transcripts were undetectable in the majority of TGCTs, and would therefore not expect T cell responses to be generated against these antigens. For that reason it was important to determine the frequency of NY-ESO-1 and MAGEB1-specific cells in TGCT patients compared to healthy donors. Our data suggests immune responses are not generated to either of these antigens, as levels of CTAg-specific cells were similar in TGCT patients and healthy individuals, irrespective of tumour type.

In summary, both dextramer analysis and ELISPOT analysis revealed that MAGEA1 and MAGEA3 –specific T cell responses are generated in TGCT patients, whereas NY-ESO-1 responses are absent. ELISPOT analysis also demonstrated the presence of MAGEA4-specific cells in seminoma patients, which were overlooked using dextramer methodology. We extended analysis to examine the frequency of MAGEB1-specific cells by ELISPOT, but no positive responses were detected in healthy controls or TGCT patients. In this study, ELISPOT analysis suggests NSGCTTs only provoke an immune response against MAGEA3, a finding which correlates well with our dextramer analysis.

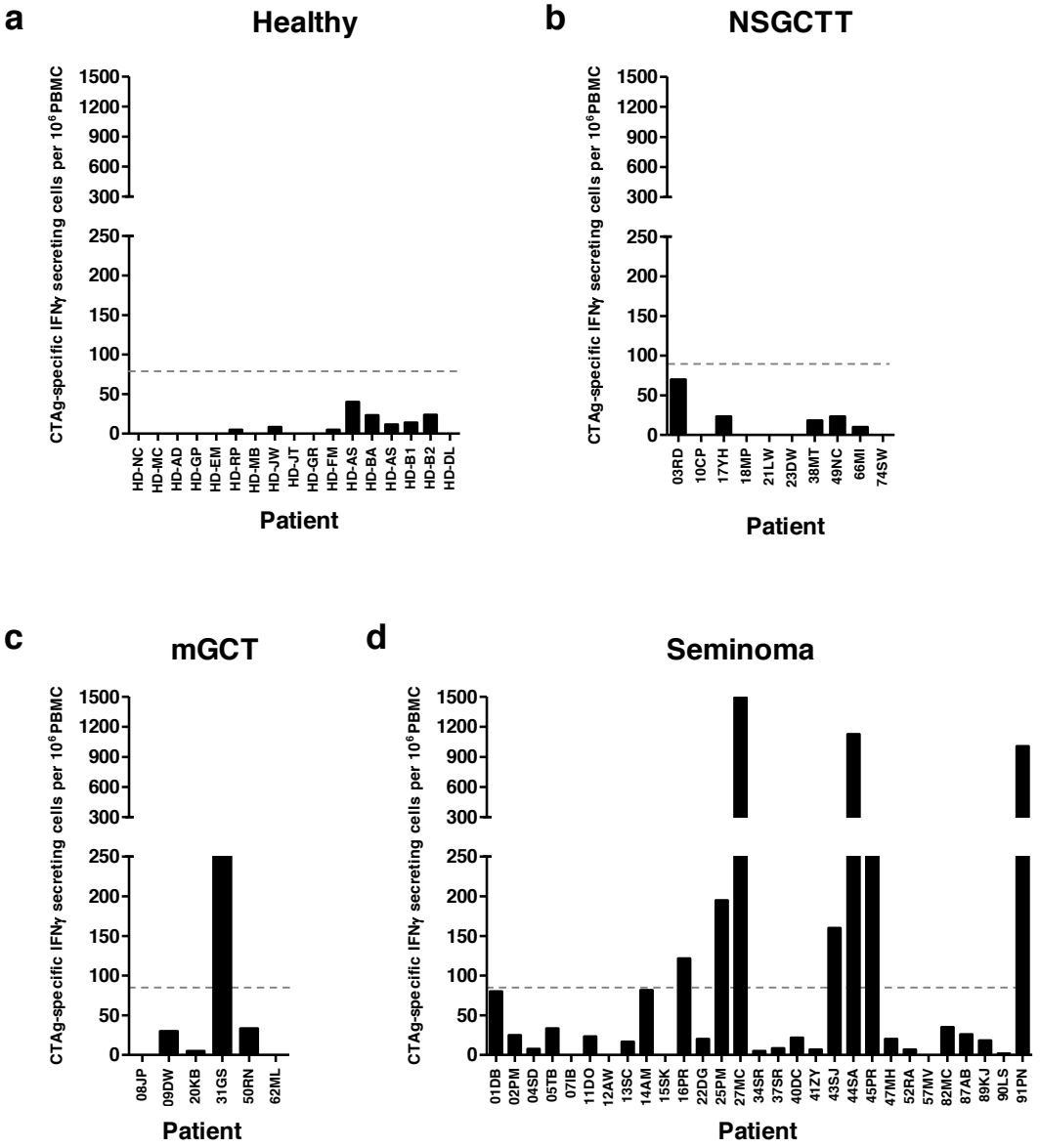

Figure 51. Frequency of MAGEA1-specific T cells in healthy donors and TGCT patients. The frequency of MAGEA1 specific T cells in healthy donors (a), NSGCTT (b), mGCT (c), and seminoma (d) patients was determined by IFNγ secretion in an ELISPOT assay. Cells were stimulated with overlapping peptides spanning the entire length of MAGEA1 protein. CEFT peptide pool was used as a positive control; DMSO was used as a negative control. Values were represented as frequency of MAGEA1 specific T cells per 10^6 PBMC. Each bar represents an individual patient. Dotted line represents the threshold for a positive response.

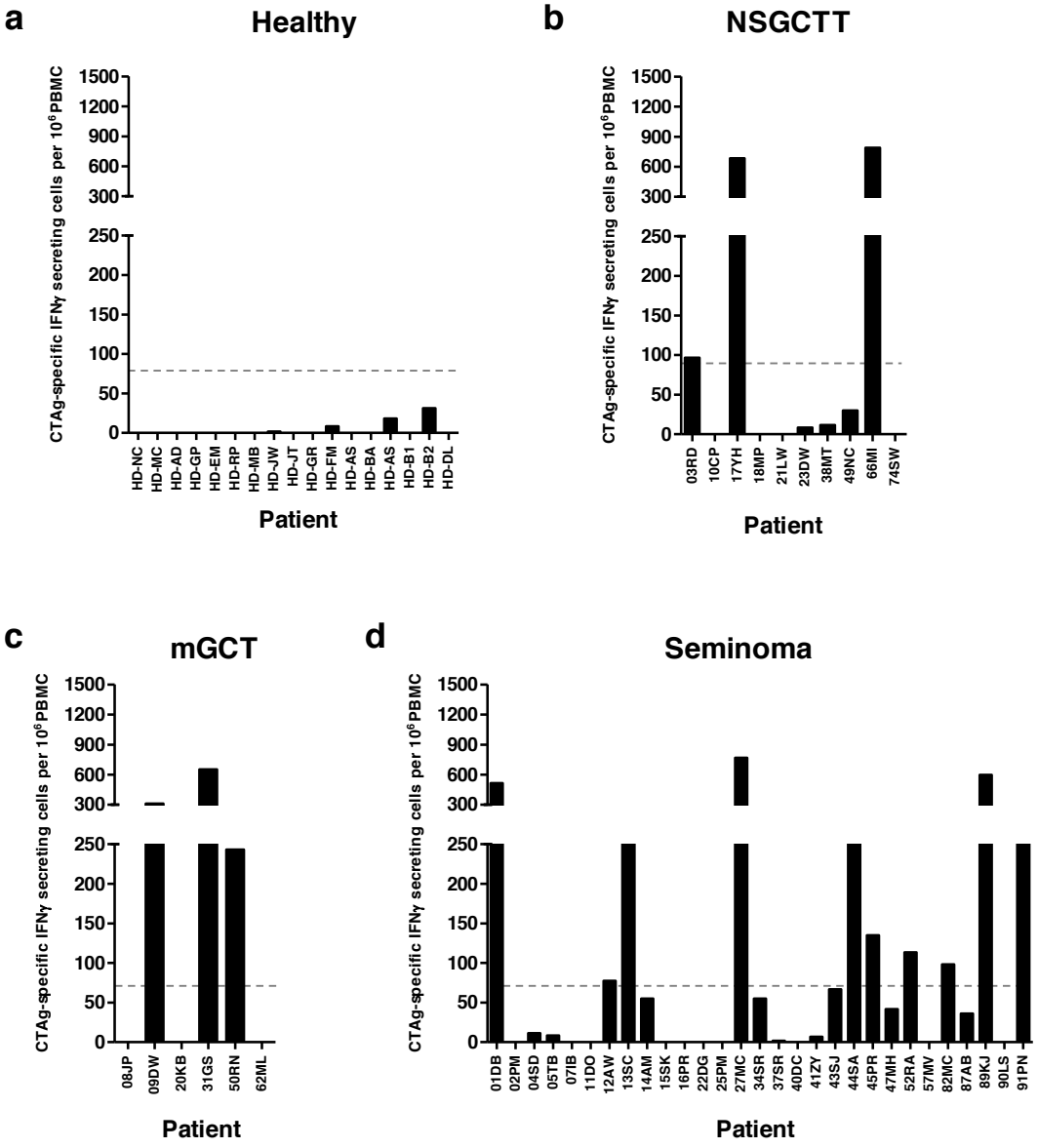

Figure 52. Frequency of MAGEA3-specific T cells in healthy donors and TGCT patients. The frequency of MAGEA3 specific T cells in healthy donors (a), NSGCTT (b), mGCT (c), and seminoma (d) patients was determined by IFNγ secretion in an ELISPOT assay. Cells were stimulated with overlapping peptides spanning the entire length of MAGEA3 protein. CEFT peptide pool was used as a positive control; DMSO was used as a negative control. Values were represented as frequency of MAGEA3 specific T cells per 10^6 PBMC. Each bar represents an individual patient. Dotted line represents the threshold for a positive response.

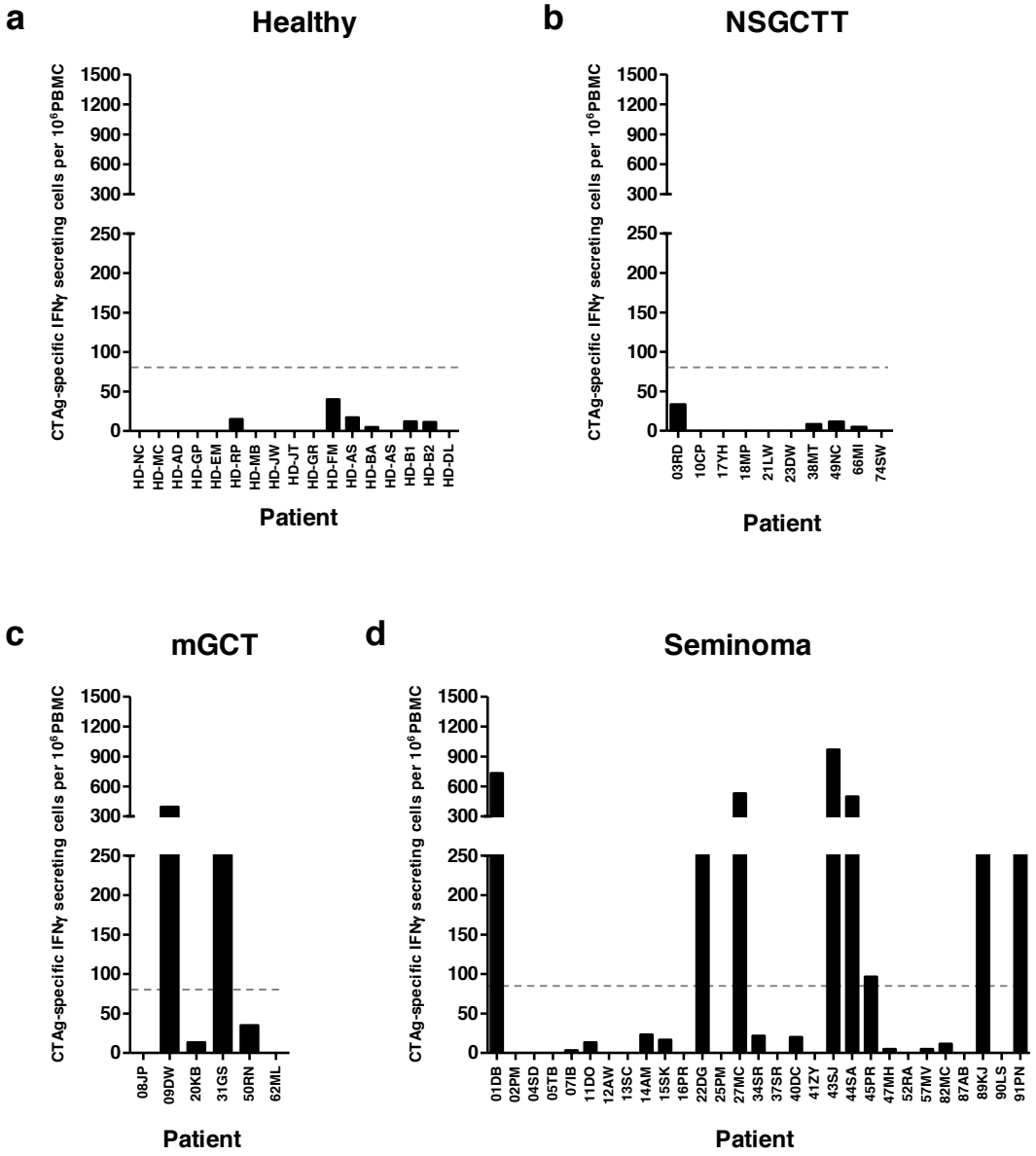

Figure 53. Frequency of MAGEA4-specific T cells in healthy donors and TGCT patients. The frequency of MAGEA4 specific T cells in healthy donors (a), NSGCTT (b), mGCT (c), and seminoma (d) patients was determined by IFNγ secretion in an ELISPOT assay. Cells were stimulated with overlapping peptides spanning the entire length of MAGEA4 protein. CEFT peptide pool was used as a positive control; DMSO was used as a negative control. Values were represented as frequency of MAGEA4 specific T cells per 10^6 PBMC. Each bar represents an individual patient. Dotted line represents the threshold for a positive response.

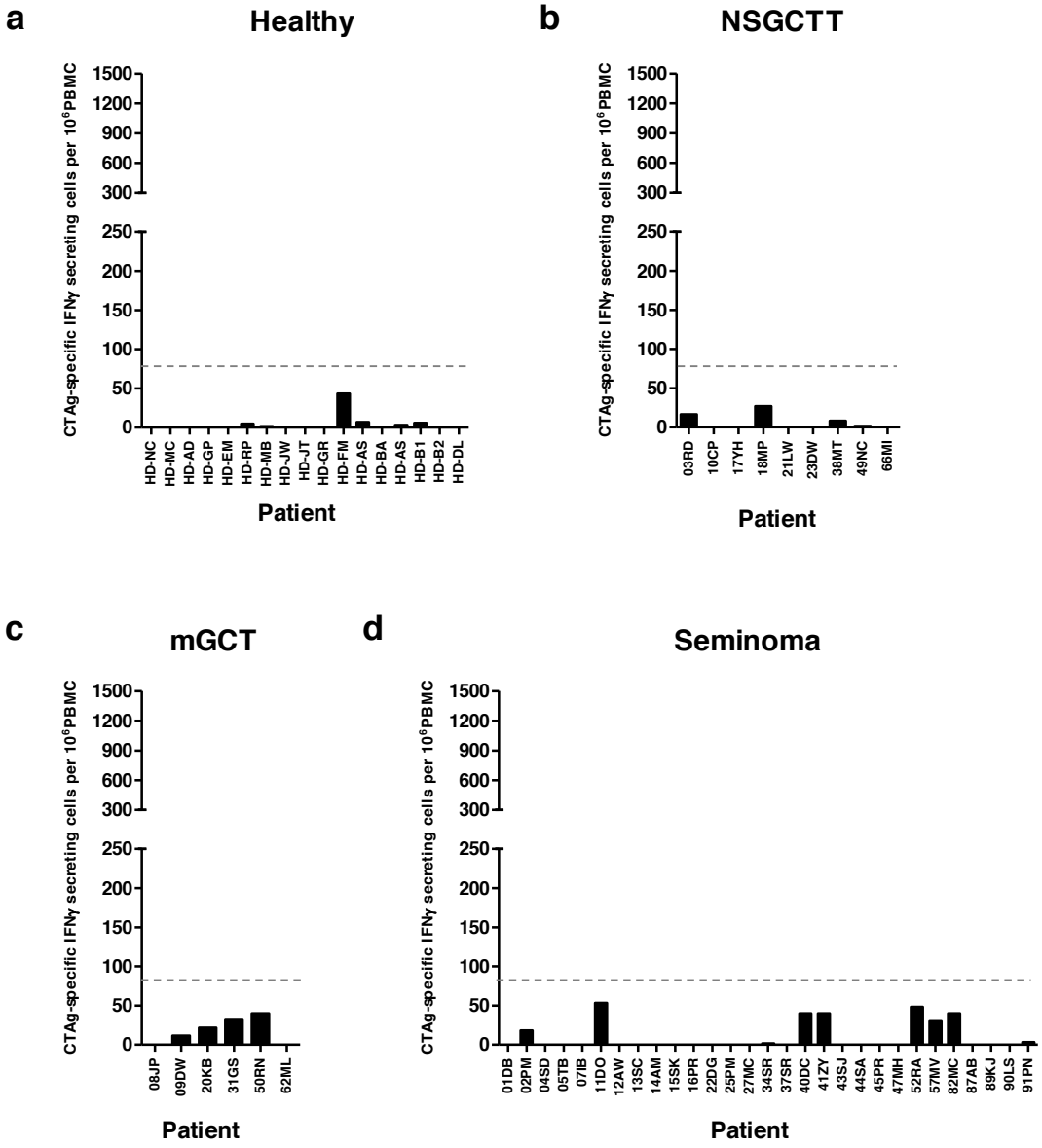

Figure 54. Frequency of NY-ESO-1-specific T cells in healthy donors and TGCT patients.

The frequency of NY-ESO-1 specific T cells in healthy donors (a), NSGCTT (b), mGCT (c), and seminoma (d) patients was determined by IFNγ secretion in an ELISPOT assay. Cells were stimulated with overlapping peptides spanning the entire length of NY-ESO-1 protein. CEFT peptide pool was used as a positive control; DMSO was used as a negative control. Values were represented as frequency of NY-ESO-1-specific T cells per 10^6 PBMC. Each bar represents an individual patient. Dotted line represents the threshold for a positive response.

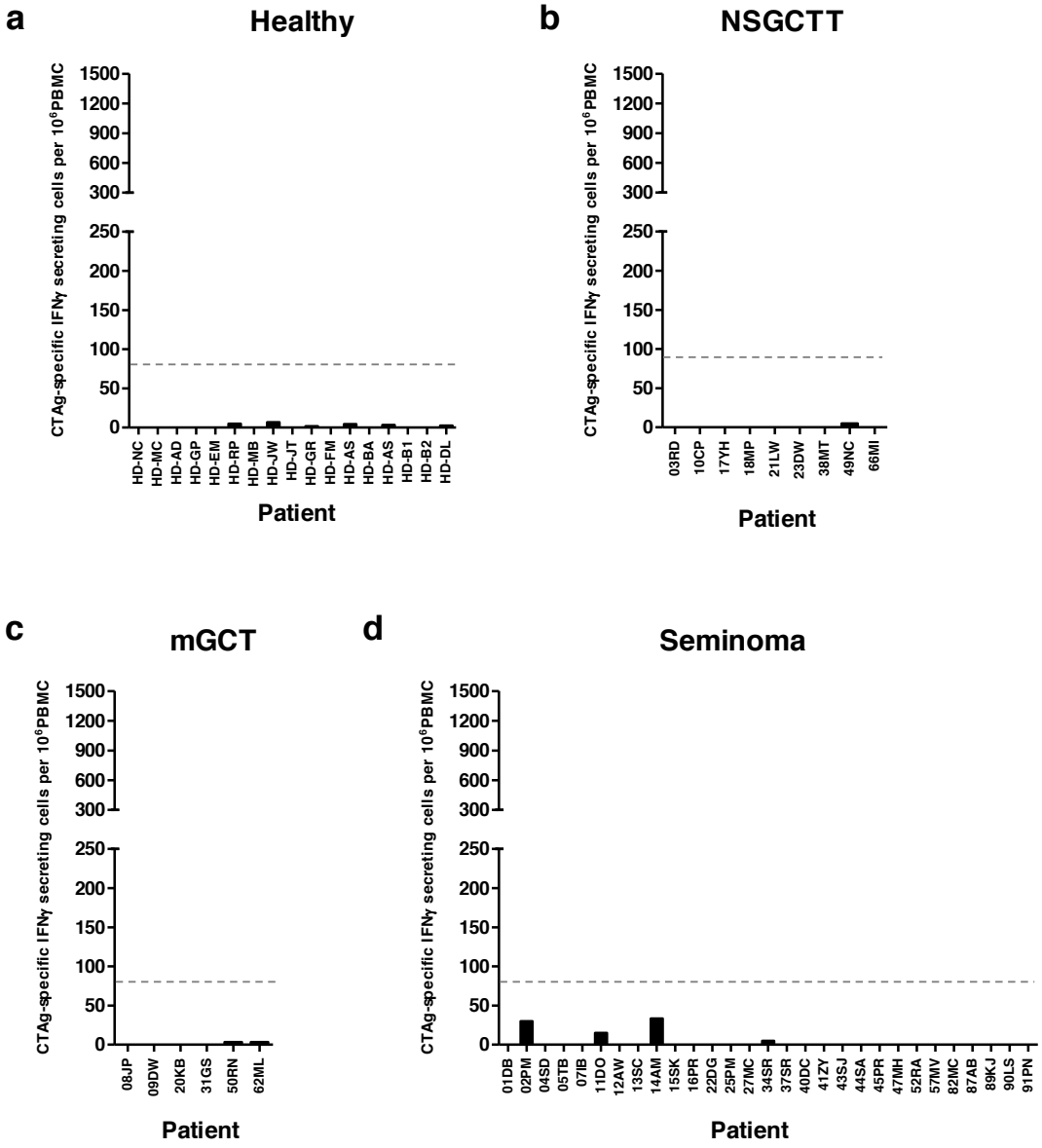

Figure 55. Frequency of MAGEB1-specific T cells in healthy donors and TGCT patients. The frequency of MAGEB1 specific T cells in healthy donors (a), NSGCTT (b), mGCT (c), and seminoma (d) patients was determined by IFNγ secretion in an ELISPOT assay. Cells were stimulated with overlapping peptides spanning the entire length of MAGEB1 protein. CEFT peptide pool was used as a positive control; DMSO was used as a negative control. Values were represented as frequency of MAGEB1-specific T cells per 10^6 PBMC. Each bar represents an individual patient. Dotted line represents the threshold for a positive response.

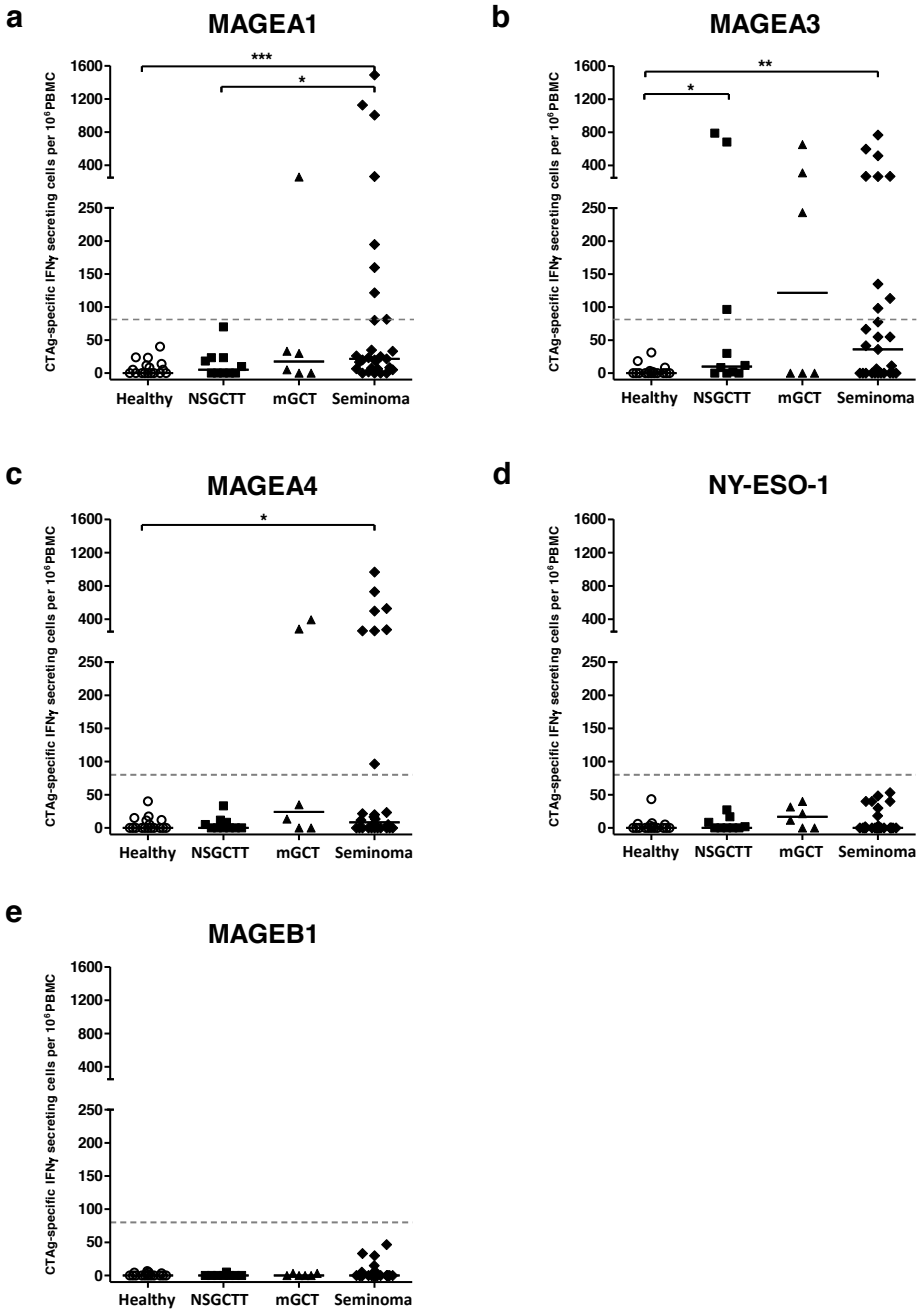

Figure 56. Overall frequency of CTAg-specific T cells in healthy donors and TGCT patients.

The frequency of MAGEA1 (a), MAGEA3 (b), MAGEA4 (c), NY-ESO-1 (d), and MAGEB1 (e) -specific T cells in healthy donors (n=17), NSGCTT (n= 10), mGCT (n= 6) and seminoma (n= 29) patients was determined. Values are represented as the frequency of CTAg-specific T cells per 10^6 PBMC. Each point represents an individual patient. Dotted line shows the threshold for positive response, defined as double the highest response determined in healthy donors. Solid horizontal line represents the median. Data analysed by Mann-Whitney test. * denotes $p<0.05$, ** denotes $p<0.01$, *** denotes $p<0.001$.

Table 28. Overall frequency of CTAg-specific T cells in healthy donors and TGCT patients.

	Healthy			NSGCTT			mGCT			Seminoma		
	Median	**25th**	**75th**	**Median**	**25th**	**75th**	**Median**	**25th**	**75th**	**Median**	**25th**	**75th**
MAGEA1	**0.0**	0.0	12.83	**5.00**	0.0	23.33	**17.5**	0.0	90.00	**21.67**	6.67	101.7
MAGEA3	**0.0**	0.0	2.92	**10.00**	0.0	243.30	**121.70**	0.0	396.7	**36.0**	0.0	124.2
MAGEA4	**0.0**	0.0	11.63	**0.0**	0.0	9.17	**24.17**	0.0	311.3	**8.33**	0	220.40
NY-ESO-1	**0.0**	0.0	4.17	**0.0**	0.0	12.50	**16.67**	0.0	33.75	**0.0**	0.0	18.33
MAGEB1	**0.0**	0.0	2.92	**0.0**	0.0	0.0	**0.0**	0.0	3.30	**0.0**	0.0	3.75

Data expressed as median (bold) with 25th and 75th quartile.

The Ability to Generate a MAGE-specific Response is Independent of Age

An aging immune system may be less efficient at generating a primary response to newly encountered antigens due to a reduced naive T cell compartment. This is primarily caused by the accumulation of highly differentiated T cell subsets generated during persistent viral infection (Wherry and Ahmed, 2004). We therefore investigated the effect of age on the ability of seminoma patients to mount a CTAg specific response. NSGCTT and mGCT patients were excluded from this analysis due to small sample size. Seminoma patients were classified into "responders" and "non-responders", depending on whether a response was detected above the positive threshold. We found the ability to generate a MAGEA1, A3 or A4-specific immune response was totally independent of patient age (Figure 57).

The Magnitude of a MAGEA4-Specific T cell Response is Age-Dependent

Next, we determined the correlation between the frequency of MAGE-specific T cells and the age of responding patients (Figure 58). There was no significant correlation between patient age and the frequency of MAGEA1 or MAGEA3-specific cells. Interestingly, strong negative correlation was observed between patient age and the frequency of MAGEA4-specific cells ($p=0.0458$). Our data suggests increasing age has a detrimental effect on the magnitude of a MAGEA4-specific immune response, but has no effect on the frequency of MAGEA1 or A3-specific cells in seminoma patients.

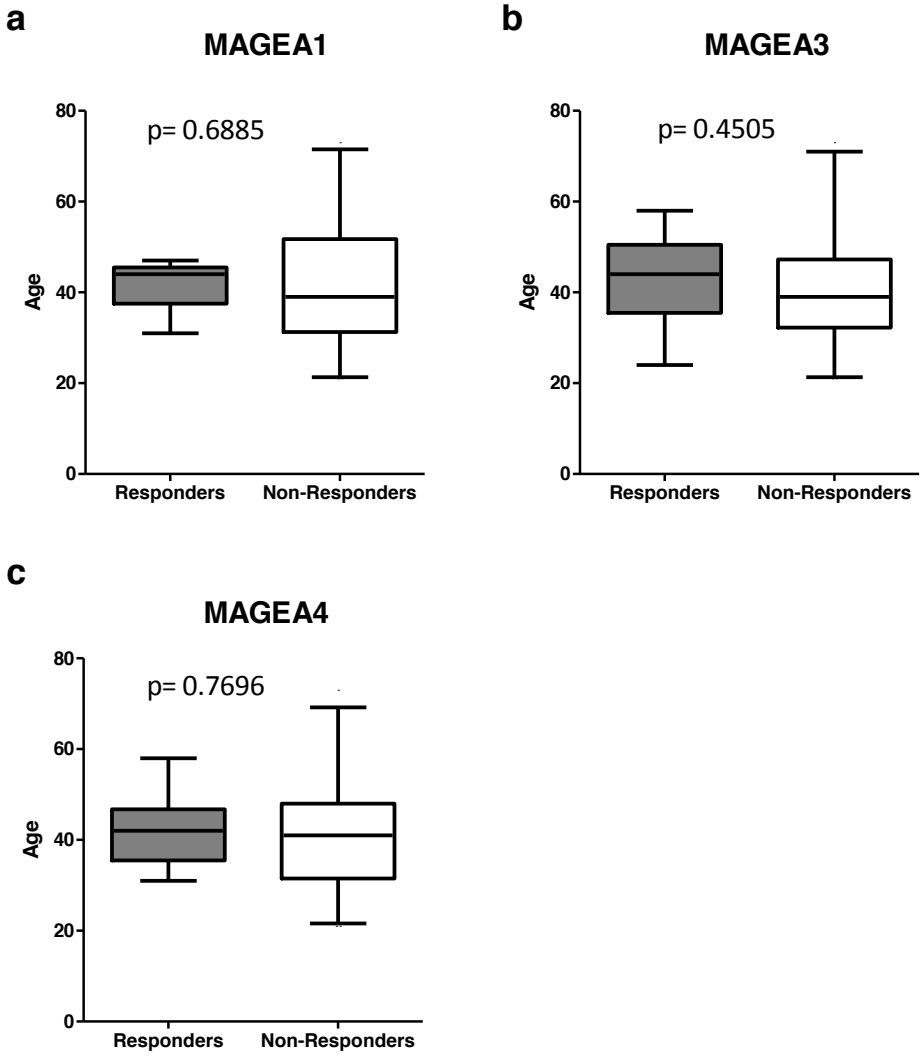

Figure 57. The effect of age on the possibility of generating a T cell response to MAGE antigens.

The age of seminoma patients with a positive response (grey) and a negative response (white) to MAGEA1 (a), MAGEA3 (b) and MAGEA4 (c) is shown. Box represents 25th and 75th percentile, line represents median, and whiskers represent 10-90 percentile. Data analysed by Mann-Whitney test.

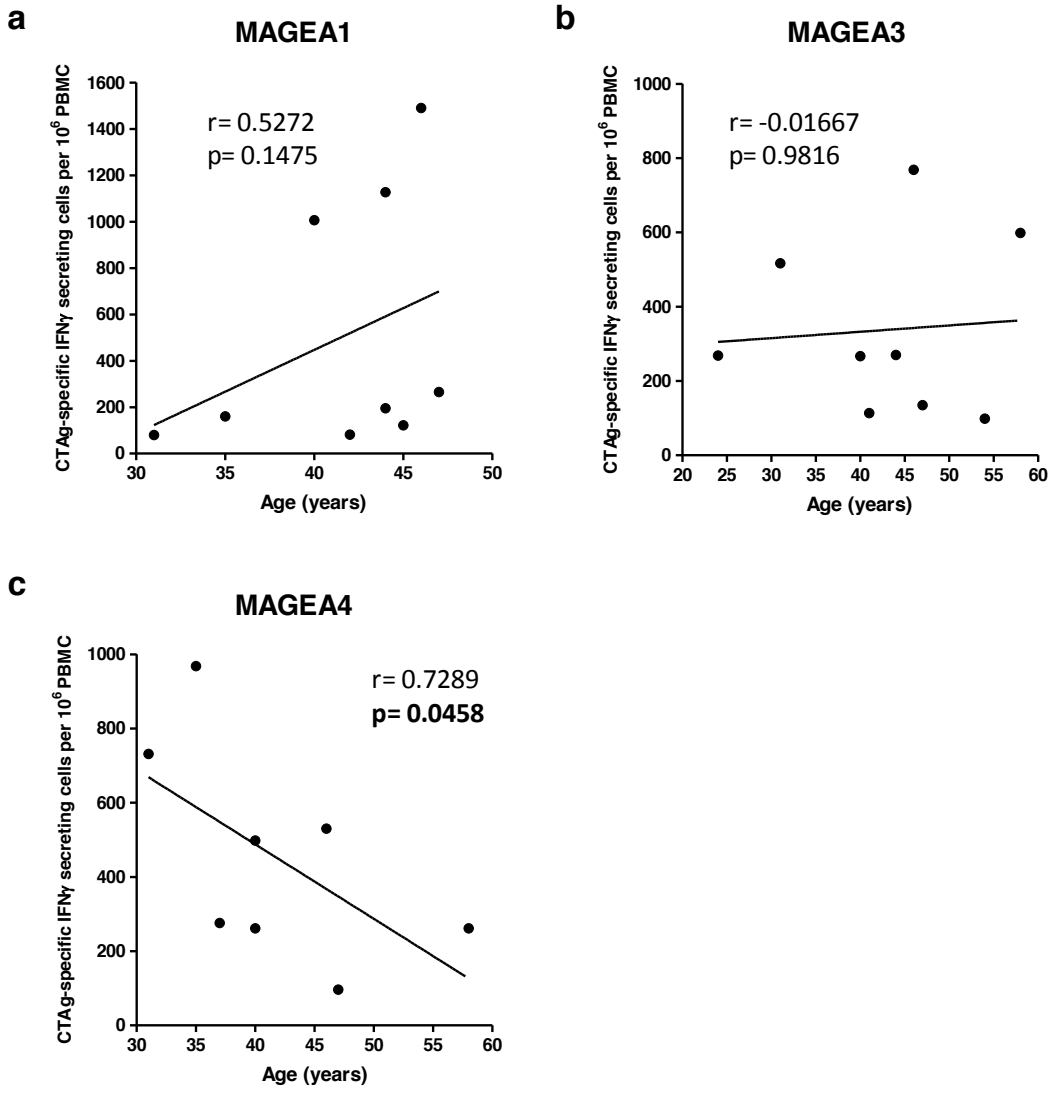

Figure 58. Correlation between frequency of CTAg-specific IFNγ secreting cells and age of seminoma patients.

Correlation between numbers of CTAg-specific IFNγ secreting cells from PBMC of seminoma patients and age for MAGEA1 (n=9) (a), MAGEA3 (n=9) (b) and MAGEA4 (n=8) (c). Spearman's rank correlation coefficient (r) and significance (p) were determined. Significant p values are highlighted in bold type. Each symbol represents an individual patient.

Patient Age of Disease Onset Differs Between Tumour Types

We observed different ages of disease onset between different testicular tumour types (Figure 59). Specifically, the age of disease onset in seminoma patients (mean age: 41) was significantly higher than NSGCTT patients (mean age: 26) (p=0.0007). Similarly, the mean age of mGCT patients in this cohort was 39, compared with a median age of 26 for NSGCTT (p=0.001). Seminoma patients have increased MAGE responses compared to NSGCTT patients, even though the average age is significantly higher. This suggests tumour type has a greater effect than age in the generation of MAGE-specific responses.

Metastatic Potential of the Tumour is Associated with Elevated Levels of MAGEA3-specific T Cells in NSGCTT Patients

Clinical grading of TGCTs depends on the subtype of disease. Generally, tumours are categorised using a combination of factors including tumour size, vascular invasion and metastasis, and the levels of specific tumour markers. In this study, mGCT patients had localised disease with undetectable lymph node metastasis. Consequently, these patients could not be effectively categorised and were subsequently omitted from further analysis.

We categorised NSGCTT patients based on the presence of tumour tissue solely in the testis (localised), or which had evident lymphovascular invasion or retroperitoneal lymph node metastasis (metastatic). We found that all NSGCTT patients with a MAGEA3-response had secondary tumour masses in the retroperitoneal lymph nodes. All patients in this group demonstrated elevated levels of MAGEA3-specific T cells in peripheral blood, compared to patients with localised disease (p=0.0396) (Figure 60a). Based on these results,

we hypothesise that disease progression and metastasis of NSGCTTs is associated with the development of a MAGEA3-specific T cell response.

Generation of a MAGE-Specific Response is not determined by Tumour Stage in Seminoma Patients

We categorised seminoma patients into two groups depending on the stage of disease. The majority of patients with seminomatous tumours are presented with clinical stage I disease (Stage I). To generate groups large enough for effective comparison, we grouped together all patients with clinical stage II and above (Stage II-IV). We detected no significant association between tumour stage and the presence or magnitude of an immune response to any MAGE antigen assessed (Figure 60b). MAGE responses were detected in approximately 30% of patients with stage I disease and 30% of patients with stage II-IV disease.

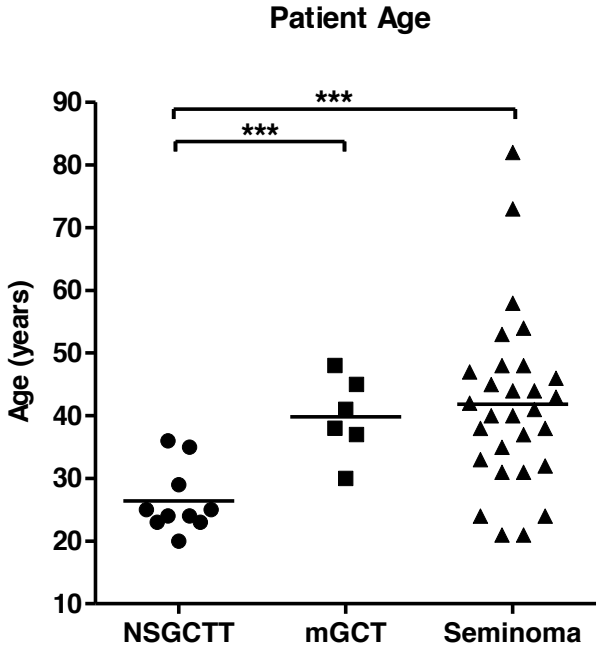

Figure 59. Age of TGCT patients used in ELISPOT assay, categorised by tumour type. Age of patients with NSGCTT (n=10), mGCT (n=6) or seminoma (n=29) used in the ELISPOT assay. Horizontal line represents the mean. Data analysed by student T test. *** denotes $p<0.001$.

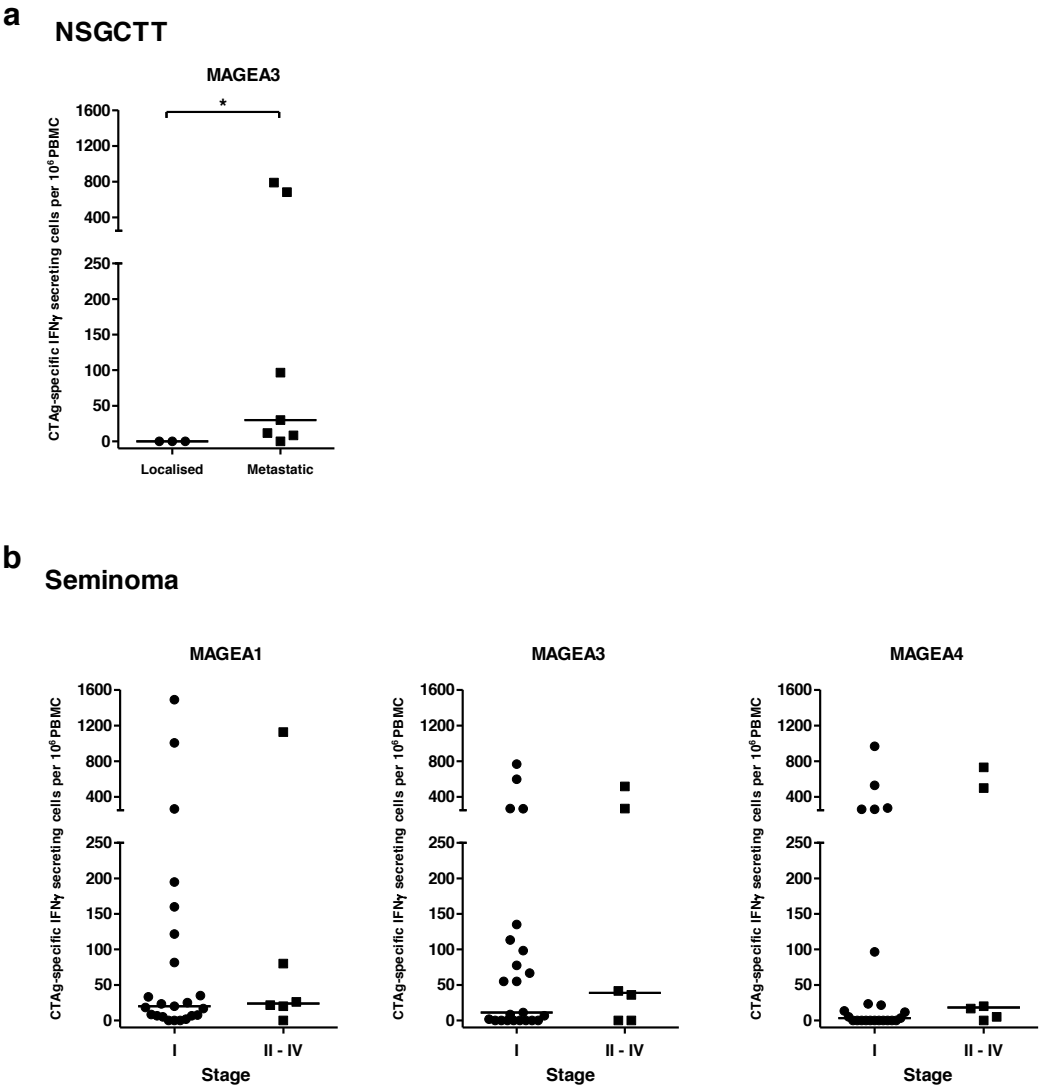

Figure 60. Effect of tumour stage on the frequency of CTAg-specific IFNγ secreting cells in TGCT patients.

Numbers of CTAg-specific IFNγ secreting cells per 10^6 PBMC were determined in NSGCTT (a), and seminoma (b) patients grouped by tumour form (localised or metastasis, NSGCTT) or tumour stage (I or II-IV, seminoma). Each symbol represents an individual patient, and horizontal line represents median. Data analysed by Mann-Whitney test.

* denotes $p<0.05$.

Multiple MAGE Responses are Generated in TGCT Patients

Several studies show the expression of multiple MAGE antigens in tumours of various histopathological types (Mashino *et al*., 2001). In this study, we have demonstrated the expression of multiple MAGEA family antigens in TGCT tissue. Assessment of MAGE responses by dextramer analysis revealed a patient who had both a MAGEA1 and a MAGEA3-specific CD8 T cell response. These observations led us to investigate the incidence of multiple MAGE responses in a cohort of TGCT patients where a MAGE response was detected, as defined by a positive IFNγ ELISPOT result (n=21).

Figure 61 outlines the frequency of MAGEA1, A3 and A4-specific cells for individual patients in this cohort. As previously shown, NSGCTT patients only generate MAGEA3 responses thus multiple MAGE responses were not generated (Figure 61a). In contrast, the majority of mGCT patients (2 out of 3) and nearly half the seminoma patients (7 out of 15), responded to at least two of the MAGEA-family antigens assessed (Figure 62). Moreover, four seminoma patients exhibited responses to all three MAGE antigens. We did not observe any association between the number of MAGEA family responses and tumour stage or patient age in seminoma patients (data not shown).

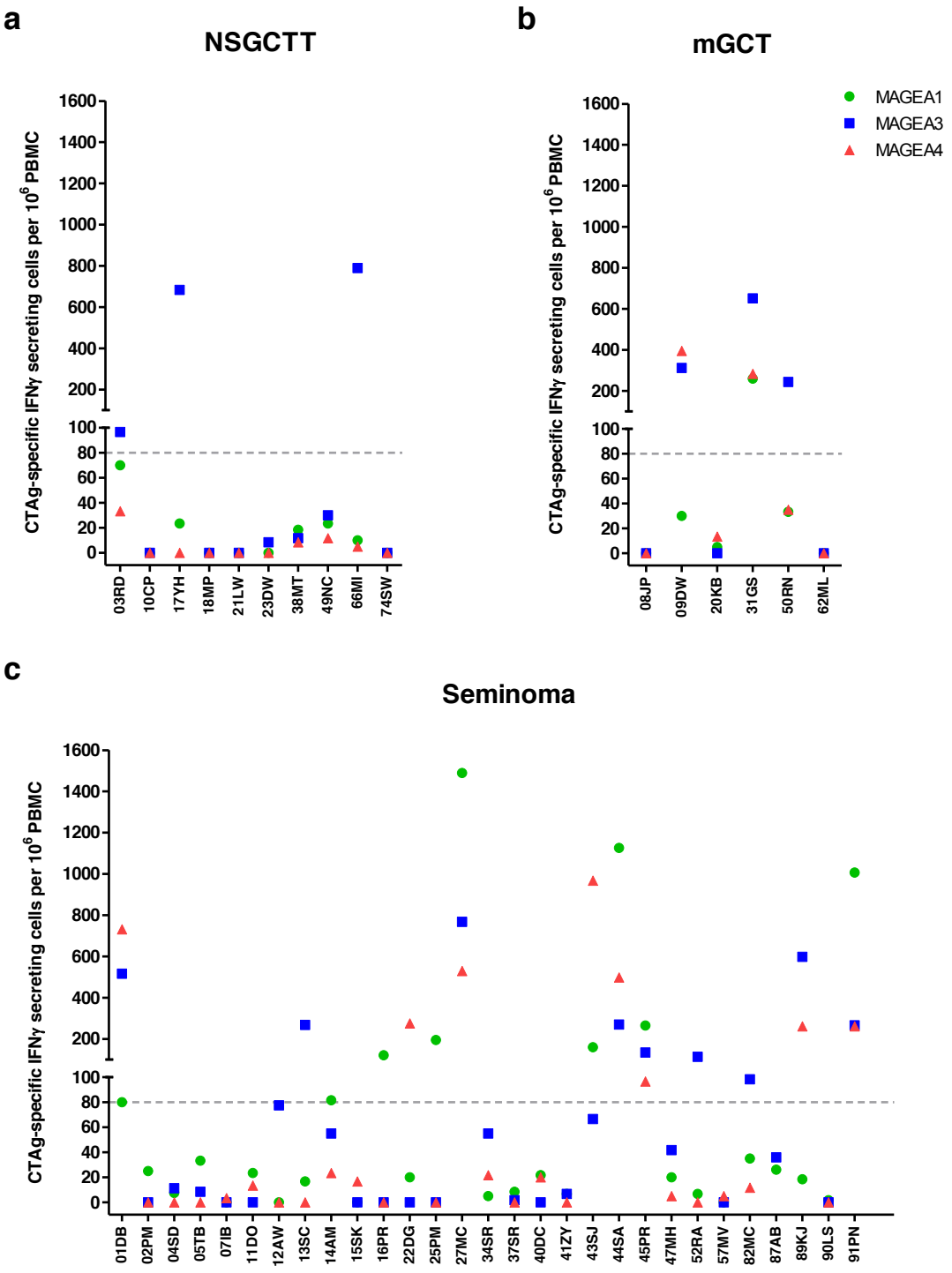

Figure 61. TGCT patients with single and multiple MAGEA family responses.
Numbers of CTAg-specific IFNγ secreting cells in PBMC for each patient in NSGCTT (a), mGCT (b) and seminoma (c). Dotted line shows the threshold for positive response, defined as double the highest response present in healthy donors. Responses to MAGEA1 (green circle), MAGEA3 (blue square), and MAGEA4 (red triangle) are shown.

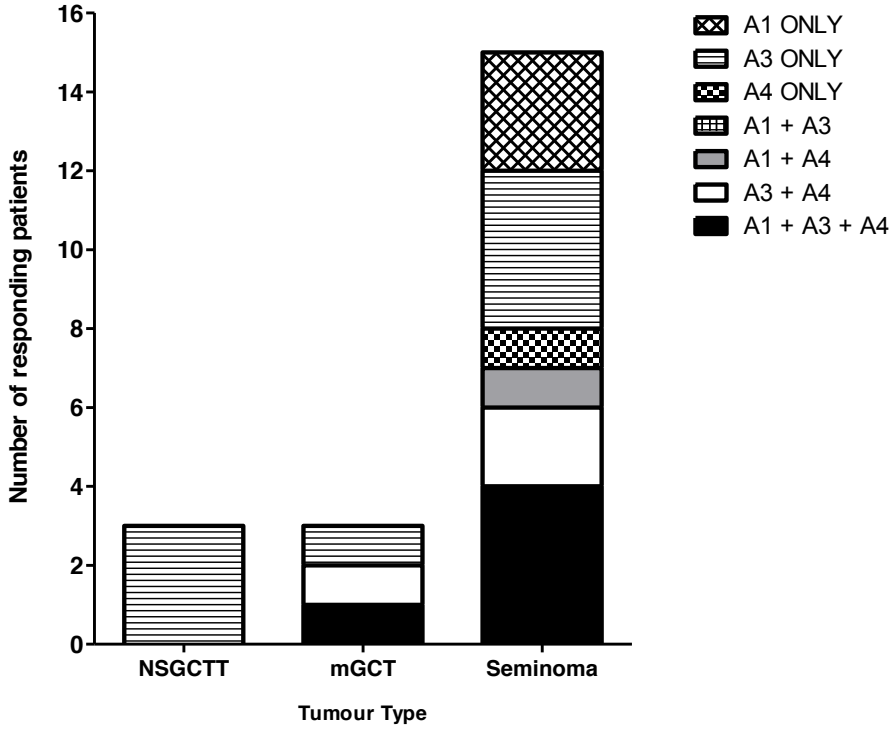

Figure 62. Frequency of responses to multiple MAGE antigens according to tumour type.

The number of patients which respond to MAGEA1, MAGEA3, MAGEA4 or a combination of these antigens is shown. Responding patients are divided according to tumour type. NSGCTT n=3, mGCT n=3, seminoma n=15.

MAGE-specific T cell Frequency Diminishes Over Time

The majority of TGCT patients were treated by radical orchidectomy to remove the primary tumour, thus reducing tumour antigen load. Highly elevated levels of MAGE-specific T cells detected in a significant proportion of TGCT patients imply repeated antigenic stimulation of these cells, and subsequent clonal expansion. We therefore investigated whether the removal of tumour antigens affected the magnitude of MAGE-specific responses in TGCT patients. Specifically, we compared the levels of MAGE-specific T cells in patients shortly after tumour removal but before chemotherapy, and at various intervals following treatment. Figure 63 shows the representative kinetics of a MAGEA3 and MAGEA4-specific response in a patient with and a patient without a response prior to chemotherapy.

We further demonstrate the dynamics of MAGE-specific responses in individual patients, pre and post adjuvant chemotherapy. A clear reduction in the frequency of MAGE-specific cells over time was observed in all patients assessed (Figure 64). We observed a significant reduction in MAGE-specific T cells as soon as two weeks after treatment, in patients with a known response before treatment. The diminishing frequency of MAGE-specific T cells was even more apparent at later time points post chemotherapy. Next we compared the frequency of MAGE-specific T cells before treatment with the frequency of MAGE-specific T cells at the latest time point at which a blood sample was obtained for a particular patient (between 3 and 18 months after treatment). We show that the frequency of MAGE-specific T cells was significantly lower at the later time point for all MAGE antigens ($p=0.0156$), in all patients assessed (Figure 65a). We then determined the extent of the reduction in MAGE-specific T cells over time by calculating the percentage decrease in cell

numbers relative to the frequency of MAGE-specific cells before treatment (0%). The median decrease was shown from all available time points and grouped into 2 categories. We observed a stepwise decrease in the frequency of MAGE-specific cells over time, for all MAGE antigens (Figure 65b). Specifically, MAGEA1 responses were reduced by a median of 93.1% over the course of observation. Similarly, MAGEA3-specific cells were diminished by 87.4% and MAGEA4 by 94.8%. It is important to note that these responses were greatly reduced but low frequencies of cells were still detectable in the majority of patients.

To compliment these results, we ascertained whether patients with dextramer responses prior to treatment experienced a reduction in the proportion of MAGE-specific T cells following treatment. We investigated the frequency of MAGE-specific T cells in three patients, each with a response to a different peptide, before, and at two intervals after chemotherapy. Representative examples show the detection levels of MAGE-specific CD8 T cells pre and post chemotherapy (Figure 66a). We observed a general reduction in the proportion of MAGE-specific T cells over time. In all cases, frequencies had diminished to levels below the positive response threshold nine months post chemotherapy (Figure 66b). These observations are in agreement with our ELISPOT results where we demonstrate a decline in MAGE-specific T cells over time following treatment.

We also investigated the frequency of MAGE-specific T cells at various time points after treatment in patients who did not have a detectable response prior to treatment. Patients where a response was not detected before chemotherapy showed no significant change in the frequency of MAGE-specific T cells at intervals post treatment (Figure 67).

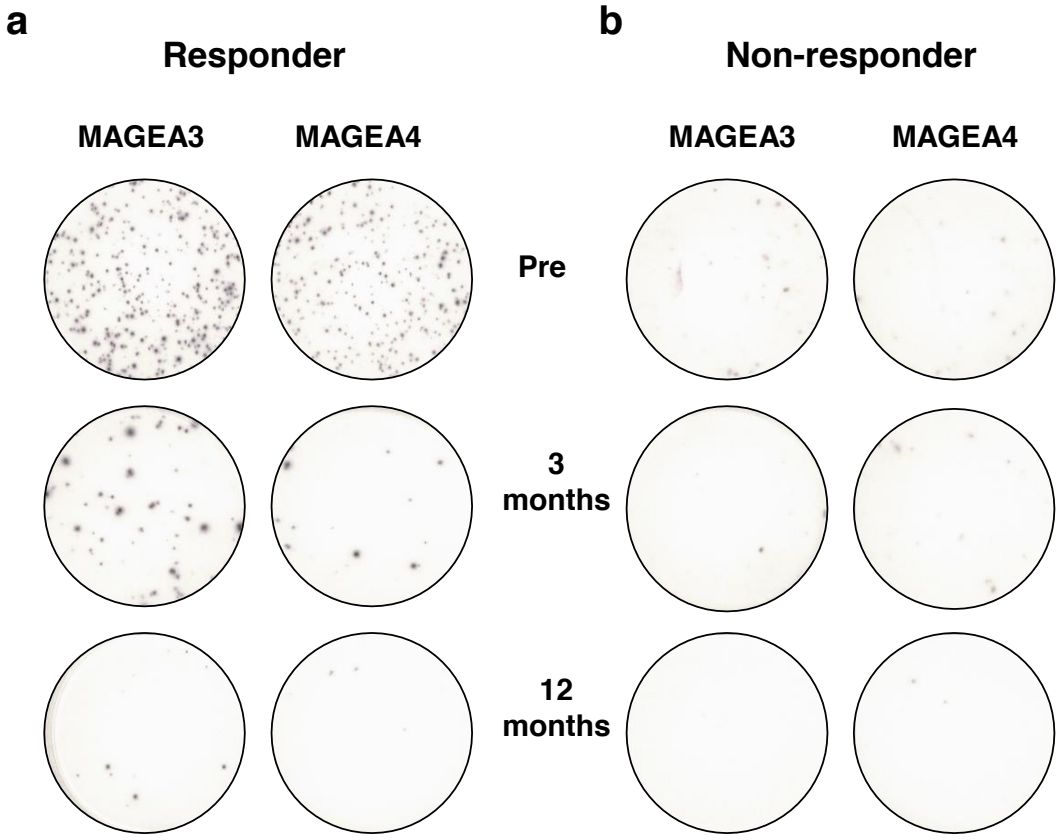

Figure 63. Kinetics of MAGE-specific responses determined using ELISPOT assay.
Representative ELISPOT spots from a TGCT patient with (a) and without (b) a MAGEA3 and MAGEA4 response prior to chemotherapy (pre). Each spot represents a single antigen-specific IFNγ secreting cell. The presence of MAGE-specific cells at pre, 3 months and 12 months post chemotherapy are shown. A reduction in the frequency of spots indicates a reduction in the proportion of CTAg specific cells in PBMC of TGCT patients.

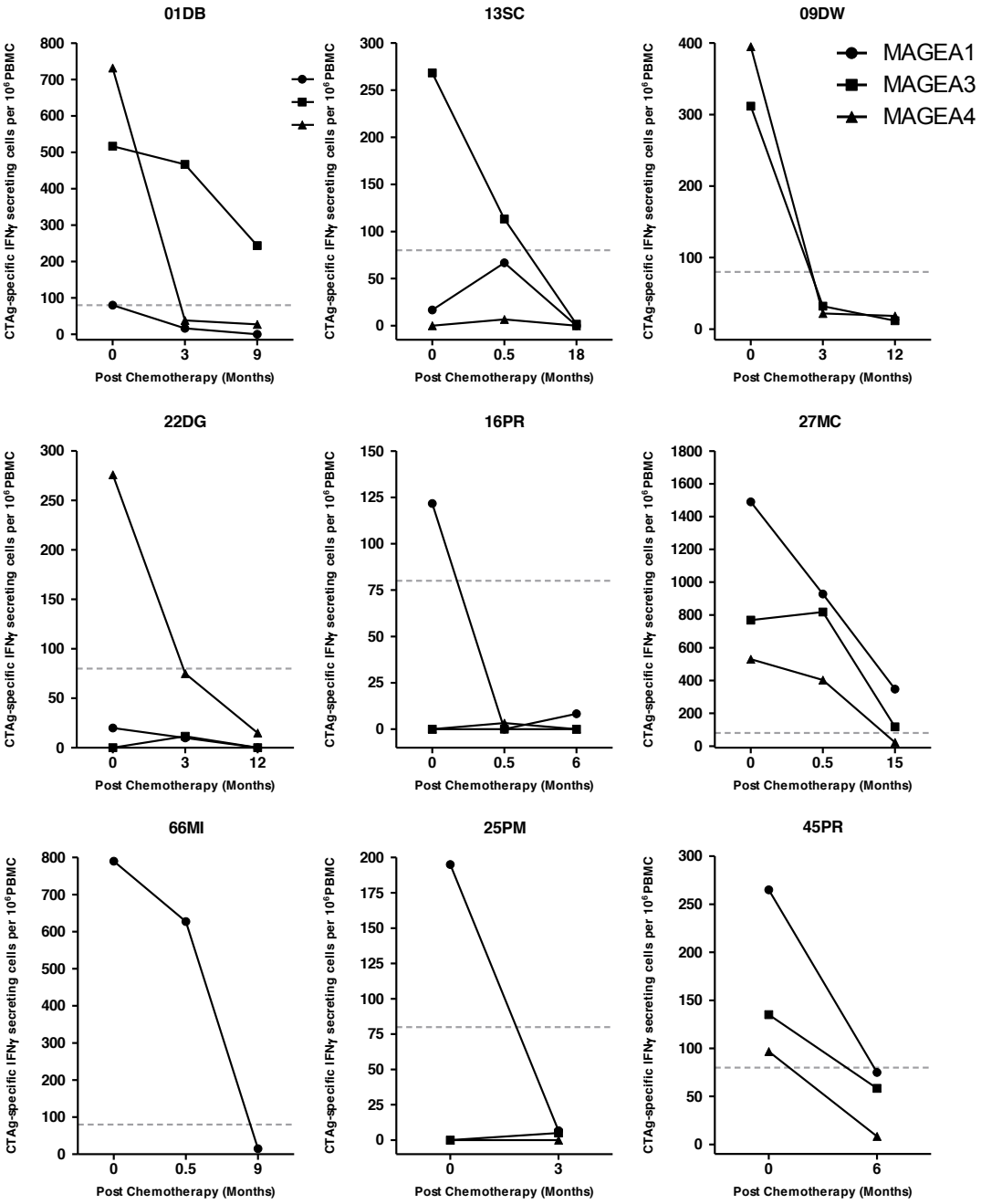

Figure 64. Kinetics of MAGE-specific responses in TGCT patients with a positive response prior to chemotherapy.

Numbers of CTAg-specific IFNγ secreting cells were determined prior to chemotherapy treatment (0 months), and then at specific time-points following the onset of treatment (0.5,3,6,9,12,15,18 months). Each graph shows one patient. Dashed horizontal line shows the threshold for positive response, defined as double the highest response determined in healthy donors.

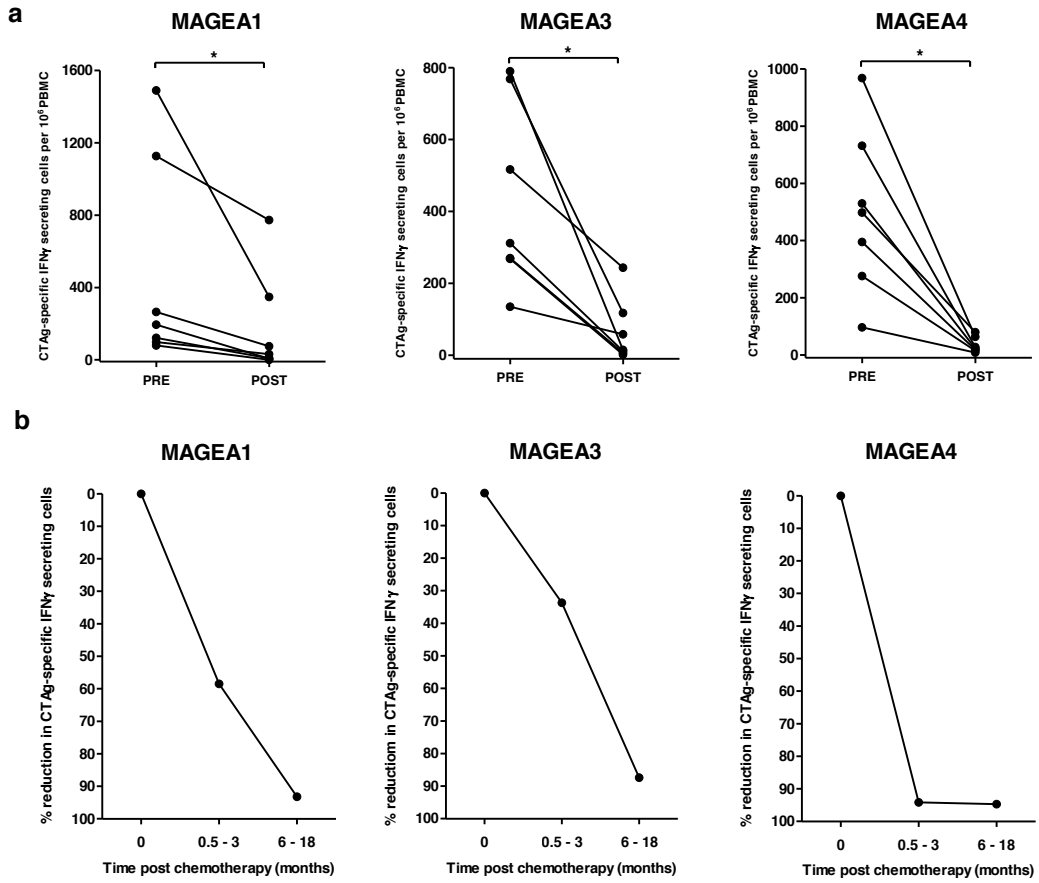

Figure 65. The reduction of MAGE-specific T cells following chemotherapy.
The frequency of MAGEA1, MAGEA3, and MAGEA4 -specific T cells at pre and post chemotherapy (a). Post chemotherapy is defined as the latest time point available in this patient cohort, and is between 3 and 18 months post treatment. The overall reduction of MAGEA1, MAGEA3, and MAGEA4 -specific T cells at various time points post chemotherapy, of all TGCT patients with a positive response prior to chemotherapy (b). Chemotherapy onset defined as 0 months. Each point represents the median value.

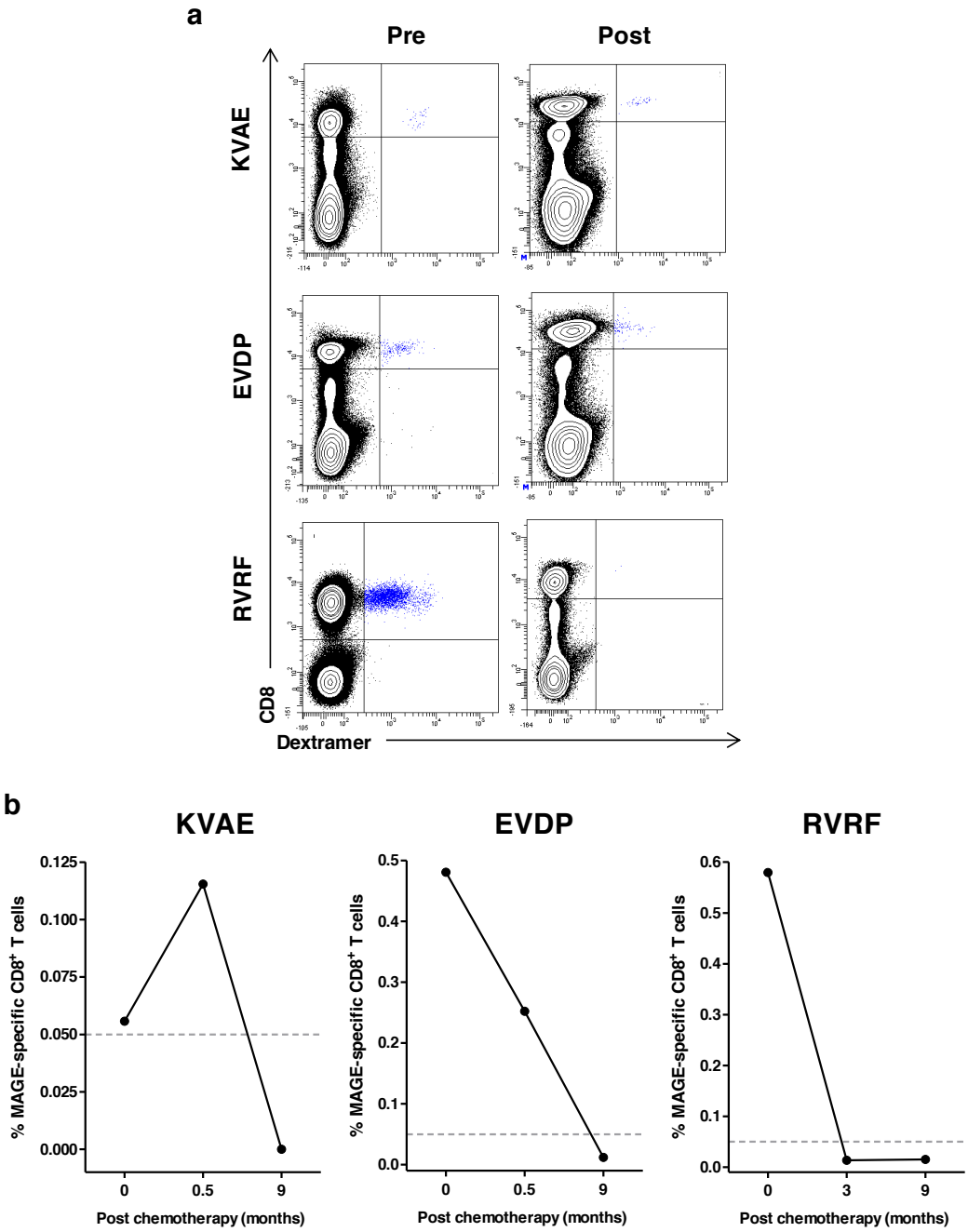

Figure 66. Dynamics of a single epitope MAGE-specific CD8 T cell response following chemotherapy.

Flow cytometry contour plots illustrate the detection of KVAE, EVDP and RVRF-specific T cells pre (left column) and post (right column) chemotherapy (a). Dextramer positive cells are highlighted in blue. The frequency of MAGE responses were determined at 2 intervals post chemotherapy and represented as percentage of total CD8 T cells (b). The dotted line represents the 0.05% threshold for a positive response.

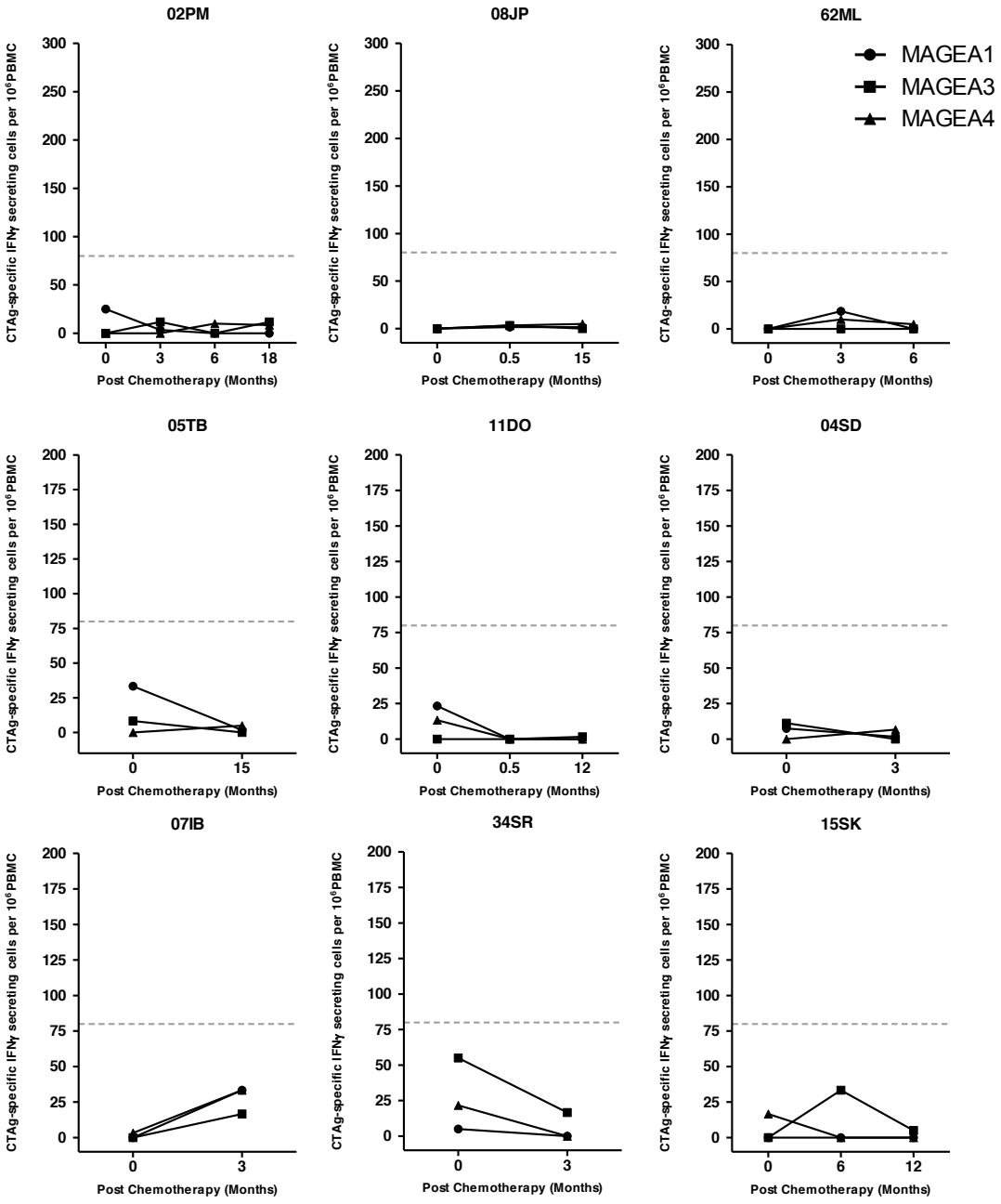

Figure 67. Kinetics of MAGE-specific responses in TGCT patients without a response prior to chemotherapy.

Numbers of CTAg-specific IFNγ secreting cells were determined prior to chemotherapy treatment (0 months), and then at specific time-points following the onset of treatment (0.5,3,6,12,15,18 months). Each graph shows one patient. Dashed horizontal line shows the threshold for positive response, defined as double the highest response determined in healthy donors.

MAGE-specific Cells are Predominantly Cytotoxic CD8 T Cells

In a smaller cohort of patients (n=10) where a positive MAGE-specific response was detected, we defined the subtype and functionality of cytokine secreting T cells. PBMC from TGCT patients were stimulated with appropriate overlapping MAGE peptides, and IFNγ and TNFα production was assessed. The majority of cells secreting inflammatory cytokines in response to MAGE peptide stimulation were found to be CD8 T cells (Figure 68a,b). However, cytokine secreting MAGE-specific CD4 T cells were present at lower frequencies in the majority of patients, and correlated positively with the frequency of MAGE-specific CD8 T cells (p=0.0156) (Figure 68c). Interestingly, CD8 T cells were predominantly TNFα only secreting cells (IFNγ^-TNFα^+), whereas CD4 T cells comprise equal proportions of TNFα only and dual secreting (IFNγ^+TNFα^+) cells. MAGE-specific IFNγ only secreting cells (IFNγ^+TNFα^-) were at particularly low levels in the majority of patients. Noticeably, IFNγ only secreting cells were readily detectable when stimulated with CEFT peptides, whereas TNFα only secreting cell were very rare. The results suggest tumour-specific T cells, specifically MAGE-specific CD8 T cells, have a unique cytokine profile.

Next we determined the cytotoxic capacity of CD8 T cells in relation to the cytokines they secrete, by assessing CD107a surface expression (Figure 69). A median of 99.89% of the IFNγ^+TNFα^+ cells expressed CD107a on their surface, and 88.51% of the IFNγ^-TNFα^+ subset. Surprisingly, only 21.67% of IFNγ^+TNFα^- cells had detectable cytotoxic potential. The cytokine and cytotoxicity profile of these cells is similar to that described earlier with the MAGEA3-specific T cell clone.

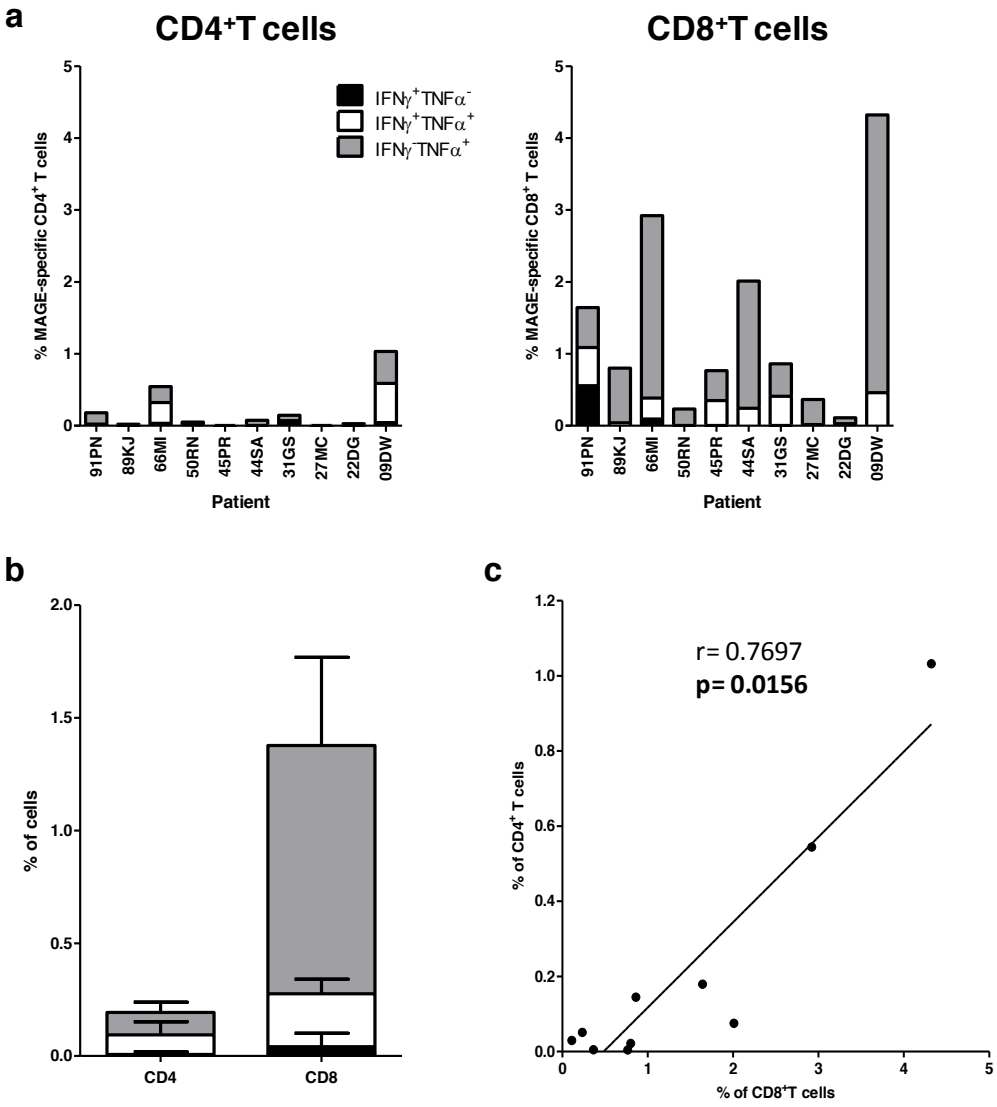

Figure 68. The secretion of inflammatory cytokines, IFNγ and TNF*α*, from CD4 and CD8 T cells following MAGE peptide stimulation.

Patients with MAGE-specific T cell responses were determined by IFNγ ELISPOT. PBMC from a number of these patients (n=10) were stimulated with the appropriate MAGE overlapping peptides to determine the T cell subset(s) (CD4 and/or CD8) that are releasing inflammatory cytokines. The proportion of IFNγ$^+$TNF*α*$^-$, IFNγ$^-$TNF*α*$^+$ and IFNγ$^+$TNF*α*$^+$ T cells following stimulation was determined for each patient (a) and the average of all ten patients (b), and represented as a percentage of total CD4 or CD8 T cells. Error bars represent SEM. Correlation between the proportion of cytokine secreting CD4 T cells and CD8 T cells was determined (c). Spearman's rank correlation coefficient (r) and significance (p) were determined. Significant p values are highlighted in bold type. Each symbol represents an individual patient.

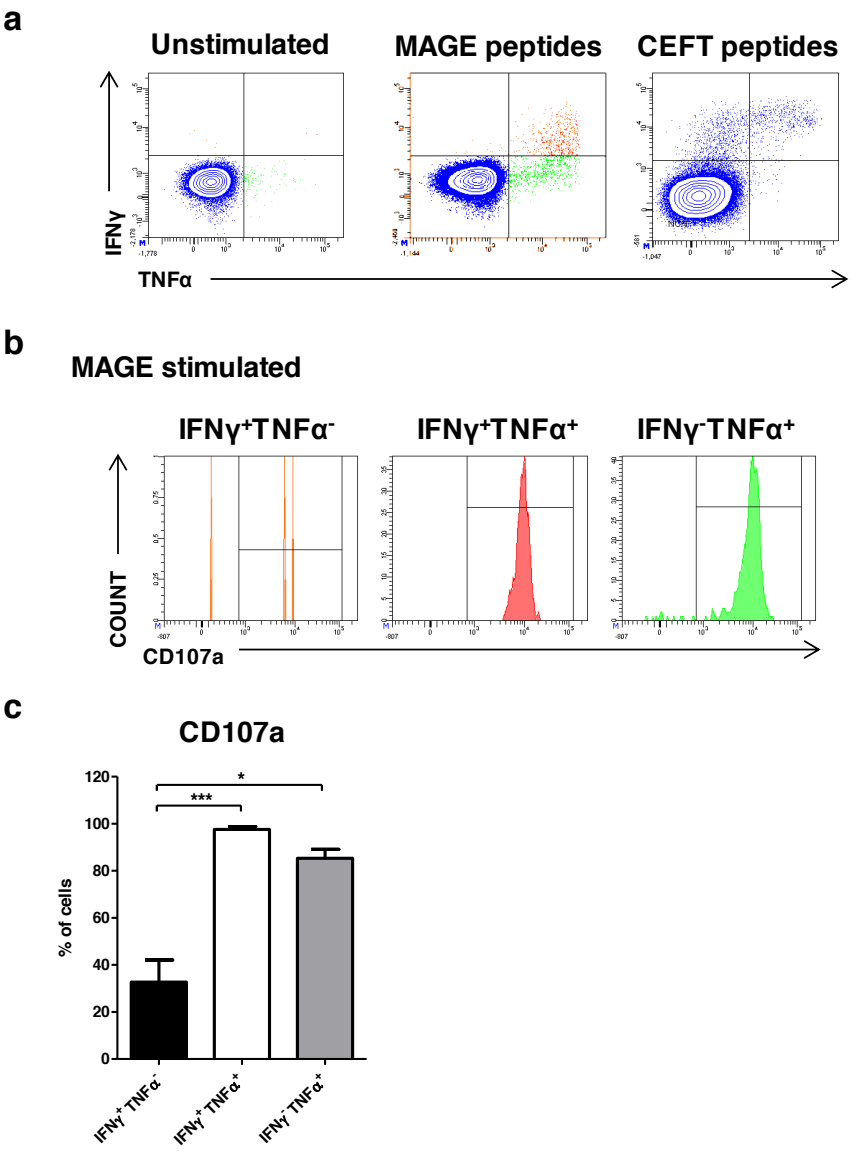

Figure 69. The magnitude of degranulation of CD8 T cells that secrete single or multiple cytokines.

CD8 T cells were identified by the positive expression of CD3 and CD8. They were analysed for expression of IFNγ and TNFα following stimulation with the appropriate MAGE overlapping peptides. Unstimulated cells were used as a negative control, CEFT peptides were used as a positive control (a). Representative histograms of CD107a surface expression on IFNγ$^+$TNFα$^-$, IFNγ$^+$TNFα$^+$, and IFNγ$^-$TNFα$^+$ subsets following MAGE peptide stimulation is shown (b). The proportion of CD107a expressing cells within each cytokine subset is shown (c). Bars represent mean. Error bars indicate SEM. Data analysed by Kruskal-Wallis with Dunn's multiple comparison test. * denotes $p<0.05$, *** denotes $p<0.001$.

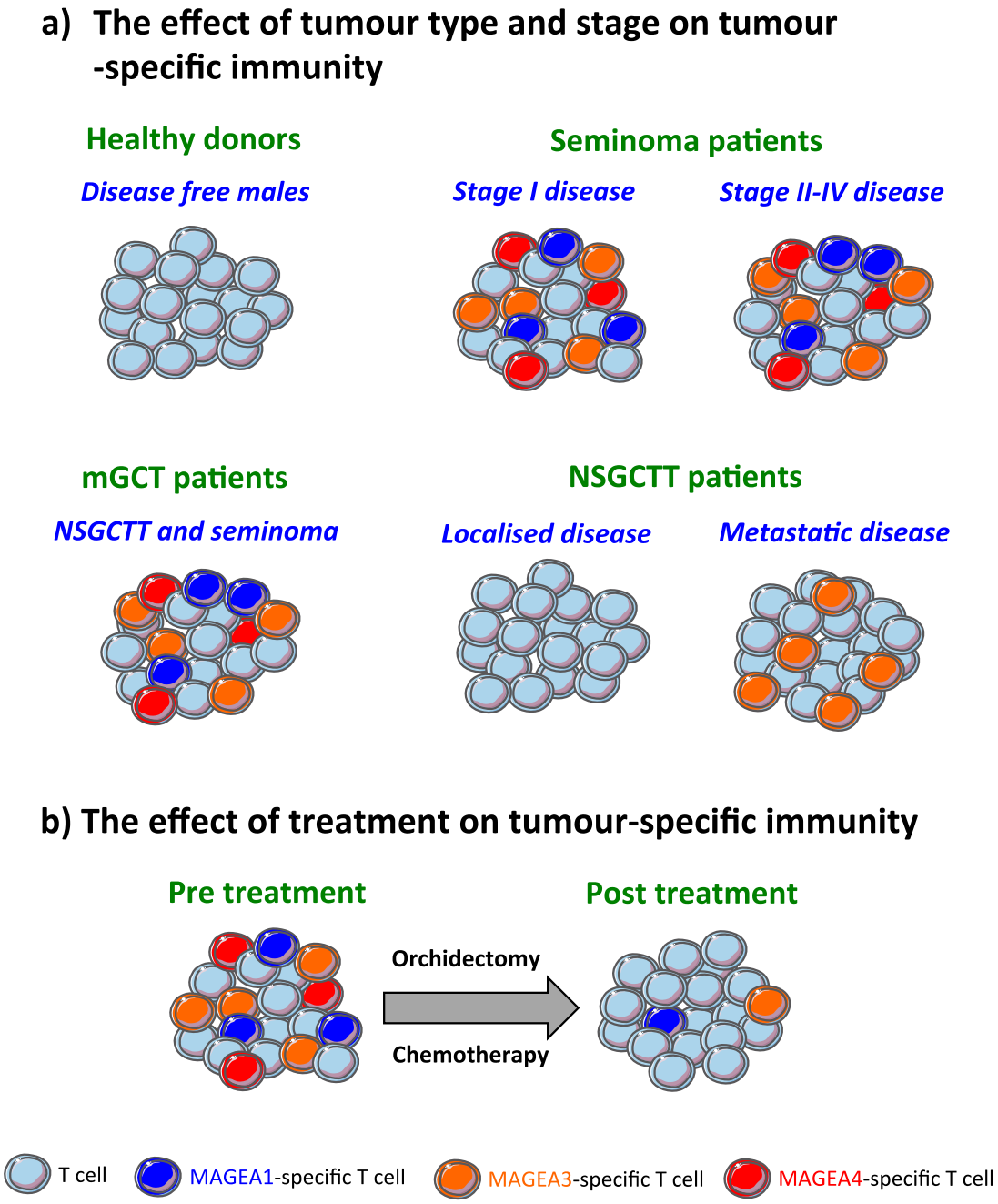

Figure 70. Summary of MAGE-specific T cell immunity in TGCT patients
Diagrammatic representation of the presence of MAGE-specific T cells in patients according to disease type and stage (a). The frequency of MAGE-specific T cells is low or absent in healthy donors and NSGCTT patients with localised disease. Multiple MAGE responses are frequently detected in seminoma patients regardless of tumour stage. MAGEA3 responses, but not MAGEA1 or A4, are detectable in NSGCTT patients with metastatic disease. The frequency of peripheral blood-derived MAGE-specific T cells declines by up to 95% following treatment (b).

Discussion

The main finding in this chapter is the frequent development of spontaneous T cell immunity in TGCT patients to multiple tumour-specific antigens, namely MAGEA1, A3 and A4. We show a decline in MAGE-specific T cells overtime, which is likely to be associated with reduced tumour-antigen load. In addition, CD8 T cell responses dominate the MAGE-specific T cell pool. The key points are summarised in Figure 70.

Dextramer analysis reveals MAGE-specific CD8 T cells in TGCT patients

CTAg expression has been observed in a wide range of tumours and can induce a cellular immune response towards the tumour, which could play an important role in controlling disease progression (Boon and van der Bruggen, 1996). Many classical seminomas have been shown to express MAGEA1, MAGEA3 (Cheville and Roche, 1999) or MAGEA4 (Aubry *et al*., 2001), yet NSGCTT have been negative in the majority of cases (Grobholz *et al*., 2000, Chen *et al*., 2013). Another study demonstrated greater levels of MAGEA1, A3, and A4 mRNA transcripts in seminoma patients compared to NSGCTT patients, although transcripts were detectable in both tumour types (Hara *et al*., 1999). We examined CTAg expression in TGCTs at both the gene and protein level. Most importantly, we show that concomitant expression of different MAGE proteins in the same specimen. Other studies have shown NY-ESO-1 expression in carcinoma *in situ* (CIS) cells, which are the pre-cancerous lesions from which all germ cell tumours arise, although the later tumours cease to express this antigen (Satie *et al*., 2002). In this present study, we found a single seminoma patient with NY-ESO-1 expression, which suggests this tissue contained elements of immature cancer precursors and is rarely expressed in fully differentiated disease. MAGEB1 expression has previously been shown in all seminomatous tumours

(Yuasa *et al*., 2001). Conversely, we demonstrate a lack of expression of this antigen in all seminoma tissues, although expression in healthy testis was detected. The vast lymphocytic infiltrate observed in seminoma may underestimate the level of CTAg expression, as our method determined the expression of antigens in whole tumour tissue and could not discriminate against immune cells. In addition, focal antigen expression may be missed in a single small biopsy, and may not be representative of the entire tumour mass.

An interesting question is whether spontaneous CD8 T cell responses are generated to MAGE antigens in TGCT patients. The detection of such responses would suggest the priming of naive antigen specific CD8 T cells directly by the tumour or through cross-presentation by APCs. The resulting expansion of such cells following recognition of cognate antigen, if they do indeed exist, should be detectable in peripheral blood of TGCT patients. We initially performed a comprehensive examination of peripheral blood-derived CD8 T cell responses to CTAgs in patients with testicular cancer, using dextramer complexes. The only previously documented CD8 T cell response to CTAg proteins in TGCT patients was detected using *in situ* tetramer staining, where they demonstrated the presence of MAGEA3-specific T cells in primary TGCT tissue (Hadrup *et al*., 2006).

In the present study, dextramer analysis revealed that MAGEA1 and MAGEA3 -specific CD8 T cells are detectable in peripheral blood of TGCT patients. Detectable levels of MAGE specific CD8 T cells were demonstrated in 8/22 patients following short-term epitope specific expansion. MAGEA1 and MAGEA3 responses were detected in seminoma patients, which correspond with the expression profile of these antigens in this tumour

subtype. Interestingly, one seminoma patient in this cohort generated both a MAGEA1 and MAGEA3 response, and another patient generated a MAGEA3 response against two peptides which are presented through different HLA molecules. Combined, the findings from both patients demonstrate the broad immunogenicity of seminomatous tumours, and the efficient presentation of these antigens to CD8 T cells.

In this assay, it is possible that a significant proportion of the MAGE- specific CD8 T cells we have observed may be attributable to *in vitro* expansion. Therefore we are unable to unequivocally determine whether MAGE-specific T cells in patients were in fact spontaneous tumour-specific responses, or inflation of naive MAGE-specific T cells *in vitro.* Due to the small volume of blood received from patients, T cells had to be expanded *in vitro*, which did not allow us to accurately surface phenotype these cells and therefore determine if they were derived from the naive or memory T cell pool. We assume that a single round of short term antigenic stimulation would not expand antigen specific naive T cells to a detectable level. In support of this assumption, a previous study using PBMCs from healthy donors, showed that five rounds of peptide loaded autologous DC stimulation was required to elevate antigen specific effector T cells to detectable levels (Li *et al*., 2004). Spontaneous and readily detectable MAGE-specific responses may be underestimated as some patients may have mounted a response below the detection limit of this assay. Overall, we speculate that MAGE-specific effector memory T cells are preferentially expanded following short-term culture with epitope specific peptides, which were originally derived from *in vivo* primed T cells.

In this set of experiments, we did not observe a single CD8 T cell response to MAGEA4. As previously discussed, MAGEA4 is expressed in seminoma tissues and therefore a MAGEA4-specific T cell response could potentially be mounted in these patients. It is important to note that the present methodology only covered a single MAGEA4 epitope thus we cannot be certain that a MAGEA4 response is not generated in these patients. The fact that more than 50 CTAg genes have been described with many immunogenic epitopes, of which we are only covering a few of these antigens suggests we are considerably underestimating the frequency and spectrum of the CTAg-specific response in TGCT patients using dextramer analysis.

The development of multiple MAGEA family specific T cell responses is dependent on tumour type

Next, we determined the actual frequency of CTAg-specific T cells in healthy donors and TGCT patients using an IFNγ ELISPOT method, in combination with full protein-spanning overlapping 15mer peptides. This method allowed the simultaneous detection of functional CTAg-specific CD8 T cells and CD4 Th1 cells, covering all known and unknown epitopes for a particular antigen. This methodology relies on the presentation of peptides to T cells by APCs and by T cells themselves (Burrows *et al*., 1992).

As expected, all CTAg-specific T cells were absent or at low frequencies in all 17 healthy donor where specific cells were at frequencies between 0 and 0.0041% of total PBMC for each antigen. It is not surprising that these cells are detectable in healthy donors, where they presumably reside in the naive T cell repertoire, ready for primary encounter of cognate antigen. In agreement with this, it has been estimated that in the naive CD8 T cell

pool a frequency of approximately $1/10^5$ T cells are specific for a given pMHC complex (Arstila *et al*., 1999). Undetectable levels in tumour-free individuals could be explained by levels present below the detectable threshold of this assay, or the fact that naive T cells predominantly circulate in lymphoid tissue and therefore are undetectable in peripheral blood.

MAGEA-specific responses were found in 21/49 TGCT patients, many of which had responses to 2 or more MAGEA antigens with up to 0.149% of cells being specific to a particular MAGE antigen. In agreement with our dextramer assay, NSGCTT patients only generated a response towards MAGEA3. Interestingly, mGCT patients also demonstrate multiple MAGE responses suggesting it is the seminoma elements in these tumours that are provoking the responses. We speculate that the generation of a MAGEA3 response in the absence of primary MAGEA3 expression in NSGCTT tissue, could be explained in two ways. Firstly by immunoediting of the antigenic phenotype of the tumours by specific cytotoxic immune responses (Dunn *et al*., 2004a). Here, particular MAGE antigens would have been expressed in some tumour cells at some point in time, but have now been eradicated by the immune system, so protein expression is no longer detectable. Secondly, distant metastases may develop that express MAGEA3 and the immune response may be generated toward this secondary tumour tissue. In support of the latter, tumour diagnosis indicated that patients with a MAGEA3 response in this NSGCTT cohort did indeed exhibit metastatic disease. We therefore wonder whether the expression of MAGEA3 is required by tumour cells to aid the migration from the primary tumour, and the presence of MAGEA3-specific cells may act as a useful indicator of disease progression and metastatic potential of NSGCTTs. In support of this, previous studies have associated

MAGEA family antigen expression with lymph node metastasis and lymphatic vessel invasion (Kavalar *et al*., 2001, Katano *et al*., 1997). MAGEA3 has been shown to be a mediator of extracellular matrix protein function, which promotes tumour cell migration and enhances invasive cancer cell growth (Liu *et al*., 2008). We speculate that tumour metastases derived from primary NSGCTTs express MAGEA3 to enable effective migration. In doing so, MAGEA3 expression increases the immunogenicity of the tumour, subsequently provoking an anti-MAGEA3 response, which is detectable in affected patients. Interestingly, we show that the stage of disease in seminoma patients does not affect the probability of generating an immune response towards MAGE antigens, nor does it correlate with the magnitude or multitude of the detectable responses.

Concerning the relationship between MAGE expression and the presence of detectable MAGE-specific T cell responses, one responding patient (91PN) in whom we detected multiple MAGE responses showed very low or absent MAGE protein expression in tumour tissue. As mentioned previously, this may simply reflect the incomplete covering of antigen expression due to the small biopsy size which therefore may not be representative of the entire tumour mass. The only other patient (47MH) in which we have CTAg expression data, showed very low or absent levels of MAGE proteins in tumour tissue and accordingly elevated levels of MAGE-specific T cells were not detected.

Patients with testicular tumours containing seminomatous elements commonly exhibited responses to a combination of MAGEA1, A3 and A4 antigens. MAGEA family antigens are co-expressed in various tumours, which suggest their regulation is part of a coordinated gene expression programme. The inclination towards genome-wide demethylation of CpG

islands in cancer (De Smet C, 1996), may largely explain the existence of multiple CTAg expression in seminoma tissue, and the multiple MAGE-specific responses we found in these patients. Sequence homology between all three MAGE antigens examined in this study is around 80% (Lurquin *et al*., 1997). Consequently, overlapping peptides spanning the length of one particular MAGE antigen could potentially present a proportion of very similar peptides, stimulating the same T cells even though a different set of peptides were used. Interestingly, if this were the case then elucidating the exact peptide would be of particular interest, in the context of future treatments, to develop immunotherapies which target multiple MAGE-antigens with a single TCR specificity. Unfortunately, we could not determine the exact peptides in which responding T cells were specific given that single peptides from the overlapping peptide pools were unavailable.

In this study it was noted that MAGEA4 responses were highly prevalent in TGCT patients as demonstrated using the ELISPOT and overlapping peptide method. This suggests the dextramer assay may hugely underestimate the rate of a CTAg response. Importantly, it also suggests many immunogenic epitopes exist that are currently undefined and future works requires the elucidation of such epitopes.

NY-ESO-1 and MAGEB1 –specific T cell responses are not generated in TGCT patients

As previously discussed, both tumour development and chemotherapy may inadvertently breakdown the blood-testis-barrier (BTB). We and others show that MAGEA family, NY-ESO-1 and MAGEB1 antigens are highly expressed in healthy testicular tissue. If breakdown of the BTB occurs, spermatogenic cells expressing many highly immunogenic proteins, including these CTAgs, may be compromised and released antigens could be

subsequently presented to T cells. If this were the case, we would expect to detect elevated responses to these antigens, especially towards NY-ESO-1, which has been described as one of the most immunogenic CTAgs. We clearly demonstrated that responses are not generated against NY-ESO-1 or MAGEB1 in patients with testicular cancer. This suggests MAGE responses observed in TGCT patients are provoked by tumours expressing these antigens and not indirectly by disruption of healthy testicular architecture during tumour progression. Further work is required to examine T cell responses to other CTAgs, particularly MAGEC1, which has recently been shown to be expressed in seminoma (Chen *et al*., 2011), although very few T cell epitopes of MAGEC1 have been described to date. Using our ELISPOT method and overlapping peptides to MAGEC1 would enable the discovery of new T cell epitopes.

The effects of age on MAGE-specific T cell responses in TGCT patients

Next, we investigated the effect of age on the development of an immune response to MAGE antigens and correlated this with the magnitude of the response. We showed that the likelihood of generating a response to a MAGE antigen is not dependent on age, although the magnitude of a MAGEA4 response does decline with age. The mechanism whereby the frequency of MAGEA4-specific cells is affected by ageing whilst the other antigens are not is unclear. We show that the majority of MAGEA4 responses (88%) are accompanied by other MAGE responses. It could be that MAGEA4 is less immunogenic than other MAGE antigens and the subsequent proliferation of MAGEA4-specific cells is lower, which may be further exacerbated in older patients. An aging immune system may be less efficient at generating a primary response to newly encountered antigens due to a reduced naive T cell compartment. Here, an unexplained preferential reduction of naive T

cells specific to MAGEA4 epitopes may occur with increased age. We demonstrated that the age of disease onset in seminoma patients was significantly higher than NSGCTT patients. Since MAGE responses are more common in seminoma patients, even though the mean age of disease onset was 15 years greater than NSGCTT patients, we speculate that tumour type has a far greater effect on the generation of MAGE responses than age.

MAGE-specific T cell responses diminish over time

The treatment schedule for patients with testicular cancer involves radical orchidectomy to remove the primary tumour, followed by adjuvant chemotherapy to eradicate residual disease. Combined, this treatment schedule reduces tumour burden and tumour antigen load, as proven clinically by the simultaneous reduction in peripheral blood tumour markers. Elevated levels of MAGE-specific T cells, which we have observed in patients shortly after tumour removal (but before chemotherapy), diminish considerably following treatment. Patient 09DW had elevated frequencies of both MAGEA3 and MAGEA4 - specific T cells, however, within 3 months these levels had dropped considerably. Interestingly, this patient did not receive chemotherapy treatment following orchidectomy, suggesting it may be the loss of tumour antigens following tumour removal and not the cytotoxic effects of chemotherapy that leads to the decline of MAGE-specific T cells over time.

We followed a cohort of patients for several months post treatment and found that during this time the majority of MAGE-specific cells were lost; although detectable levels were still observed in most patients up to 18 months later. We also demonstrated this in an epitope-specific manner by dextramer analysis, and found a marked decrease in T cells

specific to single MAGEA1 and MAGEA3 epitopes in all patients analysed. We speculate that the decline in MAGE-specific response over time mimics the kinetics of adaptive immunity following acute infection. Here, we assume the presentation of tumour antigens to naive T cells activates the primary immune response leading to elevated levels of MAGE-specific T cells, which we have described. Many of these cells are likely to enter the inflamed tumour environment, hence the large lymphocytic infiltrate observed in TGCTs. We have demonstrated the presence of large frequencies of MAGE-specific T cells in circulation of many TGCT patients, which were lost following tumour removal. Usually, an infection is cleared by the adaptive immune response, but in our case the tumour is not cleared by the immune system, but is done so by treatment. Nevertheless, the dose of tumour antigen falls below the response threshold and we assume this leads to the death of the majority (85 to 95%) of activated MAGE-specific effector T cells by apoptosis, similar to that observed following clearance of viral and bacterial infections (Badovinac *et al*., 2002, Kaech *et al*., 2002b). Following this contraction phase, a small fraction of the effector pool differentiate further to form the memory pool, which is maintained in the absence of antigen for long periods of time (Lau *et al*., 1994).

We postulate that the remaining MAGE-specific T cells which we observed in some patients many months after tumour antigen removal, are in fact these long-lived memory pool. Previous studies have shown that this long-lived memory pool retains the potential to rapidly produce IFNγ and TNFα and to quickly reacquire cytotoxic activity when exposed to antigen (Barber *et al*., 2003, Kaech *et al*., 2002a). It would be interesting to speculate that these long-lived memory T cells in TGCT patients may protect them from

subsequent tumour development. Protection could be generated not only against TGCTs but also against other cancers that express MAGEA-family antigens.

Interestingly, many but not all patients we examined had detectable levels of MAGEA-specific T cells following tumour removal, suggesting a substantial memory pool may not have been generated in some patients. Many experimental models have demonstrated that effective CD8 T cell immunity requires CD4 T cells for initiating and maintaining antitumor immune responses, and also to enable the generation of sustainable memory cells (Klebanoff *et al*., 2006). We have definitively shown that MAGE-specific CD4 T cells do exist alongside MAGE-specific CD8 T cells in the majority of TGCT patients, but are at significantly lower frequency than the CD8 T cell counterparts. Although the frequency of MAGE-specific CD4 T cells correlates positively with the MAGE-specific CD8 T cell repertoire, this low frequency may not be adequate to induce the generation of long-lived memory T cells. In addition, CD8 T cells that do populate the memory pool without CD4 T cell help have been shown to respond poorly to re-stimulation with antigen (Wherry and Ahmed, 2004).

The complete loss of MAGE-specific T cells over time, which was demonstrated in some TGCT patients in the present study, may be due to the lack of MAGE-specific CD4 T cells. We cannot rule out however the possibility that overlapping MAGE peptide pools made of 15-mer peptides more efficiently stimulated CD8 T cells than CD4 T cells. However, the majority of known MAGE immunogenic peptides expressed through MHC class II are between 13 and 22 amino acids long, suggesting CD4 T cell responses should be induced as efficiently as CD8 T cell responses.

The consequences of MAGE-specific responses in clinical outcome of TGCT patients are not definitively clear. In this context, it would be useful to conduct follow-up studies to determine whether TGCT patients with recurrent disease generated a MAGE response in the first instance. Low relapse rates in these patients would hinder this analysis, however the fact that relapse usually occurs within the first two years following treatment, would suggest it may be quickly achieved with a large enough patient cohort. We performed a follow-up survey in a small cohort of TGCT patients where MAGE-specific T cell responses had been assessed. In this cohort, only one patient (HP07) experienced tumour recurrence and he lacked responses for all MAGE antigens. Whether relapse was due to the absence of natural T cell immunity towards the tumour could not be determined.

Next, we determined whether a MAGEA response could be generated in seminoma and mGCT patients following chemotherapy. A response was not detected in these patients prior to chemotherapy, nor was one generated following chemotherapy. This could imply that chemotherapy-induced lysis of residual tumour cells does not provoke a T cell response, or that residual tumour cells are simply not present in these patients. Alternatively, a T cell response is being generated but not towards MAGE antigens, possibly due to the lack of expression of MAGE antigens in these cells.

The functionality of MAGE-specific T cells from TGCT patients

Next, we determined the functionality of CTAg-specific CD8 T cells isolated from peripheral blood of TGCT patients. MAGE-specific CD8 T cell responses were detected in a number of patients using dextramers, yet the frequency was too low to effectively analyse their functionality. Instead we generated a T cell clone from a seminoma patient,

which was specific for MAGEA3$_{168-176}$ peptide (EVDP), where expression was restricted through HLA-A1. The EVDP-specific clone demonstrated cytokine production and cytolytic activity towards peptide-loaded targets. More importantly, cytotoxicity was directed towards an HLA-A1-expressing tumour cell line (HT-29) presenting endogenously processed MAGEA3 antigen. Interestingly, HT-29 cells induced cytotoxicity (degranulation) in up to 40% of MAGEA3-specific cells without inducing cytokine production; a phenomenon that was practically absent when cells were stimulated with peptide loaded targets. We assume this is due to the nature of stimulation, which may be more physiological than transformed B cells (LCLs) to present antigen. HT-29 cells are known to express MICA on their surface (Salih *et al*., 2002), and it could be the interaction with NKG2D on the T cell surface that induced this greater cytotoxic capacity we observed.

We show that MAGE-specific CD8 T cell responses are generated in TGCT patients although the cytokine profile of these cells following stimulation was unexpected. The majority of cytokine secreting cells secreted TNFα alone; a smaller proportion produced both TNFα and IFNγ, and very few produced IFNγ alone. We confirmed this observation by stimulating PBMC, from patients with a known response, with overlapping MAGE peptides and examined subsequent cytokine production. Similarly, we found the majority of MAGE-specific CD8 T cells that produced cytokine, only secreted TNFα. This was also apparent in CD4 T cells but to a lesser extent. Only a very small percentage of cytokine secreting cells secreted IFNγ alone, but the ones that did showed a diminished ability to degranulate. In agreement with our observations, a recent study investigating TAA-specific CD8 T cells in hepatocellular carcinoma demonstrated their impaired ability to

produce IFNγ (Flecken *et al*., 2013). Others have shown impaired IFNγ secreting capacity of HCMV-specific CD8 T cells among kidney transplant recipients (Yang *et al*., 2008). This suggests that the efficacy of MAGE-specific CD8 T cell response is functionally limited, presumably due to an exhausted or anergic phenotype induced within the suppressive tumour environment.

High-avidity recognition of tumour antigens has been shown to be essential for effective *in vivo* anti-tumour responses (Zeh *et al*., 1999). We therefore determined the avidity of the MAGEA3-specific T cell clone for its cognate antigen, EVDPIGHLY. The avidity of this T cell clone was defined by the concentration of peptide required to elicit a T cell response after loading onto target cells (LCLs). We showed that its avidity was similar to MAGE-specific clones previously generated in our laboratory from AML and myeloma patients. In this assay, a high avidity T cell was classified as requiring < 1 nM peptide loaded on target cells for activation and subsequent cytokine release. Our clone required between 100 and 1000 nM peptide to induce a half maximal response (EC_{50}), suggesting our clone has a low avidity for cognate antigen (Snyder *et al*., 2003). Among the many immunosuppressive mechanisms mediated by the tumour microenvironment, impaired T cell activation and clonal expansion and diminished effector function would fit with the generation of low avidity MAGE-specific CD8 T cells, as detected in this present study.

However, we have shown that these low avidity MAGE-specific T cells are able to sufficiently recognise and induce cytotoxicity towards presented antigen even though the avidity for cognate antigen may be low. From this data we could speculate that MAGE-specific T cells were anergised or exhausted *in vivo* and may regain full functional

competence, including cytokine secretion, upon repeated *in vitro* peptide stimulation with IL-2. The IFNγ ELISPOT method used to quantify the magnitude of specific MAGE responses may underestimate the frequency of MAGE-specific cells, since multiple cytokine profiles exist. Populations of both MAGE-specific CD4 T cells and CD8 T cells show differential secretion of inflammatory cytokines, whereby many did not secrete IFNγ but were still cytotoxic. Future studies would perhaps utilise TNFα as a means to quantify MAGE-specific cells in an ELISPOT assay, as TNFα only secreting cells demonstrate cytotoxic potential. In addition, granzyme B and perforin would also be measured to quantify more specifically the cytotoxicity of MAGE-specific T cells.

Due to the rare availability of TIL, we have only explored the specificity of tumour-specific T cells in peripheral blood. At this stage, we can only assume that MAGE-specific T cells found in the peripheral blood of TGCT patients also exist within the tumour mass. Whether the functionality of these cells mimics what we have demonstrated *in vitro* is unclear. We speculate that immunosuppressive mechanisms are at play within the tumour, which may have a detrimental effect on the anti-MAGE response.

Conclusion

In conclusion, we show that pMHC dextramer complexes are valuable in the detection and isolation of epitope-specific CTAg responses from peripheral blood of TGCT patients. However, the poor detection threshold, the requirement for *in vitro* expansion and the incomplete picture of the spectrum and magnitude of responses, meant a more comprehensive and quantitative approach had to be undertaken. By combining MAGE overlapping peptides with a highly sensitive IFNγ ELISPOT assay, we show for the first time that multiple MAGEA family-specific T cells are elevated in seminoma and mGCT patients. Interestingly, NSGCTT patients only developed responses towards MAGEA3 and were shown to be associated with disease progression. MAGE-specific T cells were cytotoxic *in vitro,* but many had an impaired ability to produce IFNγ following peptide stimulation. The physiological relevance of MAGE responses in limiting tumour growth and metastasis *in vivo* remains to be determined.

CHAPTER 5: GENERAL DISCUSSION

The importance of the immune system in protecting against cancer was originally proposed in Burnet's theory of cancer immunosurveillance. This model states that the immune system recognises transformed cells as they arise and together, the innate and adaptive arms of the immune system eradicate these cells. Supporting this model is the fact that immunocompromised patients are more susceptible to tumour development (reviewed in (Dunn *et al*., 2004b, Zitvogel *et al*., 2006)). In addition, the generation of endogenous immunity to tumour antigens, as demonstrated in this study, provides compelling evidence in support of natural immunosurveillance. Expression of stress ligands such as MICA/B and ULBPs, or the presentation of tumour-antigens, such as the MAGEA family, on the surface of tumour cells targets them for destruction. Despite the diverse range of immune mechanisms that target transformed cells, the high prevalence of cancer would indicate that the immune response is unable to effectively control its growth and spread (Dranoff, 2009). One mechanism of tumour immune escape is the promotion of immune cell dysfunction or exhaustion.

In the present study, we have frequently detected multiple MAGEA family-specific T cells in peripheral blood of patients with tumours containing seminomatous elements. In contrast, MAGE-specific cells were only present at very low levels in healthy individuals and are only elevated in NSGCTT patients with metastatic disease. We presume the low levels we detect in healthy individuals are antigen inexperienced and are therefore contained within the naive T cell pool. We show that the majority of T cells within TGCT

lesion are T_{EM} cells. We believe the significant increase in peripheral blood T_{EM} cells in TGCT patients correlates with the elevated incidence of tumour-specific T cells, some of which are antigen-experienced MAGE-specific T cells. We observed considerable enrichment of the TCRVβ repertoire of TIL, however we failed to find evidence of restricted TCRVβ usage between patients. This suggests that there is likely to be extensive TCR diversity among tumour reactive T cells, along with multiple MAGE antigen specificities and TCR affinities.

Intracellular cytokine staining following MAGE overlapping peptide stimulation revealed the presence of both MAGE-specific CD4 and CD8 T cells in peripheral blood of TGCT patients. Pro-inflammatory MAGE-specific CD8 T cells were more prevalent than their MAGE-specific CD4 T cell counterparts. We did notice however a significant proportion of T cells within the tumour that did not secrete inflammatory cytokine following *in vitro* stimulation. We speculate that these T cells are irreversibly dysfunctional or are releasing immunoregulatory cytokines. Although CD8 T cells are predominately associated with the production of inflammatory cytokines, there is evidence suggesting they secrete immunoregulatory cytokines including IL-4 and IL-10 (Schuler *et al*., 2001). Moreover, CD4 T cell subsets including Th2 and Tregs are associated with the release of immunosuppressive cytokines including IL-4, IL-10 and TGFβ. In addition, we detected a significant increase in CD161-expressing CD4 T cells in the tumour indicative of IL-17-secreting Th17 cells. Further studies are required to determine the extent of pro-tumour and anti-tumour activity of these T cell subsets in TGCTs. We may however be underestimating the extent of MAGE-specific responses, especially in the case of CD4 T cells. There could potentially be a greater proportion of MAGE-specific CD4 T cells that

secrete pro-tumour associated cytokines, which were not investigated in this study. The secretion of immunoregulatory cytokines by MAGE-specific cells may favour an immunoregulatory response, contributing to tumour immune escape and consequently tumour progression. Understanding the potential roles of Th1, Th2, Th17 and Treg subsets in a MAGE-specific response may help develop improved therapeutic strategies for boosting an anti-tumour response.

The locality of initial tumour antigen recognition is currently unclear but our findings suggest that MAGE-expressing tumours do provoke a T cell response to such antigens. Unfortunately, we were unable to clarify whether T cells infiltrating the tumour were CTAg-specific due to the rare availability of tumour tissue, and the potentially unresponsiveness of TIL to TCR stimulation with native antigen. Nevertheless, the fact that they are detectable in peripheral blood would suggest that TIL are likely to contain a vast number of T cells with MAGE specificity. With this in mind, the lack of T cell proliferation and cytokine production by cells isolated from tumour tissue without *in vitro* stimulation, suggests initial antigen presentation occurs prior to tumour infiltration and clonal expansion commences here. In addition, LN-activated CD8 T cells may proliferate further within the tumour microenvironment, as described previously in brain tumours (Masson *et al*., 2007). Generally, cross-presentation of tumour antigens by DCs in the tumour-draining LN is considered the primary mode of naive tumour-specific CD8 T cell activation (Nelson *et al*., 2001, Hargadon *et al*., 2006). We hypothesise that T cell priming occurs via this mechanism and subsequent activation presumably occurs within the tumour mass, as signified by the expression of recent activation marker CD69 on tumour-residing T cells. The exact mechanism of T cell activation within the tumour remains to be

determined. However, we speculate that this may occur by either direct interaction with the tumour or through antigen presentation by tumour-residing professional APCs. Various studies have demonstrated low or absent expression of MHC class I on TGCT tissue (Nouri *et al*., 1993, Bols *et al*., 2000, Hadrup *et al*., 2006), suggesting the latter may be the most likely mechanism of tumour antigen recognition and activation within the tumour mass.

The mechanisms operating in the capture, processing and presentation of released tumour antigens to T cells in TGCTs *in vivo* is unknown. Rapid proliferation of tumour cells during normal tumour growth and development is associated with a degree of tumour cell apoptosis and necrosis, subsequently releasing tumour antigens in the process. In addition, we have observed the presence of NK cells within tumour lesions and demonstrated the cytotoxicity of these NK cells against MHC class I deficient target cells. This implies that this cell type could contribute to the release of MAGE antigens by direct lysis of TGCT cells. This would suggest that TGCT-residing NK cells may play a fundamental role in the initial recognition and subsequent lysis of tumour cells. DCs are present in TGCT lesion (Bols *et al*., 2000), and we propose these cells are important in the capture of released tumour antigens and subsequent processing and presentation to T cells.

A striking feature of the current study is that although NK cells are effective killers of tumour cell lines, they do not effectively eliminate tumours in TGCT patients. Moreover, multiple MAGEA family-specific T cell responses were detected in TGCT patients. However, there was no indication of these cells limiting tumour growth, which suggests

that expanded MAGE-specific immunity has limited value in controlling tumour growth *in vivo* despite the potent effector function of MAGE-specific T cells *in vitro*. It is difficult to determine the efficacy of a tumour-specific response that is observed in TGCT patients, as mortality is low and recurrence is very rare, even in patients with metastatic disease. We can therefore assume that MAGE-specific T cells are deficient in their ability of tumour clearance, although they may slow tumour growth and progression. The indolent course that seminoma follows may be due to the presence of a vast lymphocytic infiltrate, unlike primary NSGCTTs, which are more aggressive, exhibit a lesser immune infiltrate and fail to provoke a MAGE-specific response.

Aside from tumours reducing immunogenicity, additional mechanisms must be at play to enable them to evade immune destruction. Here, we propose possible routes of immunoregulation within TGCTs that could potentially lead to T cell hyporesponsiveness. These include the upregulation of inhibitory receptors TIM-3 and PD-1, and the downregulation of activating receptor NKG2D on tumour infiltrating T cells. We determined that TGCT tissue, especially seminoma, expressed PD-1 ligands. It is unknown whether this expression is by the tumour *per se* or by the immune infiltrate. Nonetheless, T cell activation in an environment with inadequate costimulation, or in the elevated presence of co-inhibitory molecules (PD-L1 and PD-L2), could lead to the induction of T cell anergy. In addition, prolonged antigen stimulation within the tumour microenvironment can lead to an exhausted T cell phenotype, which is associated with the high expression of multiple inhibitory receptors including TIM-3 and PD-1. This can further contribute to T cell dysfunction, as signalling through these receptors can lead to cell cycle arrest and disruption of cytotoxic potential.

We propose that anergy and exhaustion may both contribute towards T cell dysfunction in TGCTs. T cell anergy may be induced at the time of first antigen stimulation whereas exhaustion is a progressive, hierarchical process where dysfunction worsens, and correlates with the acquisition of multiple inhibitory receptors over time (Wherry *et al*., 2007). We observed both single and dual staining of PD-1 and TIM-3 on CD8 T cells, and we speculate that dual inhibitory receptor-expressing T cells are more dysfunctional than single inhibitory receptor-expressing T cells. It has been reported that dual expressing NY-ESO-1–specific CD8 T cells are highly dysfunctional compared to single-expressing or non- expressing − NY-ESO-1–specific CD8 T cells (Fourcade *et al*., 2010). In the future, we would assess the expression of additional inhibitory receptors on the surface of MAGE-specific T cells and correlate this with the extent of T cell dysfunction.

MAGE-specific T cells are only likely to have a direct effect on testicular tumour growth if they are able to enter the tumour microenvironment. We readily detected these cells in the peripheral blood of TGCT patients prior to adjuvant chemotherapy. We were intrigued to find that the vast majority of MAGE-specific cells had diminished a few months later, although low frequencies were still detectable in some patients up to 18 months later. In the future, we would investigate the memory phenotype of these cells *ex vivo*, to definitively confirm whether or not MAGE-specific T cells are antigen experienced and to determine the phenotype of the low frequency persistent population. We speculate that the elevated MAGE-specific populations we detect are T_{EM} cells, as we have observed elevated levels of T_{EM} in TGCT patients. In addition, the decline in MAGE-specific T cells over time correlates with the reduced proportion of T_{EM} cells in peripheral blood of TGCT patients. Furthermore, it is likely that the remaining MAGE-specific T cells contribute to

immunological memory and confer long-term protection. MAGE-specific immunological memory is not present in the peripheral blood all patients, which is probably due to biological factors such as the homing and tissue distribution of these T cells. In conclusion, we show a decline in MAGE-specific immunity following treatment, which may mimic the death phase of an adaptive immune response in a human cancer scenario, whereby, the tumour-specific T cell pool contracts in the absence of cognate antigen.

Much of our knowledge regarding cancer immunology is derived from research using animal models of the disease. Studies on TGCT patient samples offer potential data that is more readily translatable to clinical therapeutics. Firstly, TGCTs are an ideal model to investigate tumour immune evasion, since multiple regulatory mechanisms exist, many of which are apparent in other tumour types. Secondly, spontaneous immunity towards MAGE antigens is developed and detectable in the peripheral blood of these patients. Thirdly, the findings in this study are transferable across many solid tumours that express MAGE antigens. Finally, TGCT patients are predominantly young to middle-aged men and therefore have an efficiently functioning immune system. This removes the complications related to inadequate tumour-specific responses as a consequence of a limited naive T cell repertoire and age-related immune senescence.

Testicular cancer is a relatively rare cancer but incidence is rising fast, with an estimated doubling over the last 40 years in the UK (Toledano *et al*., 2001, Swerdlow *et al*., 1998) and USA (McGlynn *et al*., 2003). Although treatment currently provides a long-term cure in the majority of patients, there are a small number that succumb to this disease. Moreover,

many adverse side effects including major cardiovascular complications, nephrotoxicity, and infertility are commonly associated with cisplatin-based chemotherapy treatment. The increasing number of long-term survivors of this disease highlights the long-term side effects of such treatments, many of which are more detrimental than cancer recurrence. Alternative treatments which may include immunotherapy regimens could be put into practice in order to minimise the occurrence and severity of chemotherapy-induced long-term side effects.

The frequent, concomitant expression of multiple CTAgs in TGCTs, in addition to the existence of spontaneous MAGE-specific CD4 and CD8 T cells, demonstrated in this study, supports the development of specific vaccination protocols. We observe patients with a pre-existing response to MAGE antigens and such patients are more likely to generate a further response following vaccination with the same antigen (Reynolds *et al*., 2003). It would be interesting to consider a combination of vaccine strategies to induce a secondary MAGE-specific T cell response with PD-1 or TIM-3 blockade, to improve the efficacy of a tumour-specific T cell response. Many anti-cancer drugs have been shown to upregulate NKG2D ligands on the surface of tumour cells, which induce direct NK cell-mediated tumour cell lysis (He *et al*., 2013, Yang *et al*., 2013, Wu *et al*., 2012). However, we show a significant downregulation of NKG2D expression on NK cells and T cells, presumably due to overexpression or shedding of NKG2D ligands from the tumour surface. Our findings do not support this particular rationale for increasing the immunogenicity of TGCTs, which may in fact augment immunosuppressive mechanisms by further reducing the expression of NKG2D on tumour infiltrating immune cells.

Spontaneous humoral immune responses, in addition to cell-mediated immune responses, have been detected towards various tumour types (Fossa *et al*., 2004, Akcakanat *et al*., 2004, Lendvai *et al*., 2010). Since B cell frequencies in TGCTs are high (Bols *et al*., 2000), future studies should include the examination of antibody responses towards the tumour, including those generated towards MAGE antigens. Isolation of tumour-specific B cells would allow the generation of therapeutic antibodies, which could be utilised to induce an anti-tumour antibody dependent cell cytotoxicity (ADCC) response.

In conclusion, we have found antigen experienced, recently activated and exhausted T cells within TGCT lesions. Despite the reversibility of T cell effector function *in vitro*, immune-mediated tumour clearance in these patients is not observed, suggesting multiple tumour immune evasion mechanisms operate. Engagement of PD-1 and TIM-3 with their respective ligands may account for the lack of an efficient anti-tumour response *in vivo*. The main finding of this study was the demonstration of spontaneous T cell immunity to MAGEA family antigens in TGCT patients. MAGE-specific T cell responses may be mere markers of exposure to antigen without functional relevance, which is substantiated by the fact that low or absent MHC class I expression on testicular tumour cells has been reported. Nonetheless, our results suggest that multiple tumour-specific T cell responses are generated against primary seminoma tumours, whereas a response to NSGCTT is only provoked by the development of a secondary tumour. We have established for the first time that elevated frequencies of MAGE-specific T cells diminish over time, which may be strongly associated with the loss of cognate antigen following treatment.

Combined, our findings lead to the possibility that this family of tumour-specific antigens could be manipulated along with inhibitory receptor blockade to enhance the anti-tumour response in cancer patients. Further exploration into the interactions between tumour cells, stromal cells and TIL in the tumour microenvironment will be important in the design of more efficacious cancer immunotherapies, which are widely applicable across many tumour types.

REFERENCES

ABE, R., PENG, T., SAILORS, J., BUCALA, R. & METZ, C. N. 2001. Regulation of the CTL response by macrophage migration inhibitory factor. *J Immunol,* 166**,** 747-53.

ACKERMAN, A. L. & CRESSWELL, P. 2004. Cellular mechanisms governing cross-presentation of exogenous antigens. *Nat Immunol,* 5**,** 678-84.

AHMADZADEH, M., JOHNSON, L. A., HEEMSKERK, B., WUNDERLICH, J. R., DUDLEY, M. E., WHITE, D. E. & ROSENBERG, S. A. 2009. Tumor antigen-specific CD8 T cells infiltrating the tumor express high levels of PD-1 and are functionally impaired. *Blood,* 114**,** 1537-44.

AKCAKANAT, A., KANDA, T., KOYAMA, Y., WATANABE, M., KIMURA, E., YOSHIDA, Y., KOMUKAI, S., NAKAGAWA, S., ODANI, S., FUJII, H. & HATAKEYAMA, K. 2004. NY-ESO-1 expression and its serum immunoreactivity in esophageal cancer. *Cancer Chemother Pharmacol,* 54**,** 95-100.

ALAS, S., EMMANOUILIDES, C. & BONAVIDA, B. 2001. Inhibition of interleukin 10 by rituximab results in down-regulation of bcl-2 and sensitization of B-cell non-Hodgkin's lymphoma to apoptosis. *Clin Cancer Res,* 7**,** 709-23.

ALBERT, M. L., SAUTER, B. & BHARDWAJ, N. 1998. Dendritic cells acquire antigen from apoptotic cells and induce class I-restricted CTLs. *Nature,* 392**,** 86-9.

ALEGRE, M. L., FRAUWIRTH, K. A. & THOMPSON, C. B. 2001. T-cell regulation by CD28 and CTLA-4. *Nat Rev Immunol,* 1**,** 220-8.

ALLISON, J., GEORGIOU, H. M., STRASSER, A. & VAUX, D. L. 1997. Transgenic expression of CD95 ligand on islet beta cells induces a granulocytic infiltration but does not confer immune privilege upon islet allografts. *Proceedings of the National Academy of Sciences of the United States of America,* 94**,** 3943-7.

ANDERSON, M. S., VENANZI, E. S., KLEIN, L., CHEN, Z., BERZINS, S. P., TURLEY, S. J., VON BOEHMER, H., BRONSON, R., DIERICH, A., BENOIST, C. & MATHIS, D. 2002. Projection of an immunological self shadow within the thymus by the aire protein. *Science,* 298**,** 1395-401.

ANDREYEV, H. J. N., DEARNALEY, D. P. & HORWICH, A. 1993. Testicular Nonseminoma with High Serum Human Chorionic-Gonadotropin - the Trophoblastic Teratoma Syndrome. *Diagnostic Oncology,* 3**,** 67-71.

ANNUNZIATO, F., COSMI, L., SANTARLASCI, V., MAGGI, L., LIOTTA, F., MAZZINGHI, B., PARENTE, E., FILI, L., FERRI, S., FROSALI, F., GIUDICI, F., ROMAGNANI, P., PARRONCHI, P., TONELLI, F., MAGGI, E. & ROMAGNANI, S. 2007. Phenotypic and functional features of human Th17 cells. *J Exp Med,* 204**,** 1849-61.

ANTONY, P. A. & RESTIFO, N. P. 2005. CD4(+)CD25(+) T regulatory cells, immunotherapy of cancer, and interleukin-2. *Journal of Immunotherapy,* 28**,** 120-128.

APPAY, V. 2004. The physiological role of cytotoxic CD4(+) T-cells: the holy grail? *Clin Exp Immunol,* 138**,** 10-3.

APPAY, V., ZAUNDERS, J. J., PAPAGNO, L., SUTTON, J., JARAMILLO, A., WATERS, A., EASTERBROOK, P., GREY, P., SMITH, D., MCMICHAEL, A. J., COOPER, D. A., ROWLAND-JONES, S. L. & KELLEHER, A. D. 2002. Characterization of CD4(+) CTLs ex vivo. *J Immunol,* 168**,** 5954-8.

APTE, R. S., SINHA, D., MAYHEW, E., WISTOW, G. J. & NIEDERKORN, J. Y. 1998. Cutting edge: role of macrophage migration inhibitory factor in inhibiting NK cell activity and preserving immune privilege. *J Immunol,* 160**,** 5693-6.

ARAI, H., CHAN, S. Y., BISHOP, D. K. & NABEL, G. J. 1997. Inhibition of the alloantibody response by CD95 ligand. *Nature Medicine,* 3**,** 843-8.

ARINA, A., MURILLO, O., HERVAS-STUBBS, S., AZPILIKUETA, A., DUBROT, J., TIRAPU, I., HUARTE, E., ALFARO, C., PEREZ-GRACIA, J. L., GONZALEZ-ASEGUINOLAZA, G., SAROBE, P., LASARTE, J. J., JAMIESON, A., PRIETO, J., RAULET, D. H. & MELERO, I. 2007. The combined actions of NK and T lymphocytes are necessary to reject an EGFP+ mesenchymal tumor through mechanisms dependent on NKG2D and IFN gamma. *Int J Cancer,* 121**,** 1282-95.

ARSTILA, T. P., CASROUGE, A., BARON, V., EVEN, J., KANELLOPOULOS, J. & KOURILSKY, P. 1999. A direct estimate of the human alphabeta T cell receptor diversity. *Science,* 286**,** 958-61.

ASANO, M., TODA, M., SAKAGUCHI, N. & SAKAGUCHI, S. 1996. Autoimmune disease as a consequence of developmental abnormality of a T cell subpopulation. *J Exp Med,* 184**,** 387-96.

ATTIG, S., HENNENLOTTER, J., PAWELEC, G., KLEIN, G., KOCH, S. D., PIRCHER, H., FEYERABEND, S., WERNET, D., STENZL, A., RAMMENSEE, H. G. & GOUTTEFANGEAS, C. 2009. Simultaneous infiltration of polyfunctional effector and suppressor T cells into renal cell carcinomas. *Cancer Res,* 69**,** 8412-9.

AUBRY, F., SATIE, A. P., RIOUX-LECLERCQ, N., RAJPERT-DE MEYTS, E., SPAGNOLI, G. C., CHOMEZ, P., DE BACKER, O., JEGOU, B. & SAMSON, M. 2001. MAGE-A4, a germ cell specific marker, is expressed differentially in testicular tumors. *Cancer,* 92**,** 2778-85.

AVRIL, T., SAIKALI, S., VAULEON, E., JARY, A., HAMLAT, A., DE TAYRAC, M., MOSSER, J. & QUILLIEN, V. 2010. Distinct effects of human glioblastoma immunoregulatory molecules programmed cell death ligand-1 (PDL-1) and indoleamine 2,3-dioxygenase (IDO) on tumour-specific T cell functions. *Journal of Neuroimmunology,* 225**,** 22-33.

BADOVINAC, V. P., PORTER, B. B. & HARTY, J. T. 2002. Programmed contraction of CD8(+) T cells after infection. *Nat Immunol,* 3**,** 619-26.

BAI, X. F., LIU, J. Q., LI, O., ZHENG, P. & LIU, Y. 2003. Antigenic drift as a mechanism for tumor evasion of destruction by cytolytic T lymphocytes. *Journal of Clinical Investigation,* 111**,** 1487-1496.

BALZER, B. L. & ULBRIGHT, T. M. 2006. Spontaneous regression of testicular germ cell tumors: an analysis of 42 cases. *Am J Surg Pathol,* 30**,** 858-65.

BARBER, D. L., WHERRY, E. J. & AHMED, R. 2003. Cutting edge: rapid in vivo killing by memory CD8 T cells. *J Immunol,* 171**,** 27-31.

BARBER, D. L., WHERRY, E. J., MASOPUST, D., ZHU, B., ALLISON, J. P., SHARPE, A. H., FREEMAN, G. J. & AHMED, R. 2006. Restoring function in exhausted CD8 T cells during chronic viral infection. *Nature,* 439**,** 682-7.

BARKER, R. N., ERWIG, L. P., HILL, K. S., DEVINE, A., PEARCE, W. P. & REES, A. J. 2002. Antigen presentation by macrophages is enhanced by the uptake of necrotic, but not apoptotic, cells. *Clin Exp Immunol,* 127**,** 220-5.

BART, J., GROEN, H. J. M., VAN DER GRAAF, W. T. A., HOLLEMA, H., HENDRIKSE, N. H., VAALBURG, W., SLEIJFER, D. T. & DE VRIES, E. G. E. 2002. An oncological view on the blood-testis barrier. *The Lancet Oncology,* 3**,** 357-363.

BAUER, S., GROH, V., WU, J., STEINLE, A., PHILLIPS, J. H., LANIER, L. L. & SPIES, T. 1999. Activation of NK cells and T cells by NKG2D, a receptor for stress-inducible MICA. *Science,* 285**,** 727-9.

BELLGRAU, D., GOLD, D., SELAWRY, H., MOORE, J., FRANZUSOFF, A. & DUKE, R. C. 1995. A role for CD95 ligand in preventing graft rejection. *Nature,* 377**,** 630-2.

BENITEZ, R., GODELAINE, D., LOPEZ-NEVOT, M. A., BRASSEUR, F., JIMENEZ, P., MARCHAND, M., OLIVA, M. R., VAN BAREN, N., CABRERA, T., ANDRY, G., LANDRY, C., RUIZ-CABELLO, F., BOON, T. & GARRIDO, F. 1998. Mutations of the beta(2)-microglobulin gene result in a lack of HLA class I molecules on melanoma cells of two patients immunized with MAGE peptides. *Tissue Antigens,* 52**,** 520-529.

BENNETT, F., LUXENBERG, D., LING, V., WANG, I. M., MARQUETTE, K., LOWE, D., KHAN, N., VELDMAN, G., JACOBS, K. A., VALGE-ARCHER, V. E., COLLINS, M. & CARRENO, B. M. 2003. Program death-1 engagement upon TCR activation has distinct effects on costimulation and cytokine-driven proliferation: attenuation of ICOS, IL-4, and IL-21, but not CD28, IL-7, and IL-15 responses. *J Immunol,* 170**,** 711-8.

BETTS, M. R., BRENCHLEY, J. M., PRICE, D. A., DE ROSA, S. C., DOUEK, D. C., ROEDERER, M. & KOUP, R. A. 2003. Sensitive and viable identification of antigen-specific CD8+ T cells by a flow cytometric assay for degranulation. *J Immunol Methods,* 281**,** 65-78.

BEVAN, M. J. 1976. Minor H antigens introduced on H-2 different stimulating cells cross-react at the cytotoxic T cell level during in vivo priming. *J Immunol,* 117**,** 2233-8.

BEVAN, M. J. 2004. Helping the CD8(+) T-cell response. *Nat Rev Immunol,* 4**,** 595-602.

BEVAN, M. J. 2006. Cross-priming. *Nat Immunol,* 7**,** 363-5.

BEVERLY, B., KANG, S. M., LENARDO, M. J. & SCHWARTZ, R. H. 1992. Reversal of in vitro T cell clonal anergy by IL-2 stimulation. *Int Immunol,* 4**,** 661-71.

BIRKELAND, S. A., STORM, H. H., LAMM, L. U., BARLOW, L., BLOHME, I., FORSBERG, B., EKLUND, B., FJELDBORG, O., FRIEDBERG, M., FRODIN, L., GLATTRE, E., HALVORSEN, S., HOLM, N. V., JAKOBSEN, A., JORGENSEN, H. E., LADEFOGED, J., LINDHOLM, T., LUNDGREN, G. & PUKKALA, E. 1995. Cancer Risk after Renal-Transplantation in the Nordic Countries, 1964-1986. *International Journal of Cancer,* 60**,** 183-189.

BLACKBURN, S. D., SHIN, H., FREEMAN, G. J. & WHERRY, E. J. 2008. Selective expansion of a subset of exhausted CD8 T cells by alphaPD-L1 blockade. *Proc Natl Acad Sci U S A,* 105**,** 15016-21.

BLADERGROEN, B. A., STRIK, M. C., BOVENSCHEN, N., VAN BERKUM, O., SCHEFFER, G. L., MEIJER, C. J., HACK, C. E. & KUMMER, J. A. 2001. The granzyme B inhibitor, protease inhibitor 9, is mainly expressed by dendritic cells and at immune-privileged sites. *J Immunol,* 166**,** 3218-25.

BLANK, C., KUBALL, J., VOELKL, S., WIENDL, H., BECKER, B., WALTER, B., MAJDIC, O., GAJEWSKI, T. F., THEOBALD, M., ANDREESEN, R. & MACKENSEN, A. 2006. Blockade of PD-L1 (B7-H1) augments human tumor-specific T cell responses in vitro. *Int J Cancer,* 119**,** 317-27.

BOLS, B., JENSEN, L., JENSEN, A. & BRAENDSTRUP, O. 2000. Immunopathology of in situ seminoma. *Int J Exp Pathol,* 81**,** 211-7.

BOON T, O. L. 1997. Cancer Tumor antigens. *Curr Opin Immunol***,** 681-3.

BOON, T. & OLD, L. J. 1997. Cancer Tumor antigens. *Curr Opin Immunol,* 9**,** 681-3.

BOON, T. & VAN DER BRUGGEN, P. 1996. Human tumor antigens recognized by T lymphocytes. *J Exp Med,* 183**,** 725-9.

BOUVIER, M. 2003. Accessory proteins and the assembly of human class I MHC molecules: a molecular and structural perspective. *Mol Immunol,* 39**,** 697-706.

BRACK, C., HIRAMA, M., LENHARD-SCHULLER, R. & TONEGAWA, S. 1978. A complete immunoglobulin gene is created by somatic recombination. *Cell,* 15**,** 1-14.

BROWN, D. M. 2010. Cytolytic CD4 cells: Direct mediators in infectious disease and malignancy. *Cellular Immunology,* 262**,** 89-95.

BUBENIK, J. 2004. MHC class I down-regulation: Tumour escape from immune surveillance? (Review). *International Journal of Oncology,* 25**,** 487-491.

BUNCE, M., O'NEILL, C. M., BARNARDO, M. C., KRAUSA, P., BROWNING, M. J., MORRIS, P. J. & WELSH, K. I. 1995. Phototyping: comprehensive DNA typing for HLA-A, B, C, DRB1, DRB3, DRB4, DRB5 & DQB1 by PCR with 144 primer mixes utilizing sequence-specific primers (PCR-SSP). *Tissue Antigens,* 46**,** 355-67.

BURROWS, S. R., SUHRBIER, A., KHANNA, R. & MOSS, D. J. 1992. Rapid visual assay of cytotoxic T-cell specificity utilizing synthetic peptide induced T-cell-T-cell killing. *Immunology,* 76**,** 174-5.

BUTLER, L. M., HEWETT, P. J., BUTLER, W. J. & COWLED, P. A. 1998. Down regulation of Fas gene expression in colon cancer is not a result of allelic loss or gene rearrangement. *British Journal of Cancer,* 77**,** 1454-1459.

CABALLERO, O. L. & CHEN, Y. T. 2009a. Cancer/testis (CT) antigens: potential targets for immunotherapy. *Cancer Sci,* 100**,** 2014-21.

CABALLERO, O. L. & CHEN, Y. T. 2009b. Cancer/testis (CT) antigens: potential targets for immunotherapy. *Cancer Science,* 100**,** 2014-21.

CALLAN, M. F., FAZOU, C., YANG, H., ROSTRON, T., POON, K., HATTON, C. & MCMICHAEL, A. J. 2000. CD8(+) T-cell selection, function, and death in the primary immune response in vivo. *J Clin Invest,* 106**,** 1251-61.

CAMPBELL, J. J., QIN, S., UNUTMAZ, D., SOLER, D., MURPHY, K. E., HODGE, M. R., WU, L. & BUTCHER, E. C. 2001. Unique subpopulations of CD56+ NK and NK-T peripheral blood lymphocytes identified by chemokine receptor expression repertoire. *J Immunol,* 166**,** 6477-82.

CANADAY, D. H., PARKER, K. E., AUNG, H., CHEN, H. E., NUNEZ-MEDINA, D. & BURANT, C. J. 2013. Age-dependent changes in the expression of regulatory cell surface ligands in activated human T-cells. *BMC Immunol,* 14**,** 45.

CASPI, R. R. 2006. Ocular autoimmunity: the price of privilege? *Immunol Rev,* 213**,** 23-35.

CEBRIAN, M., YAGUE, E., RINCON, M., LOPEZBOTET, M., DELANDAZURI, M. O. & SANCHEZMADRID, F. 1988. Triggering of T-Cell Proliferation through Aim, an Activation Inducer Molecule Expressed on Activated Human-Lymphocytes. *Journal of Experimental Medicine,* 168**,** 1621-1637.

CERBONI, C., ARDOLINO, M., SANTONI, A. & ZINGONI, A. 2009. Detuning CD8+ T lymphocytes by down-regulation of the activating receptor NKG2D: role of NKG2D ligands released by activated T cells. *Blood,* 113**,** 2955-64.

CHEMNITZ, J. M., PARRY, R. V., NICHOLS, K. E., JUNE, C. H. & RILEY, J. L. 2004. SHP-1 and SHP-2 associate with immunoreceptor tyrosine-based switch motif of programmed death 1 upon primary human T cell stimulation, but only receptor ligation prevents T cell activation. *J Immunol,* 173**,** 945-54.

CHEN, Y. T., CAO, D., CHIU, R. & LEE, P. 2013. Chromosome X-encoded Cancer/Testis antigens are less frequently expressed in non-seminomatous germ cell tumors than in seminomas. *Cancer Immun,* 13**,** 10.

CHEN, Y. T., CHIU, R., LEE, P., BENECK, D., JIN, B. & OLD, L. J. 2011. Chromosome X-encoded cancer/testis antigens show distinctive expression patterns in developing gonads and in testicular seminoma. *Hum Reprod,* 26**,** 3232-43.

CHENG, C. Y. & MRUK, D. D. 2002. Cell junction dynamics in the testis: Sertoli-germ cell interactions and male contraceptive development. *Physiol Rev,* 82**,** 825-74.

CHENG, X., DAI, H., WAN, N., MOORE, Y., VANKAYALAPATI, R. & DAI, Z. 2009. Interaction of programmed death-1 and programmed death-1 ligand-1 contributes to testicular immune privilege. *Transplantation,* 87**,** 1778-86.

CHEVILLE, J. C. & ROCHE, P. C. 1999. MAGE-1 and MAGE-3 tumor rejection antigens in human germ cell tumors. *Mod Pathol,* 12**,** 974-8.

CHIN, Y., JANSEENS, J., VANDEPITTE, J., VANDENBRANDE, J., OPDEBEEK, L. & RAUS, J. 1992. Phenotypic analysis of tumor-infiltrating lymphocytes from human breast cancer. *Anticancer Res,* 12**,** 1463-6.

CHO, S. S., BACON, C. M., SUDARSHAN, C., REES, R. C., FINBLOOM, D., PINE, R. & O'SHEA, J. J. 1996. Activation of STAT4 by IL-12 and IFN-alpha: evidence for the involvement of ligand-induced tyrosine and serine phosphorylation. *J Immunol,* 157**,** 4781-9.

CILENSEK, Z. M., YEHIELY, F., KULAR, R. K. & DEISS, L. P. 2002. A member of the GAGE family of tumor antigens is an anti-apoptotic gene that confers resistance to Fas/CD95/APO-1, Interferon-gamma, taxol and gamma-irradiation. *Cancer Biol Ther,* 1**,** 380-7.

CLARK, W. H., JR., ELDER, D. E., GUERRY, D. T., BRAITMAN, L. E., TROCK, B. J., SCHULTZ, D., SYNNESTVEDT, M. & HALPERN, A. C. 1989. Model predicting survival in stage I melanoma based on tumor progression. *J Natl Cancer Inst,* 81**,** 1893-904.

CLEMENTE, C. G., MIHM, M. C., JR., BUFALINO, R., ZURRIDA, S., COLLINI, P. & CASCINELLI, N. 1996. Prognostic value of tumor infiltrating lymphocytes in the vertical growth phase of primary cutaneous melanoma. *Cancer,* 77**,** 1303-10.

COCA, S., PEREZPIQUERAS, J., MARTINEZ, D., COLMENAREJO, A., SAEZ, M. A., VALLEJO, C., MARTOS, J. A. & MORENO, M. 1997. The prognostic significance of intratumoral natural killer cells in patients with colorectal carcinoma. *Cancer,* 79**,** 2320-2328.

COOPER, M. A. & CALIGIURI, M. A. 2004. Isolation and characterization of human natural killer cell subsets. *Curr Protoc Immunol,* Chapter 7**,** Unit 7 34.

COOPER, M. A., FEHNIGER, T. A. & CALIGIURI, M. A. 2001. The biology of human natural killer-cell subsets. *Trends Immunol,* 22**,** 633-40.

COSMI, L., DE PALMA, R., SANTARLASCI, V., MAGGI, L., CAPONE, M., FROSALI, F., RODOLICO, G., QUERCI, V., ABBATE, G., ANGELI, R., BERRINO, L., FAMBRINI, M., CAPRONI, M., TONELLI, F., LAZZERI, E., PARRONCHI, P., LIOTTA, F., MAGGI, E., ROMAGNANI, S. & ANNUNZIATO, F. 2008. Human interleukin 17-producing cells originate from a CD161+CD4+ T cell precursor. *J Exp Med,* 205**,** 1903-16.

COULIE, P. G. 1997. Human tumour antigens recognized by T cells: new perspectives for anti-cancer vaccines? *Molecular Medicine Today,* 3**,** 261-268.

COULIE, P. G., KARANIKAS, V., LURQUIN, C., COLAU, D., CONNEROTTE, T., HANAGIRI, T., VAN PEL, A., LUCAS, S., GODELAINE, D., LONCHAY, C., MARCHAND, M., VAN BAREN, N. & BOON, T. 2002. Cytolytic T-cell responses of cancer patients vaccinated with a MAGE antigen. *Immunol Rev,* 188**,** 33-42.

COUPLAND, C. A., CHILVERS, C. E., DAVEY, G., PIKE, M. C., OLIVER, R. T. & FORMAN, D. 1999. Risk factors for testicular germ cell tumours by histological tumour type. United Kingdom Testicular Cancer Study Group. *Br J Cancer,* 80**,** 1859-63.

CRANE, C. A., HAN, S. J., BARRY, J. J., AHN, B. J., LANIER, L. L. & PARSA, A. T. 2010. TGF-beta downregulates the activating receptor NKG2D on NK cells and CD8+ T cells in glioma patients. *Neuro Oncol,* 12**,** 7-13.

CRESSWELL, P., ACKERMAN, A. L., GIODINI, A., PEAPER, D. R. & WEARSCH, P. A. 2005. Mechanisms of MHC class I-restricted antigen processing and cross-presentation. *Immunol Rev,* 207**,** 145-57.

CURIEL, T. J., COUKOS, G., ZOU, L., ALVAREZ, X., CHENG, P., MOTTRAM, P., EVDEMON-HOGAN, M., CONEJO-GARCIA, J. R., ZHANG, L., BUROW, M., ZHU, Y., WEI, S., KRYCZEK, I., DANIEL, B., GORDON, A., MYERS, L., LACKNER, A., DISIS, M. L., KNUTSON, K. L., CHEN, L. & ZOU, W. 2004. Specific recruitment of regulatory T cells in ovarian carcinoma fosters immune privilege and predicts reduced survival. *Nat Med,* 10**,** 942-9.

DAL SECCO, V., RICCIOLI, A., PADULA, F., ZIPARO, E. & FILIPPINI, A. 2008. Mouse Sertoli cells display phenotypical and functional traits of antigen-presenting cells in response to interferon gamma. *Biol Reprod,* 78**,** 234-42.

DALBETH, N., GUNDLE, R., DAVIES, R. J., LEE, Y. C., MCMICHAEL, A. J. & CALLAN, M. F. 2004. CD56bright NK cells are enriched at inflammatory sites and can engage with monocytes in a reciprocal program of activation. *J Immunol,* 173**,** 6418-26.

DAVIS, M. M. 1990. T cell receptor gene diversity and selection. *Annu Rev Biochem,* 59**,** 475-96.

DE SMET C, D. B. O., FARAONI I, LURQUIN C, BRASSEUR F, BOON T 1996. The activation of human gene MAGE-1 in tumor cells is corre-lated with genome-wide demethylation. *Proc Natl Acad Sci,* 93**,** 7149-53.

DELVES, P. J. & ROITT, I. M. 2000. The immune system. Second of two parts. *N Engl J Med,* 343**,** 108-17.

DEMARIA, R., CIFONE, M. G., TROTTA, R., RIPPO, M. R., FESTUCCIA, C., SANTONI, A. & TESTI, R. 1994. Triggering of Human Monocyte Activation through Cd69, a Member of the Natural-Killer-Cell Gene-Complex Family of Signal-Transducing Receptors. *Journal of Experimental Medicine,* 180**,** 1999-2004.

DENGJEL, J., SCHOOR, O., FISCHER, R., REICH, M., KRAUS, M., MULLER, M., KREYMBORG, K., ALTENBEREND, F., BRANDENBURG, J., KALBACHER, H., BROCK, R., DRIESSEN, C., RAMMENSEE, H. G. & STEVANOVIC, S. 2005. Autophagy promotes MHC class II presentation of peptides from intracellular source proteins. *Proc Natl Acad Sci U S A,* 102**,** 7922-7.

DERBINSKI, J., SCHULTE, A., KYEWSKI, B. & KLEIN, L. 2001. Promiscuous gene expression in medullary thymic epithelial cells mirrors the peripheral self. *Nat Immunol,* 2**,** 1032-9.

DHODAPKAR, M. V., STEINMAN, R. M., KRASOVSKY, J., MUNZ, C. & BHARDWAJ, N. 2001. Antigen-specific inhibition of effector T cell function in humans after injection of immature dendritic cells. *J Exp Med,* 193**,** 233-8.

DIEFENBACH, A. & RAULET, D. H. 2002. The innate immune response to tumors and its role in the induction of T-cell immunity. *Immunol Rev,* 188**,** 9-21.

DITZIAN-KADANOFF, R. 1999. Testicular-associated immune deviation and prevention of adjuvant-induced arthritis by three tolerization methods. *Scandinavian Journal of Immunology,* 50**,** 150-158.

DRANOFF, G. 2005. The therapeutic implications of intratumoral regulatory T cells. *Clin Cancer Res,* 11**,** 8226-9.

DRANOFF, G. 2009. Targets of protective tumor immunity. *Ann N Y Acad Sci,* 1174**,** 74-80.

DUNN, G. P., BRUCE, A. T., IKEDA, H., OLD, L. J. & SCHREIBER, R. D. 2002. Cancer immunoediting: from immunosurveillance to tumor escape. *Nat Immunol,* 3**,** 991-8.

DUNN, G. P., OLD, L. J. & SCHREIBER, R. D. 2004a. The immunobiology of cancer immunosurveillance and immunoediting. *Immunity,* 21**,** 137-48.

DUNN, G. P., OLD, L. J. & SCHREIBER, R. D. 2004b. The three Es of cancer immunoediting. *Annu Rev Immunol,* 22**,** 329-60.

DYM, M. & ROMRELL, L. J. 1975. Intraepithelial lymphocytes in the male reproductive tract of rats and rhesus monkeys. *J Reprod Fertil,* 42**,** 1-7.

FALLARINO, F., LUCA, G., CALVITTI, M., MANCUSO, F., NASTRUZZI, C., FIORETTI, M. C., GROHMANN, U., BECCHETTI, E., BURGEVIN, A., KRATZER, R., VAN ENDERT, P., BOON, L., PUCCETTI, P. & CALAFIORE, R. 2009. Therapy of experimental type 1 diabetes by isolated Sertoli cell xenografts alone. *The Journal of experimental medicine,* 206**,** 2511-26.

FINK, C., WEIGEL, R., HEMBES, T., LAUKE-WETTWER, H., KLIESCH, S., BERGMANN, M. & BREHM, R. H. 2006. Altered expression of ZO-1 and ZO-2 in Sertoli cells and loss of blood-testis barrier integrity in testicular carcinoma in situ. *Neoplasia,* 8**,** 1019-27.

FISZER D, K. M. 1998. Major histocompatibility complex expression on human, male germ cells: a review. *Am J Reprod Immunol,* 40**,** 172-76.

FISZER, D., ULBRECHT, M., FERNANDEZ, N., JOHNSON, J. P., WEISS, E. H. & KURPISZ, M. 1997. Analysis of HLA class Ib gene expression in male gametogenic cells. *European Journal of Immunology,* 27**,** 1691-5.

FIZAZI, K., CULINE, S., KRAMAR, A., AMATO, R. J., BOUZY, J., CHEN, I., DROZ, J. P. & LOGOTHETIS, C. J. 2004. Early predicted time to normalization of tumor markers predicts outcome in poor-prognosis nonseminomatous germ cell tumors. *Journal of Clinical Oncology,* 22**,** 3868-3876.

FLAVELL, R. A., SANJABI, S., WRZESINSKI, S. H. & LICONA-LIMON, P. 2010. The polarization of immune cells in the tumour environment by TGF beta. *Nature Reviews Immunology,* 10**,** 554-567.

FLECKEN, T., SCHMIDT, N., HILD, S., GOSTICK, E., DROGNITZ, O., ZEISER, R., SCHEMMER, P., BRUNS, H., EIERMANN, T., PRICE, D. A., BLUM, H. E., NEUMANN-HAEFELIN, C. & THIMME, R. 2013. Immunodominance and functional alterations of tumor-associated antigen-specific CD8 T-cell responses in hepatocellular carcinoma. *Hepatology*.

FOSSA, A., BERNER, A., FOSSA, S. D., HERNES, E., GAUDERNACK, G. & SMELAND, E. B. 2004. NY-ESO-1 protein expression and humoral immune responses in prostate cancer. *Prostate,* 59**,** 440-7.

FOURCADE, J., KUDELA, P., SUN, Z., SHEN, H., LAND, S. R., LENZNER, D., GUILLAUME, P., LUESCHER, I. F., SANDER, C., FERRONE, S., KIRKWOOD, J. M. & ZAROUR, H. M. 2009. PD-1 is a regulator of NY-ESO-1-specific CD8+ T cell expansion in melanoma patients. *J Immunol,* 182**,** 5240-9.

FOURCADE, J., SUN, Z., BENALLAOUA, M., GUILLAUME, P., LUESCHER, I. F., SANDER, C., KIRKWOOD, J. M., KUCHROO, V. & ZAROUR, H. M. 2010. Upregulation of Tim-3 and PD-1 expression is associated with tumor antigen-specific CD8+ T cell dysfunction in melanoma patients. *J Exp Med,* 207**,** 2175-86.

FREEMAN, G. J., LONG, A. J., IWAI, Y., BOURQUE, K., CHERNOVA, T., NISHIMURA, H., FITZ, L. J., MALENKOVICH, N., OKAZAKI, T., BYRNE, M. C., HORTON, H. F., FOUSER, L., CARTER, L., LING, V., BOWMAN, M. R., CARRENO, B. M., COLLINS, M., WOOD, C. R. & HONJO, T. 2000. Engagement of the PD-1 immunoinhibitory receptor by a novel B7 family member leads to negative regulation of lymphocyte activation. *J Exp Med,* 192**,** 1027-34.

FRIESE, M. A., WISCHHUSEN, J., WICK, W., WEILER, M., EISELE, G., STEINLE, A. & WELLER, M. 2004. RNA interference targeting transforming growth factor-beta enhances NKG2D-mediated antiglioma immune response, inhibits glioma cell migration and invasiveness, and abrogates tumorigenicity in vivo. *Cancer Res,* 64**,** 7596-603.

FRUMENTO, G., ROTONDO, R., TONETTI, M., DAMONTE, G., BENATTI, U. & FERRARA, G. B. 2002. Tryptophan-derived catabolites are responsible for inhibition of T and natural killer cell proliferation induced by indoleamine 2,3-dioxygenase. *J Exp Med,* 196**,** 459-68.

FRUNGIERI, M. B., CALANDRA, R. S., LUSTIG, L., MEINEKE, V., KOHN, F. M., VOGT, H. J. & MAYERHOFER, A. 2002. Number, distribution pattern, and identification of macrophages in the testes of infertile men. *Fertil Steril,* 78**,** 298-306.

GAJEWSKI, T. F., MENG, Y., BLANK, C., BROWN, I., KACHA, A., KLINE, J. & HARLIN, H. 2006. Immune resistance orchestrated by the tumor microenvironment. *Immunol Rev,* 213**,** 131-45.

GALLUCCI, S. & MATZINGER, P. 2001. Danger signals: SOS to the immune system. *Current Opinion in Immunology,* 13**,** 114-119.

GARNER, M. J., BIRKETT, N. J., JOHNSON, K. C., SHATENSTEIN, B., GHADIRIAN, P. & KREWSKI, D. 2003. Dietary risk factors for testicular carcinoma. *Int J Cancer,* 106**,** 934-41.

GASSER, S., ORSULIC, S., BROWN, E. J. & RAULET, D. H. 2005. The DNA damage pathway regulates innate immune system ligands of the NKG2D receptor. *Nature,* 436**,** 1186-90.

GERMAIN, R. N. 2002. T-cell development and the CD4-CD8 lineage decision. *Nat Rev Immunol,* 2**,** 309-22.

GHEBEH, H., MOHAMMED, S., AL-OMAIR, A., QATTAN, A., LEHE, C., AL-QUDAIHI, G., ELKUM, N., ALSHABANAH, M., BIN AMER, S., TULBAH, A., AJARIM, D., AL-TWEIGERI, T. & DERMIME, S. 2006. The B7-H1 (PD-L1) T lymphocyte-inhibitory molecule is expressed in breast cancer patients with infiltrating ductal carcinoma: correlation with important high-risk prognostic factors. *Neoplasia,* 8**,** 190-8.

GHIRINGHELLI, F., APETOH, L., TESNIERE, A., AYMERIC, L., MA, Y. T., ORTIZ, C., VERMAELEN, K., PANARETAKIS, T., MIGNOT, G., ULLRICH, E., PERFETTINI, J. L.,

SCHLEMMER, F., TASDEMIR, E., UHL, M., GENIN, P., CIVAS, A., RYFFEL, B., KANELLOPOULOS, J., TSCHOPP, J., ANDRE, F., LIDEREAU, R., MCLAUGHLIN, N. M., HAYNES, N. M., SMYTH, M. J., KROEMER, G. & ZITVOGEL, L. 2009. Activation of the NLRP3 inflammasome in dendritic cells induces IL-1 beta-dependent adaptive immunity against tumors. *Nature Medicine,* 15**,** 1170-U99.

GJERSTORFF MF, J. L., NIELSEN O, KOCK K, DITZEL HJ 2006. Restriction of GAGE protein expression to subpopulations of cancer cells is independent of genotype and may limit the use of GAGE proteins as targets for cancer immunotherapy. *Br J Cancer,* 94**,** 1864-73.

GLOBOCAN 2002. Cancer Incidence, Mortality and Prevalence Worldwide 2002 estimates.

GLYNN, S. A., GAMMELL, P., HEENAN, M., O'CONNOR, R., LIANG, Y., KEENAN, J. & CLYNES, M. 2004. A new superinvasive in vitro phenotype induced by selection of human breast carcinoma cells with the chemotherapeutic drugs paclitaxel and doxorubicin. *Br J Cancer,* 91**,** 1800-7.

GODELAINE, D., CARRASCO, J., LUCAS, S., KARANIKAS, V., SCHULER-THURNER, B., COULIE, P. G., SCHULER, G., BOON, T. & VAN PEL, A. 2003. Polyclonal CTL responses observed in melanoma patients vaccinated with dendritic cells pulsed with a MAGE-3.A1 peptide. *J Immunol,* 171**,** 4893-7.

GOH, A. M., COFFILL, C. R. & LANE, D. P. 2010. The role of mutant p53 in human cancer. *The Journal of pathology*.

GONZALEZ-GALARZA, F. F., CHRISTMAS, S., MIDDLETON, D. & JONES, A. R. 2011. Allele frequency net: a database and online repository for immune gene frequencies in worldwide populations. *Nucleic Acids Res,* 39**,** D913-9.

GOODYEAR, O., PIPER, K., KHAN, N., STARCZYNSKI, J., MAHENDRA, P., PRATT, G. & MOSS, P. 2005. CD8+ T cells specific for cancer germline gene antigens are found in many patients with multiple myeloma, and their frequency correlates with disease burden. *Blood,* 106**,** 4217-24.

GOURLEY, T. S., WHERRY, E. J., MASOPUST, D. & AHMED, R. 2004. Generation and maintenance of immunological memory. *Semin Immunol,* 16**,** 323-33.

GROBHOLZ, R., VERBEKE, C. S., SCHLEGER, C., KOHRMANN, K. U., HEIN, B., WOLF, G., BLEYL, U., SPAGNOLI, G. C., COPLAN, K., KOLB, D., IVERSEN, K. & JUNGBLUTH, A. A. 2000. Expression of MAGE antigens and analysis of the inflammatory T-cell infiltrate in human seminoma. *Urol Res,* 28**,** 398-403.

GROH, V., WU, J., YEE, C. & SPIES, T. 2002. Tumour-derived soluble MIC ligands impair expression of NKG2D and T-cell activation. *Nature,* 419**,** 734-8.

GROMME, M., UYTDEHAAG, F. G., JANSSEN, H., CALAFAT, J., VAN BINNENDIJK, R. S., KENTER, M. J., TULP, A., VERWOERD, D. & NEEFJES, J. 1999. Recycling MHC class I molecules and endosomal peptide loading. *Proc Natl Acad Sci U S A,* 96**,** 10326-31.

GROUP, T. C. S. 1994a. Aetiology of testicular cancer: association with congenital abnormalities, age at puberty, infertility, and exercise. *BMJ,* 308**,** 1393-9.

GROUP, U. T. C. S. 1994b. Social, behavioural and medical factors in the aetiology of testicular cancer: results from the UK study. *Br J Cancer,* 70**,** 513-20.

GUERMONPREZ, P., SAVEANU, L., KLEIJMEER, M., DAVOUST, J., VAN ENDERT, P. & AMIGORENA, S. 2003. ER-phagosome fusion defines an MHC class I cross-presentation compartment in dendritic cells. *Nature,* 425**,** 397-402.

GUERRA, N., TAN, Y. X., JONCKER, N. T., CHOY, A., GALLARDO, F., XIONG, N., KNOBLAUGH, S., CADO, D., GREENBERG, N. R. & RAULET, D. H. 2008. NKG2D-deficient mice are defective in tumor surveillance in models of spontaneous malignancy. *Immunity,* 28**,** 571-580.

HADRUP, S. R., BRAENDSTRUP, O., JACOBSEN, G. K., MORTENSEN, S., PEDERSEN, L. O., SEREMET, T., ANDERSEN, M. H., BECKER, J. C. & STRATEN, P. T. 2006. Tumor

infiltrating lymphocytes in seminoma lesions comprise clonally expanded cytotoxic T cells. *Int J Cancer,* 119**,** 831-8.
HAHNE, M., RIMOLDI, D., SCHROTER, M., ROMERO, P., SCHREIER, M., FRENCH, L. E., SCHNEIDER, P., BORNAND, T., FONTANA, A., LIENARD, D., CEROTTINI, J. & TSCHOPP, J. 1996. Melanoma cell expression of Fas(Apo-1/CD95) ligand: implications for tumor immune escape. *Science,* 274**,** 1363-6.
HAMERMAN, J. A., OGASAWARA, K. & LANIER, L. L. 2005. NK cells in innate immunity. *Curr Opin Immunol,* 17**,** 29-35.
HAN, Y. M., GUO, Q. L., ZHANG, M. G., CHEN, Z. B. & CAO, X. T. 2009. CD69(+)CD4(+)CD25(-) T Cells, a New Subset of Regulatory T Cells, Suppress T Cell Proliferation through Membrane-Bound TGF-beta 1. *Journal of Immunology,* 182**,** 111-120.
HARA, I., HARA, S., MIYAKE, H., YAMANAKA, K., NAGAI, H., GOHJI, K., ARAKAWA, S. & KAMIDONO, S. 1999. Expression of MAGE genes in testicular germ cell tumors. *Urology,* 53**,** 843-7.
HARA, T., JUNG, L. K., BJORNDAHL, J. M. & FU, S. M. 1986. Human T cell activation. III. Rapid induction of a phosphorylated 28 kD/32 kD disulfide-linked early activation antigen (EA 1) by 12-o-tetradecanoyl phorbol-13-acetate, mitogens, and antigens. *J Exp Med,* 164**,** 1988-2005.
HARGADON, K. M., BRINKMAN, C. C., SHEASLEY-O'NEILL S, L., NICHOLS, L. A., BULLOCK, T. N. & ENGELHARD, V. H. 2006. Incomplete differentiation of antigen-specific CD8 T cells in tumor-draining lymph nodes. *J Immunol,* 177**,** 6081-90.
HARRINGTON, L. E., HATTON, R. D., MANGAN, P. R., TURNER, H., MURPHY, T. L., MURPHY, K. M. & WEAVER, C. T. 2005. Interleukin 17-producing CD4+ effector T cells develop via a lineage distinct from the T helper type 1 and 2 lineages. *Nat Immunol,* 6**,** 1123-32.
HASTINGS, W. D., ANDERSON, D. E., KASSAM, N., KOGUCHI, K., GREENFIELD, E. A., KENT, S. C., ZHENG, X. X., STROM, T. B., HAFLER, D. A. & KUCHROO, V. K. 2009. TIM-3 is expressed on activated human CD4+ T cells and regulates Th1 and Th17 cytokines. *Eur J Immunol,* 39**,** 2492-501.
HE, S., YIN, T., LI, D., GAO, X., WAN, Y., MA, X., YE, T., GUO, F., SUN, J., LIN, Z. & WANG, Y. 2013. Enhanced interaction between natural killer cells and lung cancer cells: involvement in gefitinib-mediated immunoregulation. *J Transl Med,* 11**,** 186.
HEDGER, M. P. 1997. Testicular leukocytes: what are they doing? *Rev Reprod,* 2**,** 38-47.
HEDGER, M. P. 2002. Macrophages and the immune responsiveness of the testis. *J Reprod Immunol,* 57**,** 19-34.
HEDGER, M. P. 2011. Immunophysiology and pathology of inflammation in the testis and epididymis. *J Androl,* 32**,** 625-40.
HEIDENREICH, A., BOKEMEYER, C. & SOUCHON, R. 2009. [Stage-specific treatment for testicular germ cell tumours]. *Urologe A,* 48**,** 377-85.
HILDEMANN, S. K., EBERLEIN, J., DAVENPORT, B., NGUYEN, T. T., VICTORINO, F. & HOMANN, D. 2013. High efficiency of antiviral CD4(+) killer T cells. *PLoS One,* 8**,** e60420.
HOFFMANN, J. A., KAFATOS, F. C., JANEWAY, C. A. & EZEKOWITZ, R. A. 1999. Phylogenetic perspectives in innate immunity. *Science,* 284**,** 1313-8.
HORTON, R., WILMING, L., RAND, V., LOVERING, R. C., BRUFORD, E. A., KHODIYAR, V. K., LUSH, M. J., POVEY, S., TALBOT, C. C., JR., WRIGHT, M. W., WAIN, H. M., TROWSDALE, J., ZIEGLER, A. & BECK, S. 2004. Gene map of the extended human MHC. *Nat Rev Genet,* 5**,** 889-99.
IMMUNOPAEDIA.ORG. 2010. *Blood-Testis Barrier* [Online]. Available: http://www.immunopaedia.org.za/fileadmin/new_all/case_studies/pdfs/immune_privilege_testis_27MAY10.pdf.
INABA, K., METLAY, J. P., CROWLEY, M. T., WITMER-PACK, M. & STEINMAN, R. M. 1990. Dendritic cells as antigen presenting cells in vivo. *Int Rev Immunol,* 6**,** 197-206.

IOANNIDES, C. G., FISK, B., FAN, D., BIDDISON, W. E., WHARTON, J. T. & OBRIAN, C. A. 1993. Cytotoxic T-Cells Isolated from Ovarian Malignant Ascites Recognize a Peptide Derived from the Her-2/Neu Protooncogene. *Cellular Immunology,* 151**,** 225-234.

ISHIGAMI, S., NATSUGOE, S., TOKUDA, K., NAKAJO, A., CHE, X. M., IWASHIGE, H., ARIDOME, K., HOKITA, S. & AIKOU, T. 2000. Prognostic value of intratumoral natural killer cells in gastric carcinoma. *Cancer,* 88**,** 577-583.

ITANO, A. A. & JENKINS, M. K. 2003. Antigen presentation to naive CD4 T cells in the lymph node. *Nat Immunol,* 4**,** 733-9.

JAGER, E., KARBACH, J., GNJATIC, S., NEUMANN, A., BENDER, A., VALMORI, D., AYYOUB, M., RITTER, E., RITTER, G., JAGER, D., PANICALI, D., HOFFMAN, E., PAN, L., OETTGEN, H., OLD, L. J. & KNUTH, A. 2006. Recombinant vaccinia/fowlpox NY-ESO-1 vaccines induce both humoral and cellular NY-ESO-1-specific immune responses in cancer patients. *Proc Natl Acad Sci U S A,* 103**,** 14453-8.

JIN, H. T., ANDERSON, A. C., TAN, W. G., WEST, E. E., HA, S. J., ARAKI, K., FREEMAN, G. J., KUCHROO, V. K. & AHMED, R. 2010. Cooperation of Tim-3 and PD-1 in CD8 T-cell exhaustion during chronic viral infection. *Proc Natl Acad Sci U S A,* 107**,** 14733-8.

JONES, R. B., NDHLOVU, L. C., BARBOUR, J. D., SHETH, P. M., JHA, A. R., LONG, B. R., WONG, J. C., SATKUNARAJAH, M., SCHWENEKER, M., CHAPMAN, J. M., GYENES, G., VALI, B., HYRCZA, M. D., YUE, F. Y., KOVACS, C., SASSI, A., LOUTFY, M., HALPENNY, R., PERSAD, D., SPOTTS, G., HECHT, F. M., CHUN, T. W., MCCUNE, J. M., KAUL, R., RINI, J. M., NIXON, D. F. & OSTROWSKI, M. A. 2008. Tim-3 expression defines a novel population of dysfunctional T cells with highly elevated frequencies in progressive HIV-1 infection. *J Exp Med,* 205**,** 2763-79.

JU, S. T., PANKA, D. J., CUI, H., ETTINGER, R., EL-KHATIB, M., SHERR, D. H., STANGER, B. Z. & MARSHAK-ROTHSTEIN, A. 1995. Fas(CD95)/FasL interactions required for programmed cell death after T-cell activation. *Nature,* 373**,** 444-8.

JUNGBLUTH AA, B. K., KOLB D, IVERSEN K, COPLAN K, CHEN YT, SPAGNOLI GC, OLD LJ 2000. Expression of MAGE-antigens in normal tissues and cancer. *Int J Cancer,* 85**,** 460-5.

JUNGBLUTH AA, C. Y., BUSAM KJ, COPLAN K, KOLB D, IVERSEN K, WILLIAMSON B, VAN LANDEGHEM FK, STOCKERT E, OLD LJ 2002. CT7 (MAGE-C1) antigen expression in normal and neoplastic tissues. *Int J Cancer,* 99**,** 839-45.

JUNGBLUTH AA, C. Y., STOCKERT E, BUSAM KJ, KOLB D, IVERSEN K, COPLAN K, WILLIAMSON B, ALTORKI N, OLD LJ 2001. Immunohistochemical analysis of NY-ESO-1 antigen expression in normal and malignant human tissues. *Int J Cancer,* 92**,** 856-60.

JUNGBLUTH, A. A., STOCKERT, E., CHEN, Y. T., KOLB, D., IVERSEN, K., COPLAN, K., WILLIAMSON, B., ALTORKI, N., BUSAM, K. J. & OLD, L. J. 2000. Monoclonal antibody MA454 reveals a heterogeneous expression pattern of MAGE-1 antigen in formalin-fixed paraffin embedded lung tumours. *Br J Cancer,* 83**,** 493-497.

KAECH, S. M., HEMBY, S., KERSH, E. & AHMED, R. 2002a. Molecular and functional profiling of memory CD8 T cell differentiation. *Cell,* 111**,** 837-51.

KAECH, S. M., WHERRY, E. J. & AHMED, R. 2002b. Effector and memory T-cell differentiation: implications for vaccine development. *Nat Rev Immunol,* 2**,** 251-62.

KALINSKI, P., MAILLIARD, R. B., GIERMASZ, A., ZEH, H. J., BASSE, P., BARTLETT, D. L., KIRKWOOD, J. M., LOTZE, M. T. & HERBERMAN, R. B. 2005. Natural killer-dendritic cell cross-talk in cancer immunotherapy. *Expert Opin Biol Ther,* 5**,** 1303-15.

KARANIKAS, V., LURQUIN, C., COLAU, D., VAN BAREN, N., DE SMET, C., LETHE, B., CONNEROTTE, T., CORBIERE, V., DEMOITIE, M. A., LIENARD, D., DRENO, B., VELU, T., BOON, T. & COULIE, P. G. 2003. Monoclonal anti-MAGE-3 CTL responses in melanoma patients displaying tumor regression after vaccination with a recombinant canarypox virus. *J Immunol,* 171**,** 4898-904.

KATANO, M., NAKAMURA, M., MORISAKI, T. & FUJIMOTO, K. 1997. Melanoma antigen-encoding gene-1 expression in invasive gastric carcinoma: correlation with stage of disease. *J Surg Oncol,* 64**,** 195-201.

KAVALAR, R., SARCEVIC, B., SPAGNOLI, G. C., SEPAROVIC, V., SAMIJA, M., TERRACCIANO, L., HEBERER, M. & JURETIC, A. 2001. Expression of MAGE tumour-associated antigens is inversely correlated with tumour differentiation in invasive ductal breast cancers: an immunohistochemical study. *Virchows Arch,* 439**,** 127-31.

KAWAKAMI, Y. & ROSENBERG, S. A. 1997. Human tumor antigens recognized by T-cells. *Immunol Res,* 16**,** 313-39.

KAWAMURA, K., BAHAR, R., NATSUME, W., SAKIYAMA, S. & TAGAWA, M. 2002. Secretion of interleukin-10 from murine colon carcinoma cells suppresses systemic antitumor immunity and impairs protective immunity induced against the tumors. *Cancer Gene Ther,* 9**,** 109-15.

KEEFE, D., SHI, L., FESKE, S., MASSOL, R., NAVARRO, F., KIRCHHAUSEN, T. & LIEBERMAN, J. 2005. Perforin triggers a plasma membrane-repair response that facilitates CTL induction of apoptosis. *Immunity,* 23**,** 249-62.

KELLY-ROGERS, J., MADRIGAL-ESTEBAS, L., O'CONNOR, T. & DOHERTY, D. G. 2006. Activation-induced expression of CD56 by T cells is associated with a reprogramming of cytolytic activity and cytokine secretion profile in vitro. *Hum Immunol,* 67**,** 863-73.

KERN, S., ROBERTSON, S. A., MAU, V. J. & MADDOCKS, S. 1995. Cytokine secretion by macrophages in the rat testis. *Biol Reprod,* 53**,** 1407-16.

KHALED, Y. S., AMMORI, B. J. & ELKORD, E. 2013. Myeloid-derived suppressor cells in cancer: recent progress and prospects. *Immunol Cell Biol,* 91**,** 493-502.

KHAZAIE, K., BONERTZ, A. & BECKHOVE, P. 2009. Current developments with peptide-based human tumor vaccines. *Current Opinion in Oncology,* 21**,** 524-530 10.1097/CCO.0b013e328331a78e.

KLEBANOFF, C. A., GATTINONI, L. & RESTIFO, N. P. 2006. CD8+ T-cell memory in tumor immunology and immunotherapy. *Immunol Rev,* 211**,** 214-24.

KLEIN, L., HINTERBERGER, M., WIRNSBERGER, G. & KYEWSKI, B. 2009. Antigen presentation in the thymus for positive selection and central tolerance induction. *Nat Rev Immunol,* 9**,** 833-44.

KOSKIMIES, A. I., KORMANO, M. & LAHTI, A. 1971. A difference in the immunoglobulin content of seminiferous tubule fluid and rete testis fluid of the rat. *J Reprod Fertil,* 27**,** 463-5.

KOULIS, A., DISS, T., ISAACSON, P. G. & DOGAN, A. 1997. Characterization of tumor-infiltrating T lymphocytes in B-cell lymphomas of mucosa-associated lymphoid tissue. *Am J Pathol,* 151**,** 1353-60.

KOWALCZYK, D. W. 2002. Tumors and the danger model. *Acta Biochimica Polonica,* 49**,** 295-302.

KRANGEL, M. S. 2009. Mechanics of T cell receptor gene rearrangement. *Curr Opin Immunol,* 21**,** 133-9.

KREBS, P., BARNES, M. J., LAMPE, K., WHITLEY, K., BAHJAT, K. S., BEUTLER, B., JANSSEN, E. & HOEBE, K. 2009. NK-cell-mediated killing of target cells triggers robust antigen-specific T-cell-mediated and humoral responses. *Blood,* 113**,** 6593-602.

LADURON, S., DEPLUS, R., ZHOU, S., KHOLMANSKIKH, O., GODELAINE, D., DE SMET, C., HAYWARD, S. D., FUKS, F., BOON, T. & DE PLAEN, E. 2004. MAGE-A1 interacts with adaptor SKIP and the deacetylase HDAC1 to repress transcription. *Nucleic Acids Res,* 32**,** 4340-50.

LANZAVECCHIA, A. & SALLUSTO, F. 2005. Understanding the generation and function of memory T cell subsets. *Curr Opin Immunol,* 17**,** 326-32.

LATCHMAN, Y., WOOD, C. R., CHERNOVA, T., CHAUDHARY, D., BORDE, M., CHERNOVA, I., IWAI, Y., LONG, A. J., BROWN, J. A., NUNES, R., GREENFIELD, E. A., BOURQUE, K., BOUSSIOTIS, V. A., CARTER, L. L., CARRENO, B. M., MALENKOVICH, N.,

NISHIMURA, H., OKAZAKI, T., HONJO, T., SHARPE, A. H. & FREEMAN, G. J. 2001. PD-L2 is a second ligand for PD-1 and inhibits T cell activation. *Nat Immunol,* 2**,** 261-8.

LAU, L. L., JAMIESON, B. D., SOMASUNDARAM, T. & AHMED, R. 1994. Cytotoxic T-cell memory without antigen. *Nature,* 369**,** 648-52.

LEE, H. M., OH, B. C., LIM, D. P., LEE, D. S., CHO, J., LEE, G. & LEE, J. R. 2007. Role of complement regulatory proteins in the survival of murine allo-transplanted Sertoli cells. *J Korean Med Sci,* 22**,** 277-82.

LEHMANN, C., ZEIS, M., SCHMITZ, N. & UHAREK, L. 2000. Impaired binding of perforin on the surface of tumor cells is a cause of target cell resistance against cytotoxic effector cells. *Blood,* 96**,** 594-600.

LEIBOVITCH, I., BANIEL, J., ROWLAND, R. G., SMITH, E. R., JR., LUDLOW, J. K. & DONOHUE, J. P. 1996. Malignant testicular neoplasms in immunosuppressed patients. *J Urol,* 155**,** 1938-42.

LENDVAI, N., GNJATIC, S., RITTER, E., MANGONE, M., AUSTIN, W., REYNER, K., JAYABALAN, D., NIESVIZKY, R., JAGANNATH, S., BHARDWAJ, N., CHEN-KIANG, S., OLD, L. J. & CHO, H. J. 2010. Cellular immune responses against CT7 (MAGE-C1) and humoral responses against other cancer-testis antigens in multiple myeloma patients. *Cancer Immun,* 10**,** 4.

LEVIN, H. S. 2000. Tumors of the testis in intersex syndromes. *Urol Clin North Am,* 27**,** 543-51, x.

LI, B., HE, X., PANG, X., ZHANG, H., CHEN, J. & CHEN, W. 2004. Elicitation of both CD4 and CD8 T-cell-mediated specific immune responses to HCA587 protein by autologous dendritic cells. *Scand J Immunol,* 60**,** 506-13.

LI, H., WU, K., TAO, K., CHEN, L., ZHENG, Q., LU, X., LIU, J., SHI, L., LIU, C., WANG, G. & ZOU, W. 2012. Tim-3/galectin-9 signaling pathway mediates T-cell dysfunction and predicts poor prognosis in patients with hepatitis B virus-associated hepatocellular carcinoma. *Hepatology,* 56**,** 1342-51.

LI, M. W., MRUK, D. D., LEE, W. M. & CHENG, C. Y. 2009. Cytokines and junction restructuring events during spermatogenesis in the testis: an emerging concept of regulation. *Cytokine Growth Factor Rev,* 20**,** 329-38.

LI, Y., WANG, L. X., YANG, G., HAO, F., URBA, W. J. & HU, H. M. 2008. Efficient cross-presentation depends on autophagy in tumor cells. *Cancer Res,* 68**,** 6889-95.

LIEBERMAN, J. 2003. The ABCs of granule-mediated cytotoxicity: new weapons in the arsenal. *Nat Rev Immunol,* 3**,** 361-70.

LIU, W., CHENG, S., ASA, S. L. & EZZAT, S. 2008. The melanoma-associated antigen A3 mediates fibronectin-controlled cancer progression and metastasis. *Cancer Res,* 68**,** 8104-12.

LJUNGGREN, H. G. & KARRE, K. 1990. In search of the 'missing self': MHC molecules and NK cell recognition. *Immunol Today,* 11**,** 237-44.

LOETSCHER, M., GERBER, B., LOETSCHER, P., JONES, S. A., PIALI, L., CLARK-LEWIS, I., BAGGIOLINI, M. & MOSER, B. 1996. Chemokine receptor specific for IP10 and mig: structure, function, and expression in activated T-lymphocytes. *J Exp Med,* 184**,** 963-9.

LONDON, C. A., LODGE, M. P. & ABBAS, A. K. 2000. Functional responses and costimulator dependence of memory CD4+ T cells. *J Immunol,* 164**,** 265-72.

LUITEN, R. & VAN DER BRUGGEN, P. 2000. A MAGE-A1 peptide is recognized on HLA-B7 human tumors by cytolytic T lymphocytes. *Tissue Antigens,* 55**,** 149-52.

LURQUIN, C., DE SMET, C., BRASSEUR, F., MUSCATELLI, F., MARTELANGE, V., DE PLAEN, E., BRASSEUR, R., MONACO, A. P. & BOON, T. 1997. Two members of the human MAGEB gene family located in Xp21.3 are expressed in tumors of various histological origins. *Genomics,* 46**,** 397-408.

MACKAY, C. R. 1993. Homing of naive, memory and effector lymphocytes. *Curr Opin Immunol,* 5**,** 423-7.

MAEURER, M. J., MARTIN, D., WALTER, W., LIU, K., ZITVOGEL, L., HALUSCZCAK, K., RABINOWICH, H., DUQUESNOY, R., STORKUS, W. & LOTZE, M. T. 1996. Human intestinal Vdelta1+ lymphocytes recognize tumor cells of epithelial origin. *J Exp Med,* 183**,** 1681-96.

MALAVASI, F., DEAGLIO, S., FERRERO, E., FUNARO, A., SANCHO, J., AUSIELLO, C. M., ORTOLAN, E., VAISITTI, T., ZUBIAUR, M., FEDELE, G., AYDIN, S., TIBALDI, E. V., DURELLI, I., LUSSO, R., COZNO, F. & HORENSTEIN, A. L. 2006. CD38 and CD157 as receptors of the immune system: a bridge between innate and adaptive immunity. *Mol Med,* 12**,** 334-41.

MALLICK, C. A., DUDLEY, E. C., VINEY, J. L., OWEN, M. J. & HAYDAY, A. C. 1993. Rearrangement and diversity of T cell receptor beta chain genes in thymocytes: a critical role for the beta chain in development. *Cell,* 73**,** 513-9.

MANDRUZZATO, S., BRASSEUR, F., ANDRY, G., BOON, T. & VANDERBRUGGEN, P. 1997. A CASP-8 mutation recognized by cytolytic T lymphocytes on a human head and neck carcinoma. *Journal of Experimental Medicine,* 186**,** 785-793.

MARCHAND, M., VAN BAREN, N., WEYNANTS, P., BRICHARD, V., DRENO, B., TESSIER, M. H., RANKIN, E., PARMIANI, G., ARIENTI, F., HUMBLET, Y., BOURLOND, A., VANWIJCK, R., LIENARD, D., BEAUDUIN, M., DIETRICH, P. Y., RUSSO, V., KERGER, J., MASUCCI, G., JAGER, E., DE GREVE, J., ATZPODIEN, J., BRASSEUR, F., COULIE, P. G., VAN DER BRUGGEN, P. & BOON, T. 1999. Tumor regressions observed in patients with metastatic melanoma treated with an antigenic peptide encoded by gene MAGE-3 and presented by HLA-A1. *Int J Cancer,* 80**,** 219-30.

MARIE, M., NICOLAS VAN, B., PATRICK, W., VINCENT, B., BRIGITTE, D., MARIE-HÉLÈNE, T., ELAINE, R., GIORGIO, P., FLAVIO, A., YVES, H., ANDRÉ, B., ROMAIN, V., DANIELLE, L., MARC, B., PIERRE-YVES, D., VINCENZO, R., JOSEPH, K., GIUSEPPE, M., ELKE, J., JACQUES DE, G., JENS, A., FRANCIS, B., PIERRE, G. C., PIERRE VAN DER, B. & THIERRY, B. 1999. Tumor regressions observed in patients with metastatic melanoma treated with an antigenic peptide encoded by gene <I>MAGE-3</I> and presented by HLA-A1. *International Journal of Cancer,* 80**,** 219-230.

MARSMAN, M., JORDENS, I., GRIEKSPOOR, A. & NEEFJES, J. 2005. Chaperoning antigen presentation by MHC class II molecules and their role in oncogenesis. *Advances in Cancer Research, Vol 93,* 93**,** 129-158.

MASHINO, K., SADANAGA, N., TANAKA, F., YAMAGUCHI, H., NAGASHIMA, H., INOUE, H., SUGIMACHI, K. & MORI, M. 2001. Expression of multiple cancer-testis antigen genes in gastrointestinal and breast carcinomas. *Br J Cancer,* 85**,** 713-20.

MASSON, F., CALZASCIA, T., DI BERARDINO-BESSON, W., DE TRIBOLET, N., DIETRICH, P. Y. & WALKER, P. R. 2007. Brain microenvironment promotes the final functional maturation of tumor-specific effector CD8+ T cells. *J Immunol,* 179**,** 845-53.

MATTHEW, J. S., ALI, O. G., ACHIM, A. J., LLOYD, J. O. & YAO-TSENG, C. 2002. Cancer/testis antigens: an expanding family of targets for cancer immunotherapy. *Immunological Reviews,* 188**,** 22-32.

MATZINGER, P. 1994. Tolerance, Danger, and the Extended Family. *Annual Review of Immunology,* 12**,** 991-1045.

MCGLYNN, K. A., DEVESA, S. S., SIGURDSON, A. J., BROWN, L. M., TSAO, L. & TARONE, R. E. 2003. Trends in the incidence of testicular germ cell tumors in the United States. *Cancer,* 97**,** 63-70.

MEINHARDT, A. & HEDGER, M. P. 2011. Immunological, paracrine and endocrine aspects of testicular immune privilege. *Molecular and cellular endocrinology,* 335**,** 60-8.

MESSAL, N., SERRIARI, N. E., PASTOR, S., NUNES, J. A. & OLIVE, D. 2011. PD-L2 is expressed on activated human T cells and regulates their function. *Mol Immunol,* 48**,** 2214-9.

MITAL, P., HINTON, B. T. & DUFOUR, J. M. 2011. The Blood-Testis and Blood-Epididymis Barriers Are More Than Just Their Tight Junctions. *Biology of Reproduction*.

MIWA, K., ASANO, M., HORAI, R., IWAKURA, Y., NAGATA, S. & SUDA, T. 1998. Caspase 1-independent IL-1beta release and inflammation induced by the apoptosis inducer Fas ligand. *Nature Medicine,* 4**,** 1287-92.

MONNEY, L., SABATOS, C. A., GAGLIA, J. L., RYU, A., WALDNER, H., CHERNOVA, T., MANNING, S., GREENFIELD, E. A., COYLE, A. J., SOBEL, R. A., FREEMAN, G. J. & KUCHROO, V. K. 2002. Th1-specific cell surface protein Tim-3 regulates macrophage activation and severity of an autoimmune disease. *Nature,* 415**,** 536-41.

MONTE, M., SIMONATTO, M., PECHE, L. Y., BUBLIK, D. R., GOBESSI, S., PIEROTTI, M. A., RODOLFO, M. & SCHNEIDER, C. 2006. MAGE-A tumor antigens target p53 transactivation function through histone deacetylase recruitment and confer resistance to chemotherapeutic agents. *Proc Natl Acad Sci U S A,* 103**,** 11160-5.

MORETTA, L., BOTTINO, C., PENDE, D., VITALE, M., MINGARI, M. C. & MORETTA, A. 2004. Different checkpoints in human NK-cell activation. *Trends Immunol,* 25**,** 670-6.

MORGAN, C. D. & HOLGUIN, M. H. 2002. Chemotherapeutic stress mediated by certain antitumor antibiotics induces an atypical CD69+ surface phenotype in peripheral T-lymphocytes. *Int Immunopharmacol,* 2**,** 367-80.

MOSES, H. 2010. TGF-beta regulation of the inflammatory tumour microenvironment. *Ejc Supplements,* 8**,** 157-157.

MOSMANN, T. R. & COFFMAN, R. L. 1989. TH1 and TH2 cells: different patterns of lymphokine secretion lead to different functional properties. *Annu Rev Immunol,* 7**,** 145-73.

MUNN, D. H. & MELLOR, A. L. 2006. The tumor-draining lymph node as an immune-privileged site. *Immunological Reviews,* 213**,** 146-158.

MURPHY, E., SHIBUYA, K., HOSKEN, N., OPENSHAW, P., MAINO, V., DAVIS, K., MURPHY, K. & O'GARRA, A. 1996. Reversibility of T helper 1 and 2 populations is lost after long-term stimulation. *J Exp Med,* 183**,** 901-13.

NAITO, Y., SAITO, K., SHIIBA, K., OHUCHI, A., SAIGENJI, K., NAGURA, A. & OHTANI, H. 1998. CD8(+) T cells infiltrated within cancer cell nests as a prognostic factor in human colorectal cancer. *Cancer Research,* 58**,** 3491-3494.

NASR, I. W., WANG, Y., GAO, G., DENG, S., DIGGS, L., ROTHSTEIN, D. M., TELLIDES, G., LAKKIS, F. G. & DAI, Z. 2005. Testicular immune privilege promotes transplantation tolerance by altering the balance between memory and regulatory T cells. *J Immunol,* 174**,** 6161-8.

NAZARETH, M. R., BRODERICK, L., SIMPSON-ABELSON, M. R., KELLEHER, R. J., JR., YOKOTA, S. J. & BANKERT, R. B. 2007. Characterization of human lung tumor-associated fibroblasts and their ability to modulate the activation of tumor-associated T cells. *J Immunol,* 178**,** 5552-62.

NEIJSSEN, J., HERBERTS, C., DRIJFHOUT, J. W., REITS, E., JANSSEN, L. & NEEFJES, J. 2005. Cross-presentation by intercellular peptide transfer through gap junctions. *Nature,* 434**,** 83-8.

NELSON, D. J., MUKHERJEE, S., BUNDELL, C., FISHER, S., VAN HAGEN, D. & ROBINSON, B. 2001. Tumor progression despite efficient tumor antigen cross-presentation and effective "arming" of tumor antigen-specific CTL. *J Immunol,* 166**,** 5557-66.

NICHOLS, C. R., HEEREMA, N. A., PALMER, C., LOEHRER, P. J., SR., WILLIAMS, S. D. & EINHORN, L. H. 1987. Klinefelter's syndrome associated with mediastinal germ cell neoplasms. *J Clin Oncol,* 5**,** 1290-4.

NIERKENS, S., TEL, J., JANSSEN, E. & ADEMA, G. J. 2013. Antigen cross-presentation by dendritic cell subsets: one general or all sergeants? *Trends Immunol,* 34**,** 361-70.

NONOMURA, N., IMAZU, T., HARADA, Y., NOZAWA, M., ONO, Y., FUKUI, T., NISHIMURA, K. & OKUYAMA, A. 1999. [Molecular staging of testicular cancer using polymerase chain reaction of the testicular cancer-specific genes]. *Hinyokika Kiyo,* 45**,** 593-7.

NOURI, A. M., HUSSAIN, R. F., OLIVER, R. T., HANDY, A. M., BARTKOVA, I. & BODMER, J. G. 1993. Immunological paradox in testicular tumours: the presence of a large number of activated T-cells despite the complete absence of MHC antigens. *Eur J Cancer,* 29A**,** 1895-9.

OHIGASHI, Y., SHO, M., YAMADA, Y., TSURUI, Y., HAMADA, K., IKEDA, N., MIZUNO, T., YORIKI, R., KASHIZUKA, H., YANE, K., TSUSHIMA, F., OTSUKI, N., YAGITA, H., AZUMA, M. & NAKAJIMA, Y. 2005. Clinical significance of programmed death-1 ligand-1 and programmed death-1 ligand-2 expression in human esophageal cancer. *Clin Cancer Res,* 11**,** 2947-53.

OHKAWA, T., SEKI, S., DOBASHI, H., KOIKE, Y., HABU, Y., AMI, K., HIRAIDE, H. & SEKINE, I. 2001. Systematic characterization of human CD8+ T cells with natural killer cell markers in comparison with natural killer cells and normal CD8+ T cells. *Immunology,* 103**,** 281-90.

OKUMA, Y., SAITO, K., O'CONNOR, A. E., PHILLIPS, D. J., DE KRETSER, D. M. & HEDGER, M. P. 2005. Reciprocal regulation of activin A and inhibin B by interleukin-1 (IL-1) and follicle-stimulating hormone (FSH) in rat Sertoli cells in vitro. *J Endocrinol,* 185**,** 99-110.

OLD, L. J. 2001. Cancer/testis (CT) antigens - a new link between gametogenesis and cancer. *Cancer Immun,* 1.

OLIVER, R. T. 1997. Testis cancer. *Curr Opin Oncol,* 9**,** 287-94.

OSTRAND-ROSENBERG, S. 2004. Animal models of tumor immunity, immunotherapy and cancer vaccines. *Current Opinion in Immunology,* 16**,** 143-150.

OTTAVIANI, S., ZHANG, Y., BOON, T. & VAN DER BRUGGEN, P. 2005. A MAGE-1 antigenic peptide recognized by human cytolytic T lymphocytes on HLA-A2 tumor cells. *Cancer Immunol Immunother,* 54**,** 1214-20.

PAGES, F., BERGER, A., CAMUS, M., SANCHEZ-CABO, F., COSTES, A., MOLIDOR, R., MLECNIK, B., KIRILOVSKY, A., NILSSON, M., DAMOTTE, D., MEATCHI, T., BRUNEVAL, P., CUGNENC, P. H., TRAJANOSKI, Z., FRIDMAN, W. H. & GALON, J. 2005a. Effector memory T cells, early metastasis, and survival in colorectal cancer. *New England Journal of Medicine,* 353**,** 2654-2666.

PAGES, F., BERGER, A., CAMUS, M., SANCHEZ-CABO, F., COSTES, A., MOLIDOR, R., MLECNIK, B., KIRILOVSKY, A., NILSSON, M., DAMOTTE, D., MEATCHI, T., BRUNEVAL, P., CUGNENC, P. H., TRAJANOSKI, Z., FRIDMAN, W. H. & GALON, J. 2005b. Effector memory T cells, early metastasis, and survival in colorectal cancer. *N Engl J Med,* 353**,** 2654-66.

PAGES, F., GALON, J., DIEU-NOSJEAN, M. C., TARTOUR, E., SAUTES-FRIDMAN, C. & FRIDMAN, W. H. 2010. Immune infiltration in human tumors: a prognostic factor that should not be ignored. *Oncogene,* 29**,** 1093-102.

PALMA, L., DILORENZO, N. & GUIDETTI, B. 1978. Lymphocytic Infiltrates in Primary Glioblastomas and Recidivous Gliomas - Incidence, Fate, and Relevance to Prognosis in 228 Operated Cases. *Journal of Neurosurgery,* 49**,** 854-861.

PANG, B., NEIJSSEN, J., QIAO, X., JANSSEN, L., JANSSEN, H., LIPPUNER, C. & NEEFJES, J. 2009. Direct antigen presentation and gap junction mediated cross-presentation during apoptosis. *J Immunol,* 183**,** 1083-90.

PARK, H., LI, Z., YANG, X. O., CHANG, S. H., NURIEVA, R., WANG, Y. H., WANG, Y., HOOD, L., ZHU, Z., TIAN, Q. & DONG, C. 2005. A distinct lineage of CD4 T cells regulates tissue inflammation by producing interleukin 17. *Nat Immunol,* 6**,** 1133-41.

PARK, J. H., KONG, G. H. & LEE, S. W. 2002. hMAGE-A1 overexpression reduces TNF-alpha cytotoxicity in ME-180 cells. *Mol Cells,* 14**,** 122-9.

PEREIRA, M. L. & GARCIA E COSTA, F. 2007. The blood-testis barrier as a target of some chemotherapeutic agents. *Chemotherapy,* 53**,** 446-8.

PETERSEN, R. P., CAMPA, M. J., SPERLAZZA, J., CONLON, D., JOSHI, M. B., HARPOLE, D. H., JR. & PATZ, E. F., JR. 2006. Tumor infiltrating Foxp3+ regulatory T-cells are associated with recurrence in pathologic stage I NSCLC patients. *Cancer,* 107**,** 2866-72.

PETRIE, H. T., STRASSER, A., HARRIS, A. W., HUGO, P. & SHORTMAN, K. 1993. CD4+8- and CD4-8+ mature thymocytes require different post-selection processing for final development. *J Immunol,* 151**,** 1273-9.

PLANT, T. M. & MARSHALL, G. R. 2001. The functional significance of FSH in spermatogenesis and the control of its secretion in male primates. *Endocr Rev,* 22**,** 764-86.

POLLANEN, P. & NIEMI, M. 1987. Immunohistochemical identification of macrophages, lymphoid cells and HLA antigens in the human testis. *International journal of andrology,* 10**,** 37-42.

PRESTWICH, R. J., ERRINGTON, F., HATFIELD, P., MERRICK, A. E., ILETT, E. J., SELBY, P. J. & MELCHER, A. A. 2008. The immune system--is it relevant to cancer development, progression and treatment? *Clin Oncol (R Coll Radiol),* 20**,** 101-12.

QIN, S., ROTTMAN, J. B., MYERS, P., KASSAM, N., WEINBLATT, M., LOETSCHER, M., KOCH, A. E., MOSER, B. & MACKAY, C. R. 1998. The chemokine receptors CXCR3 and CCR5 mark subsets of T cells associated with certain inflammatory reactions. *J Clin Invest,* 101**,** 746-54.

RAJPERT-DE MEYTS, E., KVIST, M. & SKAKKEBAEK, N. E. 1996. Heterogeneity of expression of immunohistochemical tumour markers in testicular carcinoma in situ: pathogenetic relevance. *Virchows Arch,* 428**,** 133-9.

RAJPERT-DE MEYTS, E. & SKAKKEBAEK, N. E. 1994. Expression of the c-kit protein product in carcinoma-in-situ and invasive testicular germ cell tumours. *International journal of andrology,* 17**,** 85-92.

RAPLEY, E. A., CROCKFORD, G. P., TEARE, D., BIGGS, P., SEAL, S., BARFOOT, R., EDWARDS, S., HAMOUDI, R., HEIMDAL, K., FOSSA, S. D., TUCKER, K., DONALD, J., COLLINS, F., FRIEDLANDER, M., HOGG, D., GOSS, P., HEIDENREICH, A., ORMISTON, W., DALY, P. A., FORMAN, D., OLIVER, T. D., LEAHY, M., HUDDART, R., COOPER, C. S., BODMER, J. G., EASTON, D. F., STRATTON, M. R. & BISHOP, D. T. 2000. Localization to Xq27 of a susceptibility gene for testicular germ-cell tumours. *Nat Genet,* 24**,** 197-200.

RAUSER, S., LANGER, R., TSCHERNITZ, S., GAIS, P., JUTTING, U., FEITH, M., HOFLER, H. & WALCH, A. 2010. High number of CD45RO+ tumor infiltrating lymphocytes is an independent prognostic factor in non-metastasized (stage I-IIA) esophageal adenocarcinoma. *BMC Cancer,* 10**,** 608.

REAL, L. M., JIMENEZ, P., KIRKIN, A., SERRANO, A., GARCIA, A., CANTON, J., ZEUTHEN, J., GARRIDO, F. & RUIZ-CABELLO, F. 2001. Multiple mechanisms of immune evasion can coexist in melanoma tumor cell lines derived from the same patient. *Cancer Immunology Immunotherapy,* 49**,** 621-628.

REDMOND, W. L. & SHERMAN, L. A. 2005. Peripheral tolerance of CD8 T lymphocytes. *Immunity,* 22**,** 275-84.

REIK, W., DEAN, W. & WALTER, J. 2001. Epigenetic Reprogramming in Mammalian Development. *Science,* 293**,** 1089-1093.

REINHERZ, E. L., MEUER, S., FITZGERALD, K. A., HUSSEY, R. E., LEVINE, H. & SCHLOSSMAN, S. F. 1982. Antigen recognition by human T lymphocytes is linked to surface expression of the T3 molecular complex. *Cell,* 30**,** 735-43.

RENGARAJAN, J., SZABO, S. J. & GLIMCHER, L. H. 2000. Transcriptional regulation of Th1/Th2 polarization. *Immunol Today,* 21**,** 479-83.

REYNOLDS, S. R., ZELENIUCH-JACQUOTTE, A., SHAPIRO, R. L., ROSES, D. F., HARRIS, M. N., JOHNSTON, D. & BYSTRYN, J. C. 2003. Vaccine-induced CD8+ T-cell responses to MAGE-3 correlate with clinical outcome in patients with melanoma. *Clin Cancer Res,* 9**,** 657-62.

RICHIE, J. P. 2005. Familial risk in testicular cancer as a clue to a heritable and environmental aetiology. *J Urol,* 173**,** 832-3.

RINCON-OROZCO, B., KUNZMANN, V., WROBEL, P., KABELITZ, D., STEINLE, A. & HERRMANN, T. 2005. Activation of V gamma 9V delta 2 T cells by NKG2D. *J Immunol,* 175**,** 2144-51.

RIVAL, C., LUSTIG, L., IOSUB, R., GUAZZONE, V. A., SCHNEIDER, E., MEINHARDT, A. & FIJAK, M. 2006. Identification of a dendritic cell population in normal testis and in chronically inflamed testis of rats with autoimmune orchitis. *Cell Tissue Res,* 324**,** 311-8.

ROBBINS, P. F., EL-GAMIL, M., LI, Y. F., FITZGERALD, E. B., KAWAKAMI, Y. & ROSENBERG, S. A. 1997. The intronic region of an incompletely spliced gp100 gene transcript encodes an epitope recognized by melanoma-reactive tumor-infiltrating lymphocytes. *J Immunol,* 159**,** 303-8.

ROBERTS, A. I., LEE, L., SCHWARZ, E., GROH, V., SPIES, T., EBERT, E. C. & JABRI, B. 2001. NKG2D receptors induced by IL-15 costimulate CD28-negative effector CTL in the tissue microenvironment. *J Immunol,* 167**,** 5527-30.

ROBERTSON, M. J., SOIFFER, R. J., WOLF, S. F., MANLEY, T. J., DONAHUE, C., YOUNG, D., HERRMANN, S. H. & RITZ, J. 1992. Response of human natural killer (NK) cells to NK cell stimulatory factor (NKSF): cytolytic activity and proliferation of NK cells are differentially regulated by NKSF. *J Exp Med,* 175**,** 779-88.

ROCK, K. L., GRAMM, C., ROTHSTEIN, L., CLARK, K., STEIN, R., DICK, L., HWANG, D. & GOLDBERG, A. L. 1994. Inhibitors of the proteasome block the degradation of most cell proteins and the generation of peptides presented on MHC class I molecules. *Cell,* 78**,** 761-71.

ROGERS, P. R. & CROFT, M. 1999. Peptide dose, affinity, and time of differentiation can contribute to the Th1/Th2 cytokine balance. *J Immunol,* 163**,** 1205-13.

ROSENBERG, S. A. 2001. Progress in human tumour immunology and immunotherapy. *Nature,* 411**,** 380-4.

ROT, A. & VON ANDRIAN, U. H. 2004. Chemokines in innate and adaptive host defense: basic chemokinese grammar for immune cells. *Annu Rev Immunol,* 22**,** 891-928.

ROUVIER, E., LUCIANI, M. F. & GOLSTEIN, P. 1993. Fas involvement in Ca(2+)-independent T cell-mediated cytotoxicity. *J Exp Med,* 177**,** 195-200.

ROZALI, E. N., HATO, S. V., ROBINSON, B. W., LAKE, R. A. & LESTERHUIS, W. J. 2012. Programmed death ligand 2 in cancer-induced immune suppression. *Clin Dev Immunol,* 2012**,** 656340.

RUDENSKY, A., PRESTON-HURLBURT, P., HONG, S. C., BARLOW, A. & JANEWAY, C. A., JR. 1991. Sequence analysis of peptides bound to MHC class II molecules. *Nature,* 353**,** 622-7.

RUSSELL, J. H. & LEY, T. J. 2002. Lymphocyte-mediated cytotoxicity. *Annu Rev Immunol,* 20**,** 323-70.

RYSCHICH, E., SCHMIDT, J., HAMMERLING, G. J., KLAR, E. & GANSS, R. 2002. Transformation of the microvascular system during multistage tumorigenesis. *International Journal of Cancer,* 97**,** 719-725.

SAARI, T., JAHNUKAINEN, K. & POLLANEN, P. 1996. Autoantigenicity of the basal compartment of seminiferous tubules in the rat. *J Reprod Immunol,* 31**,** 65-79.

SACCHERI, F., POZZI, C., AVOGADRI, F., BAROZZI, S., FARETTA, M., FUSI, P. & RESCIGNO, M. 2010. Bacteria-induced gap junctions in tumors favor antigen cross-presentation and antitumor immunity. *Sci Transl Med,* 2**,** 44ra57.

SAID, E. A., DUPUY, F. P., TRAUTMANN, L., ZHANG, Y., SHI, Y., EL-FAR, M., HILL, B. J., NOTO, A., ANCUTA, P., PERETZ, Y., FONSECA, S. G., VAN GREVENYNGHE, J., BOULASSEL, M. R., BRUNEAU, J., SHOUKRY, N. H., ROUTY, J. P., DOUEK, D. C., HADDAD, E. K. & SEKALY, R. P. 2010. Programmed death-1-induced interleukin-10 production by monocytes impairs CD4+ T cell activation during HIV infection. *Nat Med,* 16**,** 452-9.

SAINT-RUF, C., UNGEWISS, K., GROETTRUP, M., BRUNO, L., FEHLING, H. J. & VON BOEHMER, H. 1994. Analysis and expression of a cloned pre-T cell receptor gene. *Science,* 266**,** 1208-12.

SAKAGUCHI, S., ONO, M., SETOGUCHI, R., YAGI, H., HORI, S., FEHERVARI, Z., SHIMIZU, J., TAKAHASHI, T. & NOMURA, T. 2006. Foxp3+ CD25+ CD4+ natural regulatory T cells in dominant self-tolerance and autoimmune disease. *Immunol Rev,* 212**,** 8-27.

SAKUISHI, K., APETOH, L., SULLIVAN, J. M., BLAZAR, B. R., KUCHROO, V. K. & ANDERSON, A. C. 2010. Targeting Tim-3 and PD-1 pathways to reverse T cell exhaustion and restore anti-tumor immunity. *J Exp Med,* 207**,** 2187-94.

SALIH, H. R., RAMMENSEE, H. G. & STEINLE, A. 2002. Cutting edge: down-regulation of MICA on human tumors by proteolytic shedding. *J Immunol,* 169**,** 4098-102.

SALLUSTO, F., LENIG, D., FORSTER, R., LIPP, M. & LANZAVECCHIA, A. 1999. Two subsets of memory T lymphocytes with distinct homing potentials and effector functions. *Nature,* 401**,** 708-12.

SANBERG, P. R., BORLONGAN, C. V., SAPORTA, S. & CAMERON, D. F. 1996. Testis-derived Sertoli cells survive and provide localized immunoprotection for xenografts in rat brain. *Nat Biotechnol,* 14**,** 1692-5.

SANDOVAL-MONTES, C. & SANTOS-ARGUMEDO, L. 2005. CD38 is expressed selectively during the activation of a subset of mature T cells with reduced proliferation but improved potential to produce cytokines. *J Leukoc Biol,* 77**,** 513-21.

SANTIS, A. G., CAMPANERO, M. R., ALONSO, J. L., TUGORES, A., ALONSO, M. A., YAGUE, E., PIVEL, J. P. & SANCHEZMADRID, F. 1992. Tumor-Necrosis-Factor-Alpha Production Induced in Lymphocytes-T through the Aim/Cd69 Activation Pathway. *European Journal of Immunology,* 22**,** 1253-1259.

SARID, D. L., RON, I. G., AVINOACH, I., SPERBER, F. & INBAR, M. J. 2002. Spontaneous regression of retroperitoneal metastases from a primary pure anaplastic seminoma: a case report. *Am J Clin Oncol,* 25**,** 380-2.

SATIE, A. P., RAJPERT-DE MEYTS, E., SPAGNOLI, G. C., HENNO, S., OLIVO, L., JACOBSEN, G. K., RIOUX-LECLERCQ, N., JEGOU, B. & SAMSON, M. 2002. The cancer-testis gene, NY-ESO-1, is expressed in normal fetal and adult testes and in spermatocytic seminomas and testicular carcinoma in situ. *Lab Invest,* 82**,** 775-80.

SATO, E., OLSON, S., JUNGBLUTH, A. A., KUNLE, O. & OLD, L. J. 2005. Prognostic significance of tumor infiltrating lymphocytes (TILs) in ovarian cancer and their relationship to cancer-testis (CT) antigen expression. *Modern Pathology,* 18**,** 203a-203a.

SCANLAN, M. J., CHEN, Y. T., WILLIAMSON, B., GURE, A. O., STOCKERT, E., GORDAN, J. D., TURECI, O., SAHIN, U., PFREUNDSCHUH, M. & OLD, L. J. 1998. Characterization of human colon cancer antigens recognized by autologous antibodies. *Int J Cancer,* 76**,** 652-8.

SCANLAN MJ, G. A., JUNGBLUTH AA, OLD LJ, CHEN YT 2002. Cancer/testis antigens: an expanding family of targets for cancer immunotherapy. *Immunol Rev,* 188**,** 22-32.

SCANLAN, M. J., GORDAN, J. D., WILLIAMSON, B., STOCKERT, E., BANDER, N. H., JONGENEEL, V., GURE, A. O., JAGER, D., JAGER, E., KNUTH, A., CHEN, Y. T. & OLD, L. J. 1999. Antigens recognized by autologous antibody in patients with renal-cell carcinoma. *Int J Cancer,* 83**,** 456-64.

SCHMID, D., PYPAERT, M. & MUNZ, C. 2007. Antigen-loading compartments for major histocompatibility complex class II molecules continuously receive input from autophagosomes. *Immunity,* 26**,** 79-92.

SCHREIBER, R. D., OLD, L. J. & SMYTH, M. J. 2011. Cancer immunoediting: integrating immunity's roles in cancer suppression and promotion. *Science,* 331**,** 1565-70.

SCHULER, T., KAMMERTOENS, T., PREISS, S., DEBS, P., NOBEN-TRAUTH, N. & BLANKENSTEIN, T. 2001. Generation of tumor-associated cytotoxic T lymphocytes requires interleukin 4 from CD8(+) T cells. *J Exp Med,* 194**,** 1767-75.

SCHWARTZ, R. H. 2003. T cell anergy. *Annu Rev Immunol,* 21**,** 305-34.
SCHWEYER, S., SORURI, A., BAUMHOER, D., PETERS, J., CATTARUZZA, M., RADZUN, H. J. & FAYYAZI, A. 2002. Expression of CXC chemokine IP-10 in testicular germ cell tumours. *The Journal of pathology,* 197**,** 89-97.
SETCHELL, B. P. 1990. Local control of testicular fluids. *Reprod Fertil Dev,* 2**,** 291-309.
SHAH, W., YAN, X., JING, L., ZHOU, Y., CHEN, H. & WANG, Y. 2011. A reversed CD4/CD8 ratio of tumor-infiltrating lymphocytes and a high percentage of CD4(+)FOXP3(+) regulatory T cells are significantly associated with clinical outcome in squamous cell carcinoma of the cervix. *Cell Mol Immunol,* 8**,** 59-66.
SHALET, S. M. 2009. Normal testicular function and spermatogenesis. *Pediatr Blood Cancer,* 53**,** 285-8.
SHARMA, O. P., FLORES, J. A., LEONG, D. A. & VELDHUIS, J. D. 1994. Cellular basis for follicle-stimulating hormone-stimulated calcium signaling in single rat Sertoli cells: possible dissociation from effects of adenosine 3',5'-monophosphate. *Endocrinology,* 134**,** 1915-23.
SHARPE, A. H., WHERRY, E. J., AHMED, R. & FREEMAN, G. J. 2007. The function of programmed cell death 1 and its ligands in regulating autoimmunity and infection. *Nat Immunol,* 8**,** 239-45.
SHEIL, A. G. R., DISNEY, A. P. S., MATHEW, T. H., LIVINGSTON, B. E. R. & KEOGH, A. M. 1997. Lymphoma incidence, cyclosporine, and the evolution and major impact of malignancy following organ transplantation. *Transplantation Proceedings,* 29**,** 825-827.
SHEVACH, E. M. 2002. CD4(+)CD25(+) suppressor T cells: More questions than answers. *Nature Reviews Immunology,* 2**,** 389-400.
SHIGEKI, S., AKIRA, Y., KIMITAKA, S., OSAMU, I., MOTOKO, S., KOJIRO, N. & KYOGO, I. 1996. Induction of MAGE Genes in Lymphoid Cells by the Demethylating Agent 5-Aza-2'-deoxycytidine. *Cancer Science,* 87**,** 751-756.
SHUBINSKY, G. & SCHLESINGER, M. 1997. The CD38 lymphocyte differentiation marker: new insight into its ectoenzymatic activity and its role as a signal transducer. *Immunity,* 7**,** 315-24.
SIDDIK, Z. H. 2003. Cisplatin: mode of cytotoxic action and molecular basis of resistance. *Oncogene,* 22**,** 7265-79.
SIMPSON, A. J. G., CABALLERO, O. L., JUNGBLUTH, A., CHEN, Y.-T. & OLD, L. J. 2005. Cancer/testis antigens, gametogenesis and cancer. *Nat Rev Cancer,* 5**,** 615-625.
SIMS, G. P., ROWE, D. C., RIETDIJK, S. T., HERBST, R. & COYLE, A. J. 2010. HMGB1 and RAGE in Inflammation and Cancer. *Annual Review of Immunology, Vol 28,* 28**,** 367-388.
SINKOVICS, J. G. & HORVATH, J. C. 2005. Human natural killer cells: a comprehensive review. *Int J Oncol,* 27**,** 5-47.
SIPIONE, S., SIMMEN, K. C., LORD, S. J., MOTYKA, B., EWEN, C., SHOSTAK, I., RAYAT, G. R., DUFOUR, J. M., KORBUTT, G. S., RAJOTTE, R. V. & BLEACKLEY, R. C. 2006. Identification of a novel human granzyme B inhibitor secreted by cultured sertoli cells. *J Immunol,* 177**,** 5051-8.
SNYDER, J. T., ALEXANDER-MILLER, M. A., BERZOFSKYL, J. A. & BELYAKOV, I. M. 2003. Molecular mechanisms and biological significance of CTL avidity. *Curr HIV Res,* 1**,** 287-94.
SPEISER, D. E., VALMORI, D., RIMOLDI, D., PITTET, M. J., LIENARD, D., CERUNDOLO, V., MACDONALD, H. R., CEROTTINI, J. C. & ROMERO, P. 1999. CD28-negative cytolytic effector T cells frequently express NK receptors and are present at variable proportions in circulating lymphocytes from healthy donors and melanoma patients. *Eur J Immunol,* 29**,** 1990-9.
STATISTICAL INFORMATION TEAM, C. R. U. L. 2007.
STEIMLE, V., SIEGRIST, C. A., MOTTET, A., LISOWSKA-GROSPIERRE, B. & MACH, B. 1994. Regulation of MHC class II expression by interferon-gamma mediated by the transactivator gene CIITA. *Science,* 265**,** 106-9.

STEMBERGER, C., HUSTER, K. M., KOFFLER, M., ANDERL, F., SCHIEMANN, M., WAGNER, H. & BUSCH, D. H. 2007. A single naive CD8+ T cell precursor can develop into diverse effector and memory subsets. *Immunity,* 27**,** 985-97.

STOCKERT, E., JAGER, E., CHEN, Y. T., SCANLAN, M. J., GOUT, I., KARBACH, J., ARAND, M., KNUTH, A. & OLD, L. J. 1998. A survey of the humoral immune response of cancer patients to a panel of human tumor antigens. *J Exp Med,* 187**,** 1349-54.

STRAND, S., HOFMANN, W. J., HUG, H., MULLER, M., OTTO, G., STRAND, D., MARIANI, S. M., STREMMEL, W., KRAMMER, P. H. & GALLE, P. R. 1996. Lymphocyte apoptosis induced by CD95 (APO-1/Fas) ligand-expressing tumor cells--a mechanism of immune evasion? *Nat Med,* 2**,** 1361-6.

STRID, J., ROBERTS, S. J., FILLER, R. B., LEWIS, J. M., KWONG, B. Y., SCHPERO, W., KAPLAN, D. H., HAYDAY, A. C. & GIRARDI, M. 2008. Acute upregulation of an NKG2D ligand promotes rapid reorganization of a local immune compartment with pleiotropic effects on carcinogenesis. *Nat Immunol,* 9**,** 146-54.

SUESCUN, M. O., CALANDRA, R. S. & LUSTIG, L. 1994. Alterations of testicular function after induced autoimmune orchitis in rats. *J Androl,* 15**,** 442-8.

SWANN, J. B. & SMYTH, M. J. 2007. Immune surveillance of tumors. *J Clin Invest,* 117**,** 1137-46.

SWERDLOW, A. J., DOS SANTOS SILVA, I., REID, A., QIAO, Z., BREWSTER, D. H. & ARRUNDALE, J. 1998. Trends in cancer incidence and mortality in Scotland: description and possible explanations. *Br J Cancer,* 77 Suppl 3**,** 1-54.

TAAMS, L. S., SMITH, J., RUSTIN, M. H., SALMON, M., POULTER, L. W. & AKBAR, A. N. 2001. Human anergic/suppressive CD4(+)CD25(+) T cells: a highly differentiated and apoptosis-prone population. *European Journal of Immunology,* 31**,** 1122-1131.

TAKAHASHI K, S. S., NOGUCHI M, HIROHATA M, ITOH K 1995. Identification of MAGE-1 and MAGE-4 proteins in spermatogonia and primary spermatocytes of testis. *Cancer Res,* 55**,** 3478-82.

TAKAHASHI, T., DEJBAKHSH-JONES, S. & STROBER, S. 2006. Expression of CD161 (NKR-P1A) defines subsets of human CD4 and CD8 T cells with different functional activities. *J Immunol,* 176**,** 211-6.

TAKAHASHI, T., KUNIYASU, Y., TODA, M., SAKAGUCHI, N., ITOH, M., IWATA, M., SHIMIZU, J. & SAKAGUCHI, S. 1998. Immunologic self-tolerance maintained by CD25+CD4+ naturally anergic and suppressive T cells: induction of autoimmune disease by breaking their anergic/suppressive state. *Int Immunol,* 10**,** 1969-80.

TAKANAMI, I., TAKEUCHI, K. & GIGA, M. 2001. The prognostic value of natural killer cell infiltration in resected pulmonary adenocarcinoma. *Journal of Thoracic and Cardiovascular Surgery,* 121**,** 1058-1063.

TANCHOT, C., ROSADO, M. M., AGENES, F., FREITAS, A. A. & ROCHA, B. 1997. Lymphocyte homeostasis. *Semin Immunol,* 9**,** 331-7.

TARKKANEN, J., SAKSELA, E. & LANIER, L. L. 1986. Bacterial activation of human natural killer cells. Characteristics of the activation process and identification of the effector cell. *J Immunol,* 137**,** 2428-33.

TENCA, C., MERLO, A., ZARCONE, D., SAVERINO, D., BRUNO, S., DE SANTANNA, A., RAMARLI, D., FABBI, M., PESCE, C., DEAGLIO, S., CICCONE, E., MALAVASI, F. & GROSSI, C. E. 2003. Death of T cell precursors in the human thymus: a role for CD38. *Int Immunol,* 15**,** 1105-16.

TESTI, R., D'AMBROSIO, D., DE MARIA, R. & SANTONI, A. 1994. The CD69 receptor: a multipurpose cell-surface trigger for hematopoietic cells. *Immunol Today,* 15**,** 479-83.

THOMAS, D. A. & MASSAGUE, J. 2005. TGF-beta directly targets cytotoxic T cell functions during tumor evasion of immune surveillance. *Cancer Cell,* 8**,** 369-380.

THOMPSON, E. D., ENRIQUEZ, H. L., FU, Y. X. & ENGELHARD, V. H. 2010. Tumor masses support naive T cell infiltration, activation, and differentiation into effectors. *Journal of Experimental Medicine,* 207**,** 1791-1804.

THOMPSON, R. H., KUNTZ, S. M., LEIBOVICH, B. C., DONG, H., LOHSE, C. M., WEBSTER, W. S., SENGUPTA, S., FRANK, I., PARKER, A. S., ZINCKE, H., BLUTE, M. L., SEBO, T. J., CHEVILLE, J. C. & KWON, E. D. 2006. Tumor B7-H1 is associated with poor prognosis in renal cell carcinoma patients with long-term follow-up. *Cancer Res,* 66**,** 3381-5.

TOLEDANO, M. B., JARUP, L., BEST, N., WAKEFIELD, J. & ELLIOTT, P. 2001. Spatial variation and temporal trends of testicular cancer in Great Britain. *Br J Cancer,* 84**,** 1482-7.

TOLLERUD, D. J., BLATTNER, W. A., FRASER, M. C., BROWN, L. M., POTTERN, L., SHAPIRO, E., KIRKEMO, A., SHAWKER, T. H., JAVADPOUR, N., O'CONNELL, K. & ET AL. 1985. Familial testicular cancer and urogenital developmental anomalies. *Cancer,* 55**,** 1849-54.

TORRES, A., CASANOVA, J. F., NISTAL, M. & REGADERA, J. 1997. Quantification of immunocompetent cells in testicular germ cell tumours. *Histopathology,* 30**,** 23-30.

TRAVERSARI, C., VAN DER BRUGGEN, P., LUESCHER, I. F., LURQUIN, C., CHOMEZ, P., VAN PEL, A., DE PLAEN, E., AMAR-COSTESEC, A. & BOON, T. 1992. A nonapeptide encoded by human gene MAGE-1 is recognized on HLA-A1 by cytolytic T lymphocytes directed against tumor antigen MZ2-E. *J Exp Med,* 176**,** 1453-7.

TUCK, R. R., SETCHELL, B. P., WAITES, G. M. & YOUNG, J. A. 1970. The composition of fluid collected by micropuncture and catheterization from the seminiferous tubules and rete testis of rats. *Pflugers Arch,* 318**,** 225-43.

TUNG, K. S., TEUSCHER, C. & MENG, A. L. 1981. Autoimmunity to spermatozoa and the testis. *Immunol Rev,* 55**,** 217-55.

TUNG, K. S., YULE, T. D., MAHI-BROWN, C. A. & LISTROM, M. B. 1987. Distribution of histopathology and Ia positive cells in actively induced and passively transferred experimental autoimmune orchitis. *Journal of Immunology,* 138**,** 752-9.

TUREK, P. J. & LIPSHULTZ, L. I. 1994. Immunologic infertility. *Urol Clin North Am,* 21**,** 447-68.

UGUR, S., ÖZLEM, T., YAO-TSENG, C., GERHARD, S., CARLOS, V.-H., LLOYD, J. O. & MICHAEL, P. 1998. Expression of multiple cancer/testis (CT) antigens in breast cancer and melanoma: Basis for polyvalent CT vaccine strategies. *International Journal of Cancer,* 78**,** 387-389.

UNDERHILL, D. M., BASSETTI, M., RUDENSKY, A. & ADEREM, A. 1999. Dynamic interactions of macrophages with T cells during antigen presentation. *J Exp Med,* 190**,** 1909-14.

UYTTENHOVE, C., PILOTTE, L., THEATE, I., STROOBANT, V., COLAU, D., PARMENTIER, N., BOON, T. & VAN DEN EYNDE, B. J. 2003. Evidence for a tumoral immune resistance mechanism based on tryptophan degradation by indoleamine 2,3-dioxygenase. *Nat Med,* 9**,** 1269-74.

VAN DE BERG, P. J., VAN LEEUWEN, E. M., TEN BERGE, I. J. & VAN LIER, R. 2008. Cytotoxic human CD4(+) T cells. *Curr Opin Immunol,* 20**,** 339-43.

VAN DEN EYNDE, B. J. & BOON, T. 1997. Tumor antigens recognized by T lymphocytes. *Int J Clin Lab Res,* 27**,** 81-6.

VAN DER BRUGGEN P, T. C., CHOMEZ P, LURQUIN C, DE PLAEN E, VAN DEN EYNDE B, KNUTH A, BOON T 1991. A gene encoding an antigen recognized by cytolytic T lymphocytes on a human melanoma. *Science,* 254**,** 1643-7.

VAN DER BRUGGEN, P., TRAVERSARI, C., CHOMEZ, P., LURQUIN, C., DE PLAEN, E., VAN DEN EYNDE, B., KNUTH, A. & BOON, T. 1991. A gene encoding an antigen recognized by cytolytic T lymphocytes on a human melanoma. *Science,* 254**,** 1643-7.

VERAJANKORVA, E., SETALA, N., TEROS, T., SALMI, A. A. & POLLANEN, P. 2002. Testicular-associated immune deviation: flushing of the testicular lymph sinusoids induces immunosuppression and inhibits formation of EAE in SJL mice. *Scand J Immunol,* 55**,** 478-83.

VILLADANGOS, J. A. & SCHNORRER, P. 2007. Intrinsic and cooperative antigen-presenting functions of dendritic-cell subsets in vivo. *Nat Rev Immunol,* 7**,** 543-55.

VON EYBEN, F. E., BLAABJERG, O., HYLTOFT-PETERSEN, P., MADSEN, E. L., AMATO, R., LIU, F. & FRITSCHE, H. 2001. Serum lactate dehydrogenase isoenzyme 1 and prediction of death in patients with metastatic testicular germ cell tumors. *Clinical Chemistry and Laboratory Medicine,* 39**,** 38-44.

WAKABAYASHI, O., YAMAZAKI, K., OIZUMI, S., HOMMURA, F., KINOSHITA, I., OGURA, S., DOSAKA-AKITA, H. & NISHIMURA, M. 2003. CD4+ T cells in cancer stroma, not CD8+ T cells in cancer cell nests, are associated with favorable prognosis in human non-small cell lung cancers. *Cancer Sci,* 94**,** 1003-9.

WAKIM, L. M. & BEVAN, M. J. 2011. Cross-dressed dendritic cells drive memory CD8+ T-cell activation after viral infection. *Nature,* 471**,** 629-32.

WALDHAUER, I. & STEINLE, A. 2006. Proteolytic release of soluble UL16-binding protein 2 from tumor cells. *Cancer Res,* 66**,** 2520-6.

WALKER, L. S. & ABBAS, A. K. 2002. The enemy within: keeping self-reactive T cells at bay in the periphery. *Nat Rev Immunol,* 2**,** 11-9.

WALKER, W. H., FUCCI, L. & HABENER, J. F. 1995. Expression of the gene encoding transcription factor cyclic adenosine 3',5'-monophosphate (cAMP) response element-binding protein (CREB): regulation by follicle-stimulating hormone-induced cAMP signaling in primary rat Sertoli cells. *Endocrinology,* 136**,** 3534-45.

WATTS, C. 2004. Class II MHC: sweetening the peptide only diet? *Cell,* 117**,** 558-9.

WEISER, T. S., GUO, Z. S., OHNMACHT, G. A., PARKHURST, M. L., TONG-ON, P., MARINCOLA, F. M., FISCHETTE, M. R., YU, X., CHEN, G. A., HONG, J. A., STEWART, J. H., NGUYEN, D. M., ROSENBERG, S. A. & SCHRUMP, D. S. 2001. Sequential 5-Aza-2'-deoxycytidine-Depsipeptide FR901228 Treatment Induces Apoptosis Preferentially in Cancer Cells and Facilitates Their Recognition by Cytolytic T Lymphocytes Specific for NY-ESO-1. *Journal of Immunotherapy,* 24**,** 151-161.

WHERRY, E. J. & AHMED, R. 2004. Memory CD8 T-cell differentiation during viral infection. *J Virol,* 78**,** 5535-45.

WHERRY, E. J., HA, S. J., KAECH, S. M., HAINING, W. N., SARKAR, S., KALIA, V., SUBRAMANIAM, S., BLATTMAN, J. N., BARBER, D. L. & AHMED, R. 2007. Molecular signature of CD8+ T cell exhaustion during chronic viral infection. *Immunity,* 27**,** 670-84.

WIEMANN, K., MITTRUCKER, H. W., FEGER, U., WELTE, S. A., YOKOYAMA, W. M., SPIES, T., RAMMENSEE, H. G. & STEINLE, A. 2005. Systemic NKG2D down-regulation impairs NK and CD8 T cell responses in vivo. *J Immunol,* 175**,** 720-9.

WOLF, D., WOLF, A. M., RUMPOLD, H., FIEGL, H., ZEIMET, A. G., MULLER-HOLZNER, E., DEIBL, M., GASTL, G., GUNSILIUS, E. & MARTH, C. 2005. The expression of the regulatory T cell-specific forkhead box transcription factor FoxP3 is associated with poor prognosis in ovarian cancer. *Clin Cancer Res,* 11**,** 8326-31.

WOLFERS, J., LOZIER, A., RAPOSO, G., REGNAULT, A., THERY, C., MASURIER, C., FLAMENT, C., POUZIEUX, S., FAURE, F., TURSZ, T., ANGEVIN, E., AMIGORENA, S. & ZITVOGEL, L. 2001. Tumor-derived exosomes are a source of shared tumor rejection antigens for CTL cross-priming. *Nat Med,* 7**,** 297-303.

WOO, E. Y., YEH, H., CHU, C. S., SCHLEINGER, K., CARROLL, R. G., RILEY, J. L., KAISER, L. R. & JUNE, C. H. 2002. Cutting edge: Regulatory T cells from lung cancer patients directly inhibit autologous T cell proliferation. *Journal of Immunology,* 168**,** 4272-4276.

WU, X., TAO, Y., HOU, J., MENG, X. & SHI, J. 2012. Valproic acid upregulates NKG2D ligand expression through an ERK-dependent mechanism and potentially enhances NK cell-mediated lysis of myeloma. *Neoplasia,* 14**,** 1178-89.

YAKIREVICH, E., LEFEL, O., SOVA, Y., STEIN, A., COHEN, O., IZHAK, O. B. & RESNICK, M. B. 2002. Activated status of tumour-infiltrating lymphocytes and apoptosis in testicular seminoma. *The Journal of pathology,* 196**,** 67-75.

YAMAMOTO, R., NISHIKORI, M., KITAWAKI, T., SAKAI, T., HISHIZAWA, M., TASHIMA, M., KONDO, T., OHMORI, K., KURATA, M., HAYASHI, T. & UCHIYAMA, T. 2008. PD-1-PD-1 ligand interaction contributes to immunosuppressive microenvironment of Hodgkin lymphoma. *Blood,* 111**,** 3220-4.

YANG, B., O'HERRIN, S. M., WU, J., REAGAN-SHAW, S., MA, Y., BHAT, K. M., GRAVEKAMP, C., SETALURI, V., PETERS, N., HOFFMANN, F. M., PENG, H., IVANOV, A. V., SIMPSON, A. J. & LONGLEY, B. J. 2007. MAGE-A, mMage-b, and MAGE-C proteins form complexes with KAP1 and suppress p53-dependent apoptosis in MAGE-positive cell lines. *Cancer Res,* 67**,** 9954-62.

YANG, F., SHAO, Y., LIU, M., HUANG, J., ZHU, K., GUO, C., LUO, J., LI, W., YANG, B., SHI, J. & ZHENG, J. 2013. Valproic acid upregulates NKG2D ligand expression and enhances susceptibility of human renal carcinoma cells to NK cell-mediated cytotoxicity. *Arch Med Sci,* 9**,** 323-31.

YANG, R., XIA, T., XU, G., LI, Z., YING, Z. & XU, X. 2008. Human cytomegalovirus specific CD8(+) T lymphocytes display interferon-gamma secretion impairment in kidney transplant recipients with pp65 antigenemia. *Transplant Proc,* 40**,** 3500-4.

YOSHIMOTO, M., SAKAMOTO, G. & OHASHI, Y. 1993. Time Dependency of the Influence of Prognostic Factors on Relapse in Breast-Cancer. *Cancer,* 72**,** 2993-3001.

YOSHINO, I., YANO, T., MURATA, M., ISHIDA, T., SUGIMACHI, K., KIMURA, G. & NOMOTO, K. 1992. Tumor-reactive T-cells accumulate in lung cancer tissues but fail to respond due to tumor cell-derived factor. *Cancer Res,* 52**,** 775-81.

YUAN, J., GNJATIC, S., LI, H., POWEL, S., GALLARDO, H. F., RITTER, E., KU, G. Y., JUNGBLUTH, A. A., SEGAL, N. H., RASALAN, T. S., MANUKIAN, G., XU, Y., ROMAN, R. A., TERZULLI, S. L., HEYWOOD, M., POGORILER, E., RITTER, G., OLD, L. J., ALLISON, J. P. & WOLCHOK, J. D. 2008. CTLA-4 blockade enhances polyfunctional NY-ESO-1 specific T cell responses in metastatic melanoma patients with clinical benefit. *Proc Natl Acad Sci U S A,* 105**,** 20410-5.

YUASA, T., OKAMOTO, K., KAWAKAMI, T., MISHINA, M., OGAWA, O. & OKADA, Y. 2001. Expression patterns of cancer testis antigens in testicular germ cell tumors and adjacent testicular tissue. *J Urol,* 165**,** 1790-4.

YULE, T. D., MONTOYA, G. D., RUSSELL, L. D., WILLIAMS, T. M. & TUNG, K. S. 1988. Autoantigenic germ cells exist outside the blood testis barrier. *J Immunol,* 141**,** 1161-7.

ZAUNDERS, J. J., DYER, W. B., WANG, B., MUNIER, M. L., MIRANDA-SAKSENA, M., NEWTON, R., MOORE, J., MACKAY, C. R., COOPER, D. A., SAKSENA, N. K. & KELLEHER, A. D. 2004. Identification of circulating antigen-specific CD4+ T lymphocytes with a CCR5+, cytotoxic phenotype in an HIV-1 long-term nonprogressor and in CMV infection. *Blood,* 103**,** 2238-47.

ZEH, H. J., 3RD, PERRY-LALLEY, D., DUDLEY, M. E., ROSENBERG, S. A. & YANG, J. C. 1999. High avidity CTLs for two self-antigens demonstrate superior in vitro and in vivo antitumor efficacy. *J Immunol,* 162**,** 989-94.

ZERBINI, A., PILLI, M., SOLIANI, P., ZIEGLER, S., PELOSI, G., ORLANDINI, A., CAVALLO, C., UGGERI, J., SCANDROGLIO, R., CRAFA, P., SPAGNOLI, G. C., FERRARI, C. & MISSALE, G. 2004. Ex vivo characterization of tumor-derived melanoma antigen encoding gene-specific CD8+cells in patients with hepatocellular carcinoma. *J Hepatol,* 40**,** 102-9.

ZHANG, L., GAJEWSKI, T. F. & KLINE, J. 2009. PD-1/PD-L1 interactions inhibit antitumor immune responses in a murine acute myeloid leukemia model. *Blood,* 114**,** 1545-52.

ZHANG, Y., STROOBANT, V., RUSSO, V., BOON, T. & VAN DER BRUGGEN, P. 2002. A MAGE-A4 peptide presented by HLA-B37 is recognized on human tumors by cytolytic T lymphocytes. *Tissue Antigens,* 60**,** 365-71.

ZHAO, Q., KUANG, D. M., WU, Y., XIAO, X., LI, X. F., LI, T. J. & ZHENG, L. 2012. Activated CD69+ T cells foster immune privilege by regulating IDO expression in tumor-associated macrophages. *J Immunol,* 188**,** 1117-24.

ZHAO, X., WEI, Y. Q., KARIYA, Y., TESHIGAWARA, K. & UCHIDA, A. 1995. Accumulation of gamma/delta T cells in human dysgerminoma and seminoma: roles in autologous tumor killing and granuloma formation. *Immunol Invest,* 24**,** 607-18.

ZHOU, F. 2009. Molecular mechanisms of IFN-gamma to up-regulate MHC class I antigen processing and presentation. *Int Rev Immunol,* 28**,** 239-60.

ZHU, C., ANDERSON, A. C., SCHUBART, A., XIONG, H., IMITOLA, J., KHOURY, S. J., ZHENG, X. X., STROM, T. B. & KUCHROO, V. K. 2005. The Tim-3 ligand galectin-9 negatively regulates T helper type 1 immunity. *Nat Immunol,* 6**,** 1245-52.

ZITVOGEL, L., TESNIERE, A. & KROEMER, G. 2006. Cancer despite immunosurveillance: immunoselection and immunosubversion. *Nat Rev Immunol,* 6**,** 715-27.

ZOU, W. 2006. Regulatory T cells, tumour immunity and immunotherapy. *Nat Rev Immunol,* 6**,** 295-307.

APPENDIX

Table 29. Patient Information of Recruited TGCT Patients.

Patient ID	Age	Primary Tumour Type	Tumour Stage	Localised (L) or Metastatic (M)	Chemotherapy Regimen	Date of Reoccurrence (if any)	Date of 1st Sample
01DB	30	Pure Seminoma	Stage 2b	M	3 x EP120		24/11/2010
02PM	52	Pure Seminoma	Stage 1	L	Carboplatin		07/12/2010
03RD	35	NSGCTT	IGCCCG - Good	M	3 x BEP165		07/12/2010
04SD	41	Pure Seminoma	Stage 1	L	Carboplatin		07/12/2010
05TB	23	Pure Seminoma	Stage 1	L	Carboplatin		11/01/2011
06JB	32	Pure Seminoma	Stage 2a	M	3 x EP120		17/01/2011
07IB	47	Pure Seminoma	Stage 1	L	Carboplatin	17/01/2013	18/01/2011
08JP	37	Mixed GCT	Stage 1 vi+	L	2 x BEP120		18/01/2011
09DW	48	Mixed GCT	Stage 1 vi-	L	Surveillance		18/01/2011
10CP	28	NSGCTT	Stage 1 vi-	L	2 x BEP120		24/01/2011

11DO	20	Pure Seminoma	Stage 1	L	Carboplatin	22/02/2011
12AW	30	Pure Seminoma	Stage 1	L	Carboplatin	15/03/2011
13SC	24	Pure Seminoma	Stage 1	L	Carboplatin	15/03/2011
14AM	39	Pure Seminoma	Stage 1	L	Carboplatin	29/03/2011
15SK	47	Pure Seminoma	Stage 2a	M	3 x EP120	31/03/2011
16PR	44	Pure Seminoma	Stage 1	L	Carboplatin	17/05/2011
17YH	26	NSGCTT	IGCCCG - Good	M	3 x BEP165	20/05/2011
18MP	25	NSGCTT	Stage 1 vi-	L	2 x BEP120	24/05/2011
20KB	41	Mixed GCT	IGCCCG - Good	L	2 x BEP120	31/05/2011
21LW	24	NSGCTT	IGCCCG - Good	M	3 x BEP165	14/06/2011
22DG	37	Pure Seminoma	Stage 1	L	Carboplatin	21/06/2011
23DW	22	NSGCTT	IGCCCG - Good	M	3 x BEP165	21/06/2011
25PM	44	Pure Seminoma	Stage 1	L	Carboplatin	28/06/2011

26MP	55	Pure Seminoma	Stage 2b	M	3 x EP120	28/06/2011
27MC	45	Pure Seminoma	Stage 1	L	Carboplatin	05/07/2011
31GS	30	Mixed GCT	Stage 1 vi-	L	2 x BEP120	30/08/2011
33LH	46	Pure Seminoma	Stage 1	L	Carboplatin	04/10/2011
34SR	39	Pure Seminoma	Stage 1	L	Carboplatin	04/10/2011
35NM	31	Pure Seminoma	Stage 1	L	Carboplatin	04/10/2011
36GC	40	Pure Seminoma	Stage 1	L	Carboplatin	11/10/2011
37SR	21	Pure Seminoma	Stage 1	L	Carboplatin	11/10/2011
38MT	26	NSGCTT	IGCCCG - Good	M	3 x BEP165	11/10/2011
39DT	67	Pure Seminoma	Stage 1	L	Carboplatin	18/10/2011
40DC	72	Pure Seminoma	Stage 3	L	3 x EP120	18/10/2011
41ZY	31	Pure Seminoma	Stage 1	L	Carboplatin	18/10/2011
42GM	37	Pure Seminoma	Stage 1	L	Carboplatin	18/10/2011

43SJ	35	Pure Seminoma	Stage 1	L	Carboplatin	25/10/2011
44SA	43	Pure Seminoma	Stage IV	M	4 x BEP100	25/10/2011
45PR	47	Pure Seminoma	Stage 1	L	Carboplatin	08/11/2011
47MH	37	Pure Seminoma	Stage 2a	M	3 x EP120	09/12/2011
48JL	54	Pure Seminoma	Stage 1	L	Carboplatin	10/01/2012
49NC	20	NSGCTT	IGCCCG - Good	M	3 x BEP165	10/01/2012
50RN	45	Mixed GCT	Stage 1 vi-	L	2 x BEP120	10/01/2012
52RA	42	Pure Seminoma	Stage 1	L	Carboplatin	24/01/2012
53LR	33	Pure Seminoma	Stage 1	L	Carboplatin	24/01/2012
54SH	23	Mixed GCT	Stage 1 vi+	L	1 x BEP165	24/01/2012
56AP	34	Pure Seminoma	Stage 1	L	Carboplatin	31/01/2012
57MV	32	Pure Seminoma	Stage 1	L	Carboplatin	31/01/2012
58CL	31	Pure Seminoma	Stage 1	L	3 x EP120	02/02/2012

59BS	27	Pure Seminoma	Stage 1	L	Carboplatin		03/02/2012
61ZQ	25	NSGCTT	Stage 1 vi+	L	1 x BEP165		07/02/2012
62ML	37	Mixed GCT	Stage 1 vi-	L	2 x BEP120		07/02/2012
63JL	24	Mixed GCT	Stage 1 vi-	L	2 x BEP120		21/02/2012
65FB	32	Pure Seminoma	Stage 1	L	Carboplatin		21/03/2012
66MI	36	NSGCTT	IGCCCG - Good	M	3 x BEP165		18/04/2012
67TC	22	NSGCTT	Stage 1 vi+	L	1 x BEP165		20/04/2012
68CJ	28	Pure Seminoma	Stage 1	L	Carboplatin		26/04/2012
69HB	45	NSGCTT	IGCCCG - Inter	M	4 x BEP165	16/04/2012	27/04/2012
70DS	23	Pure Seminoma	Stage 1	L	Carboplatin		01/05/2012
71DM	41	Pure Seminoma	Stage 1	L	Carboplatin		01/05/2012
72TC	51	NSGCTT	IGCCCG - Good	M	EP 165		04/05/2012
74SW	24	Embryonal Carcinoma	Stage 1 vi-	L	2 x BEP120		04/05/2012

75NS	43	Pure Seminoma	Stage 1	L	Carboplatin	04/05/2012
76AM	20	Mixed GCT	Stage 1 vi+	L	1 x BEP165	04/05/2012
77DS	33	Mixed GCT	Stage 1 vi-	L	2 x BEP120	08/05/2012
80JD	28	NSGCTT	Stage 1 vi+	L	2 x BEP120	26/06/2012
82MC	54	Pure Seminoma	Stage 1	L	Carboplatin	10/07/2012
83PR	49	Pure Seminoma	Stage 1	L	Surveillance	10/07/2012
84JM	23	Embryonal Carcinoma	Stage 1 vi+	L	n/a	03/08/2012
85JJ	43	Pure Seminoma	Stage 1	L	Carboplatin	21/08/2012
86CE	39	Mixed GCT	Stage 1 vi-	L	2 x BEP120	21/08/2012
87AB	82	Pure Seminoma	Stage 2b	M	Radiotherapy	26/09/2012
89KJ	57	Pure Seminoma	Stage 1	L	Carboplatin	08/10/2012
90LS	36	Pure Seminoma	IGCCCG - Good	L	3 x EP120	16/10/2012
91PN	39	Pure Seminoma	Stage 1	L	Carboplatin	19/10/2012